On the theory of TM- electromagnetic guided waves in a nonlinear planar slab structure

Dissertation

zur Erlangung des Grades

eines Doktors der Naturwissenschaften

von

Kadriya Yuskaeva

vorgelegt dem Fachbereich Physik der

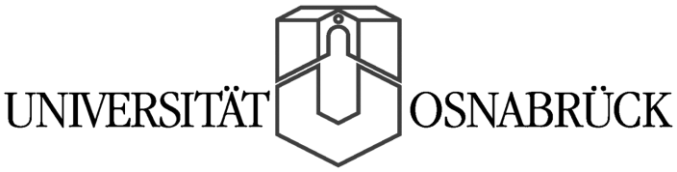

August 2012

Contents

1 Introduction

Propagation of electromagnetic waves in nonlinear dielectric layered structures is the subject of intensive theoretical and experimental studies since 1970's [for example, see Tables 2, 3 below]. At present dielectric waveguides take a central place in integrated optics, optical communications, photonics, etc.[1] The most applicable types of waveguides are planar waveguides, strips and optical fibers, shown in Figure 1[2].

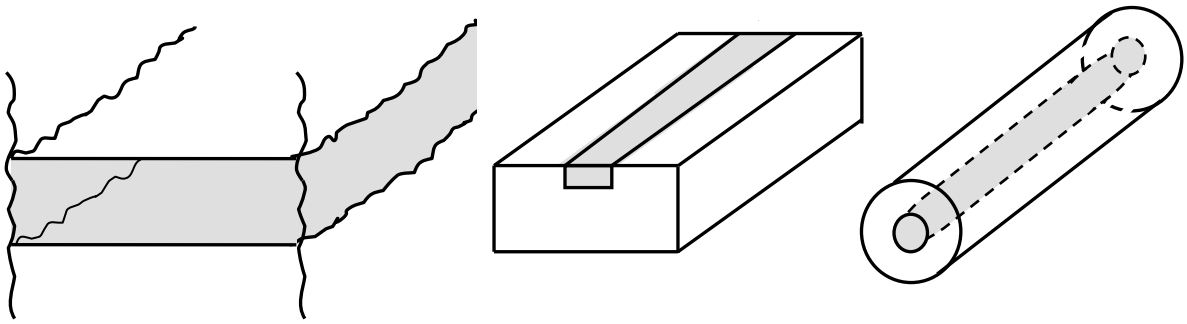

a) Planar (slab) waveguide **b)** Strip **c)** Fiber

Figure 1: Optical waveguides

The present dissertation deals with slab waveguides in a three- medium configuration. The corresponding media exhibit intensity- dependent dielectric properties (the Kerr- type nonlinearity). The optical Kerr- effect belongs to the most important nonlinear effects in optical waveguides leading to such phenomena as, for example, self- phase modulation, cross- phase modulation, four- wave mixing, modulational instability or optical solitons[3].

As well known, the general vector solution of Maxwell's equations for the electromagnetic wave propagating in the layered linear structure can be presented as the superposition of TE- (transverse electric) and TM- (transverse magnetic) solutions, having only one component of the electric and magnetic field, respectively. These components are parallel to the layers and

perpendicular to the propagation direction[1]. This is not valid in the nonlinear case; the separate mathematical treatment of TE- or TM- polarization is ad hoc but simplifies the analysis essentially.

Propagation of nonlinear TE- polarized waves at an interface between a two media as well as in a three- layer structure has been successfully investigated by many researchers. The most interesting and important publications are presented in Table 1 (given below).

The mathematical treatment of TM- polarized guided waves is more complicated than that of the TE- polarized waves. Expressing the dielectric function $\varepsilon(|\mathbf{E}|)$ in terms of the magnetic field **H** leads to a complicated equation containing **H** and the derivative of **H** [6, Table 2]. The problem in this case can be reduced to a one differential equation for **H** that cannot be solved exactly [9, Table 3]. Presenting the nonlinear dielectric function ε in terms of the electric field **E** implies a simple form, but, the occurrence of two electric field components leads in general to a dielectric tensor even for isotropic media [9, Table 3]. This makes the analysis of TM guided waves more difficult.

Propagation of TM- polarized waves has been the object of many researches in the past few decades. Tables 2 and 3 present an overview of the main theoretical results for two- and three layered configurations, respectively.

At the same time as the present dissertation has been prepared the problem of TM- wave propagation in a Kerr nonlinear film surrounded by semi- infinite linear media (special case of the present work, see subsection 4.1) has been solved using an approach similar to the present one by Valovik and Smirnov [21, 25, 27, Table 3]. The exact dispersion relation obtained in [21] has been considered in [25] as the boundary eigenvalue problem, the existence theorem for the solution has been formulated. Numerical results corresponding to the problem have been presented and analyzed in [27]. It should be noted here that there is full agreement between the results presented in subsection 4.1 and those given in [21, 25, 27] (the relation between the film thickness and the

propagation constant, corresponding field patterns)[4]. In [28, Table 3] Valovik generalized the method used in [21, 25, 27] to a case when the tensorial dielectric function in the film is an arbitrary function of the electric field components $\varepsilon_{xx} \sim f(|E_x|^2, |E_z|^2), \varepsilon_{zz} \sim g(|E_x|^2, |E_z|^2)$ by satisfying the integrability condition $\partial f / \partial E_z^2 = \partial g / \partial E_x^2$ (or $\partial f / \partial E_x^2 = \partial g / \partial E_z^2$). The first integral given in [28] has been used in the present dissertation applied to the case of the saturating film with the linear substrate and cladding (subsection 4.3).

The problem of TM- waves propagation in a plasmonic waveguide (metal substrate- Kerr nonlinear film- metal cladding) has been considered by Rukhlenko et. al. [29- 30, Table 3]. It is interesting to note here that the solution method used by the authors is similar to that presented in this dissertation[4].

To the best of my knowledge, the problem of TM- wave propagation in a three-layer structure in which all three media are anisotropic and exhibit a Kerr- like nonlinearity is addressed for the first time in this work.

The statement of the problem is given in Section 2, where Maxwell's equations written for the present case are reduced to a system of two nonlinear differential equations (SDE) containing three unknowns: two electric field components and the propagation constant of TM waves.

A method to obtain a solution of the problem is described in Section 3. It is shown that the first integral for the SDE exists so that one field component can be eliminated. Combining this result with the boundary conditions (tangential components of the electric and magnetic fields are continuous at the interfaces) an exact dispersion relation establishing a link between the parameters of the problem (in particular between the film width, the propagation constant, and the electric field intensity at the substrate – film interface) is derived. An expression for the total power flow carried by TM waves through the structure is given, too.

Numerical results for a wide range of cases to which the presented method is applicable are given in Section 4: linear substrate – nonlinear self (de)- focusing

film – linear cladding, linear substrate – nonlinear metamaterial film – linear cladding, linear substrate – nonlinear uniaxial film – linear cladding etc.

If the dielectric permittivity is a function of the field intensity as well as of the transverse coordinate ($\varepsilon(|\boldsymbol{E}|^2, x)$) the method proposed in Section 3 is not valid because the SDE with the given dielectric permittivity cannot be reduced to an exact differential equation. In such a case the problem can be solved with the help of an integral equations approach outlined in Section 5.

A summary of the results and possible directions for further investigations are discussed in Section 6.

1.1 Table 1

Table 1: Publications to the problem

of TE- wave propagation in a two– and three- layer structure

N°	Author(s)	Publication
1	**Litvak A. G., Mironov V. A.**	„Surface waves on the sepation boundary between nonlinear media“, Izv. Vuz. Radiofiz. (1968), No. 11, pp. 1911- 1912
2	**Miyagi M., Nishida S.**	„Guided waves in bounded nonlinear medium (11)- Dielectric boundaries“, Rep. Res. Inst. Elect. Commun., Tohoku Univ. (1973), Vol. B24, pp. 53- 66
3	**Tomlinson W. J.**	„Surface waves at a nonlinear interface“, Optics Letters (1980), Vol. 5,Issue 7, pp. 323- 325
4	**Maradudin A. A.**	„s- Polarized nonlinear surface polaritons“, Zeitschrif für Physik B, Condensed Matter (1981), Vol. 41, No. 4, pp. 341-344
5	**Agranovich V. M., Mills D. L.**	„Surface polaritons: Electromagnetic waves at surfaces and interfaces“, North- Holland, Amsterdam (1982)
6	**Seaton C., Valera J., Shoemaker R., Stegeman G., Chilwell J., Smith S.**	„Calculations of nonlinear TE waves guided by thin dielectric films bounded by nonlinear media“, IEEE, Journal of Quantum Electronics (1985), Vol. 21, Issue 7, pp. 774- 783
7	**Boardman A. D., Egan P.**	„Optically nonlinear waves in thin films“, IEEE, Journal of Quantum Electronics (1986), Vol. 22, Issue 2, pp. 319- 324
8	**Mihalache D., Mazilu D., Bertolotti M., Sibilia C.**	„Exact solution for nonlinear thin- film guided waves in higher- order nonlinear media“, JOSA B (1988), Vol. 5, Issue 2, pp. 565- 570

9	**Schürmann H. W.**	„On the theory of TE- polarized waves guided by a nonlinear three- layer structure“, Zeitschrift für Physik B 97 (1995), pp. 515- 522
10	**Schürmann H. W., Schmoldt R.**	„Optical response of a nonlinear absorbing dielectric film“, Optics Letters (1996), Vol. 21, Issue 6, pp. 387- 389
11	**Schürmann H. W., Serov V.S., Shestopalov Yu. V.**	„TE- polarized waves guided by a lossless nonlinear three- layer structure“, Physical Review Ea (1998), Vol. 58, No. 1, pp. 1040- 1050
12	**Schürmann H. W., Serov V.S., Shestopalov Yu. V.**	„Reflection and transmission of a plane TE-waveat a lossless nonlinear dielectric film“, Physica D 158 (2001), pp. 197- 215

1.2 Table 2

Table 2: Publications to the problem

of TM- wave propagation in a two- layer structure

N°	Author(s), Publication	Considered problem (ω- the wave frequency, $E_{\parallel}$ and $E_{\perp}$- electric field parallel and perpendicular to the surface, respectively)
1	**Agranovich V. M. et. al.** „Nonlinear surface polaritons“, Pis´ma Zh. Eksp. Teor. Fiz. (1980), Vol. 32, No. 8, pp. 532- 535 (JETP Letters (1981), Vol. 32, No. 8, pp. 512- 515)	*medium I linear, isotropic*: $\varepsilon^{I}(\omega)$ | *medium II nonlinear uniaxial*: $\varepsilon_{11} = \varepsilon_{22} = \varepsilon_0(\omega) + \alpha \left\|E_{\parallel}^{II}\right\|^2$, $\varepsilon_{33} = \varepsilon(\omega)$ | **0** An exact dispersion relation has been derived. Exact solutions for the electric and magnetic field components are obtained.
2	**Lomtev A. I.** „A new class of nonlinear surface waves“, Pis´ma Zh. Eksp. Teor. Fiz. (1981), Vol. 34, No. 2, pp. 64- 67 (JETP Letters (1981), Vol. 34, No. 2, pp. 60- 63)	*medium I (-) nonlinear uniaxial*: $\varepsilon_{11}^{-} = \varepsilon_{22}^{-} = \varepsilon_{-}^{0}(\omega) + \alpha_{-}(\omega)\left\|E_{\parallel}^{-}\right\|^2$, $\varepsilon_{33}^{-} = \varepsilon_{-}(\omega)$ | *medium II (+) nonlinear uniaxial*: $\varepsilon_{11}^{+} = \varepsilon_{22}^{+} = \varepsilon_{+}^{0}(\omega) + \alpha_{+}(\omega)\left\|E_{\parallel}^{+}\right\|^2$, $\varepsilon_{33}^{+} = \varepsilon_{+}(\omega)$ | **0** An exact dispersion relation has been derived. Exact solutions for the electric and magnetic field components are obtained. The limiting case of the boundary between two linear media, and also between linear and nonlinear media (see N° 1) has been considered.

3	**Yu M. Y.** „Surface polaritons in nonlinear media“, Physical Review A (1983), Vol. 28, No. 3, pp. 1855- 1856	***medium I*** ***nonlinear uniaxial*** | ***medium II*** ***nonlinear uniaxial*** $\varepsilon_{xx}^{I} = \varepsilon_{1}^{I}(\omega) + \alpha \left\|E_{\parallel}^{I}\right\|^{2}$ | $\varepsilon_{xx}^{II} = \varepsilon_{1}^{II}(\omega) + \alpha \left\|E_{\parallel}^{II}\right\|^{2}$ $\varepsilon_{yy}^{I} = \varepsilon_{3}^{I}(\omega) + \gamma \left\|E_{\parallel}^{I}\right\|^{2}$ | $\varepsilon_{yy}^{II} = \varepsilon_{3}^{II}(\omega) + \gamma \left\|E_{\parallel}^{II}\right\|^{2}$ $\varepsilon_{zz}^{I} = \varepsilon_{2}^{I}(\omega) + \beta \left\|E_{\parallel}^{I}\right\|^{2}$ | $\varepsilon_{zz}^{II} = \varepsilon_{2}^{II}(\omega) + \beta \left\|E_{\parallel}^{II}\right\|^{2}$ **0** The author has generalized the problem considered in N° 1. Originality of this paper is that an exact dispersion relation has been derived by using the boundary conditions only - without using the solutions in the media.
4	**Leung K. M.** „Propagation of nonlinear surface polaritons“, Physical Review A (1985), Vol. 31, No. 2, pp. 1189- 1192	***medium I*** ***nonlinear uniaxial*** | ***medium II*** ***nonlinear uniaxial*** $\varepsilon_{ij}^{I} = \delta_{ij}\left(\varepsilon_{i}^{(0)I}(\omega) + \varepsilon_{i}^{(0)I}\left(\left\|E_{\parallel}^{I}\right\|^{2}\right)\right)$ ***I,j=x,y,z*** | $\varepsilon_{ij}^{II} = \delta_{ij}\left(\varepsilon_{i}^{(0)II}(\omega) + \varepsilon_{i}^{(0)II}\left(\left\|E_{\parallel}^{II}\right\|^{2}\right)\right)$ ***I,j=x,y,z*** **0** The author has extended the results obtained in N° 3 without restrictions on the field amplitudes. An exact dispersion relation has been derived for TM- as well as for TE- wave propagation.
5	**Akhmediev N. N.** „Nonlinear theory of surface polaritons“, Zh. Eksp. Teor.Fiz. (1982), Vol. 84, pp. 1907-1917 (Sov. Phys. JETP (1983), Vol. 57, No. 5, pp. 1111- 1116)	***medium I*** ***linear, isotropic*** | ***nonlinear Kerr medium II*** ε_{l} | $\varepsilon = \varepsilon_{0} + \alpha\left(\left\|E_{\parallel}^{II}\right\|^{2} + \left\|E_{\perp}^{II}\right\|^{2}\right)$ **0** An exact dispersion relation has been derived. Superposition of the phase portraits of the media as a method to solve the problem has been proposed. Types of surface waves have been analyzed. Existence domain (parameter ranges) of the surface waves has been investigated.

6	**Leung K. M.** „p- polarized nonlinear surface polaritons in materials with intensity- dependent dielectric functions“, Physical Review B (1985), Vol. 32, No. 8, pp. 5093- 5101	***nonlinear medium I*** | ***nonlinear medium II*** $\varepsilon^{I} = \varepsilon_0^{I} + \varepsilon_2^{I}\left(\left\|\vec{E}^{I}\right\|^2\right)$ | $\varepsilon^{II} = \varepsilon_0^{II} + \varepsilon_2^{II}\left(\left\|\vec{E}^{II}\right\|^2\right)$ **0** $\varepsilon_2^{i}\left(\left\|\vec{E}^{i}\right\|^2\right)$ $(i = I, II)$ is an arbitrary function of the electric field intensity. Solution for the magnetic field component has been obtained in quadratures. An exact dispersion relation has been obtained without using solutions for the fields. Various types of the function $\varepsilon_2^{i}\left(\left\|\vec{E}^{i}\right\|^2\right)$ $(i = I, II)$ are investigated. Self- focusing and self- defocusing cases are considered. Parameter space for the physically allowed regions and wave existence are analyzed.
7	**Boardman A. D. et. al.** “Exact theory of nonlinear p- polarized optical waves”, Physical Review A (1987), Vol. 35, No. 3, pp. 1159- 1164	***linear dielectric medium I*** ε_s | ***Kerr- like nonlinear medium II*** $\varepsilon_{xx} = \varepsilon_c + \alpha_{xx}\left\|E_{\parallel}^{II}\right\|^2 + \alpha_{xz}\left\|E_{\perp}^{II}\right\|^2$ $\varepsilon_{zz} = \varepsilon_c + \alpha_{zz}\left\|E_{\perp}^{II}\right\|^2 + \alpha_{zx}\left\|E_{\parallel}^{II}\right\|^2$ ***or*** ***Non- Kerr saturating medium II*** $\varepsilon_{xx} = \varepsilon_c + \alpha_{xx} A_{xx}^2\left(1 - e^{-(A_x^2/A_{xx}^2)}\right) + \alpha_{xz} A_{xz}^2\left(1 - e^{-(A_z^2/A_{xz}^2)}\right)$ $\varepsilon_{zz} = \varepsilon_c + \alpha_{zz} A_{zz}^2\left(1 - e^{-(A_z^2/A_{zz}^2)}\right) + \alpha_{zx} A_{zx}^2\left(1 - e^{-(A_x^2/A_{zx}^2)}\right)$ (here A_{ij} $(i, j = x, z)$ are constant **0** Exact calculations have been presented. A detailed comparison with the nonlinearity approximations has been provided. Numerical results for the power flow and the field profiles, as well for the magnitude and the effect of the nonlinearity, and the behaviour of the first integral are presented.

8	**Mihalache D. et. al.** "Exact dispersion relations for transverse magnetic polarized guided waves at a nonlinear interface", Optics Letters (1987) Vol.12, No. 3, pp. 187 - 3	***medium I*** ***linear dielectric or metal*** ε_s **0** ***Kerr- like nonlinear medium II*** $\varepsilon_{xx} = \varepsilon_x + \alpha_1 \lvert E_{\parallel}^{II} \rvert^2 + \alpha_2 \lvert E_{\perp}^{II} \rvert^2$ $\varepsilon_{zz} = \varepsilon_z + \alpha_1 \lvert E_{\perp}^{II} \rvert^2 + \alpha_2 \lvert E_{\parallel}^{II} \rvert^2$ An exact dispersion relation in form of polynomial equations involving the boundary values of the electric field components, the medium parameters, and the propagation constant has been obtained. Numerical results for the dispersion curves are presented.
9	**Kushwaha Manvir S.** "Exact theory of nonlinear surface polaritons: TM case", Japanese Journal of Applied Physics (1990) Vol.29, No. 10, pp. L 1826 – L 1828	***linear medium I*** ε_l **0** ***Kerr- like nonlinear isotropic medium II*** $\varepsilon = \varepsilon_2 + \alpha \left(\lvert E_x \rvert^2 + \lvert E_z \rvert^2 \right)$ (here $E_{\parallel}^{II} = E_x, E_{\perp}^{II} = E_z$) An exact dispersion relation as well an expression for the total power flow has been obtained.

1.3 Table 3

Table 3: Publications to the problem

of TM- wave propagation in a three- layer structure

N°	Author(s), Publication	Considered problem (ω - the wave frequency, $E_{\parallel}$ and $E_{\perp}$ - the wave electric field parallel and perpendicular to the surface, respectively; d or h denotes the thickness of the film)
1	**Akhmediev N. N.** *"Novel class of* nonlinear surface waves: asymmetric modes in asymmetric *layered structure"*, Sov. Phys. JETP 56 (2), August 1982, pp. 299- 303	***nonlinear uniaxial substrate*** $\varepsilon_0 + \alpha \lvert E_{\parallel} \rvert^2$ | ***linear dielectric film*** ε_1 | ***nolinear uniaxial cladding*** $\varepsilon_0 + \alpha \lvert E_{\parallel} \rvert^2$ $-d$ $\quad$ d An exact dispersion relation has been derived. Expression for the total power flow has been given. Some interesting properties has been shown: the symmetric, and antisymmetric as well asymmetric mode can propagate in the structure; a condition for the existence of this mode is a certain minimum energy flux; in a certain range of values of the film thickness or of the wavelength, the nonlinear waves are bistable etc.
2	**Fedyanin V. K., Mihalache D.** "p- polarized nonlinear surface polaritons in layered structures", Zeitschrift für Physik B – Condensed Matter 47, (1982), pp. 167-173	***Case I:*** ***substrate (linear dielectric medium)*** $\varepsilon_1(\omega)$ | ***film (linear dielectric medium)*** $\varepsilon_2(\omega)$ | ***nolinear uniaxial anisotropic cladding*** $\varepsilon_{11} = \varepsilon_{22} = \varepsilon_{\perp}(\omega) + \alpha(\omega) \lvert E_{\parallel} \rvert^2$, $\varepsilon_{33} = \varepsilon_{\parallel}(\omega)$ 0 $\quad$ d
3	**Mikhalake D. and Fedyanin V. K.** "p- polarized nonlinear surface and bounded (guided) waves in layered structures",	***Case II:*** ***substrate (linear dielectric medium)*** $\varepsilon_1(\omega)$ | ***nolinear uniaxial anisotropic film*** $\varepsilon_{11} = \varepsilon_{22} = \varepsilon_{\perp}(\omega) + \alpha(\omega) \lvert E_{\parallel} \rvert^2$, $\varepsilon_{33} = \varepsilon_{\parallel}(\omega)$ | ***cladding (linear isotropic crystal)*** $\varepsilon_3(\omega) = \varepsilon_1(\omega)$ 0 $\quad$ d

	Teoret. Mat. Fiz. (March 1983), Vol. 54, No. 3, pp. 443- 455	An exact dispersion relation has been derived. Wave solutions in terms of Jacobi elliptic functions have been obtained. Conditions for the modes existence have been analyzed. The behaviour of nonlinear modes has been investigated. The energy flux has been evaluated.
4	**Lederer F., Langbein U. and Ponath H.- E.** "Nonlinear waves guided by a dielectric slab. II. TM-polarization", Applied Physics B (1983), Vol. 46, No. 3- 4, pp. 187- 190	*nonlinear uniaxial anisotropic substrate* / *linear dielectric film* / *nonlinear uniaxial anisotropic cladding* $\varepsilon_{xx,1} = \varepsilon$ $\varepsilon_{yy,1} = \varepsilon_{zz,1} = \bar{\varepsilon} + a\left\|E_{\parallel}\right\|^2$ $a \lessgtr 0$ ε_2 $\varepsilon_{xx,3} = \varepsilon$ $\varepsilon_{yy,3} = \varepsilon_{zz,3} = \bar{\varepsilon} + a\left\|E_{\parallel}\right\|^2$ $a \lessgtr 0$ 0 d It has been shown that such structure can be described by four nonlinear dispersion relations. Analytical expressions for the fields have been obtained. Various wave types have been classified.
5	**Langbein U., Lederer F. and Ponath H.- E.,** "A new type of nonlinear slab-guided waves", Optics Communications (July 1983), Vol. 46, No. 3-4, pp. 167- 169	*linear dielectric substrate* / *nonlinear uniaxial anisotropic film* / *linear dielectric cladding* ε_1 $\varepsilon_{xx,2} = \varepsilon$ $\varepsilon_{ij,2} = \left(\varepsilon_2 + a\left\|E_{\parallel}\right\|^2\right)\delta_{ij}$ $i,j = y,z$ $a \lessgtr 0$ ε_3 0 d Expressions for an exact dispersion relation and the field patterns have been obtained. Both cases (TE and TM) have been investigated.
6	**Mihalache D., Nazmitdinov R. G.** "p-polarized nonlinear surface waves in symmetric layered structures", Physica Scripta (1984), Vol. 29, pp. 269- 275	*nonlinear uniaxial anisotropic substrate* / *linear dielectric film* / *nonlinear uniaxial anisotropic cladding* $\varepsilon_{11} = \varepsilon_{22} = \left(\varepsilon_{\perp} + a\left\|E_{\parallel}\right\|^2\right)$ $\varepsilon_{33} = \varepsilon_{\parallel}$ ε_1 $\varepsilon_{11} = \varepsilon_{22} = \left(\varepsilon_{\perp} + a\left\|E_{\parallel}\right\|^2\right)$ $\varepsilon_{33} = \varepsilon_{\parallel}$ $-d/2$ $d/2$ An exact dispersion relation and the solutions for the field components have been obtained. The total power flow has been derived. It has been shown that the structure is optical bistable. Existence of asymmetric modes in the considered symmetric layered waveguide has been shown.

7	**Boardman A. D., Egan P.** "Nonlinear surface and guided polaritons of a general layered dielectric structure", Journal de Physique (1984), Colloque C5, supplement au n°4, Tom 46, C5- 291 – C5- 303	***nonlinear uniaxial anisotropic substrate*** | ***nonlinear uniaxial anisotropic film*** | ***nonlinear uniaxial anisotropic cladding*** $\varepsilon_{11} = \varepsilon_{22} = \tilde{\varepsilon}$ | $\varepsilon_{11} = \varepsilon_{22} = \tilde{\varepsilon}$ | $\varepsilon_{11} = \varepsilon_{22} = \tilde{\varepsilon}$ $\varepsilon_{33} = \varepsilon_{\parallel}(\omega)$ | $\varepsilon_{33} = \varepsilon_{\parallel}(\omega)$ | $\varepsilon_{33} = \varepsilon_{\parallel}(\omega)$ **0** **d** where $\tilde{\varepsilon} = \left(\varepsilon_{\perp}(\omega) + a\left\|E_{\parallel}\right\|^2\right)$ Both TE- and TM- modes have been investigated. A general exact dispersion relation has been derived. Alternative form of the dispersion relation has been given (for TE- and TM- modes, separately). The power flow of TE- waves has been evaluated for a particular case (linear layer bounded by nonlinear and uniaxial substrate and cladding).
8	**Stegeman G. I., Seaton C. T.** "Nonlinear surface plasmons guided by thin metal films", Optics Letters (1984), Vol. 9, No. 6, pp. 235- 237	***nonlinear substrate*** | ***thin metal film*** | ***nonlinear cladding*** $n = n_0 + \alpha\left\|\vec{E}\right\|^2$ | ε_m | $n = n_0 + \alpha\left\|\vec{E}\right\|^2$ **0** **h** The problem has been reduced to a nonlinear wave equation for the magnetic field **H** instead of the electric fields. Presenting the function n in terms of the magnetic field component the wave solutions inside and outside the film have been written directly. Coupled with the boundary conditions at the film interfaces these solutions lead to a dispersion relation. Some numerical results have been given.
9	**Seaton C. T., Valera J. D., Svenson B., Stegeman G. I.** "Comparison of solutions for TM-polarized nonlinear guided waves", Optics Letters (1985), Vol. 10, No. 3, pp. 149- 150	The authors have shown that the previous assumptions about the form of the uniaxial approximation ($\varepsilon \sim \left\|E_{\parallel}\right\|^2$, for example, see N° 1- 7 of the present table) lead to exact analytical solutions for the nonlinear waves that are not applicable physically. It has been argued, that the TM-wave problem should be formulated for the case of a dielectric tensor proportional to the square of the normal electric field component ($\varepsilon \sim \left|E_{\perp}\right|^2$). A suitable approximation in terms of the magnetic- field component is possible in this case with a solution similar to that derived for the exact solvable TE- case.

10	**Mihalache D. and Mazilu D.** "TM- polarized nonlinear slab-guided waves in saturable media", Solid State Communications (1986), Vol. 60, No. 4, pp. 397- 399	***nonlinear saturable cladding*** | ***linear dielectric film*** | ***linear dielectric substrate*** $\boldsymbol{\varepsilon_{xx} = \varepsilon_{yy} = \varepsilon_c}$ $\boldsymbol{\varepsilon_{zz} = \varepsilon_c \pm \varepsilon_{sat}\left(1 - e^{-\frac{\lvert\tilde{\alpha}_c\rvert H_y^2}{\varepsilon_{sat}}}\right)}$ | $\boldsymbol{\varepsilon_f}$ | $\boldsymbol{\varepsilon_s}$ $\boldsymbol{or\ \varepsilon_{zz} = \varepsilon_c \pm \frac{\lvert\tilde{\alpha}_c\rvert H_y^2}{1 + \frac{\lvert\tilde{\alpha}_c\rvert}{\varepsilon_{sat}} H_y^2}}$ **0** **d** The authors have used results obtained in N° 9. A dispersion relation and the total power flow have been derived approximately. The propagation constant has been determined as a function of the total power flow. Some numerical results have been given.
11	"Calculation of TM-polarized nonlinear waves guided- by thin dielectric films", Applied Physics B 41(1986), pp. 119- 123	***linear dielectric substrate*** | ***linear dielectric film*** | ***nonlinear uniaxial cladding*** $\boldsymbol{\varepsilon_s}$ | $\boldsymbol{\varepsilon_f}$ | $\boldsymbol{\varepsilon_{xx} = \varepsilon_{yy} = \varepsilon_c}$ $\boldsymbol{\varepsilon_{zz} = \varepsilon_c + \alpha \lvert E_\perp\rvert^2}$ **0** **d** Using results of N° 9 a dispersion relation and the wave solutions in the nonlinear cladding have been obtained approximately. As in N° 10 it has been shown that the propagation index is power dependent.
12	**Josef R. I., Christodoulides D. N.** "Exact field decomposition for TM waves in nonlinear media", Optics Letters (1987), Vol. 12, No. 10, pp. 826- 828	A nonlinear medium characterized by a dielectric subtensor $\overleftrightarrow{\varepsilon} = \varepsilon_0 \begin{bmatrix} \varepsilon_\parallel\left(\lvert E_\parallel\rvert^2, \lvert E_\perp\rvert^2\right) & 0 \\ 0 & \varepsilon_\perp\left(\lvert E_\parallel\rvert^2, \lvert E_\perp\rvert^2\right) \end{bmatrix}$ has been considered. The authors have proposed a method to analyze the propagation of the TM- waves in a two- as well as three-layer structures with the dielectric function $\overleftrightarrow{\varepsilon}$. It has been shown that the two electric field components ($\boldsymbol{E_\perp}, \boldsymbol{E_\parallel}$) are related by a conservation law if the condition $\frac{\partial \varepsilon_\parallel}{\partial E_\perp^2} = \frac{\partial \varepsilon_\perp}{\partial E_\parallel^2}$ is satisfied, so that the electric field solutions can be obtained exactly in quadratures. The method is applicable to a variety of mechanisms of Kerr- nonlinearity and has been used in the present dissertation.

13	**Kushwaha Manvir S.** "Nonlinear surface polaritons in thin films: TM case", Japanese Journal of Apllied Physics (1987) Vol. 26, No. 6, pp. L1035- L1037	***nonlinear uniaxial anisotropic substrate*** | ***linear dielectric film*** | ***nonlinear uniaxial anisotropic cladding*** $\varepsilon_{xx} = \varepsilon_s$ $\varepsilon_{zz} = \varepsilon_s + \alpha \lvert E_\perp \rvert^2$ ε_m $\varepsilon_{xx} = \varepsilon_c$ $\varepsilon_{zz} = \varepsilon_c + \alpha \lvert E_\perp \rvert^2$ 0 d The author has shown that the problem of TM- waves in the structure considered in N° 9 has an analytically and physically realizable solution without reducing the problem to the differential equation in terms of the magnetic field (as given in N° 9).
14	**Al- Bader S. J.** "TM waves in nonlinear saturable thin films: a multilayered *approach"*, Journal of Lightwave Technology (1989), Vol. 7, No. 4, pp. 717- 725	***linear dielectric substrate*** | ***Kerr nonlinear film*** | ***linear dielectric cladding*** ε_1 Subtensor $\boldsymbol{\varepsilon} = \begin{pmatrix} \varepsilon_{xx} & 0 \\ 0 & \varepsilon_{zz} \end{pmatrix}$ $\varepsilon_{xx} = \varepsilon_{20} + \frac{\alpha \lvert E_{x2} \rvert^2 + \Gamma\alpha \lvert E_{z2} \rvert^2}{1 + G(\alpha \lvert E_{x2} \rvert^2 + \Gamma\alpha \lvert E_{z2} \rvert^2)}$ $\varepsilon_{zz} = \varepsilon_{20} + \frac{\Gamma\alpha \lvert E_{x2} \rvert^2 + \alpha \lvert E_{z2} \rvert^2}{1 + G(\Gamma\alpha \lvert E_{x2} \rvert^2 + \alpha \lvert E_{z2} \rvert^2)}$ ε_3 0 a (here $E_x = E_\perp$, $E_z = E_\parallel$, a- the film width) A recursive scheme based on the stratification of the film into a large number of linear sub- layers has been proposed to solve the nonlinear wave equation within the film. The magnetic field profile, the power flow and the variation of the dielectric tensor components have been obtained. Though, a) the permittivities are (rather) different, b) the structure of results are similar (see Figure 59, p. 98).
15	**Hayata K., Misawa A., Koshiba M.** "Split- step finite- element method applied to nonlinear integrated optics*"*, Journal of the Optical Society of America B (1990), Vol. 7, No. 9, pp. 1772- 1784	***Kerr- type nonlinear substrate*** | ***linear dielectric film*** | ***linear dielectric substrate*** $\varepsilon_{yy} = n_s + \alpha\left(\lvert E_\perp \rvert^2 + \eta \lvert E_\parallel \rvert^2\right)$, $\varepsilon_{zz} = n_s + \alpha\left(\eta \lvert E_\perp \rvert^2 + \lvert E_\parallel \rvert^2\right)$ $\varepsilon_f = n_f$ $\varepsilon_s = n_c$ $-d/2$ $d/2$ (here y and z are transverse and propagation directions, respectively) A numerical method based on the finite- element and- the finite- difference methods has been proposed to solve a nonlinear guided- wave problem. Numerical results are presented.

16	**Gong Y.- J., Klemm A. D.** "Calculations on nonlinear dielectric slab waveguides by the iterative eigenfunction expansion method", Applied Mathematical Modelling (1992), Vol. 16, November, pp. 605- 609	***Kerr- nonlinear substrate*** | ***linear dielectric film*** | ***Kerr- nonlinear cladding*** $n_3, \bar{n}_3$ | n_1 | $n_2, \bar{n}_2$ $-d$ d n_i $(i = 1, 2, 3)$- the linear index of refraction $\bar{n}_i$ $(i = 1, 3)$- the nonlinear optical coefficient Considered nonlinear permittivities: $\varepsilon'_\perp = \varepsilon_0 + a\, f(E_\perp) + b\,(E_\parallel)$, $\varepsilon'_\parallel = \varepsilon_0 + b\, f(E_\perp) + a\,(E_\parallel)$, where $a \sim n, \bar{n}$; $b \sim a$ Using the iterative eigenfunction expansion method behaviour of TM nonlinear waves guided by a linear film surrounded by an arbitrary nonlinear media has been investigated. The proposed algorithm has been applied to the case of the Kerr – like nonlinearity.
17	**Misuhiro Yokota** "Guided transverse-magnetic waves supported by a weakly nonlinear slab waveguide", Journal of the Optical Society of America B (1993), Vol. 10, No. 6, pp. 1096- 1101	***linear dielectric substrate*** | ***Kerr nonlinear film*** | ***linear dielectric cladding*** ε_2 | $\varepsilon_1 + \alpha \left\vert \vec{E} \right\vert^2$ | ε_2 $-d$ d For a weak nonlinearity (the nonlinear part of the dielectric function is small compares with the linear one) in the film a singular perturbation technique with multiple space scales has been proposed. Numerical results have been presented.
18	**Qin Chen and Zi Hua Wang** "Exact dispersion relations for TM waves guided by thin dielectric films bounded by nonlinear media", Optics Letters (1993), Vol. 18, No. 4, pp. 260- 262	***Kerr nonlinear substrate*** | ***linear dielectric film*** | ***Kerr nonlinear cladding*** $\varepsilon_{3xx} = \varepsilon_{3x} + a_{31}\vert E_x\vert^2 + a_{32}\vert E_z\vert^2$ | ε_2 | $\varepsilon_{1xx} = \varepsilon_{1x} + a_{11}\vert E_x\vert^2 + a_{12}\vert E_z\vert^2$ $\varepsilon_{3zz} = \varepsilon_{3z} + a_{31}\vert E_z\vert^2 + a_{32}\vert E_x\vert^2$ | | $\varepsilon_{1zz} = \varepsilon_{1z} + a_{11}\vert E_z\vert^2 + a_{12}\vert E_x\vert^2$ 0 d (here $E_z = E_\perp$, $E_x = E_\parallel$) The method of Mihalche et.al. (see N° 8 of Table 2) has been extended for the problem of the TM- wave propagation in a three- layer structure. With the solution in the linear film and the boundary conditions an exact dispersion relation has been obtained.

19	**Stuart C. A.** "Guided TM- modes in a self- focusing anisotropic dielectric", Nonlinear problems in applied mathematics. SIAM Proceedings Series, Philadelphia (1996), pp. 225-234	TM- modes propagated in planar and cylindrical structures with a uniaxial self- focusing medium are considered. Using the amplitude of the magnetic field the problem has been reduced to a second order differential equation that has been studied purely mathematical. Only the existence problem of solutions has been discussed.
20	"Magnetic field wave equations for TM- modes in nonlinear optical waveguides", Reaction diffusion systems, Trieste (1995), Vol. 194, pp. 377-400, Lecture Notes in Pure and Applied Mathematics (1998)	As in N° 19
21	**Valovik D. V., Smirnov Yu. G.** "Propagation of TM waves in a Kerr nonlinear layer", Computational Mathematics and Mathematical Physics (2008), Vol. 48, No. 12, pp. 2217- 2225	***linear dielectric substrate*** | ***Kerr nonlinear film*** | ***linear dielectric cladding*** ε_1 | $\varepsilon_2 + a\,(\lvert E_x\rvert^2 + \lvert E_z\rvert^2)$ | ε_3 **0** **h** (here $E_x = E_\perp$, $E_z = E_\parallel$) The problem has been reduced to a system of nonlinear ordinary differential equations for the electric field components. A dispersion relation has been obtained. The limit to the linear case has been considered.

22	**Taya S. A., Shabat M. M., Khalil H. M., Jäger D. S.** "Theoretical analysis of TM nonlinear asymmetrical waveguide optical sensors", Sensors and Actuators A 147: Physical (2008), pp. 137- 141	***Kerr- nonlinear substrate*** $\varepsilon_s = \varepsilon_s + \alpha_s \left\|\vec{E}\right\|^2$ | ***linear dielectric film*** ε_f | ***Kerr- nonlinear cladding*** $\varepsilon_c = \varepsilon_c + \alpha_c \left\|\vec{E}\right\|^2$ 0 h Using results obtained in N° 8 the authors have expressed the dielectric functions in terms of the magnetic field component. A dispersion relation and the total power flow have been derived. Results of a numerical evaluation have been presented. **Note:** According to N° 9 a differential equation for the magnetic field written for a nonlinear medium can be solved approximately only. Thus, the results are presented approximately.
23	**Yuskaeva K. A., Serov V. S., Schürmann H. W.** "TM-electromagnetic guided waves in a (Kerr-) nonlinear three- layer structure", PIERS Online (2009), Vol. 5, No. 8, pp. 797- 802	***linear dielectric substrate*** ε_1 | ***Kerr nonlinear film*** $\varepsilon_2 = \begin{pmatrix} \varepsilon_x & 0 & 0 \\ 0 & \varepsilon_y & 0 \\ 0 & 0 & \varepsilon_z \end{pmatrix}$ $\varepsilon_x = \varepsilon_{21} + a\,\lvert E_x\rvert^2 + b\lvert E_z\rvert^2$ $\varepsilon_z = \varepsilon_{22} + b\,\lvert E_x\rvert^2 + a\lvert E_z\rvert^2$ | ***linear dielectric cladding*** ε_3 0 h (here $E_x = E_\perp$, $E_z = E_\parallel$) The problem has been reduced to an exact differential equation leading to a first integral relating the electric field components. Eliminating one component the other one can be found by integration. The resulting integral combined with the boundary conditions gives rise to an exact dispersion relation. Numerical results for focusing $(a > 0, b > 0)$ and defocusing $(a < 0, b < 0)$ cases have been presented.

24	**Serov V. S., Yuskaeva K. A., Schürmann H. W.** "Integral equations approach to TM-electromagnetic waves guided by a (linear/nonlinear) dielectric film with a spatially varying permittivity", PIERS Online (2009), Vol. 5, No. 8, pp. 786- 790	***linear dielectric substrate*** ε_1 | ***Kerr nonlinear film*** $\varepsilon_2 = \begin{pmatrix} \varepsilon_x & 0 & 0 \\ 0 & \varepsilon_y & 0 \\ 0 & 0 & \varepsilon_z \end{pmatrix}$ $\varepsilon_x = \varepsilon_{21} + f(x) + a\,\lvert E_x\rvert^2 + b\,\lvert E_z\rvert^2$ $\varepsilon_z = \varepsilon_{22} + f(x) + b\,\lvert E_x\rvert^2 + a\,\lvert E_z\rvert^2$ | ***linear dielectric cladding*** ε_3 **0** **h** (here $E_x = E_\perp$, $E_z = E_\parallel$) The problem has been reduced to a system of two integral equations. Applying the Banach fixed- point theorem has been shown that the solution exists in form of a uniformly convergent sequence of iterations. The exact dispersion relation has been presented and evaluated numerically in first approximation.
25	**Smirnov Yu. G., Valovik D. V.** "Boundary eigenvalue problem for Maxwell equations in a nonlinear dielectric layer", Applied Mathematics (2010), Vol. 1, No. 1, pp. 29- 36	***linear dielectric substrate*** ε_1 | ***Kerr nonlinear film*** $\varepsilon_2 + a\,(\lvert E_x\rvert^2 + \lvert E_z\rvert^2)$ | ***linear dielectric cladding*** ε_3 **0** **h** (here $E_x = E_\perp$, $E_z = E_\parallel$) This is a follow- up of N° 21 of the present table. The problem has been formulated as a boundary eigenvalue one. A theorem for the solution existence has been given. Numerical results for the dispersion relation and the electric field component have been presented.
26	**Yuskaeva K. A., Serov V. S., Schürmann H. W.** "On the theory of TM-electromagnetic guided waves in a film with nonlinear permittivity", EMTS Berlin (2010), doi: 10.1109/URSI-EMTS.2010.5637057 pp. 439- 441	***linear dielectric substrate*** ε_1 | ***Kerr nonlinear film*** $\varepsilon_2 = \begin{pmatrix} \varepsilon_x & 0 & 0 \\ 0 & \varepsilon_y & 0 \\ 0 & 0 & \varepsilon_z \end{pmatrix}$ $\varepsilon_x = \varepsilon_{21} + b\,\lvert E_z\rvert^2$ $\varepsilon_z = \varepsilon_{22} + b\,\lvert E_x\rvert^2$ | ***linear dielectric cladding*** ε_3 **0** **h** (here $E_x = E_\perp$, $E_z = E_\parallel$) Applying the method outlined in N° 23 the exact analytical dispersion relation expressed in terms of elliptic integrals has been obtained. Numerical calculations for the propagation constant have been presented.

27	**Valovik D. V., Smirnov Yu. G.** "Nonlinear effects in the problem of propagation of TM electromagnetic waves in a Kerr nonlinear layer", Journal of Communications Technology and Electronics (2011), Vol. 56, No. 3, pp. 309- 314	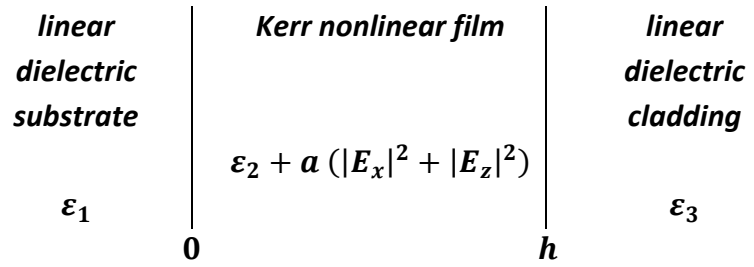 (here $\boldsymbol{E_x = E_\perp}$, $\boldsymbol{E_z = E_\parallel}$) Follow- up of N° 25. Further numerical solutions of the dispersion relation are presented.
28	**Valovik D. V.** "Propagation of TM waves in a layer with arbitrary nonlinearity", Computational Mathematics and Mathematical Physics (2011), Vol. 51, No. 9, pp. 1622- 1632	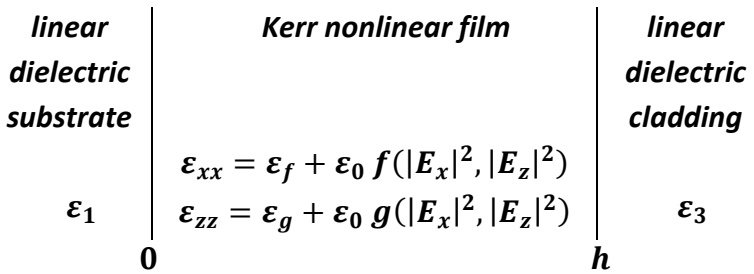 (here $\boldsymbol{E_x = E_\perp}$, $\boldsymbol{E_z = E_\parallel}$) The author has generalized the method used in his previous papers (NN° 21, 25, 27) to the case if the dielectric permittivity in the film is characterized by a tensor and depends on the electric field in an arbitrary form.

29	**Rukhlenko Ivan D. et. al.** "Dispersion relation for surface plasmon polaritons in metal/nonlinear-dielectric/metal slot waveguides", Optics Letters (2011), Vol. 36, No. 17, pp. 3374 – 3376	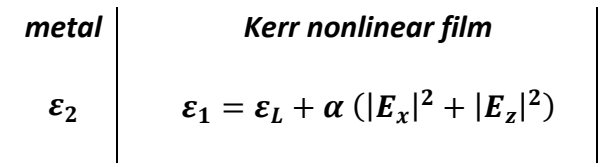 (here $E_x = E_\perp$, $E_z = E_\parallel$) The problem has been reduced to a differential equation relating both electric field components by a first integral. Using the first integral and the boundary conditions at interfaces an exact dispersion relation has been derived. Numerical results of the dispersion relation and for the profiles of the electric field components have been presented.
30	"Exact dispersion relation for nonlinear plasmonic waveguides", Physical Review B (2011), Vol. 84, No. 9, pp. 113409- 1 – 113409- 4	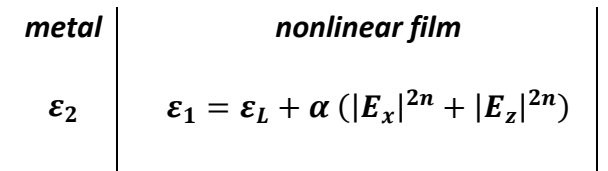 $E_x = E_\perp$, $E_z = E_\parallel$ ε_L is the linear part, α is a constant parameter $n = 1$ (corresponds to the Kerr nonlinearity)**, 2, 3…** The method presented by authors in N° 29 of the present table has been generalized for the case of more general form of the dielectric permittivity in the film.

2 Statement of the problem

The propagation of TM (transverse-magnetic) - electromagnetic waves guided by a nonlinear three-layer structure is investigated. The structure consists of a film with thickness h located between two semi-infinite half-spaces $x < 0$ (substrate) and $x > h$ (cladding). All three media are assumed to be homogeneous, lossless and nonmagnetic ($\mu = \mu_0$), characterized by a Kerr-like nonlinear tensorial dielectric function ε_ν ($\nu = s, f, c$). The geometry of the problem is shown in Figure 2. The objective is to find solutions of Maxwell's equations for various permittivity functions ε_ν (nonlinear, linear) subject to the boundary conditions.

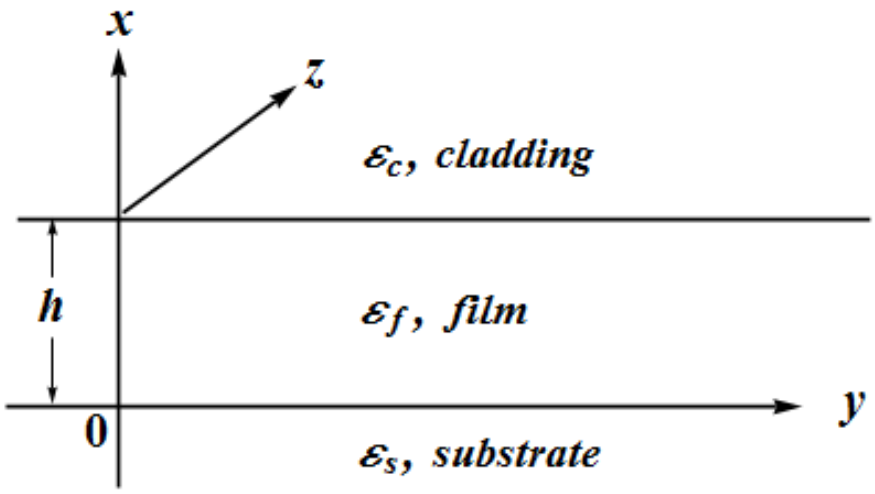

Figure 2: Geometry of the nonlinear waveguide

Specification of the problem is as follows:

An ansatz[5, 6]

$$\begin{aligned}\vec{\mathcal{E}}(x,y,z,t) &= \boldsymbol{E}(x,y,z)\, e^{-i\omega t},\\ \vec{\mathcal{H}}(x,y,z,t) &= \boldsymbol{H}(x,y,z)\, e^{-i\omega t}\end{aligned} \tag{2.1}$$

satisfies the time-dependent Maxwell's equations

$$\begin{aligned} curl\, \vec{\mathcal{H}} &= \frac{\partial \boldsymbol{D}}{\partial t},\\ curl\, \vec{\mathcal{E}} &= -\frac{\partial \boldsymbol{B}}{\partial t},\end{aligned} \tag{2.2}$$

if the complex amplitudes $\boldsymbol{E}$, $\boldsymbol{H}$ satisfy

$$\begin{aligned} curl\, \boldsymbol{H} &= -i\omega\varepsilon \boldsymbol{E},\\ curl\, \boldsymbol{E} &= i\omega\mu \boldsymbol{H}.\end{aligned} \tag{2.3}$$

For the supposed TM-polarization $\boldsymbol{E} = \{E_x, 0, E_z\}$, $\boldsymbol{H} = \{0, H_y, 0\}$ system (2.3) reads

$$\begin{cases} \dfrac{\partial H_y}{\partial z} = i\omega\varepsilon E_x,\\ \dfrac{\partial H_y}{\partial x} = -i\omega\varepsilon E_z,\\ \dfrac{\partial E_z}{\partial y} = 0,\\ \dfrac{\partial E_x}{\partial z} - \dfrac{\partial E_z}{\partial x} = i\omega\mu H_y,\\ \dfrac{\partial E_x}{\partial y} = 0,\end{cases} \tag{2.4}$$

where the dielectric permittivity ε is characterized by

I. a tensor with the Kerr- type nonlinearity[6, 7, 8]

$$\varepsilon_\nu = \begin{pmatrix} \varepsilon_{x\nu} & 0 & 0\\ 0 & \varepsilon_{y\nu} & 0\\ 0 & 0 & \varepsilon_{z\nu}\end{pmatrix}, \tag{2.5}$$

where

$$\begin{aligned}\varepsilon_{x\nu} &= \varepsilon_{1\nu} + a_\nu |E_x|^2 + b_\nu |E_z|^2,\\ \varepsilon_{z\nu} &= \varepsilon_{2\nu} + b_\nu |E_x|^2 + a_\nu |E_z|^2,\end{aligned} \tag{2.6}$$

$\varepsilon_{1\nu}$, $\varepsilon_{2\nu}$, a_ν, b_ν real constants and $\nu = s, f, c$ for the substrate, film, and cladding, respectively[9];

II. constants in the substrate and cladding , and a tensor according to[9]

$$\varepsilon_\nu = \begin{cases} \varepsilon_s = const, & \nu = s, \\ \begin{pmatrix} \varepsilon_{xf} & 0 & 0 \\ 0 & \varepsilon_{yf} & 0 \\ 0 & 0 & \varepsilon_{zf} \end{pmatrix}, & \nu = f, \\ \varepsilon_c = const, & \nu = c, \end{cases} \tag{2.7}$$

where

$$\begin{aligned} \varepsilon_{xf} &= \varepsilon_{1f} + \tilde{\varepsilon}_x, \\ \varepsilon_{zf} &= \varepsilon_{2f} + \tilde{\varepsilon}_z, \end{aligned} \tag{2.8}$$

$$\begin{aligned} \tilde{\varepsilon}_x &= f(x) + a_f|E_x|^2 + b_f|E_z|^2, \\ \tilde{\varepsilon}_z &= f(x) + b_f|E_x|^2 + a_f|E_z|^2, \end{aligned} \tag{2.9}$$

ε_{1f}, ε_{2f}, a_f, b_f are real constants and $f(x)$ is a continuously differentiable real- valued function of the transverse coordinate x.

One can see from the equations (2.4) that the components of the electric and magnetic fields $E_x = E_x(x,z)$, $E_z = E_z(x,z)$, $H_y = H_y(x,z)$ are functions independent on y.

By assuming propagation of TM- waves along z- direction, the ansatz

$$\begin{cases} E_x(x,z) = \hat{E}_x(x)e^{i\gamma z}, \\ E_z(x,z) = \hat{E}_z(x)e^{i\gamma z}, \\ H_y(x,z) = \hat{H}_y(x)e^{i\gamma z} \end{cases} \tag{2.10}$$

with γ, a real constant, transforms system (2.4) to (cf. Appendix A)

$$\begin{cases} -\dfrac{d^2Z_\nu(x)}{dx^2} + \gamma\dfrac{dX_\nu(x)}{dx} = \varepsilon_{z\nu}\,Z_\nu(x), \\ -\gamma\dfrac{dZ_\nu(x)}{dx} + \gamma^2 X_\nu(x) = \varepsilon_{x\nu}\,X_\nu(x). \end{cases} \tag{2.11}$$

Here with $k^2 = \omega^2\mu\varepsilon_0$, and normalization according to

$$\tilde{x} = kx, \tilde{z} = kz, \tilde{\gamma} = \frac{\gamma}{k}, \tilde{\varepsilon}_{j\nu} = \frac{\varepsilon_{j\nu}}{\varepsilon_0}\ (j = 1,2;\ \nu = s,c,f), \tilde{a}_\nu = \frac{a_\nu}{\varepsilon_0}, \tilde{b}_\nu = \frac{b_\nu}{\varepsilon_0} \tag{2.12}$$

and introduction of

$$Z_\nu(\tilde{x}) =: \hat{E}_z, \quad X_\nu(\tilde{x}) =: i\hat{E}_x, \quad H_\nu(\tilde{x}) =: i\sqrt{\frac{\mu_0}{\varepsilon_0}}\hat{H}_y, \quad \varepsilon_\nu =: \tilde{\varepsilon} \qquad (2.13)$$

(omitting the tilde sign) in the following have been used.

System (2.11) contains the second derivative but it can be presented as a system of two first- order differential equations as shown below.

The function $H_\nu(x)$ can be expressed in terms of $Z_\nu(x)$ and $X_\nu(x)$ as follows (cf. Appendix B)

$$H_\nu(x) = \left(\gamma X_\nu(x) - \frac{dZ_\nu(x)}{dx}\right). \qquad (2.14)$$

The diagonal elements $\varepsilon_{x\nu}, \varepsilon_{z\nu}$ (cf. (2.6)) and the nonlinear parts $\tilde{\varepsilon}_x$, $\tilde{\varepsilon}_z$ (cf. (2.9)) in new variables are

$$\begin{aligned} \varepsilon_{x\nu} &= \varepsilon_{1\nu} + a_\nu\, X_\nu^2(x) + b_\nu\, Z_\nu^2(x), \\ \varepsilon_{z\nu} &= \varepsilon_{2\nu} + b_\nu\, X_\nu^2(x) + a_\nu\, Z_\nu^2(x), \end{aligned} \qquad (2.15)$$

$$\begin{aligned} \tilde{\varepsilon}_x &= f(x) + a_f\, X_f^2(x) + b_f\, Z_f^2(x), \\ \tilde{\varepsilon}_z &= f(x) + b_f\, X_f^2(x) + a_f\, Z_f^2(x). \end{aligned} \qquad (2.16)$$

The problem is to find real solutions $Z_\nu(x)$, $X_\nu(x)$, subject to real γ and the boundary conditions at $x = 0$, $x = h$ and infinity ($Z_\nu(x)$, $X_\nu(x) \xrightarrow[|x|\to\infty]{} 0$, $\nu = s, c$).

Differentiating the second equation of (2.11) and inserting into the first one leads to a system of two first- order ordinary differential equations

$$\begin{cases} \dfrac{dZ_\nu(x)}{dx} = \dfrac{\gamma^2 - \varepsilon_{1\nu} - f(x) - a_\nu\, X_\nu^2(x) - b_\nu\, Z_\nu^2(x)}{\gamma} X_\nu(x), \\ \dfrac{dX_\nu(x)}{dx} = \dfrac{\left(\gamma^2\varepsilon_{z\nu} + 2b_\nu(\varepsilon_{x\nu} - \gamma^2)X_\nu(x)\right)Z_\nu(x) - \gamma\dfrac{df(x)}{dx}}{\gamma(\varepsilon_{1\nu} + f(x) + 3a_\nu\, X_\nu^2(x) + b_\nu Z_\nu^2(x))}. \end{cases} \qquad (2.17)$$

For the dielectric permittivity of type I (ε_ν cf. (2.5)) it is convenient to present (2.11) as (2.17) with $f(x) = 0$. If the dielectric permittivity is the type II (ε_ν cf. (2.7)) it is practical to consider (2.11).

3 Solution

The permittivity (2.5) is considered in the present Section.

3.1 Dispersion relation and fields

Multiplying the first equation of (2.11) by $2\,\frac{dZ_\nu(x)}{dx}$, the second one by $2\,\frac{dX_\nu(x)}{dx}$ and adding both equations $\left(\text{using } \frac{dZ_\nu(x)}{dx} = \left(\frac{\varepsilon_{x\nu}-\gamma^2}{\gamma}\right) X_\nu \text{ cf. (2.11)}\right)$ yields

$$(\varepsilon_{x\nu}-\gamma^2)\left(\varepsilon_{x\nu}+2X_\nu^2\frac{\partial\varepsilon_{x\nu}}{\partial X_\nu^2}\right)dX_\nu^2+\left(\gamma^2\varepsilon_{z\nu}+2X_\nu^2(\varepsilon_{x\nu}-\gamma^2)\frac{\partial\varepsilon_{x\nu}}{\partial Z_\nu^2}\right)dZ_\nu^2=0. \tag{3.1.1}$$

The differential equation is exact[10] if and only if the integrability condition

$$\frac{\partial\varepsilon_{z\nu}}{\partial X_\nu^2}=\frac{\partial\varepsilon_{x\nu}}{\partial Z_\nu^2} \tag{3.1.2}$$

is satisfied. Obviously, this holds for the permittivity (2.15)[11]. Hence, solutions of (3.1.1) are given by $\tilde{G}_\nu(Z_\nu,X_\nu)=C_\nu$, where $\tilde{G}_\nu(Z_\nu,X_\nu)$ is a function such that[10] (see (3.1.1))

$$\begin{aligned}\frac{\partial\tilde{G}_\nu(Z_\nu,X_\nu)}{\partial Z_\nu^2}&=(\varepsilon_{x\nu}-\gamma^2)\left(\varepsilon_{x\nu}+2X_\nu^2\frac{\partial\varepsilon_{x\nu}}{\partial X_\nu^2}\right),\\ \frac{\partial\tilde{G}_\nu(Z_\nu,X_\nu)}{\partial X_\nu^2}&=\gamma^2\varepsilon_{z\nu}+2X_\nu^2(\varepsilon_{x\nu}-\gamma^2)\frac{\partial\varepsilon_{x\nu}}{\partial Z_\nu^2}.\end{aligned} \tag{3.1.3}$$

Finding the function $\tilde{G}_\nu(Z_\nu,X_\nu)$ standardmethods[10] implies that solutions of (3.1.3) can be rewritten as (where $G_\nu(Z_\nu,X_\nu)=\tilde{G}_\nu(Z_\nu,X_\nu)-C_\nu$)

$$\begin{aligned}G_\nu(Z_\nu,X_\nu)\coloneqq\frac{{a_\nu}^2(X_\nu^2)^3}{2}+a_\nu\left(\varepsilon_{1\nu}+b_\nu\,Z_\nu^2-\frac{3\gamma^2}{4}\right)(X_\nu^2)^2+\\ +\frac{(\varepsilon_{1\nu}+b_\nu\,Z_\nu^2)}{2}(\varepsilon_{1\nu}+b_\nu\,Z_\nu^2-\gamma^2)X_\nu^2+\frac{\gamma^2}{4}Z_\nu^2(2\,\varepsilon_{2\nu}+a_\nu\,Z_\nu^2)+C_\nu=0\end{aligned} \tag{3.1.4}$$

where

$$C_\nu(Z_{0\nu}^2, X_{0\nu}^2) =$$

$$= -\frac{(\varepsilon_{1\nu} + a_\nu X_{0\nu}^2 + b_\nu Z_{0\nu}^2 - \gamma^2)}{2}(\varepsilon_{1\nu} + a_\nu X_{0\nu}^2 + b_\nu Z_{0\nu}^2)X_{0\nu}^2 -$$

$$-\frac{\gamma^2}{4}(2\varepsilon_{2\nu} Z_{0\nu}^2 + a_\nu (Z_{0\nu}^4 - X_{0\nu}^4)), \quad \nu = c, s, f \tag{3.1.5}$$

are constants to be determined by the boundary conditions.

Equation (3.1.4), representing the first integral of the system (2.11) (or (2.1.17) with $f(x) = 0$), is a quadratic/cubic equation with respect to Z_ν^2/X_ν^2, respectively, so that one field component (Z_ν or X_ν) can be expressed in terms of the other.

Separating the differentials in (2.1.17) (with $f(x) = 0$) leads to

$$\begin{cases} \dfrac{(\varepsilon_{1\nu} + 3a_\nu X_\nu^2(x) + b\, Z_\nu^2(x))\,\gamma}{Z_\nu(x)} \cdot \\ \cdot \dfrac{dX_\nu(x)}{\left(2a_\nu b_\nu X_\nu^4 + b_\nu(2\varepsilon_{1\nu} + 2b_\nu Z_\nu^2(X_\nu, \gamma) - \gamma^2)X_\nu^2 + \left(\varepsilon_{2\nu} + a_\nu Z_\nu^2(X_\nu, \gamma)\right)\gamma^2\right)} = dx \\ \dfrac{\gamma\, dZ_\nu(x)}{X_\nu(x)\,(\gamma^2 - \varepsilon_{1\nu} - a_\nu X_\nu^2(x) - b_\nu Z_\nu^2(x))} = dx. \end{cases} \tag{3.1.6}$$

Choosing a real root $\pm\sqrt{X_\nu^2}/\pm\sqrt{Z_\nu^2}$ of $G_\nu(Z_\nu, X_\nu) = 0$ (supposing that nonvanishing roots $\pm\sqrt{X_\nu^2}/\pm\sqrt{Z_\nu^2}$ exist) and assuming $X_\nu(x) = \pm\sqrt{X_\nu^2}$, $Z_\nu(x) = \pm\sqrt{Z_\nu^2}$ in (3.1.6), integration yields

$$\int_{Z_\nu(x_0)}^{Z_\nu(x,\gamma,Z_\nu(x_0))} F_{Z_\nu}^{\pm}(\zeta, \gamma)\, d\zeta = x - x_0, \tag{3.1.7}$$

$$\int_{X_\nu(x_0)}^{X_\nu(x,\gamma,X_\nu(x_0))} F_{X_\nu}^{\pm}(\xi, \gamma)\, d\xi = x - x_0, \tag{3.1.8}$$

where

$$F_{Z_\nu}^{\pm}(Z_\nu, \gamma) = \frac{\gamma}{\pm\sqrt{X_\nu^2(Z_\nu, \gamma)}\,(\gamma^2 - \varepsilon_{1\nu} - a_\nu X_\nu^2(Z_\nu, \gamma) - b_\nu Z_\nu^2)}, \tag{3.1.9}$$

$$F_{X_\nu}^{\pm}(X_\nu,\gamma)=\frac{1}{\pm\sqrt{Z_\nu^2(X_\nu,\gamma)}}\times$$
$$\times\frac{(\varepsilon_{1\nu}+3a_\nu X_\nu^2+b_\nu Z_\nu^2(X_\nu,\gamma))\gamma}{\left(2a_\nu b_\nu X_\nu^4+b_\nu(2\varepsilon_{1\nu}+2b_\nu Z_\nu^2(X_\nu,\gamma)-\gamma^2)X_\nu^2+\left(\varepsilon_{2\nu}+a_\nu Z_\nu^2(X_\nu,\gamma)\right)\gamma^2\right)}. \quad (3.1.10)$$

If $Z_\nu(x_0)$, $X_\nu(x_0)$ are prescribed and the propagation constant γ has been determined, equations (3.1.7) and (3.1.8) are implicite equations for $Z_\nu(x,\gamma,Z_\nu(x_0))$ and $X_\nu(x,\gamma,X_\nu(x_0))$, respectively. It seems that $Z_\nu\left(x,\gamma,Z_\nu(x_0)\right)$ and $X_\nu\left(x,\gamma,X_\nu(x_0)\right)$ cannot be found analytically by using equations (3.1.7) and (3.1.8). For the linear case ($a_\nu=b_\nu=0$) it yields the well- known result[12, 13] (see Appendix C.2).

To determine the constant C_ν the boundary conditions must be evaluated. According to (2.10), (2.13) continuity at the interfaces of the tangential component of $\boldsymbol{E}$ (E_z) implies continuity of the function $Z_\nu(x)$ at $x=x_0=0$ (for $\nu=s,f$) and $x=x_0=h$ (for $\nu=f,c$). Continuity at the film boundaries of the tangential component of $\boldsymbol{H}$ (H_y) is equivalent (cf. (2.14)) to the continuity of the function $\gamma X_\nu(x)-\frac{dZ_\nu(x)}{dx}$, and thus of the function $\varepsilon_{x\nu}X_\nu(x)$ at $x=$ $=x_0=0$ (for $\nu=s,f$) and $x=x_0=h$ (for $\nu=f,c$) (cf. the second equation (2.11)). Hence the boundary conditions read

$$\left[\varepsilon_{1s}+a_sX_s^2\left(0-0,\gamma,Z(0)\right)+b_sZ^2(0)\right]X_s(0-0,\gamma,Z(0))=$$
$$=\left[\varepsilon_{1f}+a_fX_f^2\left(0+0,\gamma,Z(0)\right)+b_fZ^2(0)\right]X_f(0+0,\gamma,Z(0)), \quad (3.1.11)$$

$$\left[\varepsilon_{1f}+a_fX_f^2\left(h-0,\gamma,Z(0)\right)+b_fZ^2(h)\right]X_f(h-0,\gamma,Z(0))=$$
$$=\left[\varepsilon_{1c}+a_cX_c^2\left(h+0,\gamma,Z(0)\right)+b_cZ^2(h)\right]X_c(h+0,\gamma,Z(0))^{14}\cdot \quad (3.1.12)$$

The boundary conditions at infinity imply

$$\begin{cases} C_s(Z_{0s}^2,X_{0s}^2)=0, \\ C_c(Z_{hc}^2,X_{hc}^2)=0 \quad (\text{with } Z_{0c}\to Z_{hc}, X_{0c}\to X_{hc} \text{ in (3.1.5)}) \end{cases} \quad (3.1.13)$$

The dispersion relation can be derived by using equation (3.1.7) according to the following steps:

I. Solution of $G_s(Z(0),\, X_s(0-0,\gamma,Z(0))) = 0$ $(C_s = 0)$ with respect to $X_s(0-0) = X_s\big(0-0,\gamma,Z(0)\big)$. Value $Z(0)$ is assumed to be prescribed[15].

II. Insertion of $X_s(0-0)$ into equation (3.1.11) and solution of (3.1.11) with respect to $X_f(0+0) = X_f\big(0+0,\gamma,Z(0)\big)$

III. Determination of $C_f = C_f\left(Z_{0f}^2 = Z^2(0), X_{0f}^2 = X_f^2(0+0)\right)$ according to (3.1.5)

IV. Solution of $G_c(Z(h),\, X_c(h+0),\gamma,Z(0)) = 0$ $(C_c = 0)$ with respect to $X_c(h+0) = X_c\big(h+0,\gamma,Z(0)\big)$

V. Solution of $G_f(Z(h), X_f(h-0,\gamma,Z(0))) = 0$ (with C_f from III.) with respect to $X_f(h-0) = X_f\big(h-0,\gamma,Z(0)\big)$

VI. Insertion of $X_c(h+0)$ (from IV.) and $X_f(h-0)$ (from V.) into equation (3.1.12) and solution of (3.1.12) with respect to $Z(h) = Z(h,\gamma,Z(0))$[16]

VII. Solution of $G_f\big(Z_f, X_f\big) = 0$ with respect to function $X_f^2\big(Z_f,\gamma\big)$ and insertion of $Z\big(h,\gamma,Z(0)\big)$ (from (VI)) and $X_f^2(\zeta,\gamma)$ into equation (3.1.7) for $\nu = f$ (with $x = h$, $x_0 = 0$ and $Z_f(0) = Z(0)$). The result reads

$$DR_Z(\gamma, Z(0), \varepsilon_{1\nu}, \varepsilon_{2\nu}, a_\nu, b_\nu) =: \int_{Z(0)}^{Z(h,\gamma,Z(0))} F_{Z_f}^{\pm}(\zeta,\gamma)\,d\zeta = h > 0. \tag{3.1.14}$$

Equation (3.1.14) represents the dispersion relation for the nonlinear TM-case. The right-hand side must be positive, and, according to the steps above, the left-hand side depends on all the material parameters of problem but not on h explicitely.

The main problem is to find real solutions $\gamma = \gamma(h, Z(0);\, \varepsilon_{1\nu},\, \varepsilon_{2\nu},\, a_\nu, b_\nu)$ associated with certain solvability conditions for (3.1.14).

A dispersion relation can be obtained also by using equation (3.1.8) as follows:
Steps I. –IV. are the same as given above.

V*. Solution of $G_f(Z(h), X_f(h-0,\gamma,Z(0)) = 0$ (with C_f from III.) for $Z(h)$

VI*. Insertion of $X_c(h+0)$ (from IV.) and $Z(h)$ (from V*.) into equation (3.1.12) and solution of (3.1.12) with respect to $X_f\big(h-0,\gamma,Z(0)\big)$[17]

VII*. Solution of $G_f\big(Z_f, X_f\big) = 0$ with respect to function $Z_f^2\big(X_f,\gamma\big)$ and insertion of $X_f\big(h-0,\gamma,Z(0)\big)$ (from VI*) and $Z_f^2(\xi,\gamma)$ into equation (3.1.8) for $\nu = f$ (with $x = h-0,\ x_0 = 0$ and $X_f(0) = X_f\big(0+0,\gamma,Z(0)\big)\big)$. Evaluation now yields

$$DR_X(\gamma, Z(0), \varepsilon_{1\nu}, \varepsilon_{2\nu}, a_\nu, b_\nu) =: \int_{X_f(0+0,\gamma,Z(0))}^{X_f(h-0,\gamma,Z(0))} F_{X_f}^{\pm}(\xi,\gamma)d\xi \ = h > 0. \tag{3.1.15}$$

It is remarkable that two dispersion relations can be derived. An interesting question is whether (3.1.14) or (3.1.15) are equivalent leading to the same $\gamma = \gamma(h, Z(0);\ \varepsilon_{1\nu},\ \varepsilon_{2\nu},\ a_\nu, b_\nu)$. Due to the complicated integrands and different upper limits in (3.1.14) and (3.1.15) equivalency could not be shown. Instead consistency is illustrated numerically (cf. Appendix F).

The sign in (3.1.9)/(3.1.10) (and hence, in (3.1.7)/(3.1.8), (3.1.14)/(3.1.15), respectively), must be fixed by choosing the real cubic/quadratic root $\big[X_f^2(Z_f,\gamma)\big]_j/\big[Z_f^2\big(X_f,\gamma\big)\big]_i$ of $G_f\big(Z_f, X_f\big) = 0$ $(j = 1,2,3;\ (i = 1,2)$ subject to

$$sgn\left[\sqrt{X_f^2\big(Z_f = Z(0),\gamma\big)}\right] \equiv sgn\big[X_f\big(0+0,\gamma,Z(0)\big)\big], \tag{3.1.16}$$

$$sgn\left[\sqrt{Z_f^2\big(X_f = X_f\big(0+0,\gamma,Z(0)\big),\gamma\big)}\right] \equiv sgn[Z(0)], \tag{3.1.17}$$

where $X_f\big(0+0,\gamma,Z(0)\big)$ is obtained by step II.. In general, the functions $X_f(x)/Z_f(x)$ can change sign, this has to be taken into account by evaluation (3.1.14)/(3.1.15) (for example see Appendix E, H).

If, for certain values of γ, $Z(0)$; $\varepsilon_{1\nu}$, $\varepsilon_{2\nu}$, a_ν, b_ν the first integral $G_f(Z_f, X_f) = 0$ describes periodic Z_f, X_f higher modes are possible. In this case, the integrals in (3.1.14) and (3.1.15) are also periodic with periods

$$T_Z = \left| \oint_{G_f(Z_f,X_f)=0} F_{Z_f}^{\pm}(\zeta,\gamma)d\zeta \right|, \tag{3.1.18}$$

$$T_X = \left| \oint_{G_f(Z_f,X_f)=0} F_{X_f}^{\pm}(\xi,\gamma)d\xi \right|, \tag{3.1.19}$$

respectively. If integration in (3.1.14) or (3.1.15) leads to $h < 0$ the period must be added to obtain $h > 0$ (see below).

Thus the dispersion relation including higher modes reads

$$h_N = (h + \mathrm{k} \cdot T_l) + N \cdot T_l\,, \tag{3.1.20}$$

where

$$\begin{aligned} &N = 1, 2, 3, \dots, \\ &\mathrm{k} = \begin{cases} 0, & \text{if } h > 0, \\ 1, & \text{if } h < 0, \end{cases} \\ &l = \begin{cases} Z, \text{ by using (3.1.14)}, \\ X, \text{ by using (3.1.15)}. \end{cases} \end{aligned} \tag{3.1.21}$$

If no periodic Z_f, X_f exist, higher modes are impossible.

If γ has been determined in dependence on $Z(0)$, h, and the material parameters of the problem $\varepsilon_{1\nu}$, $\varepsilon_{2\nu}$, a_ν, b_ν, equations (3.1.7) and (3.1.8) yield the field components Z_ν and X_ν, respectively. – Thus, the problem is solved, the complex field amplitudes are given by (expression for the magnetic field $\boldsymbol{H}$ is considered in Appendix B)

$$\begin{aligned} \boldsymbol{E} &= \big((0,0,Z(x)) - i(X(x),0,0)\big)\, e^{i\gamma z}, \\ \boldsymbol{H} &= \left(0, -i\sqrt{\frac{\varepsilon_0}{\mu_0}}\left(\gamma X(x) - \frac{dZ(x)}{dx}\right), 0\right) e^{i\gamma z} \end{aligned} \tag{3.1.22}$$

and thus the (physical) fields are

$$Re\left[\vec{\mathcal{E}}(x,y,z,t)\right] = Re\left[\boldsymbol{E}(x,y,z)\, e^{-i\omega t}\right] = \\ = (X(x)sin(\gamma z - \omega t),0,Z(x)\cos(\gamma z - \omega t)), \tag{3.1.23}$$

$$Re\left[\vec{\mathcal{H}}(x,y,z,t)\right] = Re\left[\boldsymbol{H}(x,y,z)\, e^{-i\omega t}\right] = \\ = \left(0, \sqrt{\frac{\varepsilon_0}{\mu_0}}\left(\frac{dZ(x)}{dx} - \gamma X(x)\right) sin(\gamma z - \omega t),0\right). \tag{3.1.24}$$

3.2 Power flow

By integration of the z –component of the time- averaged Poynting vector

$$\bar{S}_z = \frac{1}{2}\, Re\left[\vec{\mathcal{E}} \times \vec{\mathcal{H}}^*\right]_z \tag{3.2.1}$$

and by means of (A.0.1), (2.15) the total power flow carried by the nonlinear wave (per unit width in the y- direction) is given by (cf. Appendix D.1)

$$P = \int_{-\infty}^{\infty} \bar{S}_z(x)dx = P_s + P_f + P_c = \\ = \frac{\omega\, \varepsilon_0}{2}\left[\int_{-\infty}^{0} \frac{\varepsilon_{xs}\, X_s^2(x)}{\gamma} dx + \int_{0}^{h} \frac{\varepsilon_{xf}\, X_f^2(x)}{\gamma} dx + \int_{h}^{\infty} \frac{\varepsilon_{xc}\, X_c^2(x)}{\gamma} dx\right]. \tag{3.2.2}$$

Transforming the second equation of the system (2.11) (cf. Appendix D.2) (3.2.2) can be rewritten as follows

$$P_Z^* = \frac{P}{P_0} = \sum_{\nu=s,f,c} \int_{\alpha_{Z\nu}}^{\beta_{Z\nu}} P_{Z_\nu}^{\pm}(\zeta,\gamma)\, d\zeta, \tag{3.2.3}$$

where

$$P_0 = \frac{2}{\omega\, \varepsilon_0}, \tag{3.2.4}$$

$$P_{Z_\nu}^{\pm}(Z_\nu,\gamma) = \frac{\varepsilon_{x\nu}}{\gamma^2 - \varepsilon_{x\nu}} \cdot \left(\pm\sqrt{X_\nu^2(Z_\nu,\gamma)}\right) \tag{3.2.5}$$

and

$$\alpha_{Z\nu}=\begin{cases}0, & \nu=s\\ Z(0), & \nu=f\\ Z\big(h,\gamma,Z(0)\big), & \nu=c\end{cases},\quad \beta_{Z\nu}=\begin{cases}Z(0), & \nu=s\\ Z\big(h,\gamma,Z(0)\big), & \nu=f.\\ 0, & \nu=c\end{cases} \tag{3.2.6}$$

Rearranging the first equation of (2.11) (cf. Appendix D.3) the power flow P^* can be also evaluated according to

$$P_X^*=\frac{P}{P_0}=\sum_{\nu=s,f,c}\int_{\alpha_{X\nu}}^{\beta_{X\nu}}P_{X_\nu}^{\pm}(\xi,\gamma)\,d\xi, \tag{3.2.7}$$

where

$$P_{X_\nu}^{\pm}(X_\nu,\gamma)=\frac{\varepsilon_{x\nu}\,X_\nu^2}{\gamma}\cdot F_{X_\nu}^{\pm}(X_\nu,\gamma) \tag{3.2.8}$$

and

$$\alpha_{X\nu}=\begin{cases}0, & \nu=s,\\ X_f\big(0+0,\gamma,Z(0)\big), & \nu=f,\\ X_f\big(h-0,\gamma,Z(0)\big), & \nu=c,\end{cases}\quad \beta_{X\nu}=\begin{cases}X_f\big(0+0,\gamma,Z(0)\big), & \nu=s,\\ X_f\big(h-0,\gamma,Z(0)\big), & \nu=f,\\ 0, & \nu=c.\end{cases} \tag{3.2.9}$$

If Z_f, X_f are periodic (the first integral $G_f(Z_f,X_f,\gamma)=0$ is described for fixed γ by closed curves in the plane (Z_f,X_f)) the total power flow corresponding to the dispersion relation (3.1.20) reads

$$P_N^*=\left(P_l^*+\mathrm{k}\cdot T_l^*\right)+N\cdot T_l^* \tag{3.2.10}$$

where l,k and N are defined by (3.1.21) and

$$T_l^*=\begin{cases}\left|\oint_{G_f(Z_f,X_f)=0}P_{Z_f}^{\pm}(\zeta,\gamma)d\zeta\right|, & l=Z,\\ \left|\oint_{G_f(Z_f,X_f)=0}P_{X_f}^{\pm}(\xi,\gamma)d\xi\right|, & l=X.\end{cases} \tag{3.2.11}$$

Power flow evaluated according to (3.2.3) (or 3.2.7) for the linear case $(a_\nu=b_\nu=0)$ is consistent with that given in literature[12] (for details, see Appendix C.1).

4 Applications

Results of the subsections 4.1- 4.1.4 are obtained for the dielectric permittivity (2.5).

4.1 Nonlinear film bounded by linear substrate and cladding

TM- electromagnetic guided waves propagating in a Kerr nonlinear dielectric film sandwiched between two linear isotropic media ($\varepsilon_{1s} = \varepsilon_{2s} = \varepsilon_s,\ \varepsilon_{1c} = = \varepsilon_{2c} = \varepsilon_c,\ a_s = b_s = a_c = b_c = 0$) are considered in this subsection.

Taking into account systems (C.1.4), (C.1.6) and (C.1.7) solutions $Z_\nu(x)$, $X_\nu(x)$ and $H_\nu(x)$ $(\nu = s, c)$ for the linear substrate and cladding are written as

$$\begin{cases} \nu = s, & Z_s(x) = Z(0)e^{x\cdot\sqrt{\gamma^2-\varepsilon_s}}, & x < 0, \\ \nu = c, & Z_c(x) = Z(h)\, e^{-(x-h)\cdot\sqrt{\gamma^2-\varepsilon_c}}, & x > h, \end{cases} \tag{4.1.1}$$

$$\begin{cases} \nu = s, & X_s(x) = \dfrac{\gamma\, Z(0)}{\sqrt{\gamma^2-\varepsilon_s}} e^{x\cdot\sqrt{\gamma^2-\varepsilon_s}}, & x < 0, \\ \nu = c, & X_c(x) = -\dfrac{\gamma\, Z(h)}{\sqrt{\gamma^2-\varepsilon_c}}\, e^{-(x-h)\cdot\sqrt{\gamma^2-\varepsilon_c}}, & x > h. \end{cases} \tag{4.1.2}$$

$$\begin{cases} \nu = s, & H_s(x) = \dfrac{\varepsilon_s\, Z(0)}{\sqrt{\gamma^2-\varepsilon_s}} e^{x\cdot\sqrt{\gamma^2-\varepsilon_s}}, & x < 0, \\ \nu = c, & H_c(x) = -\dfrac{\varepsilon_c\, Z(h)}{\sqrt{\gamma^2-\varepsilon_c}}\, e^{-(x-h)\cdot\sqrt{\gamma^2-\varepsilon_c}}, & x > h. \end{cases} \tag{4.1.3}$$

From equations (4.1.1), (4.1.2) and (4.1.3) follows

$$\gamma > \max\left(\sqrt{\varepsilon_s}, \sqrt{\varepsilon_c}\right). \tag{4.1.4}$$

For the case of the linear film holds[12]

$$\gamma < \sqrt{\varepsilon_{1f}}, \tag{4.1.5}$$

but there is no general upper limit for the propagation constant in the case of the nonlinear film. For each numerical case below an arbitrary upper limit of γ is set.

Omitting hereafter (in subsections 4.1- 4.1.4) subscript $\nu = f$ (only that $\varepsilon_{xf}, \varepsilon_{zf}, \varepsilon_{1f}, \varepsilon_{2f}, C_f$) equation (3.1.11) is written here as

$$\left[\varepsilon_{1f} + a\, X^2(0+0) + b\, Z^2(0)\right] X(0+0) = \frac{\gamma\, \varepsilon_s\, Z(0)}{\sqrt{\gamma^2 - \varepsilon_s}}. \qquad (4.1.6)$$

Equation (4.1.6) is a cubic equation with respect to $X(0+0)$ and has one or three real roots in dependence on whether discriminant of (4.1.6) given by

$$D = -\frac{27\, a^2\, \varepsilon_s^2\, \gamma^2\, Z^2(0)}{\gamma^2 - \varepsilon_s} - 4\, a \left(\varepsilon_{2f} + b\, Z^2(0)\right)^3. \qquad (4.1.7)$$

is negative or positive[18].

For fixed material parameters ε_{1f}, ε_{2f}, ε_s, ε_c, a, b the sign of the discriminant D depends on the value $Z(0)$ and γ (cf. Figure 3).

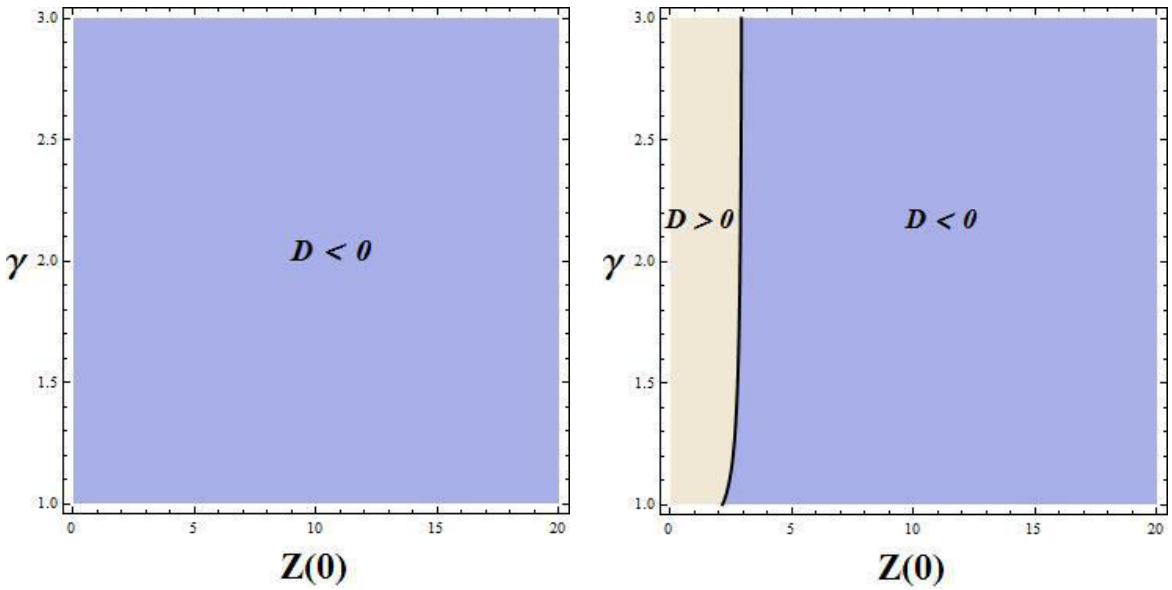

a) Focusing case **b)** Defocusing case

Figure 3: Regions of negative and positive discriminant D (cf. (4.1.7)). Parameters:

a) $\varepsilon_s = 1, \quad \varepsilon_c = 1, \quad \varepsilon_{1f} = 4, \quad \varepsilon_{2f} = 2, \quad a = 0.03, \quad b = 0.01;$

b) $\varepsilon_s = 0.8, \quad \varepsilon_c = 1, \quad \varepsilon_{1f} = 4, \quad \varepsilon_{2f} = 3, \quad a = -0.3, \quad b = -0.2.$

The present Section is organized as follows:

Taking parameters

a) (cf. Figure 3) and assuming $Z(0) = 1$ propagation in a self- focusing medium $(a > 0, b > 0\,; D < 0)$ is considered first (subsection 4.1.1). Equation (4.1.6) has a unique real root $X(0+0)$ in this case.

b) (cf. Figure 3) the self- defocusing medium $(a < 0, b < 0)$ is analyzed (subsection 4.1.2). Depending on the value $Z(0)$ three or one real root $X(0+0)$ are possible[19], leading to four cases to be considered:

$Z(0) = 1 \Rightarrow D > 0$:

Case I: Evaluation with the first root $X_1(0+0)$ of (4.1.6) (subsection 4.1.2.1).

Case II: Evaluation with the second root $X_2(0+0)$ of (4.1.6) (subsection 4.1.2.2).

Case III: Evaluation with the third root $X_3(0+0)$ of (4.1.6) (subsection 4.1.2.3).

$Z(0) = 3 \Rightarrow D < 0$:

Case IV: Evaluation with the unique real root $X(0+0)$ of (4.1.6) (subsection 4.1.2.4).

With $a = 0, b \neq 0$ a closed analytical dispersion relation of the problem is possible. This is shown in subsection 4.1.3.

In subsection 4.1.4 the propagation of TM- waves in a nonlinear metamaterial film $(\varepsilon_{1f} < 0, \varepsilon_{2f} < 0)$ is presented.

4.1.1 Self- focusing film

TM- waves, propagating in the nonlinear film with the positive coefficients of Kerr nonlinearity a, b are analyzed in this subsection (see N°23 in Table 3). Numerical results are evaluated with material parameters according to a) (cf. Figure 3) and

$$1 < \gamma \leq 4. \tag{4.1.1.1}$$

Field components Z, X satisfying equation (3.1.4) are shown in Figure 4. Obviously, there is a certain range of γ so that Z, X are periodic.

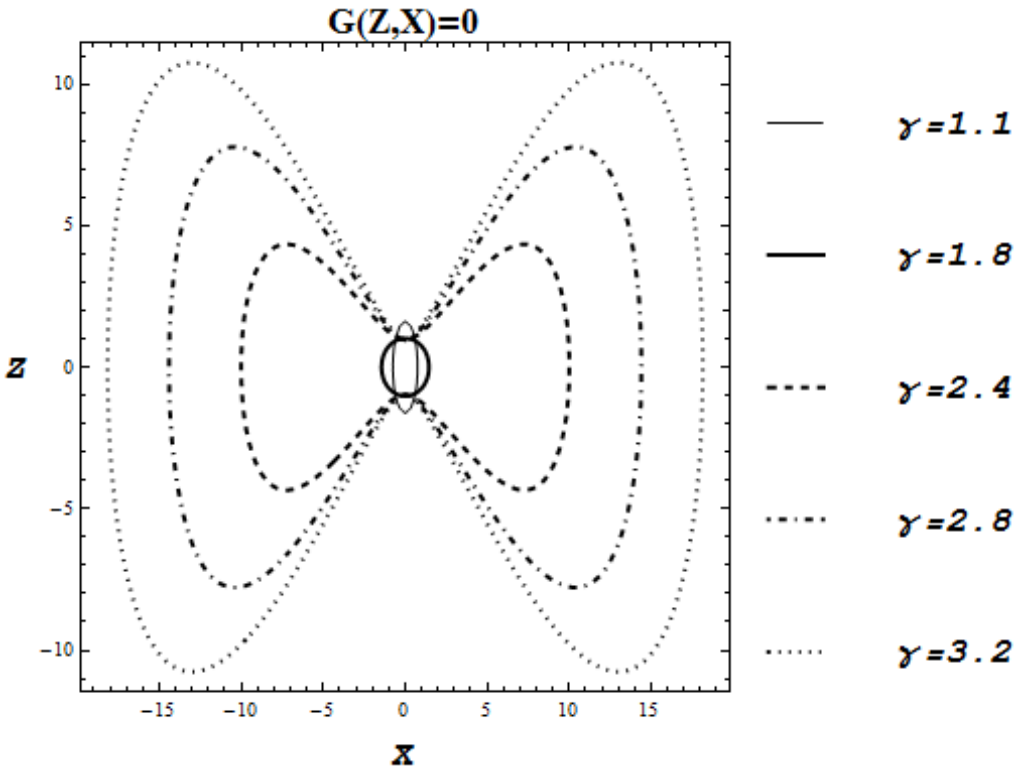

Figure 4: Contourplot of the first integral $G(Z, X) = 0$ for various γ (cf. (3.1.4))

Following the steps I- IV, V*- VII* outlined in the foregoing Section (see Appendix E for details) the dispersion relation (3.1.15) can be evaluated leading to Figure 5.

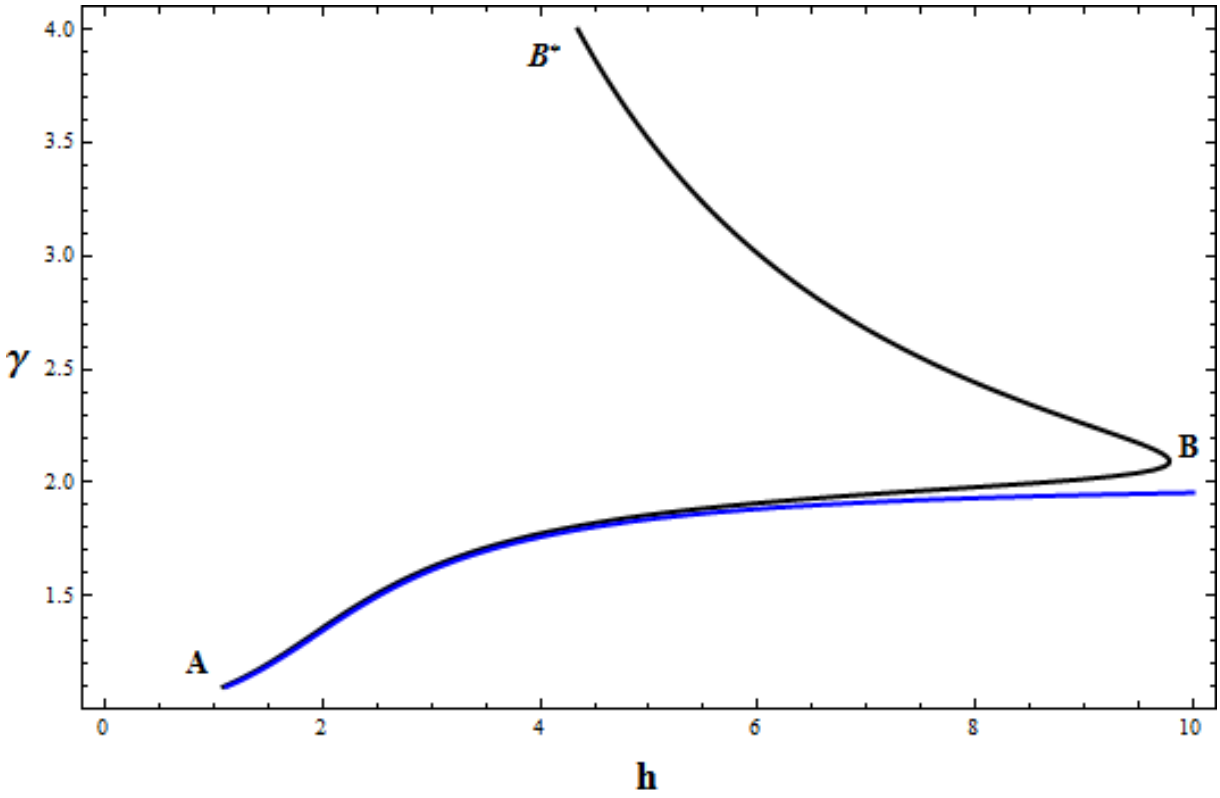

Figure 5: Black curve: solution of the dispersion relation (3.1.15) for the fundamental mode TM_0. Blue curve: solution of the dispersion relation in the linear case ($a = b = 0$, cf. (C.1.8)).

Fixing thickness h of the film and finding the corresponding propagation constant γ via the dispersion relation the patterns of the field components are plotted in Figure 6.

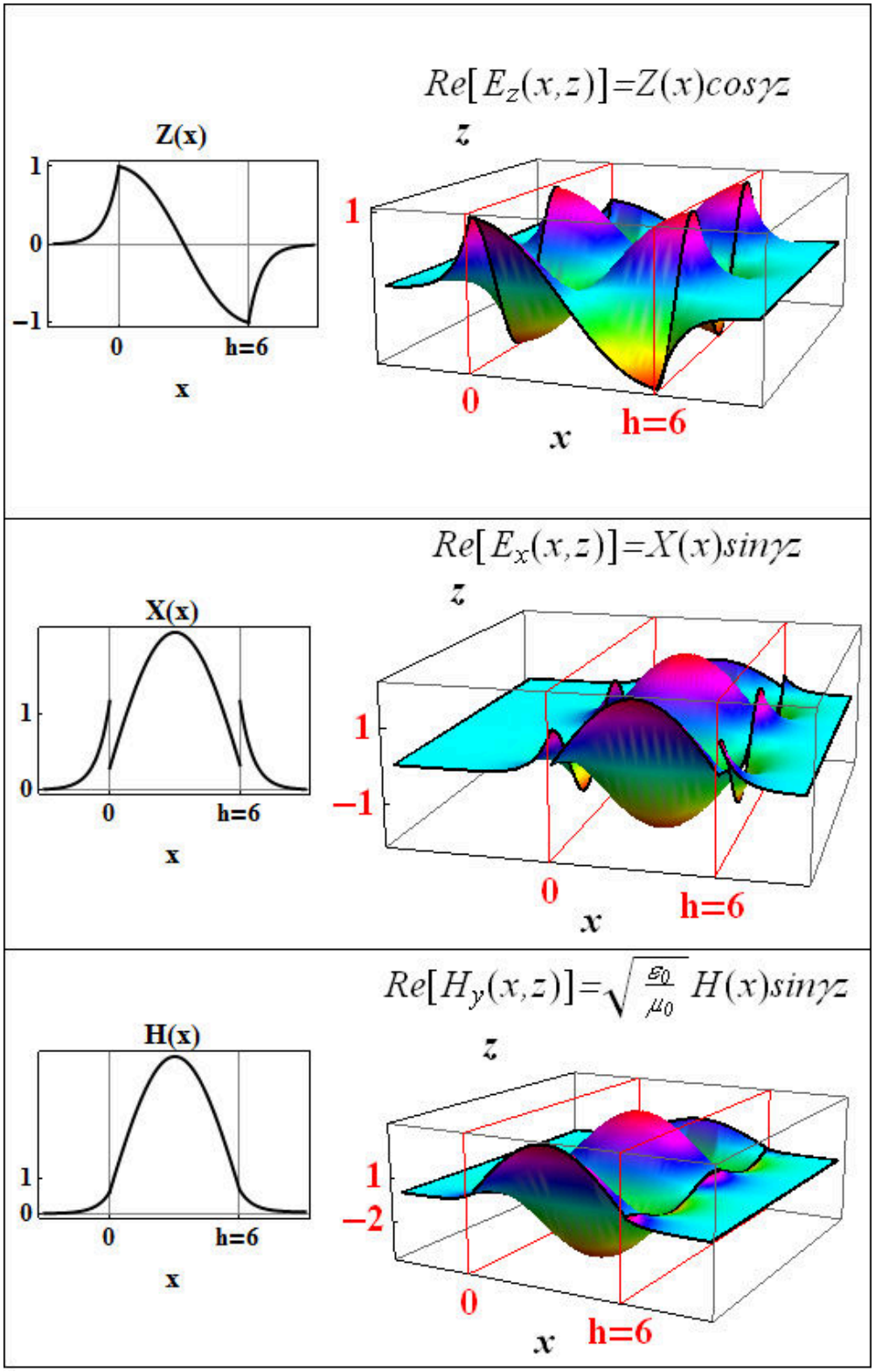

Figure 6: Field patterns of the nonlinear TM_0- wave for $h = 6, \gamma = 1.912$ (cf. (4.1.1), (4.1.2), (4.1.3), (3.1.23) and (3.1.24)[20])

Due to the periodicy of the field components higher modes are present. The corresponding dispersion curves are shown in Figure 7 (cf. equation (3.1.20)). The associated field patterns are depicted in Figure 8.

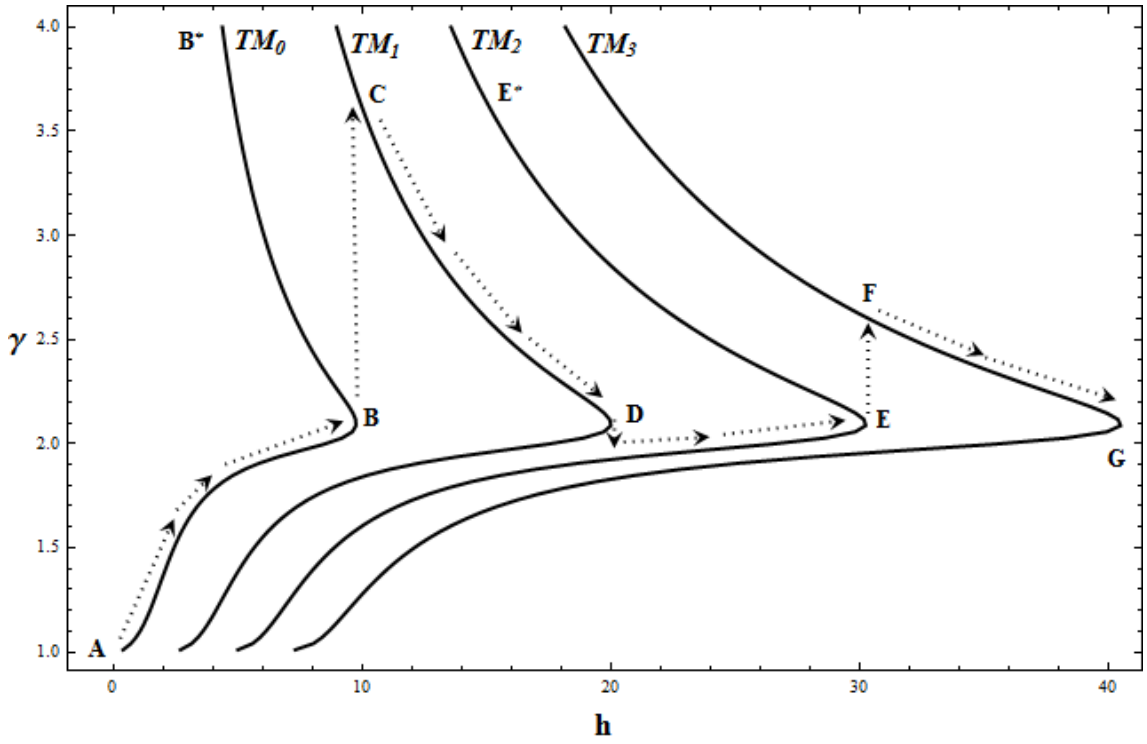

Figure 7: Higher mode solutions of the dispersion relation (3.1.20). Dotted lines and arrows indicate the direction of change of the propagation constant γ if h increases. "Switch" is represented by vertical arrows.

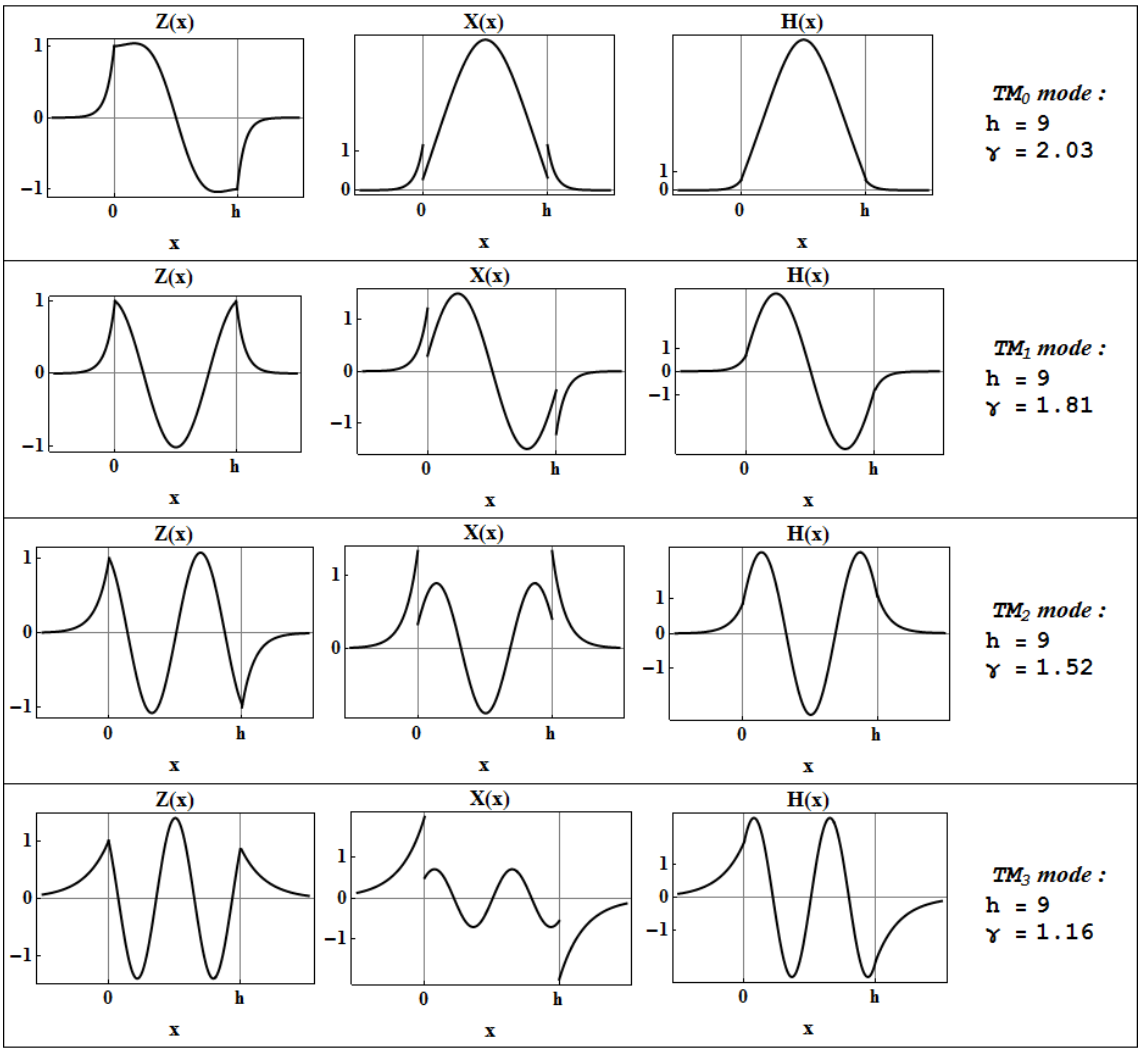

Figure 8: Field components $Z(x), X(x),$ and $H(x)$ for the TM_0- , TM_1- , TM_2- and TM_3- modes, corresponding to the dispersion curves in the Figure 7 (cf. (4.1.1), (4.1.2) and (4.1.3)[20])

The shape of the dispersion curves (Figures 5, 7) is similar to the shape in the TE case[21]. Remarkably, dispersion curves in Figures 5, 7 are not reported in the pertinent literature[22, 23]. The same holds for the dependence of the propagation constant γ on $Z^2(0)$ and on the nonlinear parameter a, b as depicted in Figure 9.

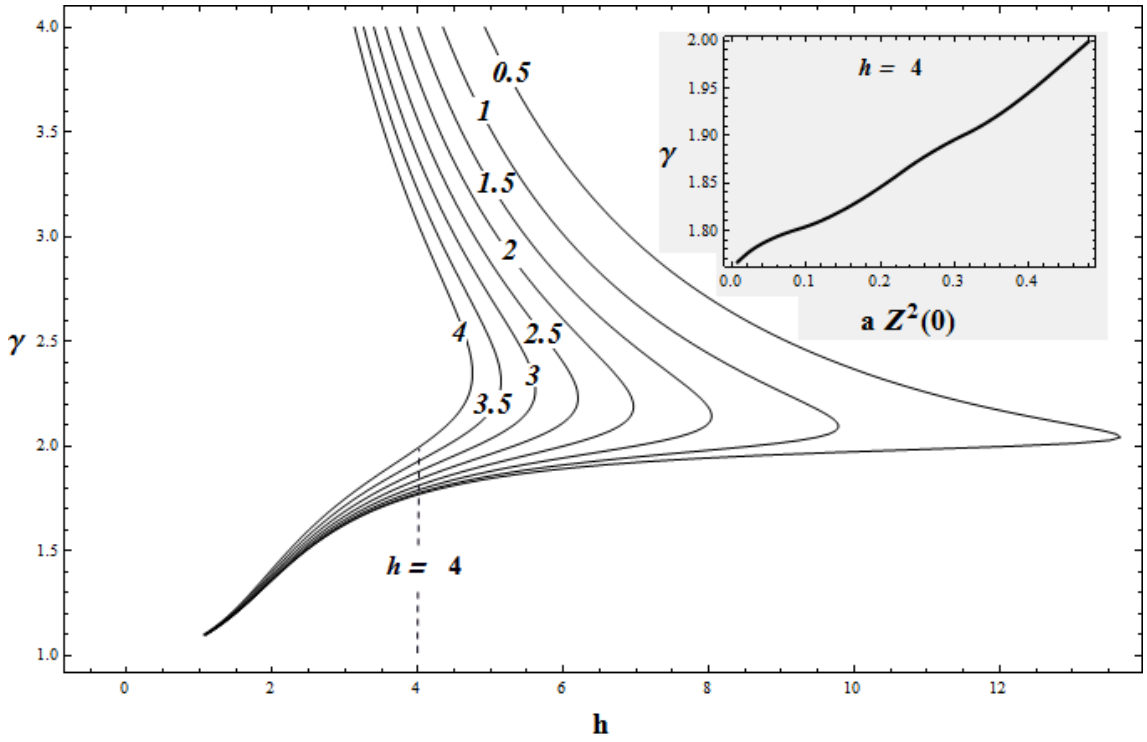

Figure 9: Dependence of the propagation constant γ on the film thickness h for the TM_0- mode evaluated for different values $Z(0)$ (cf. (3.1.15)). Dispersion curves are labelled by $Z(0)$. Gray region: dependence γ on the field intensity $a\,Z^2(0)$ for $h = 4$

Solutions of the dispersion relation (3.1.15) evaluated for various values of the nonlinearity coefficients a, b are presented in Figure 10.

Evaluation of the power flow according to equation (3.2.7) yields results represented in Figure 11 consistent with results reported in the literature if h is determined by γ via the dispersion relation[24].

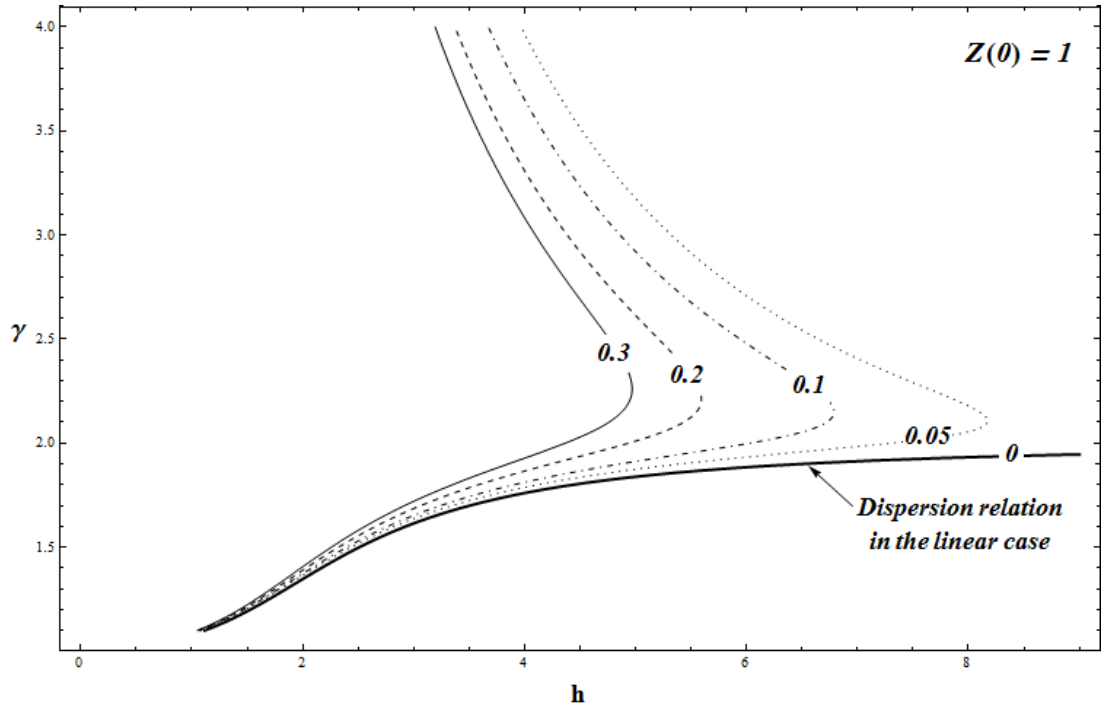

Figure 10: Propagation constant γ versus film thickness h for the TM_0- mode obtained for different values of the nonlinearity coefficients a, b (with $a = b$) (cf. (3.1.15)). Dispersion curves are labelled by a.

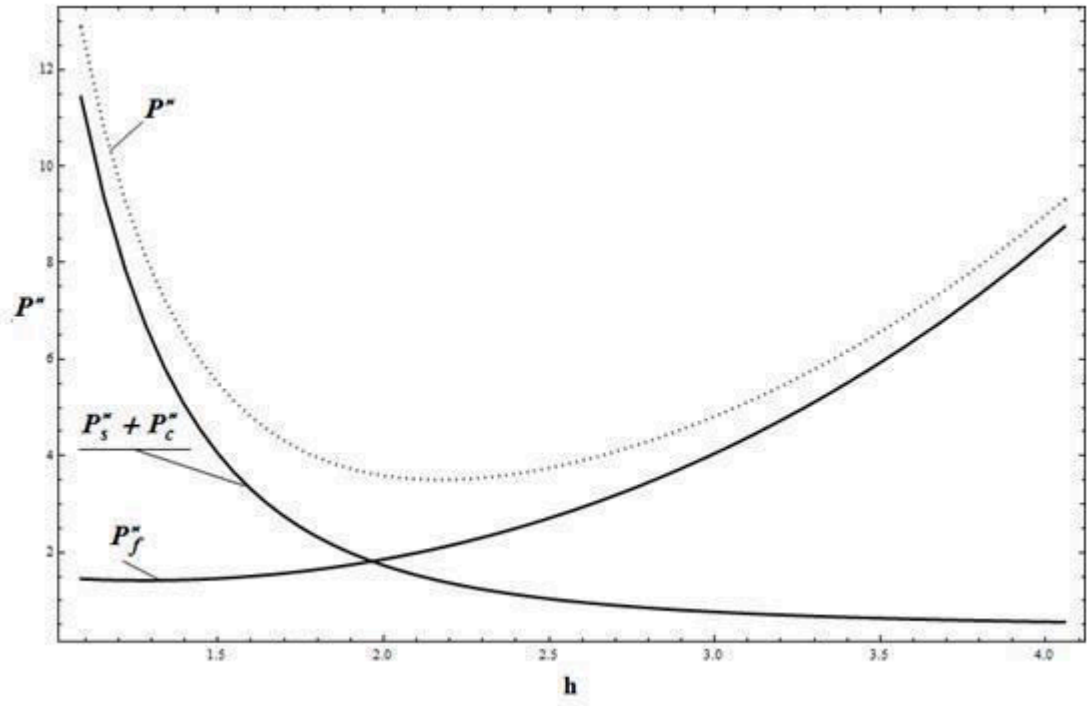

Figure 11: Total power flow P^* for the TM_0- wave (dotted curve) and its separation into power flow in the substrate and cladding ($P_s^* + P_c^*$) and the power flow in the film (P_f^*) versus film thickness h (cf. (3.2.7))

Figure 12 illustrates the normalized total power flow P^* evaluated for the fundamental (TM_0) and the first three higher modes (TM_1, TM_2, TM_3).

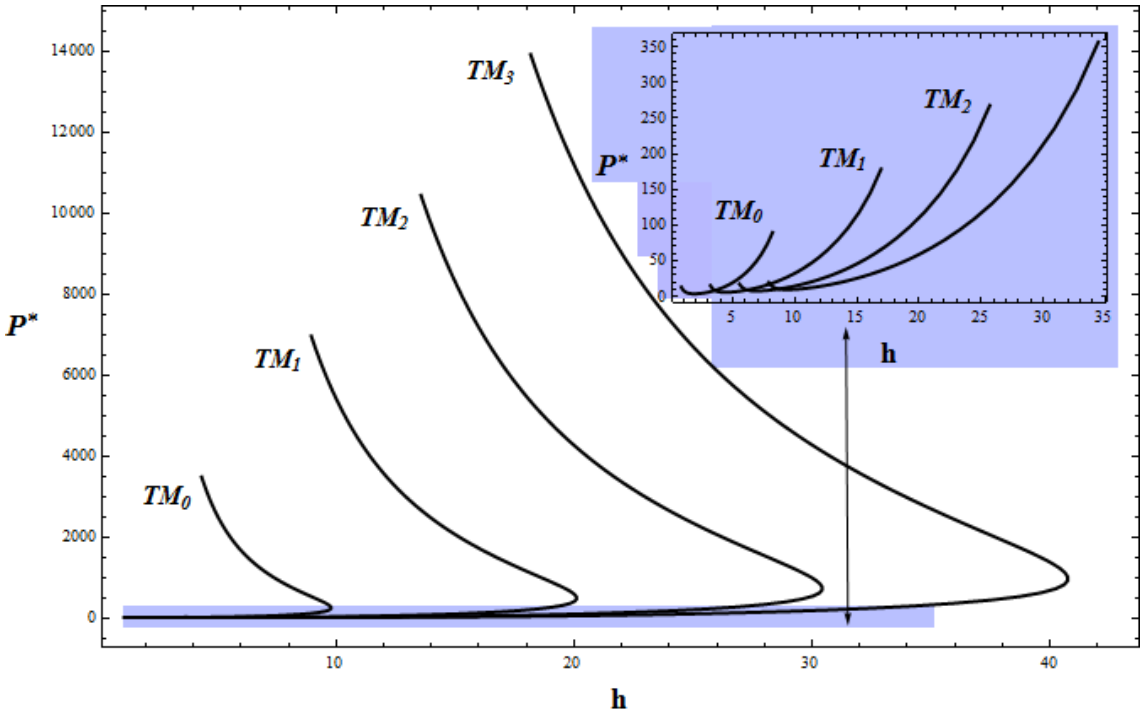

Figure 12: Total power flow P^* versus film thickness h for the different modes (cf. (3.2.10))

It should be noted here again that results of this subsection (the dispersion relation) are in full agreement with those presented in NN° 21, 25, 27 of Table 3.

4.1.2 Self- defocusing film

Four possible cases of TM- wave- propagation in a self- defocusing nonlinear film (coefficients of Kerr nonlinearity a, b are negative) are considered below. Material parameters are chosen according to b) (cf. Figure 3) with

$$Z(0)=\begin{cases}1, & \text{for Cases I, II and III,}\\ 3, & \text{for Case VI.}\end{cases}$$

4.1.2.1 Case I

$\left(\boldsymbol{Z(0)=1;\ X_1(0+0)\ cf.\ Eq.\ (4.1.6)}\right)$

Assuming

$$1<\gamma\leq 5 \qquad (4.1.2.1.1)$$

following results are obtained.

Figure 13 presents the first integral $G(Z,X,\gamma)=0$ evaluated according to equation (3.1.4).

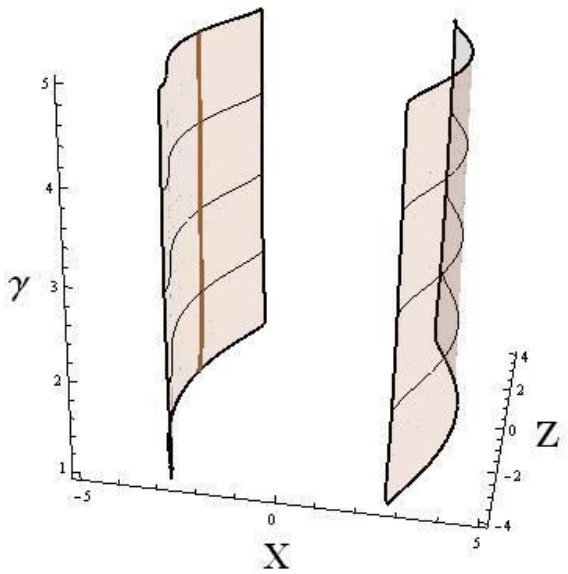

Figure 13: The first integral $G(Z,X,\gamma)=0$ (cf. (3.1.4)). Solid curve on the left surface depicts solution $X_1(0+0)$ (cf. (4.1.6)).

As shown in Figure 13 the relation between Z and X for each fixed γ is not represented by closed curves. Thus the components $Z(x)$, $X(x)$ and $H(x)$ are not periodic (for $1 < \gamma \leq 5$).

Figure 14 shows the dispersion relation obtained by using equation (3.1.14) (detailed description is given in Appendix F). Field components are depicted in Figure 15.

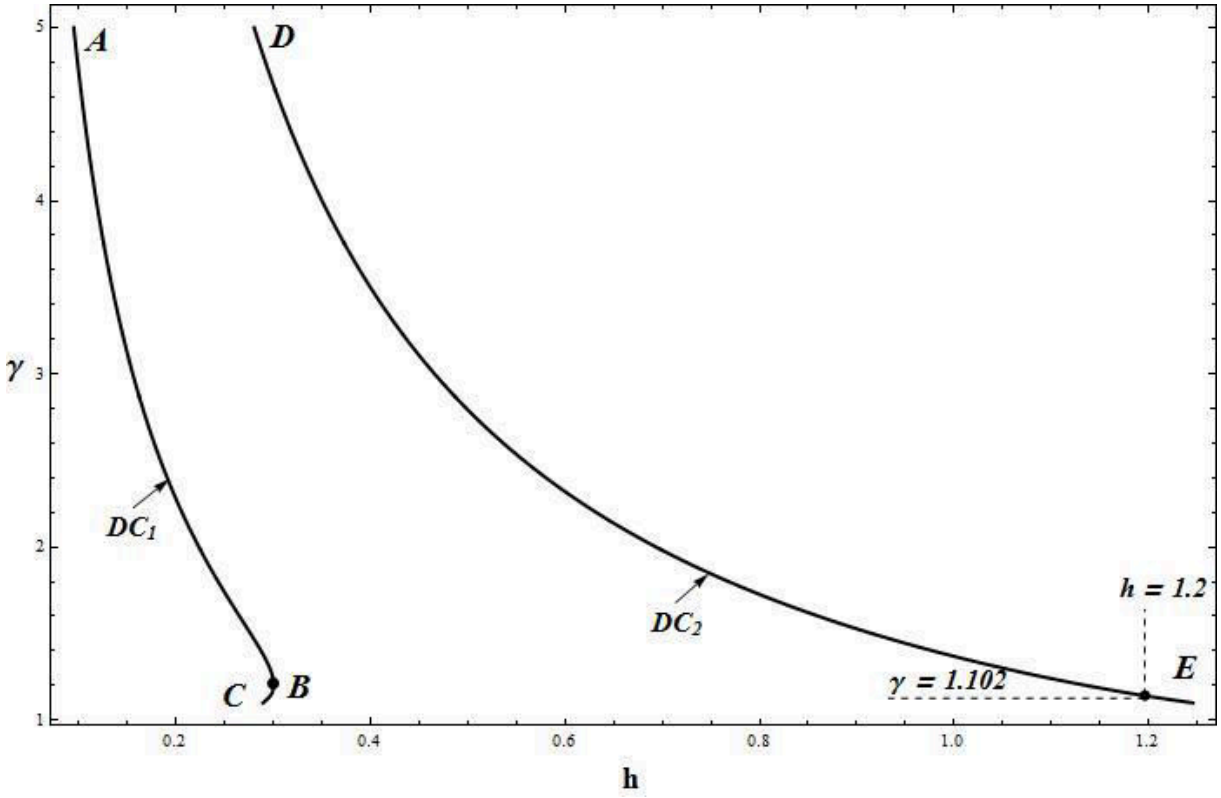

Figure 14: Solutions of the dispersion relation (cf. (3.1.14))

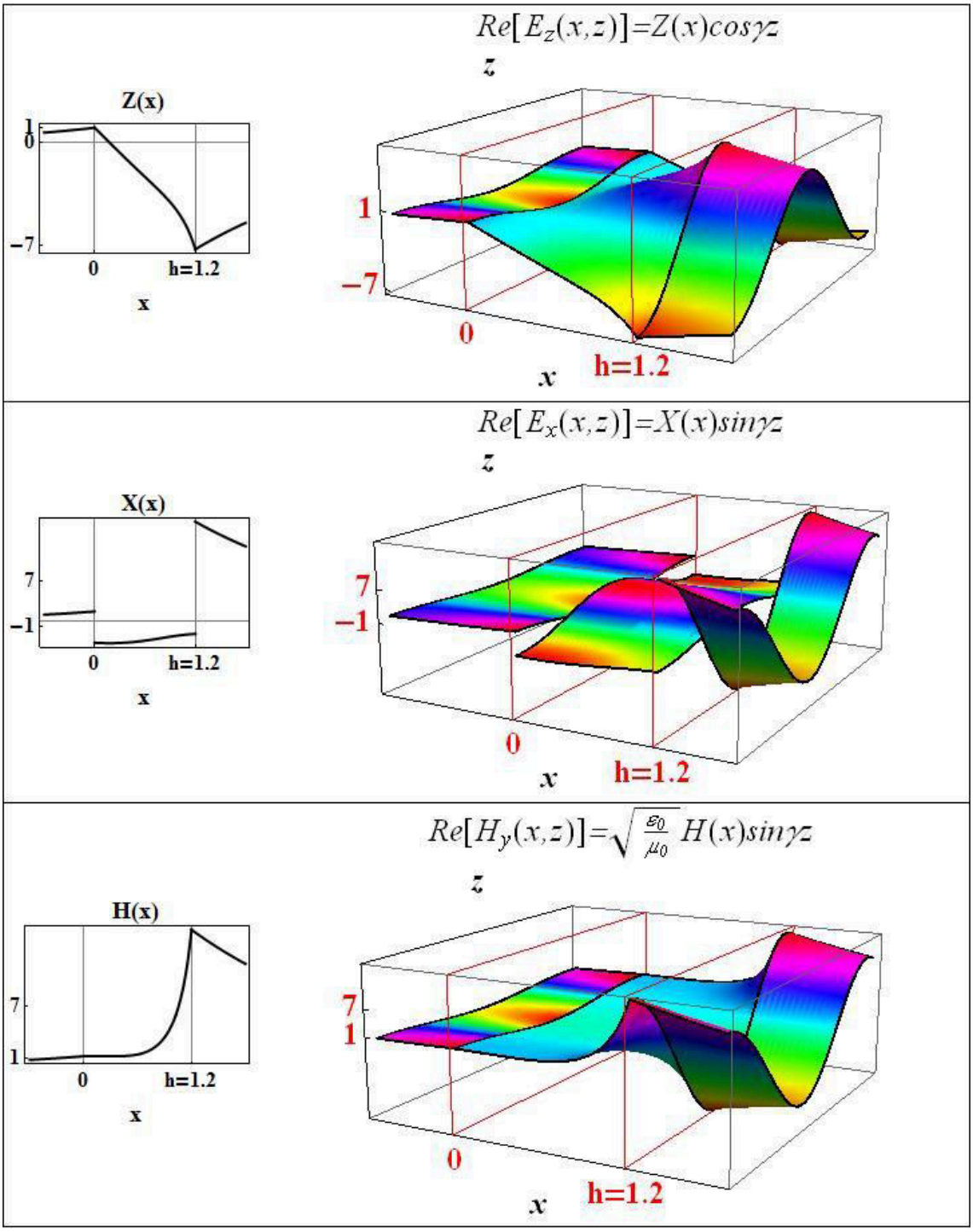

Figure 15: Field patterns of the nonlinear TM- wave for $h = 1.2, \gamma = 1.102$ (cf. Figure 14, equations (4.1.1), (4.1.2), (4.1.3), (3.1.23) and (3.1.24)[20])

Figure 16 presents solutions of the dispersion relation (3.1.14) for various values of $Z(0)$ and fixed nonlinearity coefficients $a = -0.3, b = -0.2$.

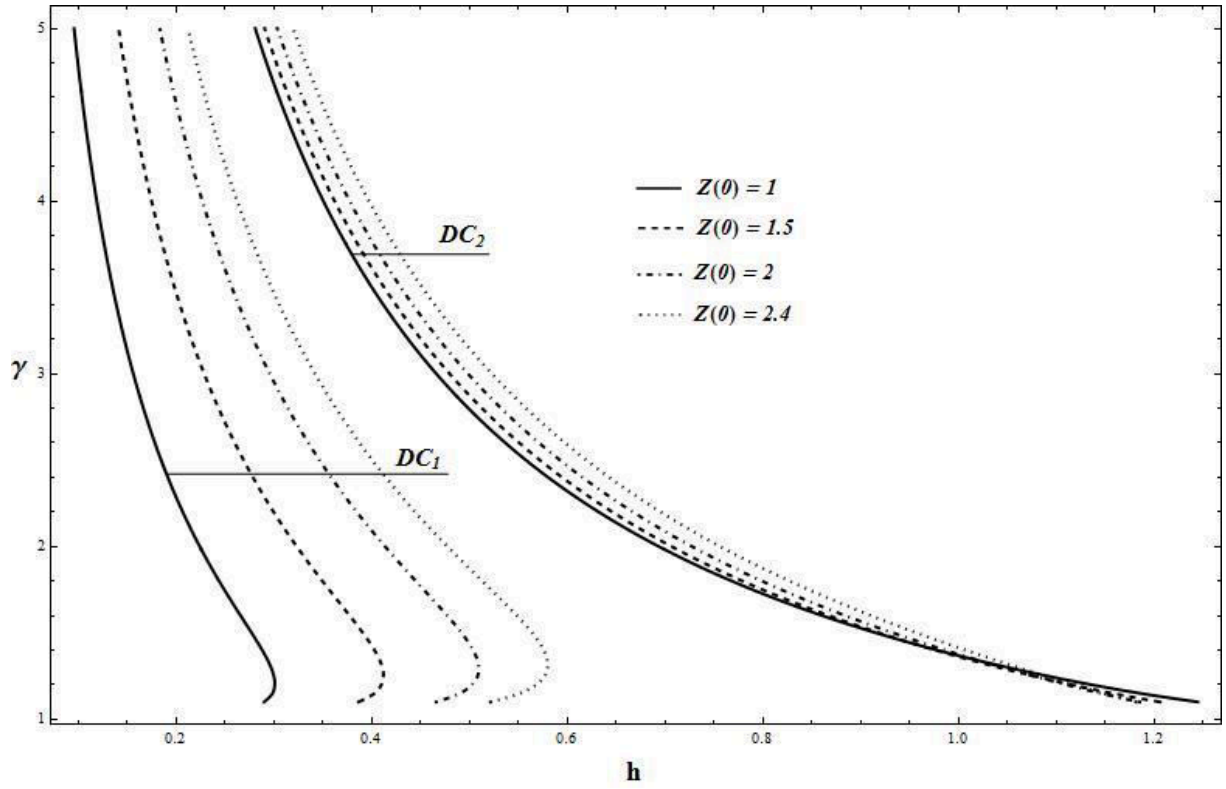

Figure 16: Dependence of the propagation constant γ on the film thickness h evaluated for different values $Z(0)$ (cf. (3.1.14))

Evaluation of the dispersion relation (3.1.14) for small nonlinearity coefficients a, b are depicted in Figure 17. Field components are shown in Figure 18.

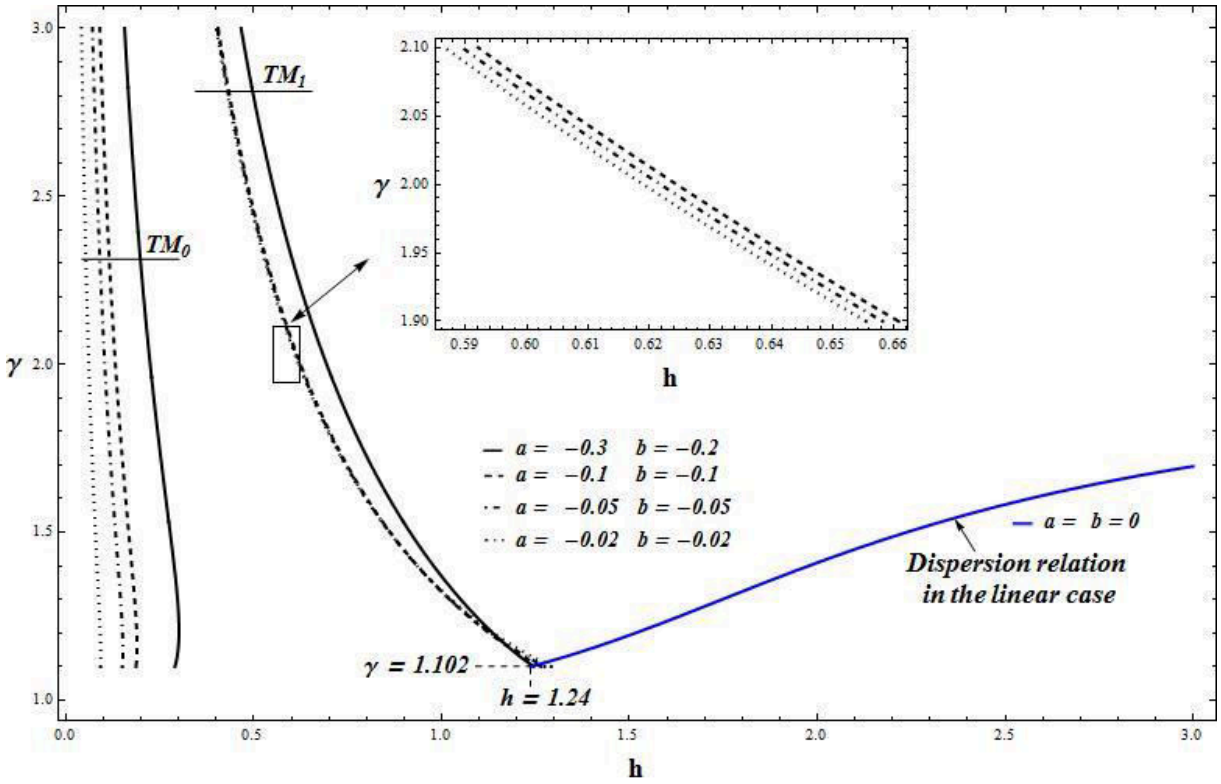

Figure 17: Propagation constant γ versus film thickness h (cf. (3.1.14)) for various nonlinearity coefficients a, b

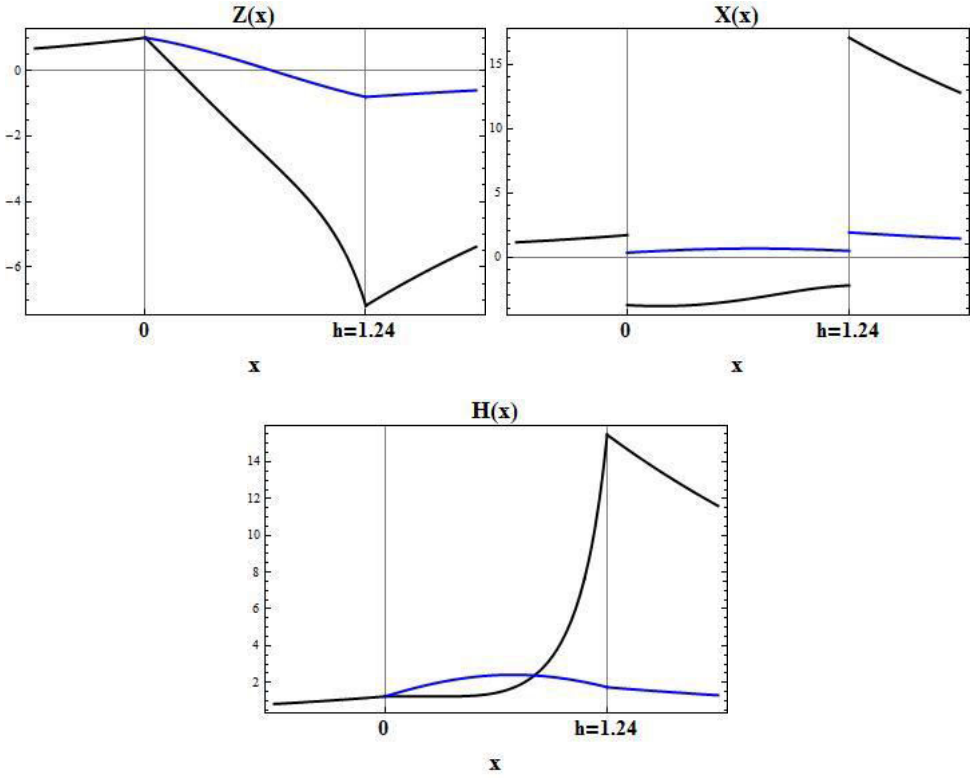

Figure 18: Field profiles for $h = 1.24$ and $\gamma = 1.102$ (cf. Figure 17). Black curve represents the solution in the nonlinear case (cf. (4.1.1), (4.1.2) and (4.1.3)[20]), blue – in the linear one (cf. (C.1.4), (C.1.6) and (C.1.7)).

Figures 19 and 20 describe the total power flow in dependence on the film thickness h associated to the dispersion curves on the Figure 14 (evaluated using equation (3.2.3)).

As shown in Figure 19 the transport of the energy by the TM- waves inside and outside the film exhibits opposite signs $\left(P_f^* < 0,\ P_s^* > 0,\ P_c^* > 0\right)$, moreover the total power flow changes sign at $h_0 = 0.285$. These remarkable results also have been obtained by Boardman A. D. et.al.[22] in the case if the one of the three layers is a metal.

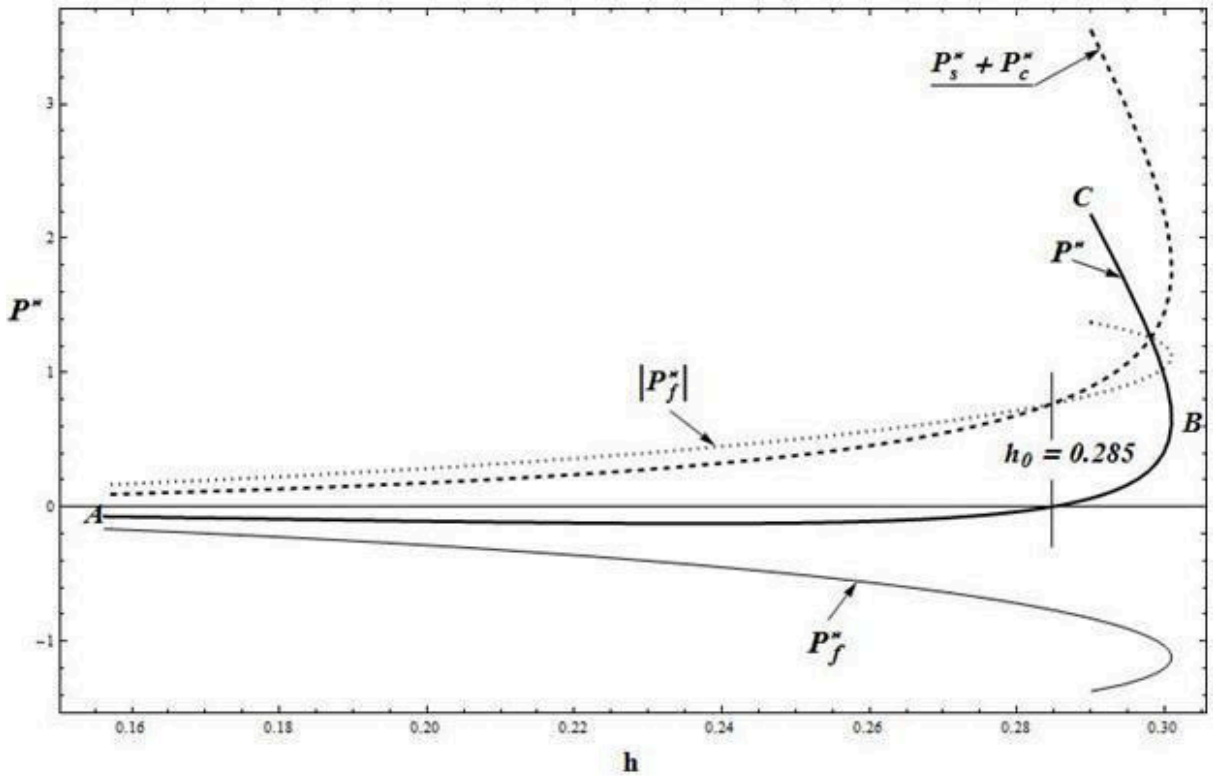

Figure 19: Total power flow P^* and components in the substrate, film and cladding versus film thickness h corresponding to the dispersion curve DC_1 (cf. Figure 14 and (3.2.3)).

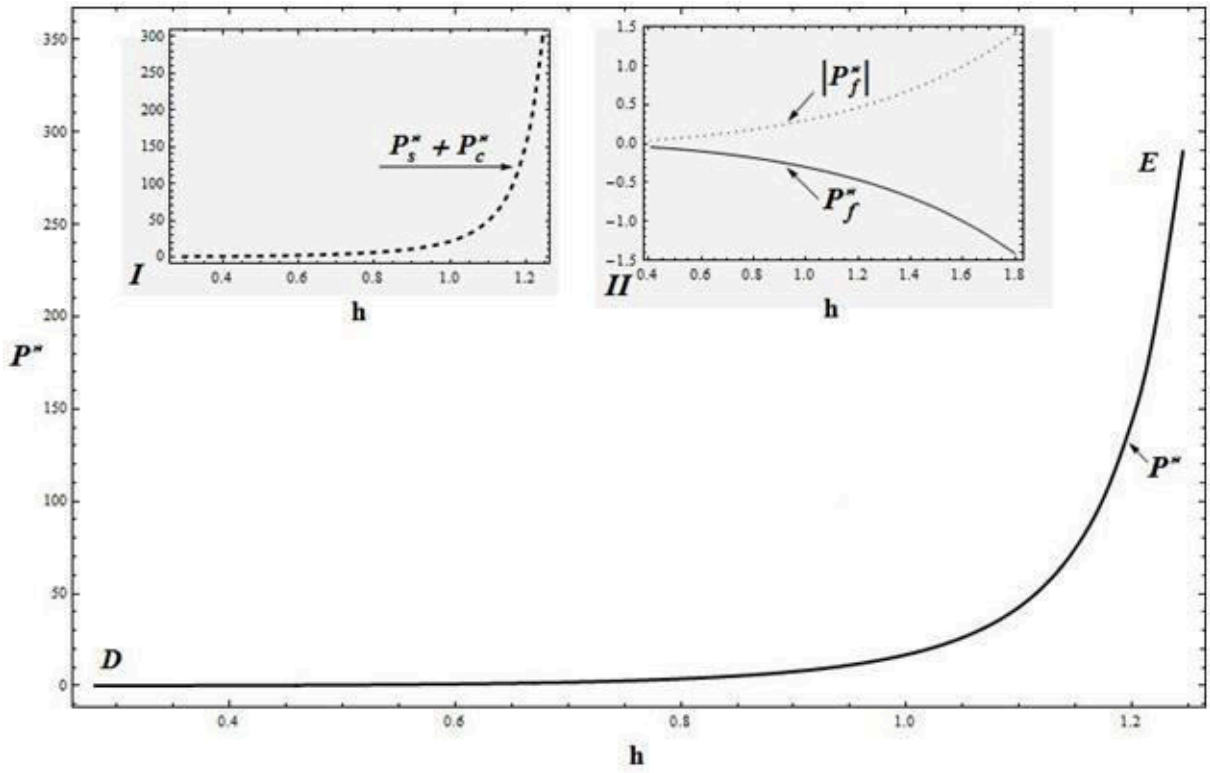

Figure 20: Total power flow P^* and components in the substrate and cladding (gray region I) and in the film (gray region II) versus film thickness h corresponding to the dispersion curve DC_2 (cf. Figure 14 and (3.2.3))

4.1.2.2 Case II

$\left(Z(0) = 1;\ X_2(0+0)\ cf.\ Eq.\ (4.1.6)\right)$

The following numerical evaluation has been performed with

$$1 < \gamma \leq 3. \qquad (4.1.2.2.1)$$

According to the steps I– VII of Section 3 the results are presented in Figures 21-25.

As can be seen in Figure 21 the field components $Z(x)$, $X(x)$ and $H(x)$ are not periodic (the first integral $G(Z,X) = 0$ is not represented by closed curves for each γ in the considered interval (4.1.2.2.1)).

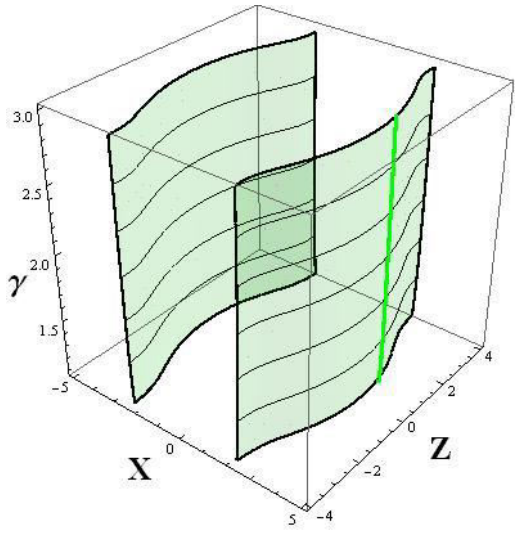

Figure 21: The first integral $G(Z,X,\gamma) = 0$ (cf. (3.1.4)). Solid curve on the right surface depicts solution $X_2(0+0)$ (cf. (4.1.6)).

In the present case solution $X_2(0+0)$ of equation (4.1.6) leads to only one solution of the dispersion relation (3.1.14) (for details see Appendix G) that is shown in Figure 22 together with the corresponding field components.

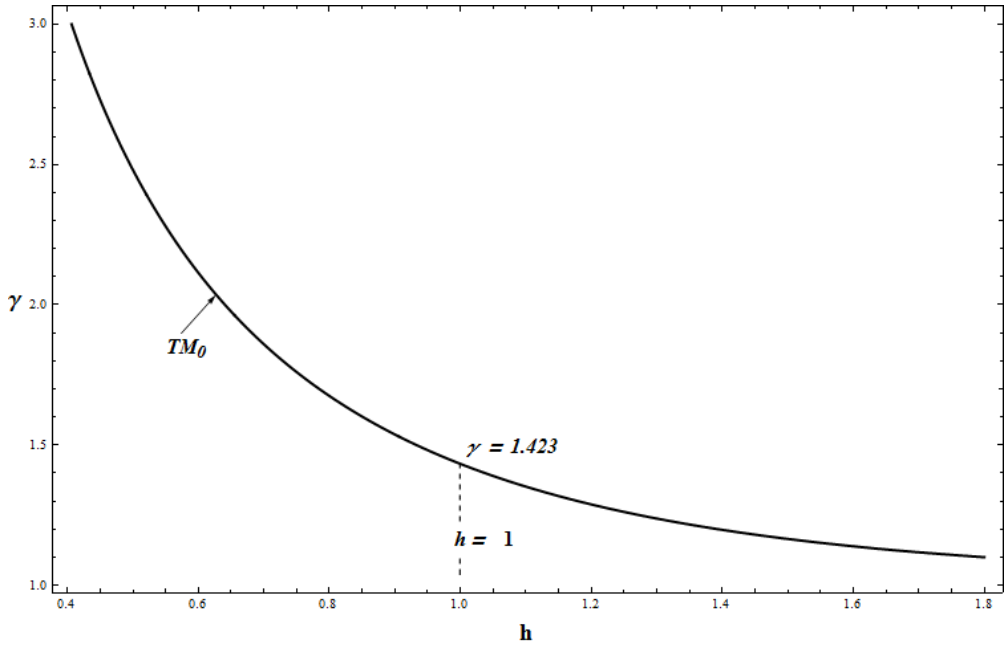

a)

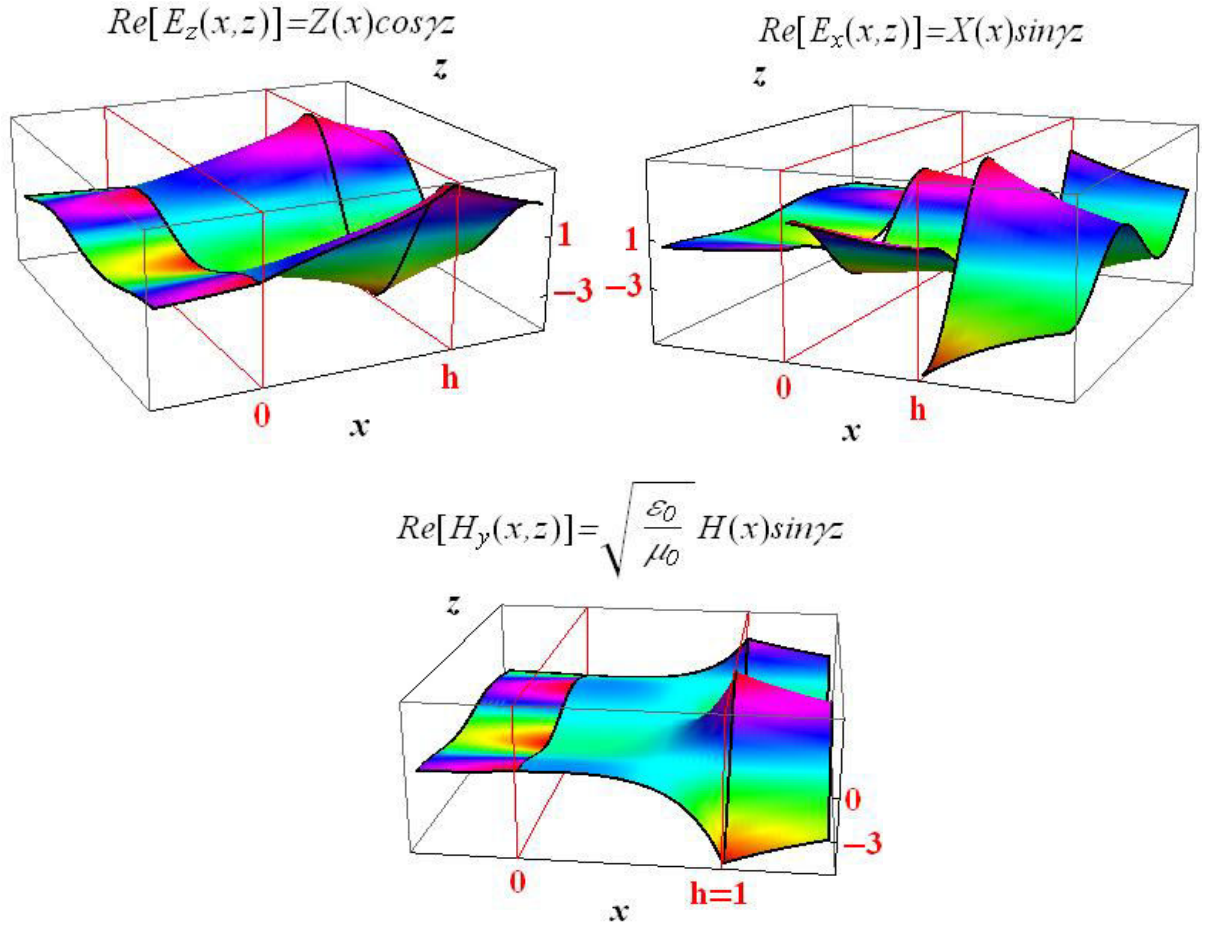

b)

Figure 22: **a)** Solution of the dispersion relation (3.1.14) (TM_0- mode). **b)** Field components for $h = 1, \gamma = 1.423$ (cf. (4.1.1), (4.1.2), (4.1.3), (3.1.23) and (3.1.24)[20])

Evaluating the dispersion relation (3.1.14) with various values $Z(0)$ leads to Figure 23.

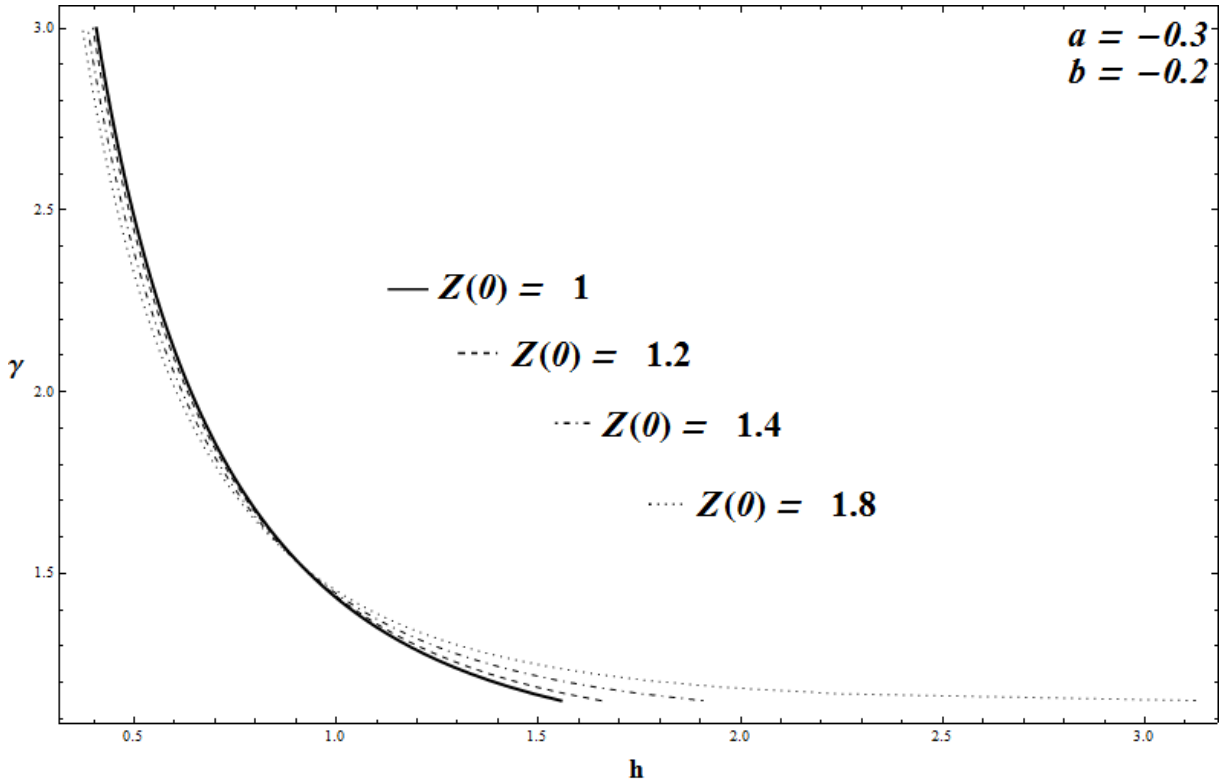

Figure 23: Dependence of propagation constant γ on film thickness h evaluated for the different values of the electric field component $Z(0)$ (cf. (3.1.14))

Figure 24 represents the dispersion relation in the limit $a \to 0,\ b \to 0$. Solutions for the wave functions $Z(x),\ X(x)$ and $H(x)$ are compared with those obtained in the linear case $a = b = 0$.

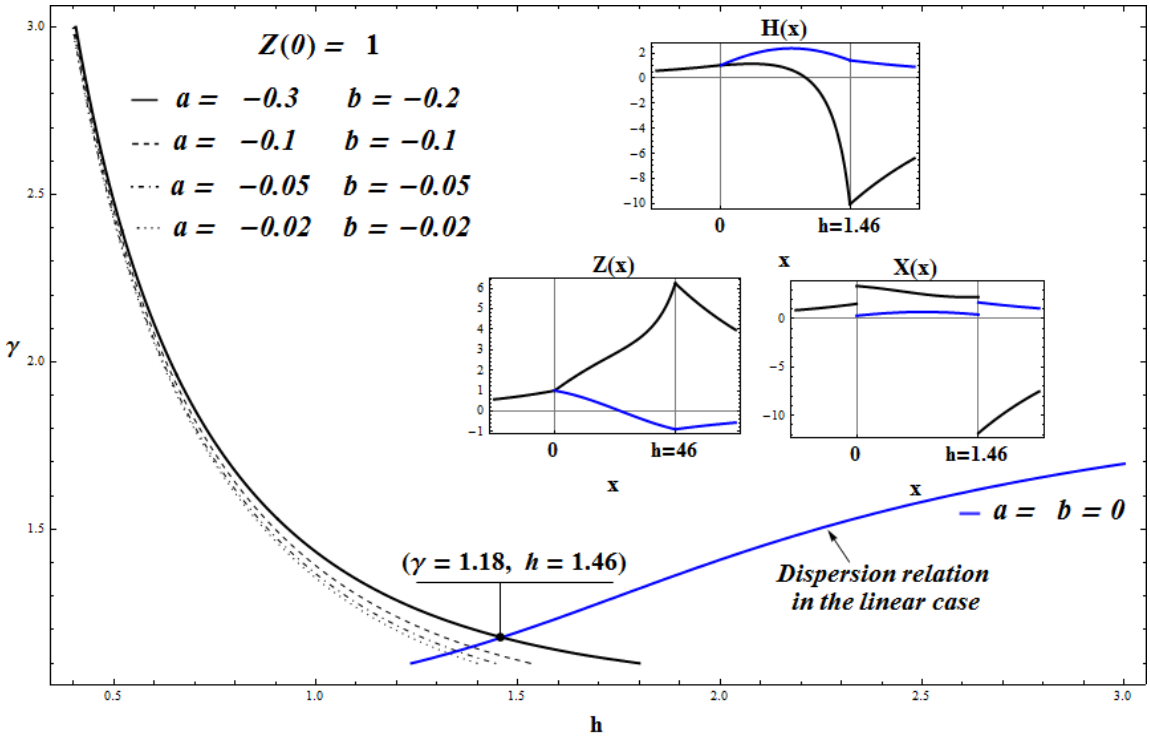

Figure 24: γ versus h (cf. (3.1.14)) for various nonlinearity coefficients a, b. Blue solid curve describes the linear case (cf. (C.1.8)). Field patterns for $h = 1.46$, $\gamma = 1.18$ (cf. (4.1.1), (4.1.2), (4.1.3)[20], (C.1.4), (C.1.6) and (C.1.7))

The power flow in the film, shown in Figure 25, depends on the thickness h similar as in the Case I (cf. Figure 20, p. 51).

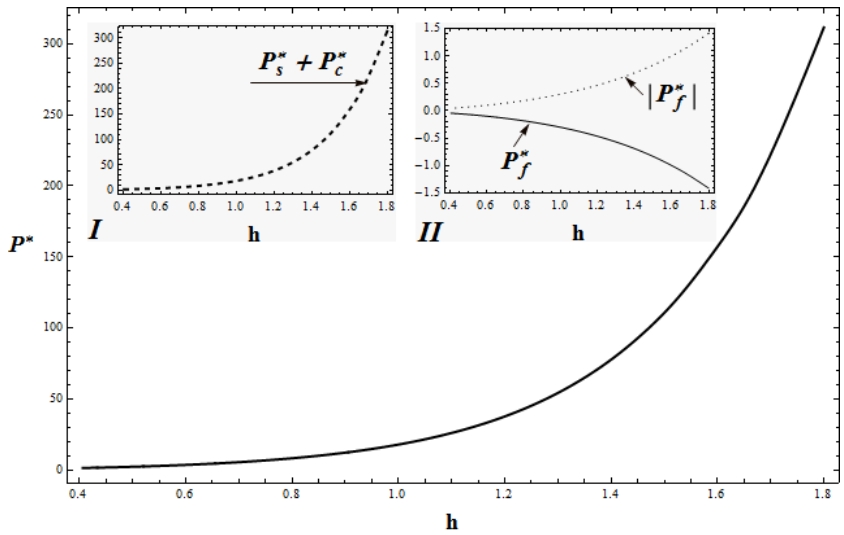

Figure 25: Total power flow P^* versus h (cf. (3.2.3)). Gray region I: power flow $P_s^* + P_c^*$ transported by the nonlinear TM_0- wave outside the film. Gray region II: power flow P_f^* carried by the film

4.1.2.3 Case III

$\left(Z(0)=1; X_3(0+0)\ cf.\ Eq.\ (4.1.6)\right)$

Using the third root $X_3(0+0)$ of (4.1.6) the first integral $G(Z,X)=0$ is represented by closed curves (for various $1<\gamma<4$) as shown in Figure 26.

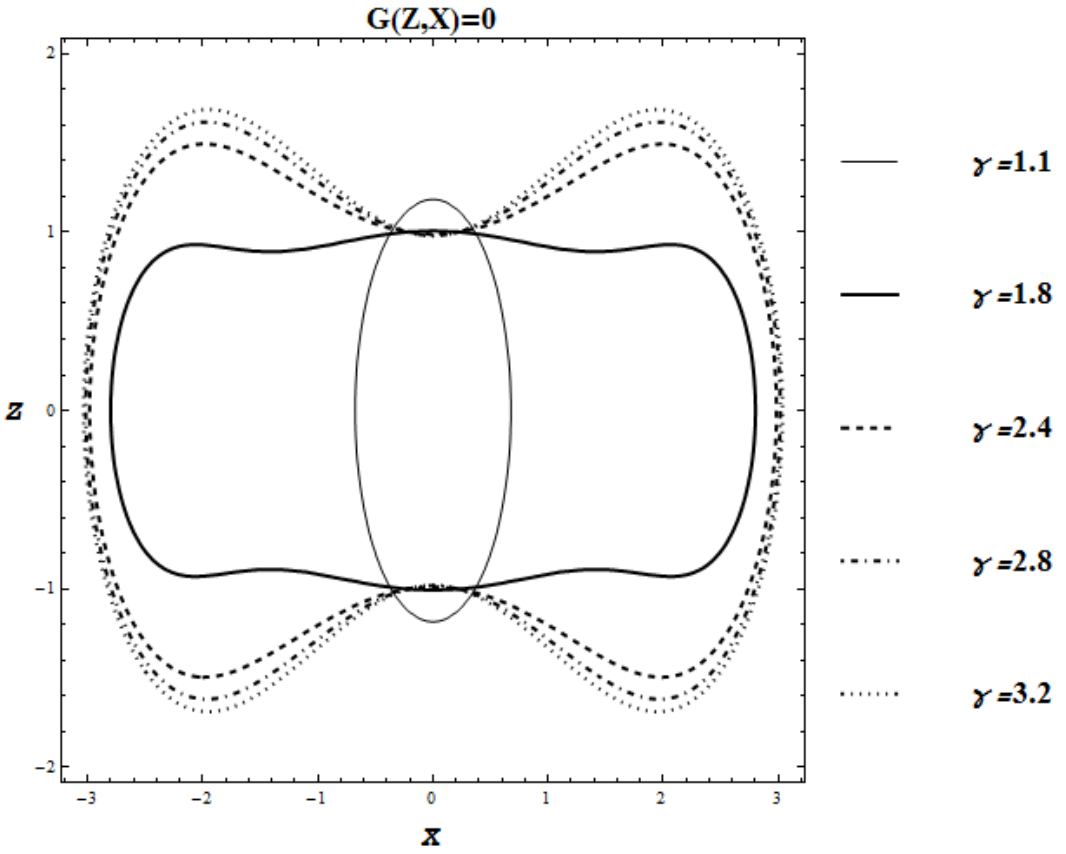

Figure 26: The first integral $G(Z,X)=0$ for various propagation constant γ (cf. (3.1.4))

The associated dispersion relation including higher modes is represented in Figure 27.

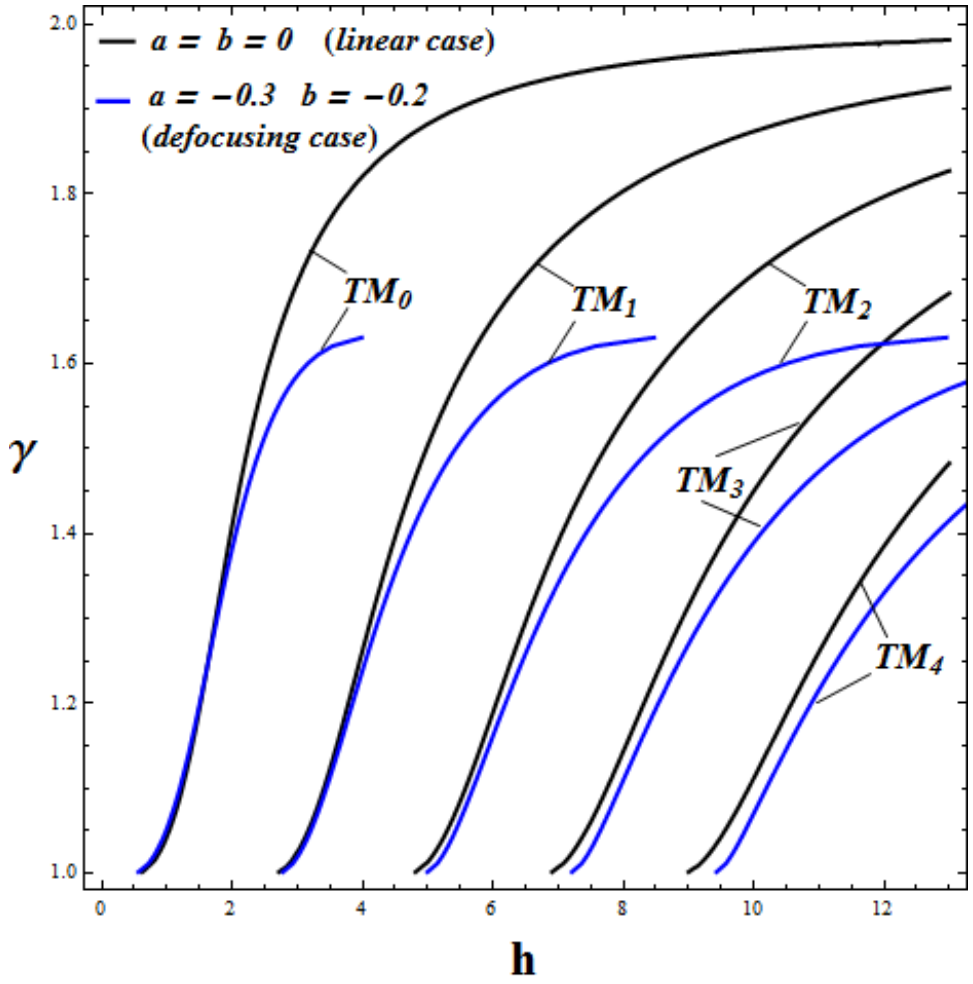

Figure 27: Dispersion relation (3.1.20) (blue curves) and dispersion relation of the linear case (C.1.8) (black curves)

Comparing Figure 26 with Figure 4 (see p. 37) it is obvious that the integral curves (for fixed γ) in the defocusing case III are similar to those in the focusing one. Figure 28 presents graphs of the corresponding dispersion relations for the defocusing, focusing, and linear case (detailed description of the solution for the defocusing case III is given in Appendix H).

For the film thickness $h = 3$ the corresponding field components are shown in Figure 29.

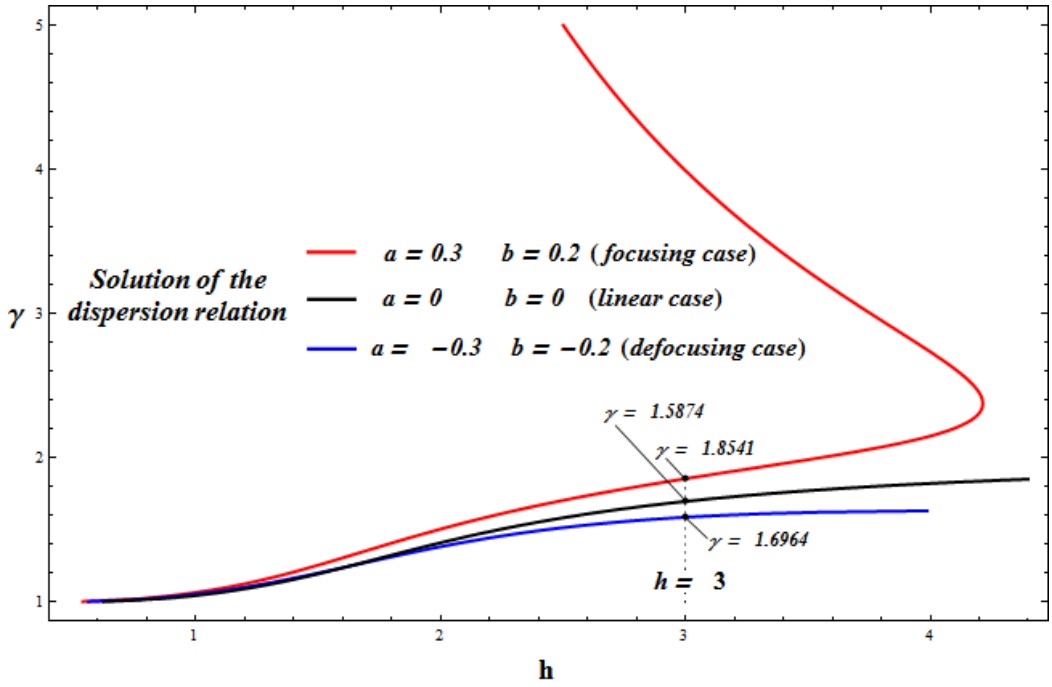

Figure 28: Dispersion relation (3.1.15) for the defocusing (blue curve), focusing (red curve) case, and the linear case (black curve) (cf. equation (C.1.8))

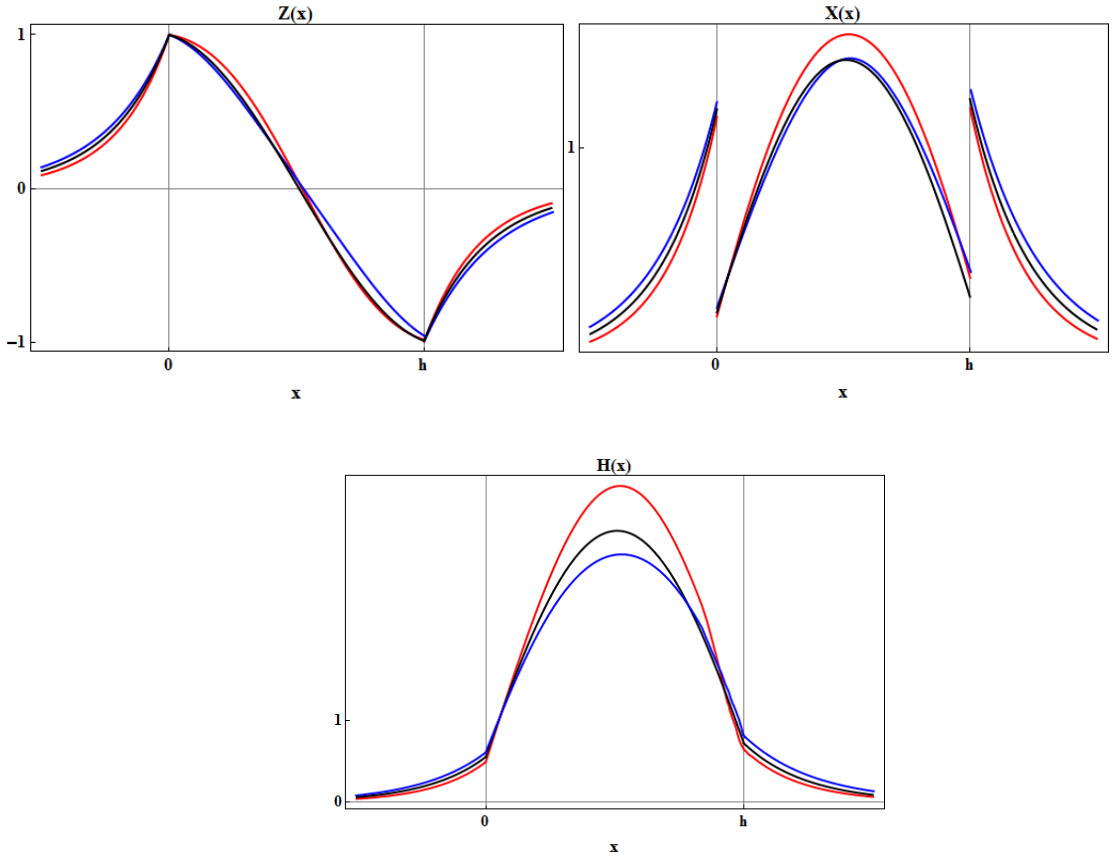

Figure 29: Field components $Z(x)$, $X(x)$ and $H(x)$ of the TM_0- mode propagating in the film of the thickness $h = 3$ (cf. Figure 28 and equations (4.1.1), (4.1.2) and (4.1.3)[20]). Parameters a, b and propagation constants γ according to Figure 28

Solutions of the dispersion relation (3.1.20) for small nonlinearity coefficients a, b are illustrated in Figure 30 (as before, compared with those for the focusing and linear case).

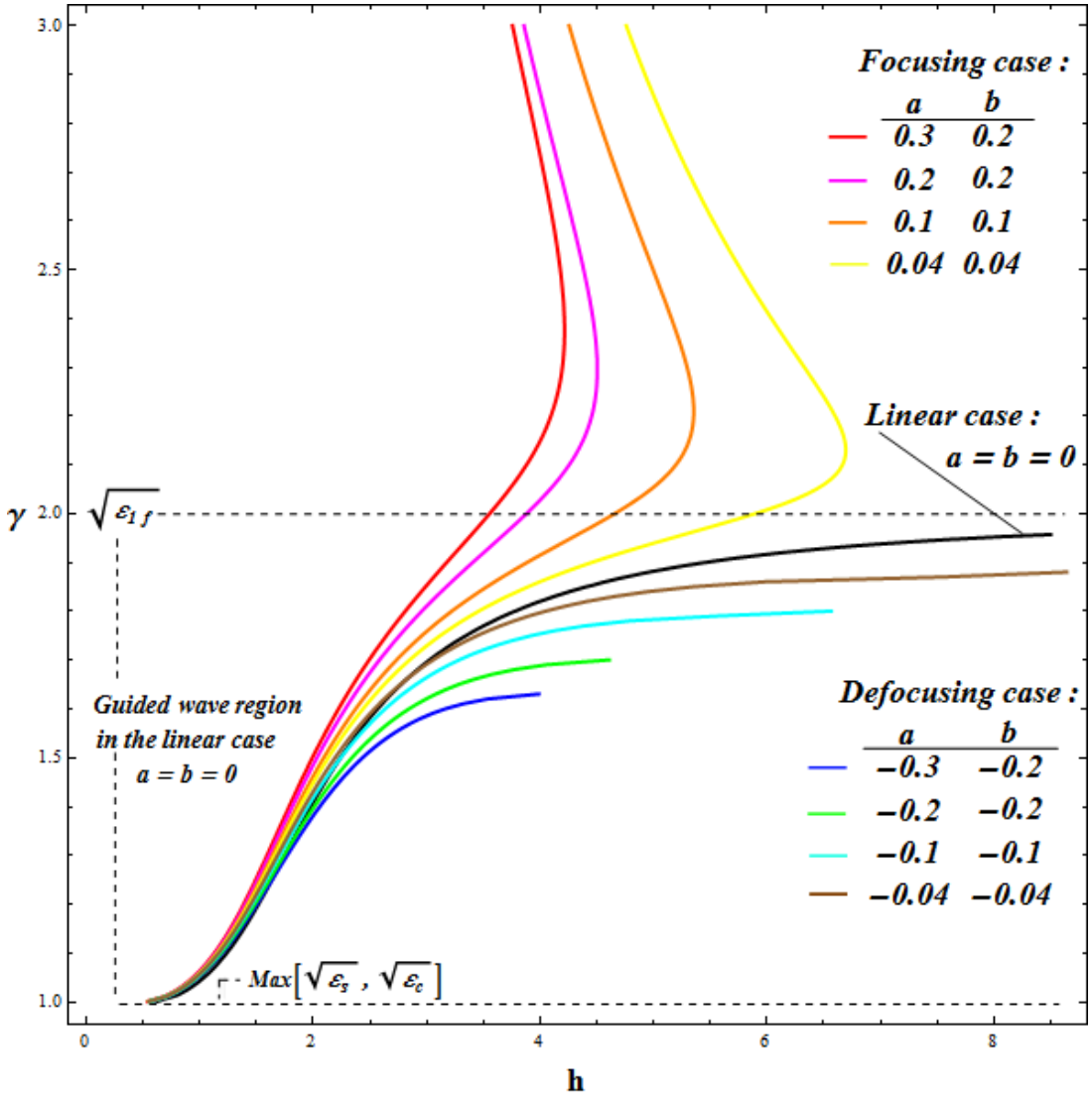

Figure 30: γ versus h for the different values of the nonlinearity coefficients a, b (cf. (3.1.20) and (C.1.8))

For different values of the field intensity $Z(0)$ in the dispersion relation (3.1.20) solutions depicted in Figure 31 are obtained (and compared with the solution for the linear case).

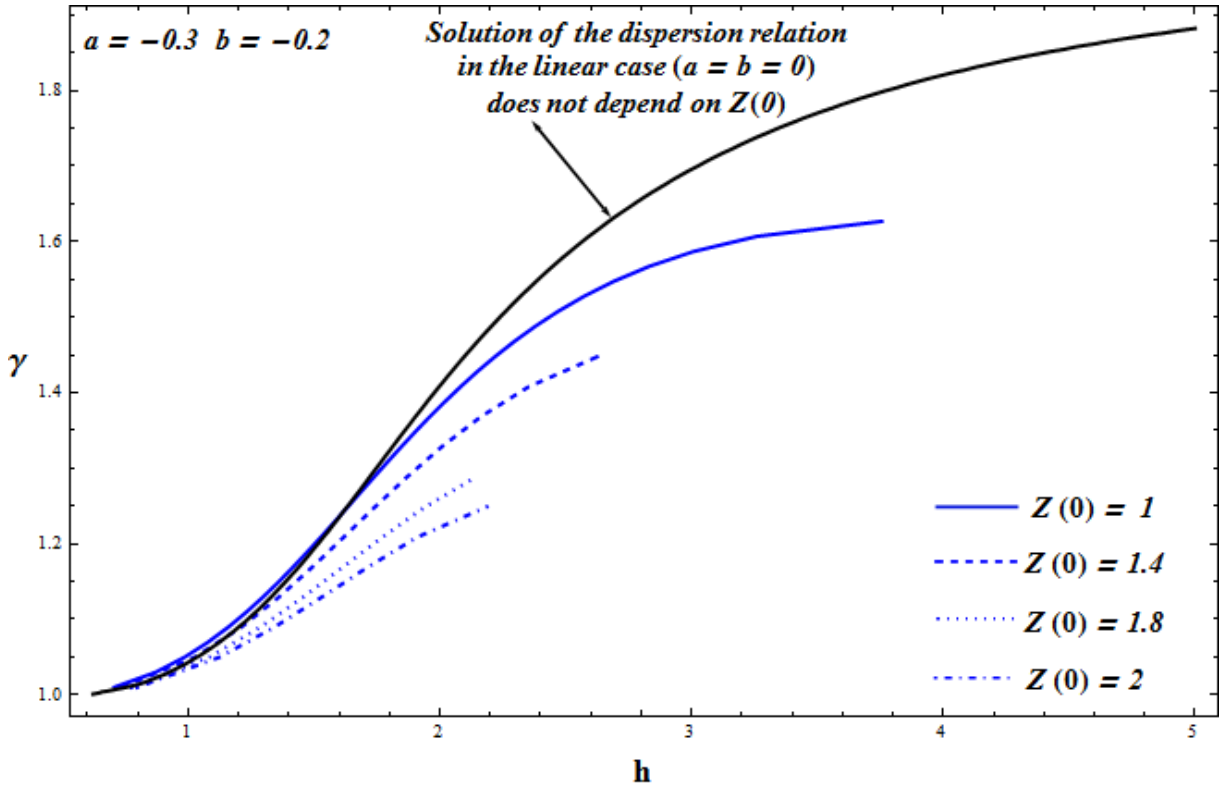

Figure 31: γ versus h for various values of the field component $Z(0)$ (cf. (3.1.20) and (C.1.8)). Colour labelling as in Figure 28

Figures 30, 31 show that the dispersion curves in the defocusing case lie in the "linear" guided wave region ($\gamma < \sqrt{\varepsilon_{1f}}$). This fact is well known in the case of TE- propagation in a defocusing medium[22].

The total power flow transported by the nonlinear TM- wave through the waveguide described by Figures 27, 28 (only defocusing case, blue curves) is shown in Figure 32. Again, the shape of the curves is similar to the shape in the TE case[22].

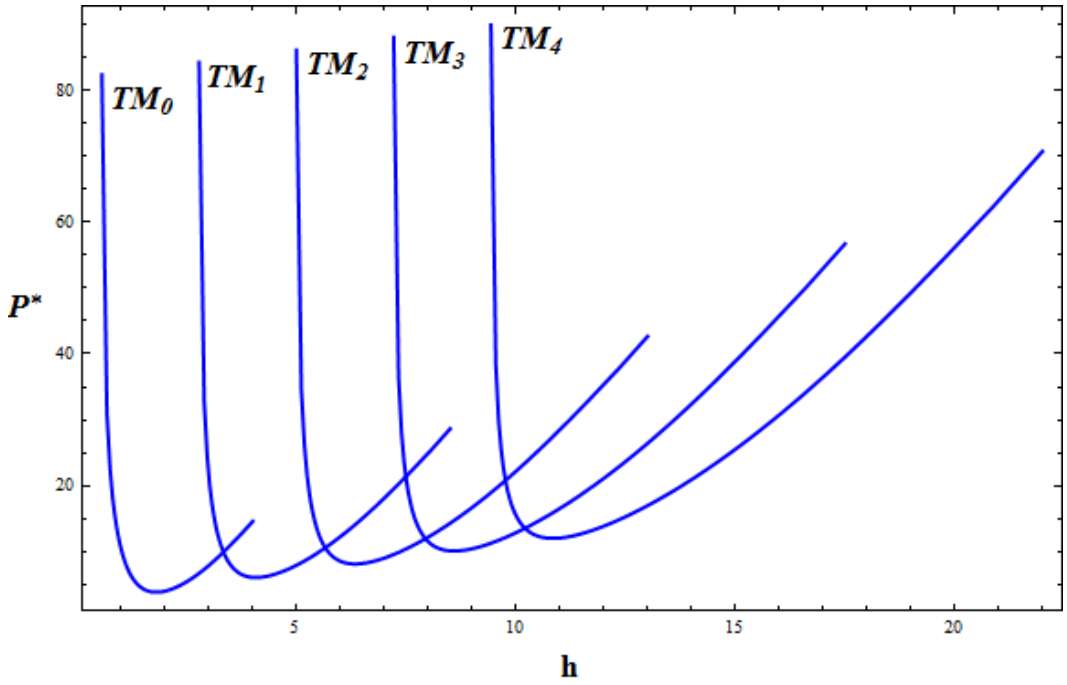

a)

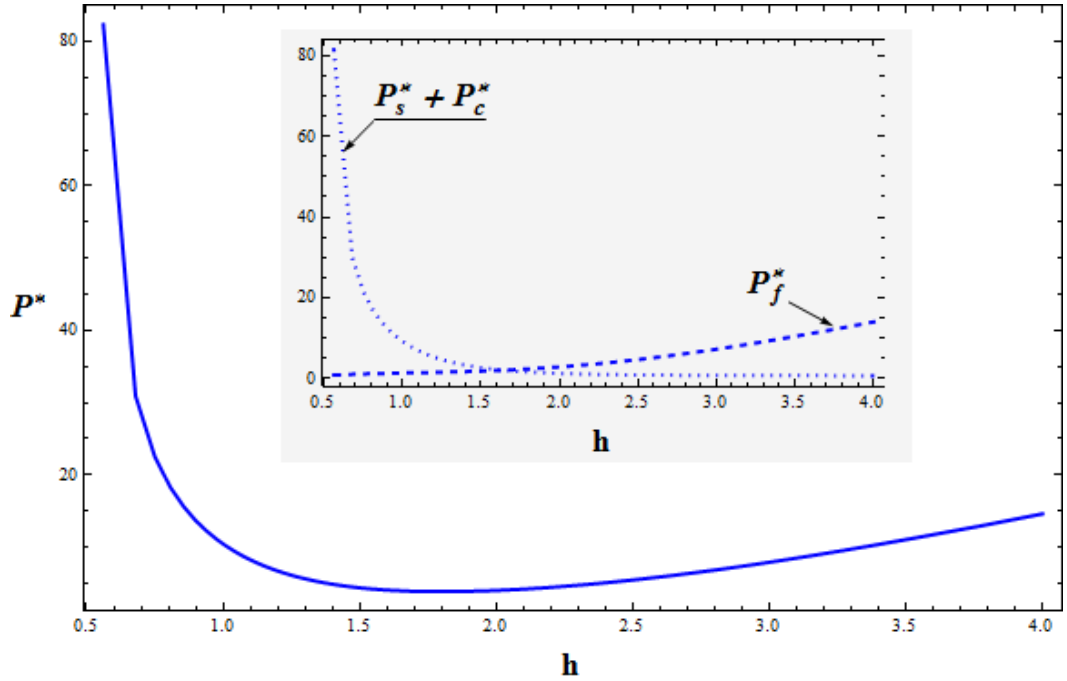

b)

Figure 32: Total power flow P^* versus film thickness h **a)** corresponding to the dispersion (blue) curves of Figure 27 (cf. (3.2.10)) **b)** corresponding to the dispersion (blue) curve of Figure 28 (cf. (3.2.7)). Gray region: separation of the total power flow into power flow carried by the substrate and cladding and power flow through the film

4.1.2.4 Case IV $\left(Z(0) = 3;$ only one real root $X(0+0)$ $cf. Eq. (4.1.6)\right)$

Field components Z and X satisfying equation (3.1.4) are represented in Figure 33 (for each fixed γ in interval $1 < \gamma < 5$). As follows from Figure 33 the functions $Z(x)$, $X(x)$ and $H(x)$ are not periodic.

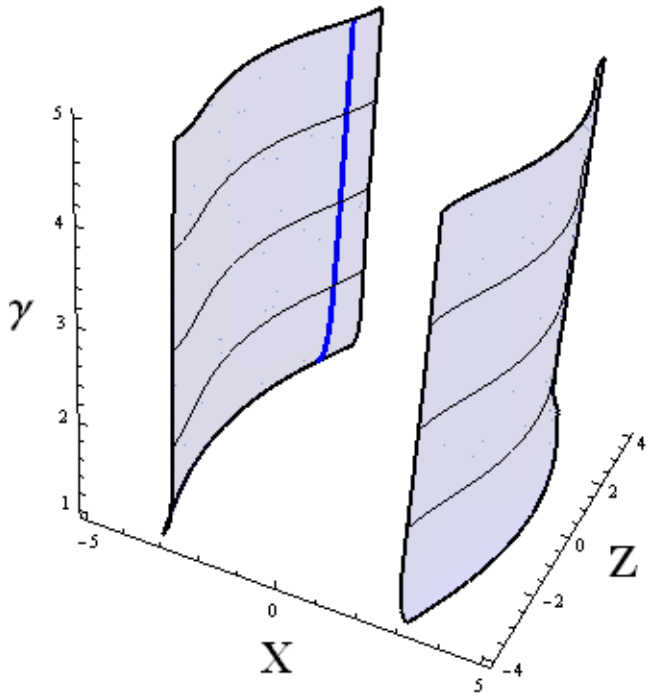

Figure 33: The first integral $G(Z, X, \gamma) = 0$ (cf. (3.1.4)). Solid curve on the right surface depicts the unique real solution $X(0+0)$ of equation (4.1.6).

Following steps I− VII, outlined in Section 3, two solutions of the dispersion relation (3.1.14) are obtained (evaluation proceeds as exemplified in Appendix F). The results are presented in Figure 34.

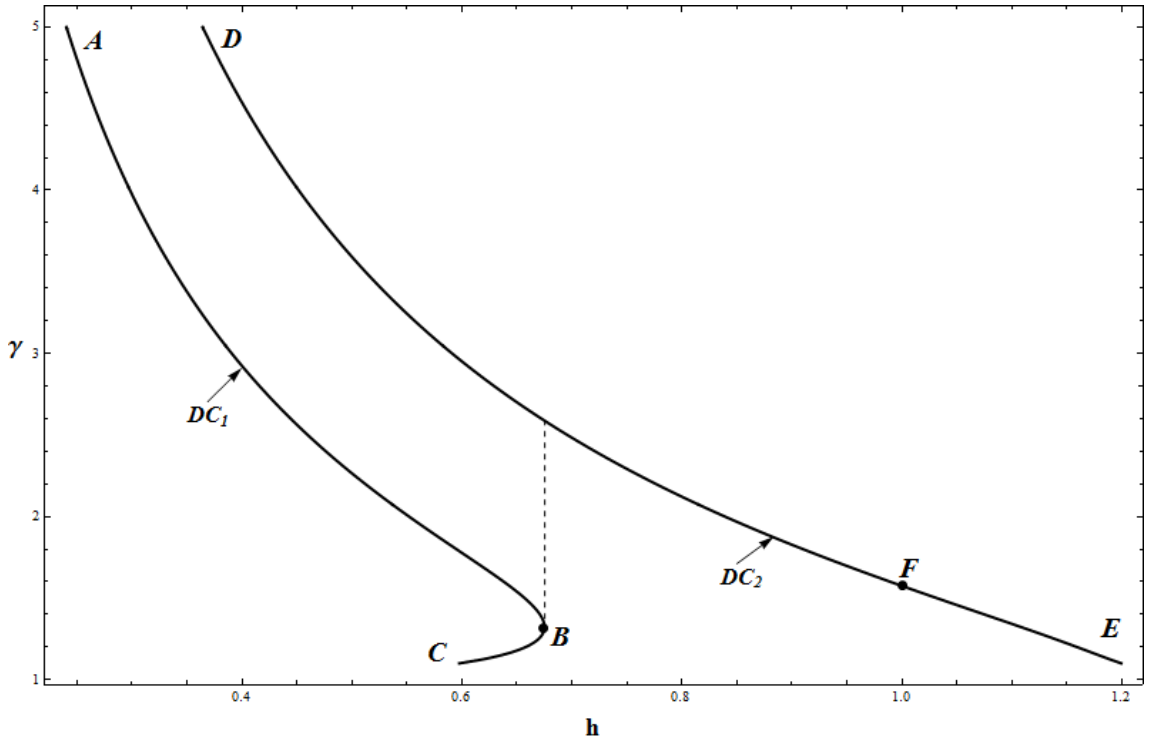

Figure 34: Two solutions of the dispersion relation (cf. (3.1.14)) labelled by DC_1 and DC_2. Point $B(h=0.67,\gamma=1.31)$ is a "switching" point with respect to h.

Profiles of the field components for the film thickness $h=0.67$ and the propagation constant $\gamma=1.31$ (point B on the dispersion curve DC_1 (cf. Figure 34)) are shown in Figure 35.

Figure 36 depicts the field patterns for the point $F\ (h=1,\gamma=1.57)$ (corresponding to the dispersion curve DC_2 (cf. Figure 34)).

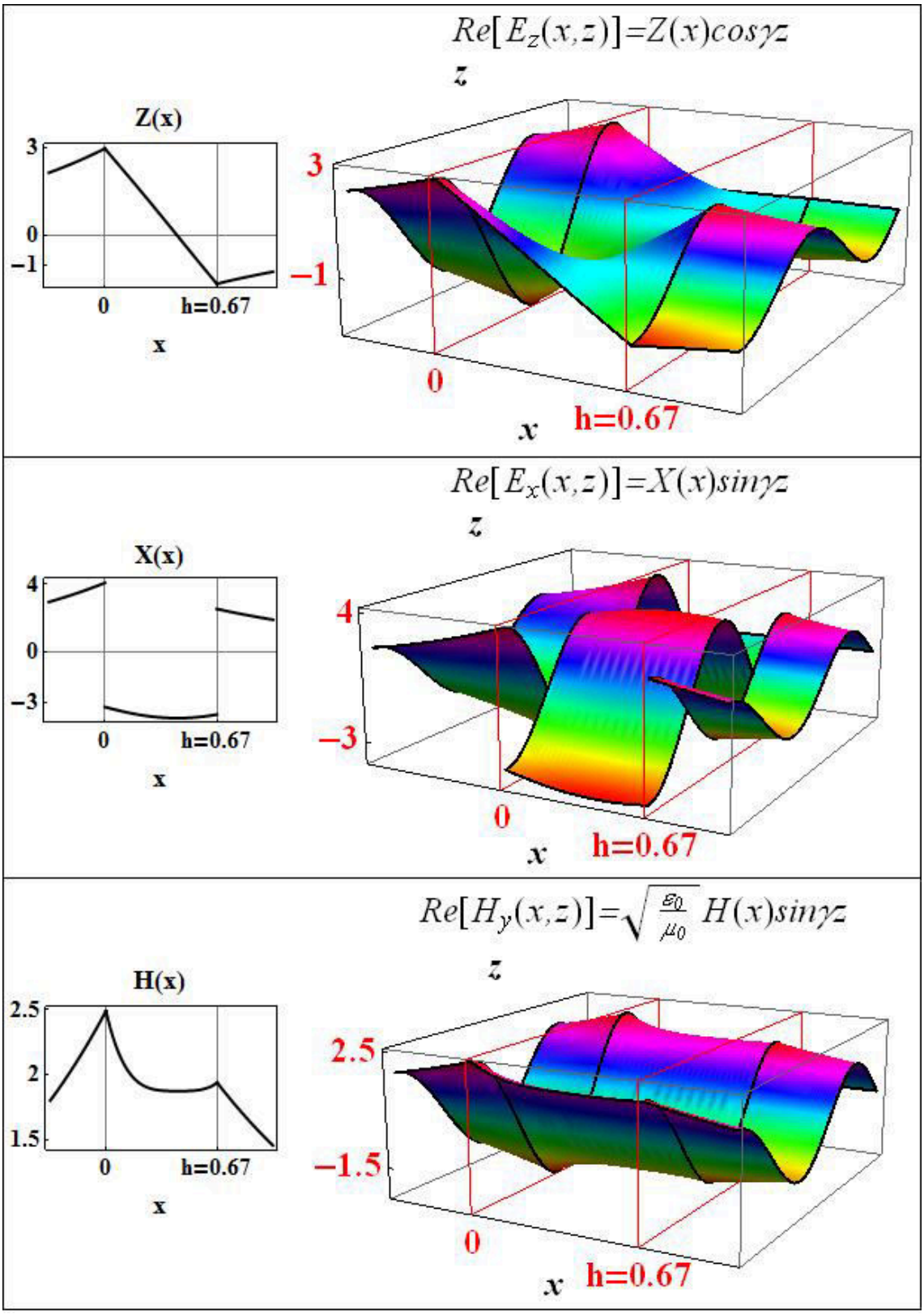

Figure 35: Field patterns of the nonlinear TM_0- wave for $h = 0.67$, $\gamma = 1.31$ (cf. (4.1.1), (4.1.2), (4.1.3), (3.1.23) and (3.1.24)[20])

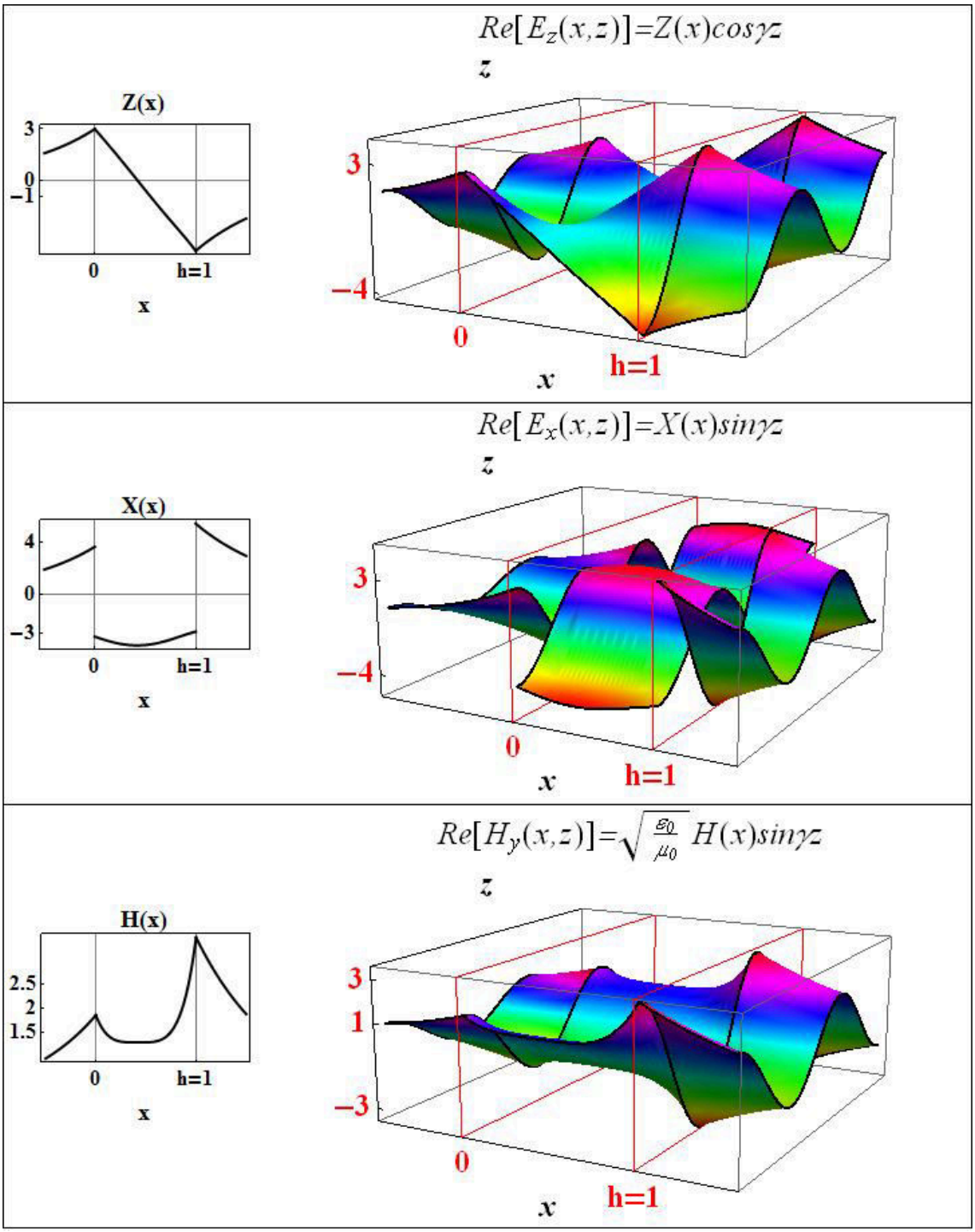

Figure 36: Field patterns of the nonlinear TM_0- wave for $h = 1, \gamma = 1.57$ (cf. (4.1.1), (4.1.2), (4.1.3), (3.1.23) and (3.1.24)[20])

The dependence of the dispersion curves DC_1 and DC_2 (cf. Figure 34) on the field component $Z(0)$ is shown in Figure 37.

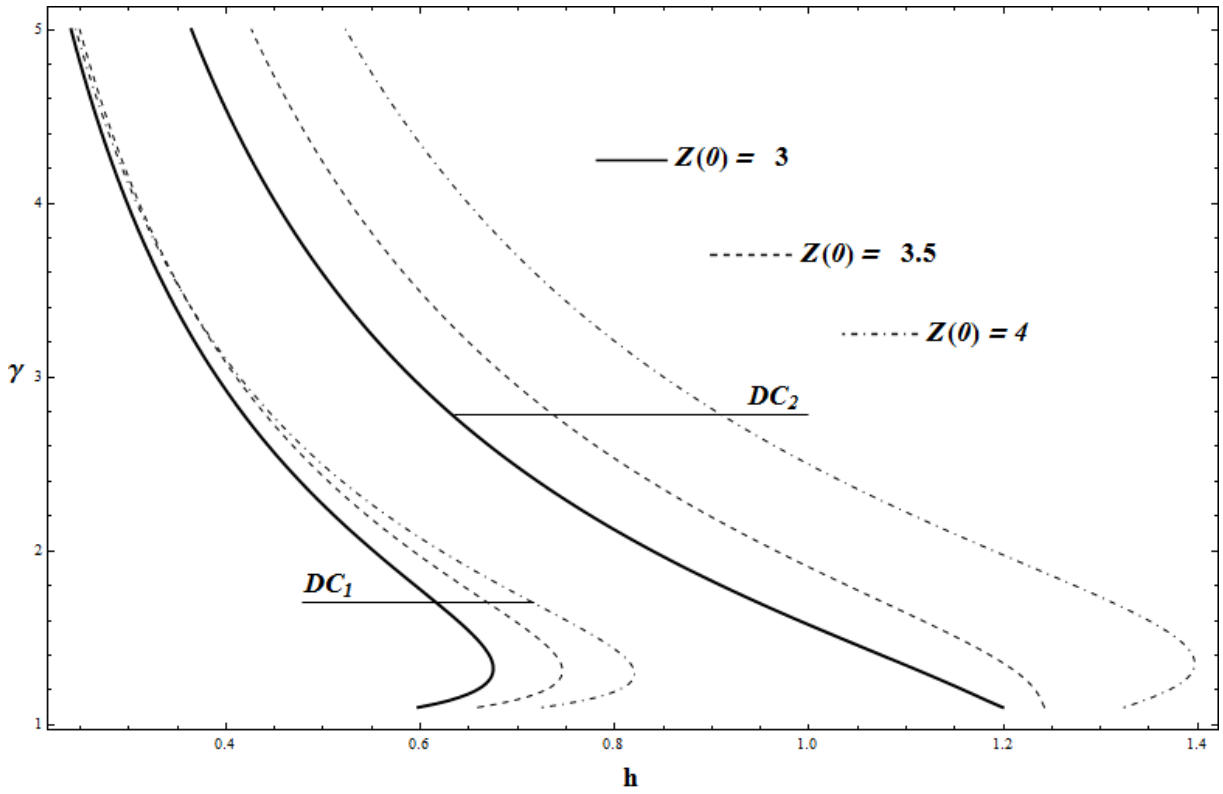

Figure 37: Two solutions of the dispersion relation (3.1.14) evaluated for different values $Z(0)$

Total power flow carried by the nonlinear TM_0- wave (corresponding to the dispersion curves DC_1 and DC_2 in the Figure 34) is given in Figures 38 and 39. As can be seen, also in the present case the total power flow depends on the thickness h similar to Case I (see Figures 19, 20 on pp. 50, 51).

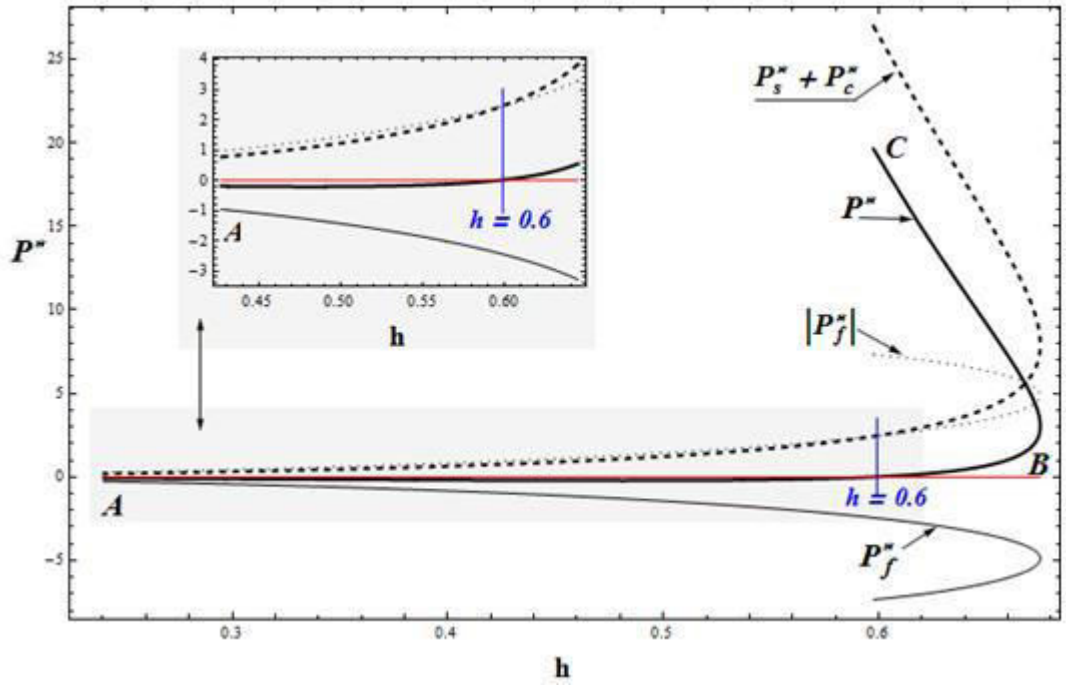

Figure 38: Total power flow P^* and its separation into power flow in the substrate and cladding $(P_s^* + P_c^*)$ and in the film (P_f^*) versus h corresponding to the dispersion curve DC_1 (cf. Figure 34 and (3.2.5)). Gray region shows a part of the total power flow that is negative (for $h < 0.6$)

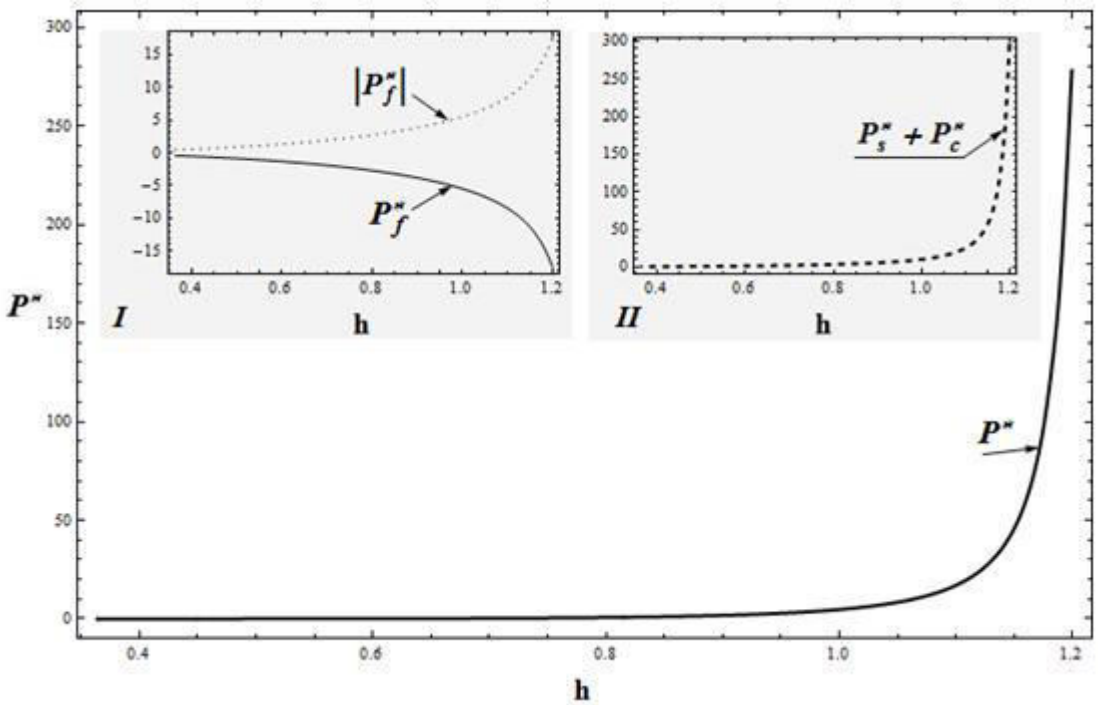

Figure 39: Total power flow P^* and its parts in the substrate and cladding (gray region I) and in the film (gray region II) versus h corresponding to the dispersion curve DC_2 (cf. Figure 34 and (3.2.3))

4.1.3 Special Kerr- nonlinearity of the film $(a_f = 0)$

The present subsection deals with the case of TM- wave- propagation in a nonlinear film by assuming $a_f = a = 0$ (the substrate and cladding are linear).

Following steps the I- VII of Section 3[25] a closed form analytical dispersion relation expressed in terms of elliptic integrals is obtained (see Appendix I).

Equations (2.6), (3.1.4), (3.1.5) and (3.1.9) with $a = 0$ and $\nu = f$ read

$$\begin{aligned} \varepsilon_{xf} &= \varepsilon_{1f} + b\, Z^2(x), \\ \varepsilon_{zf} &= \varepsilon_{2f} + b\, X^2(x), \end{aligned} \tag{4.1.3.1}$$

$$G(Z, X, \gamma) := C_f + \frac{\gamma^2 \varepsilon_{2f}\, Z^2}{2} + \frac{1}{2}\, X^2 \left(\varepsilon_{1f} + b\, Z^2\right)\left(\varepsilon_{1f} + b\, Z^2 - \gamma^2\right) = 0, \tag{4.1.3.2}$$

$$C_f = -\frac{\gamma^2\, \varepsilon_{2f}}{2}\, Z_0^2 - \frac{1}{2}\, X_0^2 \left(\varepsilon_{1f} + b\, Z_0^2\right)\left(\varepsilon_{1f} + b\, Z_0^2 - \gamma^2\right), \tag{4.1.3.3}$$

$$F_Z^{\pm}(Z, \gamma) = \frac{\gamma}{\pm\sqrt{X^2(Z, \gamma)}\left(\gamma^2 - \varepsilon_{1f} - b\, Z^2\right)}. \tag{4.1.3.4}$$

Solving (4.1.3.2) with respect to X^2 (assuming that $X^2 > 0$) and using (4.1.3.4) the dispersion relation (3.1.14) is written as

$$DR_z\left(\gamma, Z(0), \varepsilon_s, \varepsilon_{1f}, \varepsilon_{2f}, \varepsilon_c, b\right) = \int_{Z(0)}^{Z(h,\gamma,Z(0))} \frac{\gamma d\zeta}{\pm\sqrt{-\dfrac{2\, C_f + \gamma^2 \varepsilon_{2f} \zeta^2}{(\varepsilon_{1f} + b\, \zeta^2)(\varepsilon_{1f} + b\, \zeta^2 - \gamma^2)}} \times \left(\gamma^2 - \varepsilon_{1f} - b\, \zeta^2\right)} = h > 0. \tag{4.1.3.5}$$

The primitive function of the integral in (4.1.3.5) (omitting the sign " $\pm$ ") reads

$$\Phi[z] = \alpha_1(z)\, F[\varphi(s(z))|m] + \alpha_2\,(z)\, \Pi(n; \varphi(s(z))|m), \tag{4.1.3.6}$$

where $F[\varphi(s(z))|m]$ and $\Pi(n; \varphi(s(z))|m)$ denote the elliptic integrals of the first and third kinds, respectively[26], and $\alpha_1(z), \alpha_2(z), \varphi(s(z)), m, n,$ are defined in Appendix I.

The period for higher mode solutions of the dispersion relation (4.1.3.5)[27] is given by[28] (cf. (3.1.18))

$$T_Z = \left| \oint_{G(Z,X,\gamma)=0} F_Z^{\pm}(\zeta, \gamma) d\zeta \right|. \tag{4.1.3.7}$$

According to (3.1.20) $N \cdot T_Z$ $(N = 1,2,3, \dots)$ has to be added on the left- hand side of (4.1.3.5), hence, the dispersion relation including higher modes reads

$$h_N = (h + \mathrm{k} \cdot T_Z) + N \cdot T_Z\,, \tag{4.1.3.8}$$

where

$$\mathrm{k} = \begin{cases} 0, & \text{if } h > 0, \\ 1, & \text{if } h < 0. \end{cases}$$

Using (3.2.3) and (B.1.10) the total power flow is written as

$$P_Z^* = \frac{\varepsilon_{1s}\, \gamma\, Z^2(0)}{2\sqrt{(\gamma^2 - \varepsilon_{1s})^3}} + P_{film,Z}^{\pm} + \frac{\varepsilon_{1c}\, \gamma\, Z^2(h)}{2\sqrt{(\gamma^2 - \varepsilon_{1c})^3}}, \tag{4.1.3.9}$$

where the power flow in the film is

$$P_{film,Z}^{\pm} = \pm \int_{Z(0)}^{Z(h,\gamma,Z(0))} \frac{(\varepsilon_{1f} + b\,\zeta^2)}{(\gamma^2 - \varepsilon_{1f} - b\,\zeta^2)} \sqrt{-\frac{2\,C_f + \gamma^2 \varepsilon_{2f} \zeta^2}{(\varepsilon_{1f} + b\,\zeta^2)(\varepsilon_{1f} + b\,\zeta^2 - \gamma^2)}}\, d\zeta. \tag{4.1.3.10}$$

The primitive function of the integral in (4.1.3.10) (omitting sign " $\pm$ ") reads

$$\mathcal{P}[z] = \beta_1(z)\, E\big[\varphi\big(m \cdot s(x)\big)\big|m\big] + \beta_2(z)\, F\big[\varphi\big(m \cdot s(x)\big)\big|m\big] + \\ + \beta_3\,(z)\, \Pi\big(n; \varphi\big(m \cdot s(x)\big)\big|m\big) + \beta_4(z), \tag{4.1.3.11}$$

where $E\big[\varphi\big(m \cdot s(x)\big)\big|m\big]$ denotes the elliptic integrals of the second kind[26] and $\beta_1(z), \beta_2(z), \beta_3(z), \beta_4(z)$ are defined in Appendix I.

If Z, X are periodic[27] the total power flow for higher modes is given by (cf. (3.2.10) and (3.2.11))

$$P_N^* = (P_Z^* + \mathrm{k} \cdot T^*) + N \cdot T^* \tag{4.1.3.12}$$

with[28]

$$T^* = \left| \oint_{G(Z,X,\gamma)=0} P_{film,Z}^{\pm}(\zeta, \gamma) d\zeta \right|. \tag{4.1.3.13}$$

Using (4.1.3.6) and (4.1.3.11) the dispersion relation including higher modes and the total power flow can be evaluated straightforwardly (detailed description is given in Appendix I).

To illustrate the results the material parameters are chosen as:

$$\varepsilon_{1s} = \varepsilon_{2s} = \varepsilon_s = 1, \qquad \varepsilon_{1c} = \varepsilon_{2c} = \varepsilon_c = 4, \qquad \varepsilon_{1f} = 9,\ \varepsilon_{2f} = 6,$$
$$a_s = b_s = a_c = b_c = a_f = 0.$$

Figure 40 presents a contour plot of the first integral $G(Z, X) = 0$ (for fixed γ) for positive and negative nonlinear coefficient b. It seems (analytical evaluation is rather involved) that closed curves only exist for $\gamma < \sqrt{\varepsilon_{1f}} = 3$.

Further numerical evaluation for different values of b yields the same result. Thus it seems that $Z(x), X(x)$ and $H(x)$ are in general periodic only for $\gamma < \sqrt{\varepsilon_{1f}}$ (subject to the above material parameters).

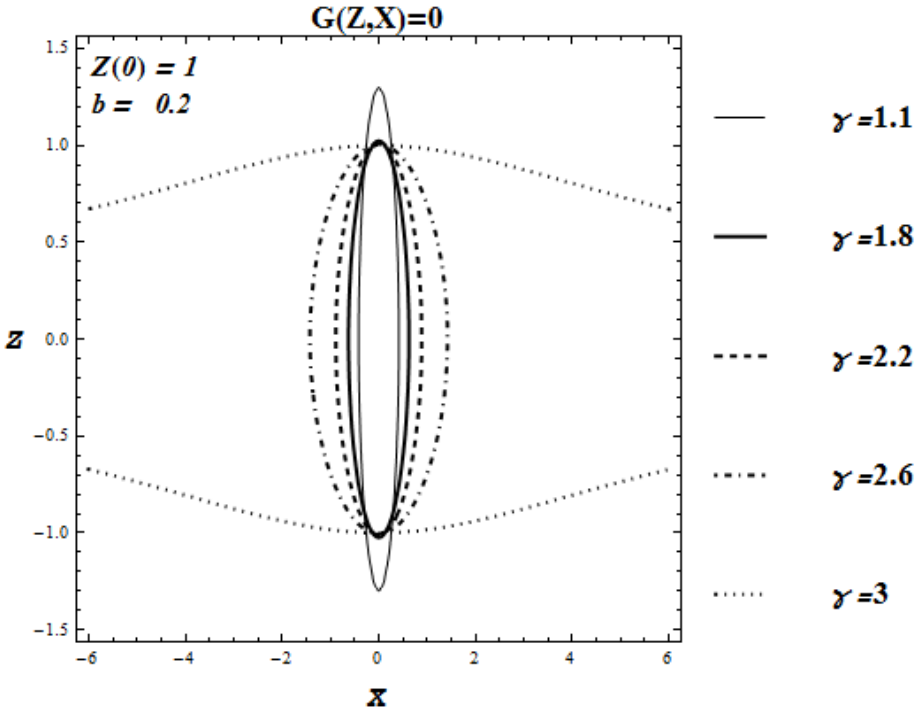

a)

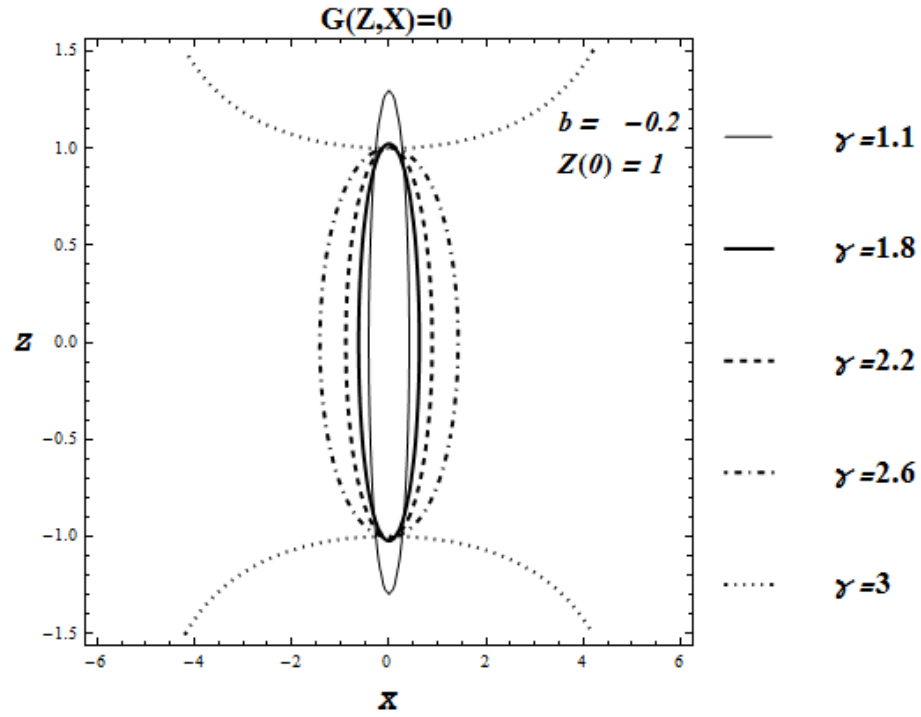

b)

Figure 40: The first integral $G(Z, X, \gamma) = 0$ (cf. (4.1.3.5)) for **a)** $b = 0.2$, **b)** $b = -0.2$

Evaluation of equation (4.1.3.5) for various nonlinearity coefficients b in comparison with the solution of the linear problem ($b = 0$) are depicted in Figure 41.

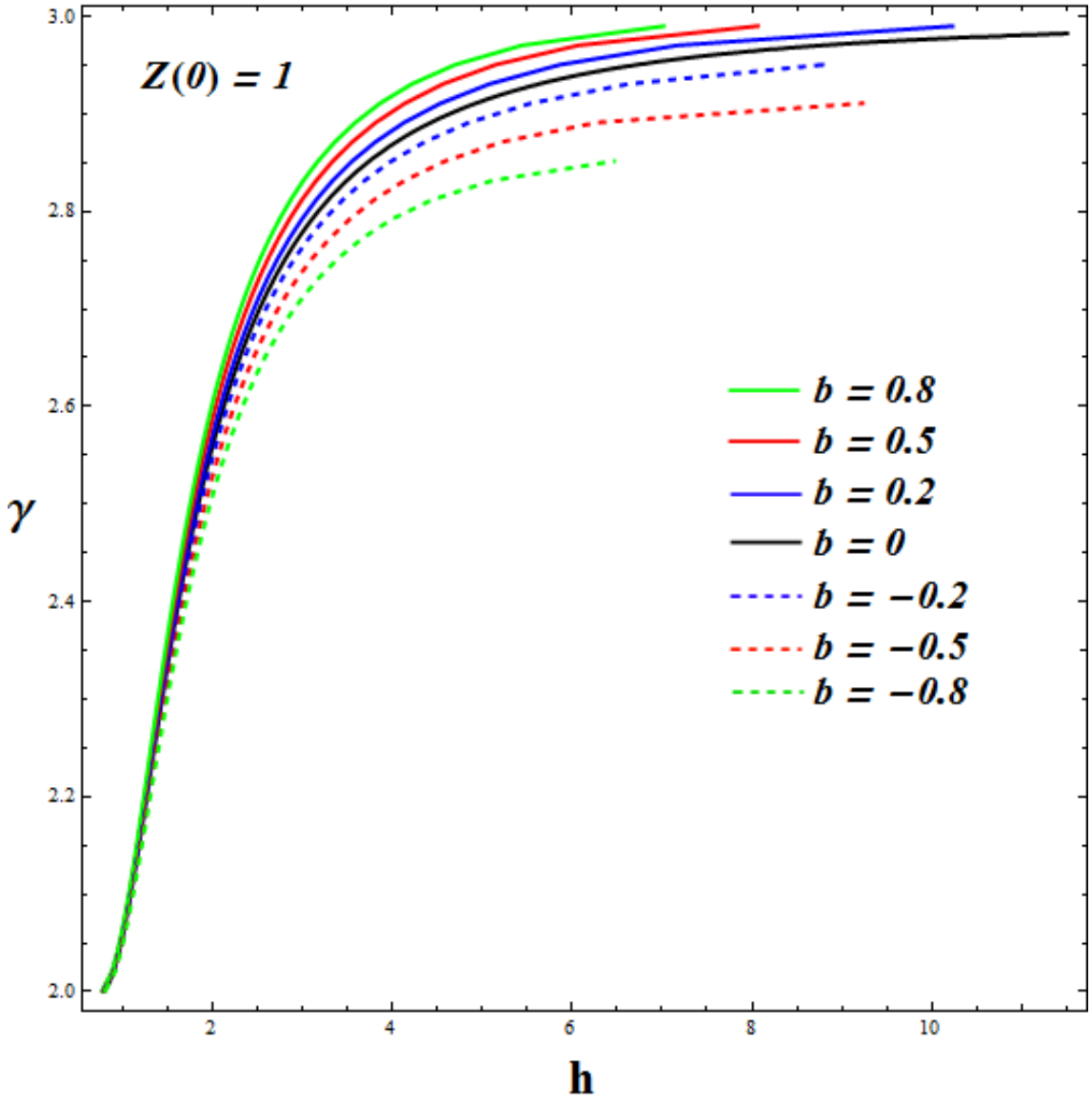

Figure 41: Dispersion relation (cf. (4.1.3.5)) evaluated for different values b $(Z(0) = 1)$

Using (4.1.3.8) the dispersion relation including higher modes is evaluated. Results are shown in Figure 42.

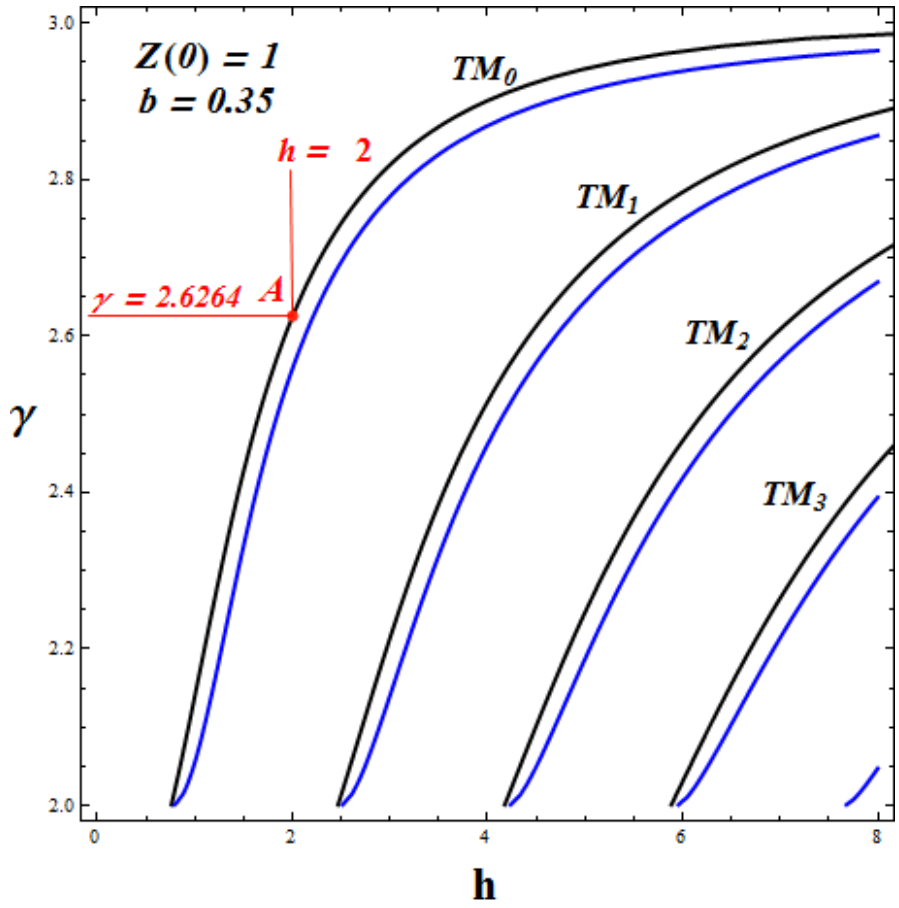

Figure 42: γ versus h (cf. (4.1.3.8)) ($b = 0.35$). Blue curves represent higher mode solutions of the linear case ($b = 0$) (cf. C.1.8).

Field patterns for the film thickness $h = 2$ and the propagation constant $\gamma = 2.6264$ (point A on the TM_0- mode in Figure 42) are presented in Figure 43.

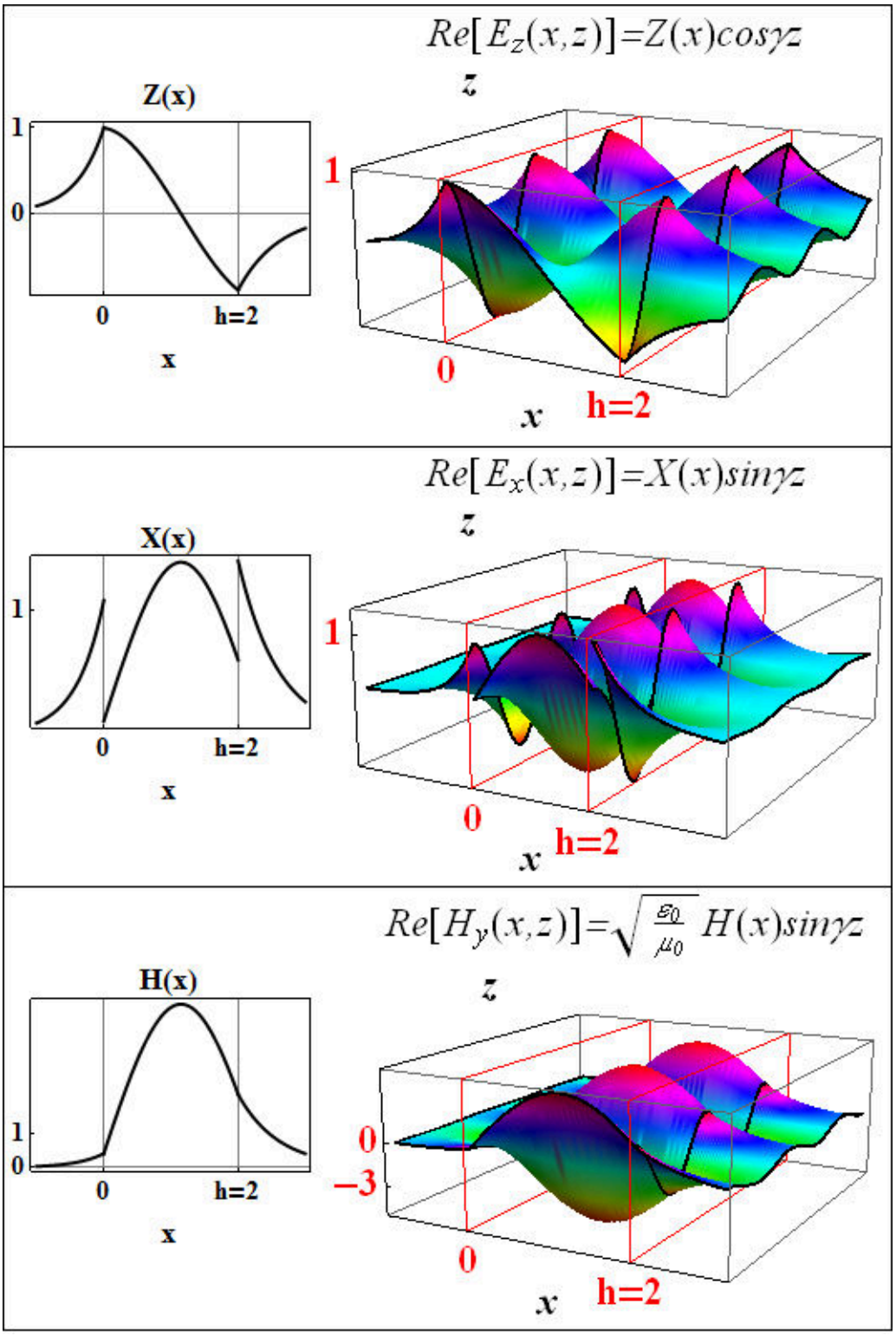

Figure 43: Field patterns $Z(x)$, $X(x)$ and $H(x)$ for the nonlinear TM_0- mode (cf. (4.1.1), (4.1.2), (4.1.3), (3.1.23) and (3.1.24)[20]) propagating in the film with the thickness $h = 2$ and the propagation constant $\gamma = 2.6264$ $(b = 0.35)$ (cf. Figure 42)

Solutions of the dispersion relation (4.1.3.5) for various $Z(0)$ are shown in Figure 44.

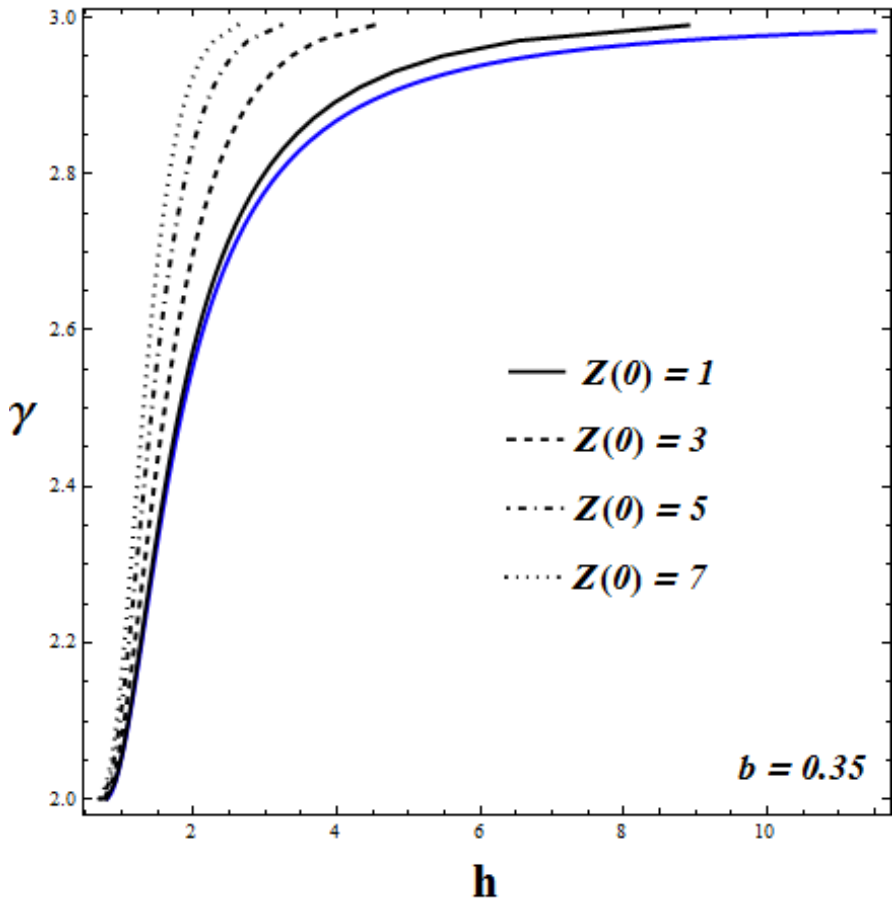

Figure 44: γ in dependence on h (cf. (4.1.3.5)) evaluated for different values of the field component $Z(0)$ ($b = 0.35$). Blue curve: linear case ($b = 0$; $Z(0) = 1$)

Using (4.3.1.9) the total power flow carried by the nonlinear TM_0- wave is evaluated for various nonlinearity coefficients b. Results are depicted in Figure 45. Figure 46 represents the total power flow for higher modes.

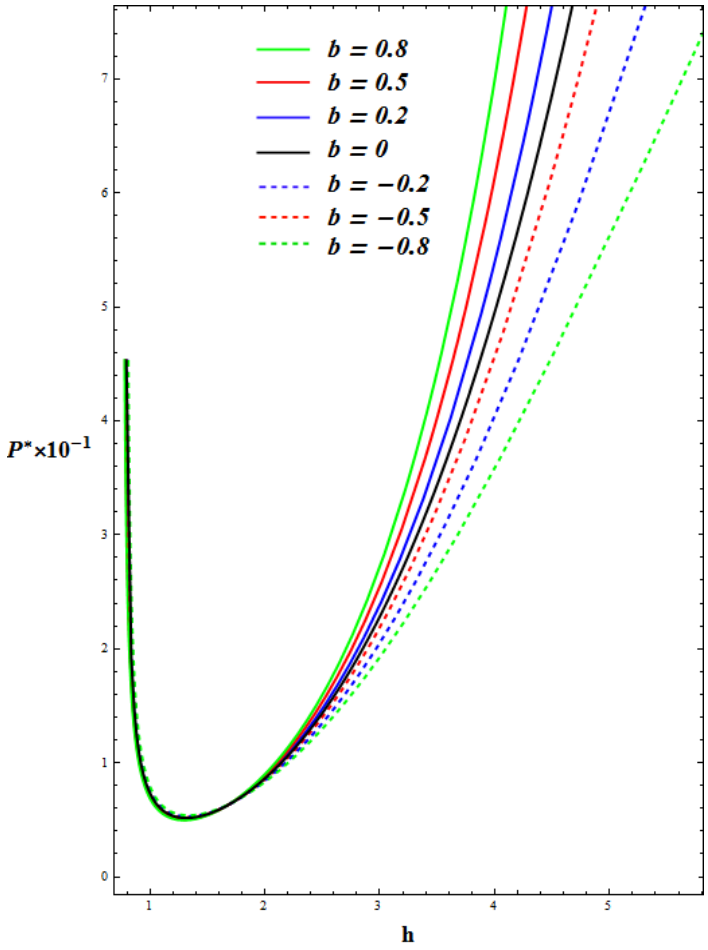

Figure 45: Total power flow P^* of the TM_0- mode versus h (cf. (4.1.3.9)) evaluated for various b $(Z(0) = 1)$

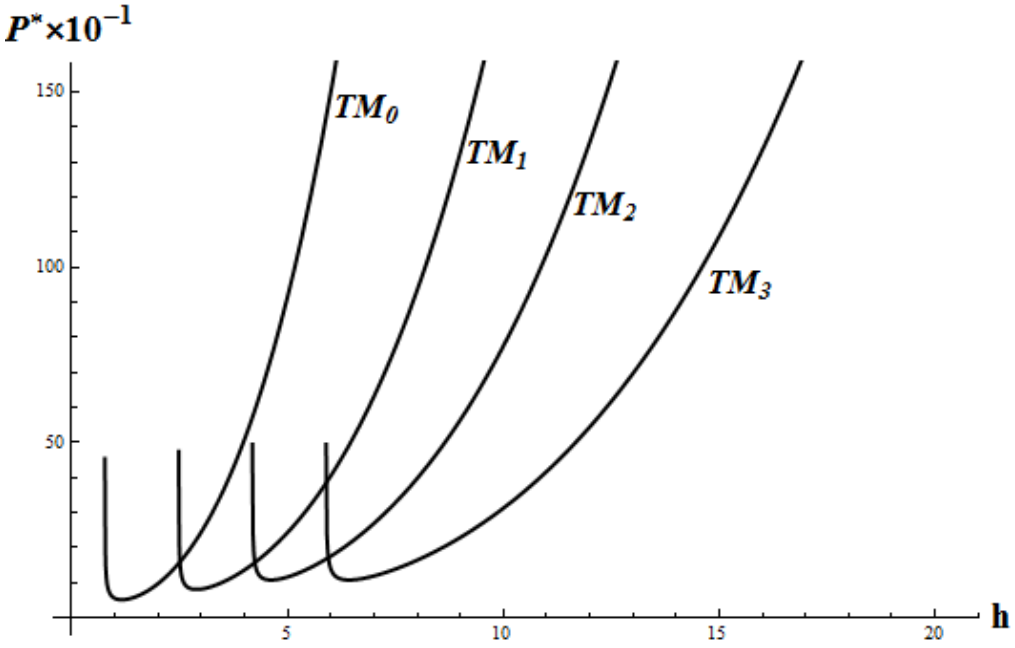

Figure 46: Total power flow P^* versus film thickness h corresponding to the dispersion (black) curves in the Figure 42 (cf. (4.1.3.12))

4.1.4 Metamaterial nonlinear film

The parameters of the present Section are chosen as follows:

$$\varepsilon_{1s} = \varepsilon_{2s} = \varepsilon_s = 0.8, \quad \varepsilon_{1c} = \varepsilon_{2c} = \varepsilon_c = 1, \quad \varepsilon_{1f} = -4, \ \varepsilon_{2f} = -3,$$

$$a_s = b_s = a_c = b_c = 0, \quad a = -0.3, \quad b = 0.2, \quad Z(0) = 1$$

The discriminant D (cf. (4.1.7)) is negative, so that equation (4.1.6) has a unique real root $X(0+0)$.

As follows from Figure 47 the field components Z, X are not periodic for certain propagation constants γ in interval $1 < \gamma < 3$.

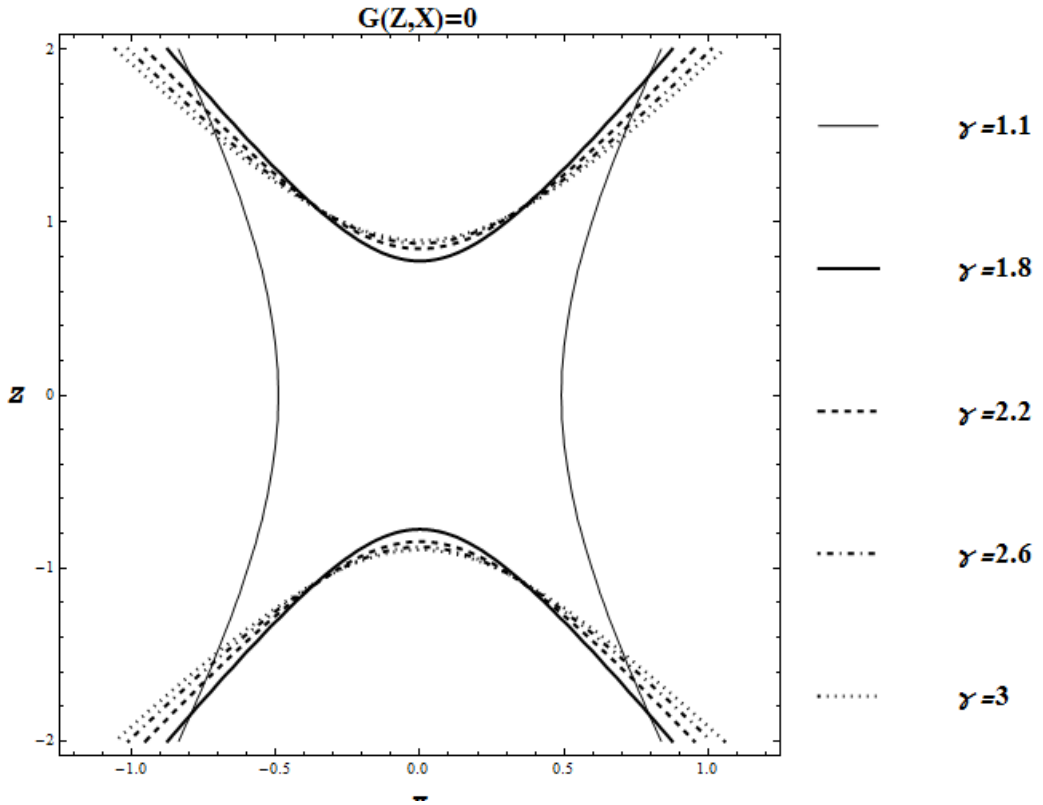

Figure 47: The first integral $G(Z, X, \gamma) = 0$ (cf. (3.1.4))

Following the steps I-VII of Section 3 three solutions of the dispersion relation (3.1.14) are obtained (evaluation proceeds as exemplified in Appendix F). Results are depicted in Figure 48.

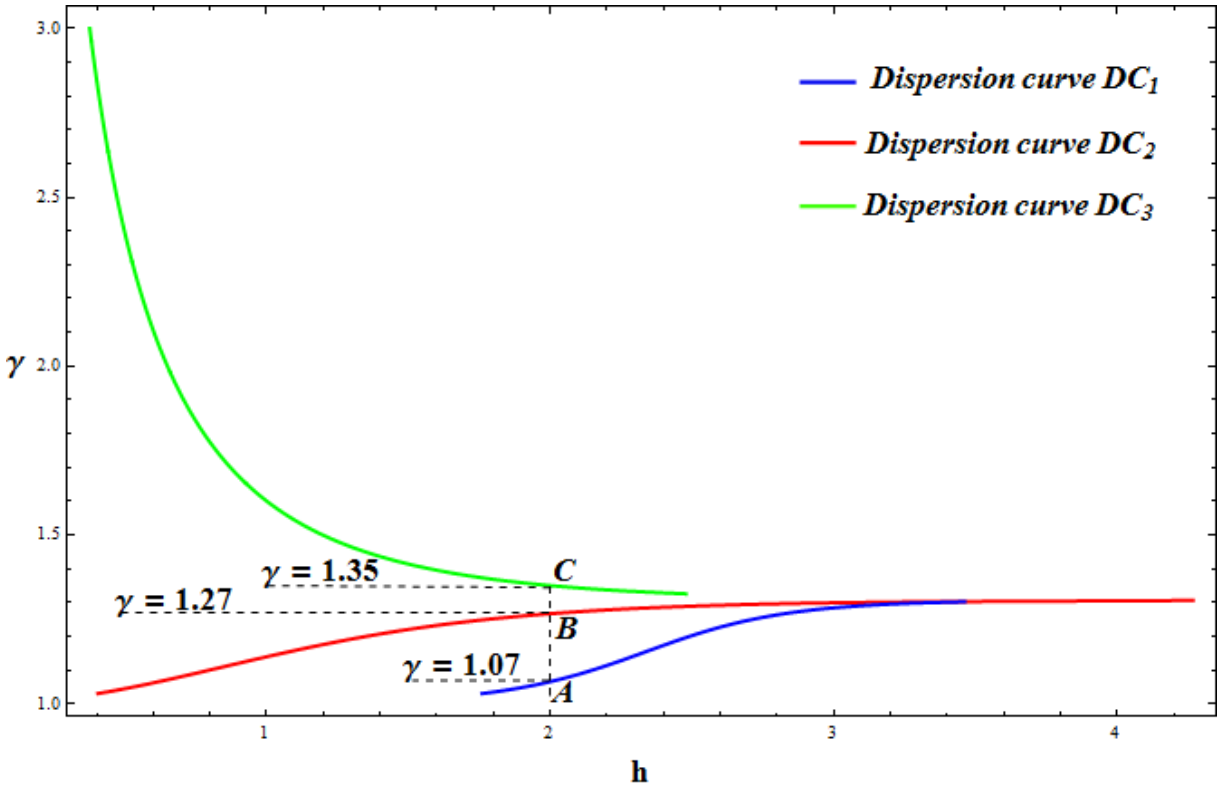

Figure 48: Three solutions of the dispersion relation (cf. (3.1.14)) (dispersion curves DC_1, DC_2 and DC_3). Points A, B and C show three different possibilities of the TM_0-wave propagation in the film with the thickness $h = 2$ (with the propagation constant $\gamma = 1.07$, $\gamma = 1.27$ and $\gamma = 1.35$, respectively)

Fixing the film thickness h and finding (via the dispersion relation (3.1.14)) the corresponding propagation constant γ (as shown by points A, B and C in the Figure 48) field components $Z(x)$, $X(x)$ and $H(x)$ are depicted in Figure 49.

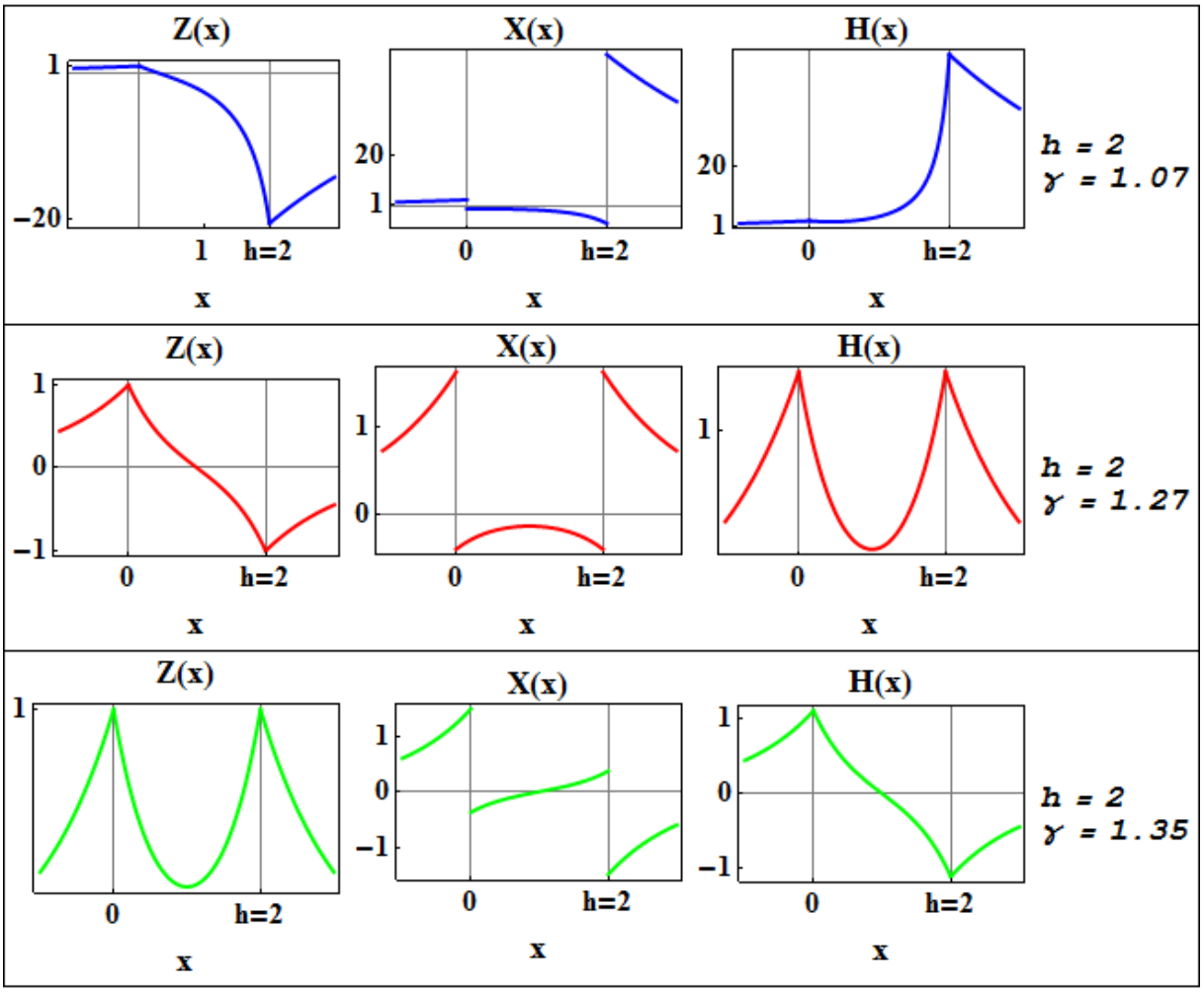

Figure 49: Field patterns $Z(x)$, $X(x)$ and $H(x)$ for the nonlinear TM_0- mode (cf. Figure 48) (evaluated by using (4.1.1), (4.1.2), (4.1.3)[20]) (blue: corresponding to the point A on the dispersion curve DC_1; red: corresponding to the point B on the dispersion curve DC_2; green: corresponding to the point C on the dispersion curve DC_3)

Figure 50 presents the total power flow carried by the nonlinear TM_0- wave (corresponding to the dispersion curves DC_1, DC_2 and DC_3 in the Figure 48). Also here as in the cases I-IV of the subection 4.1.2 the energy flow in the metamaterial film is opposite to the energy flow in the substrate and cladding (see, for example, Figure 20, p. 51).

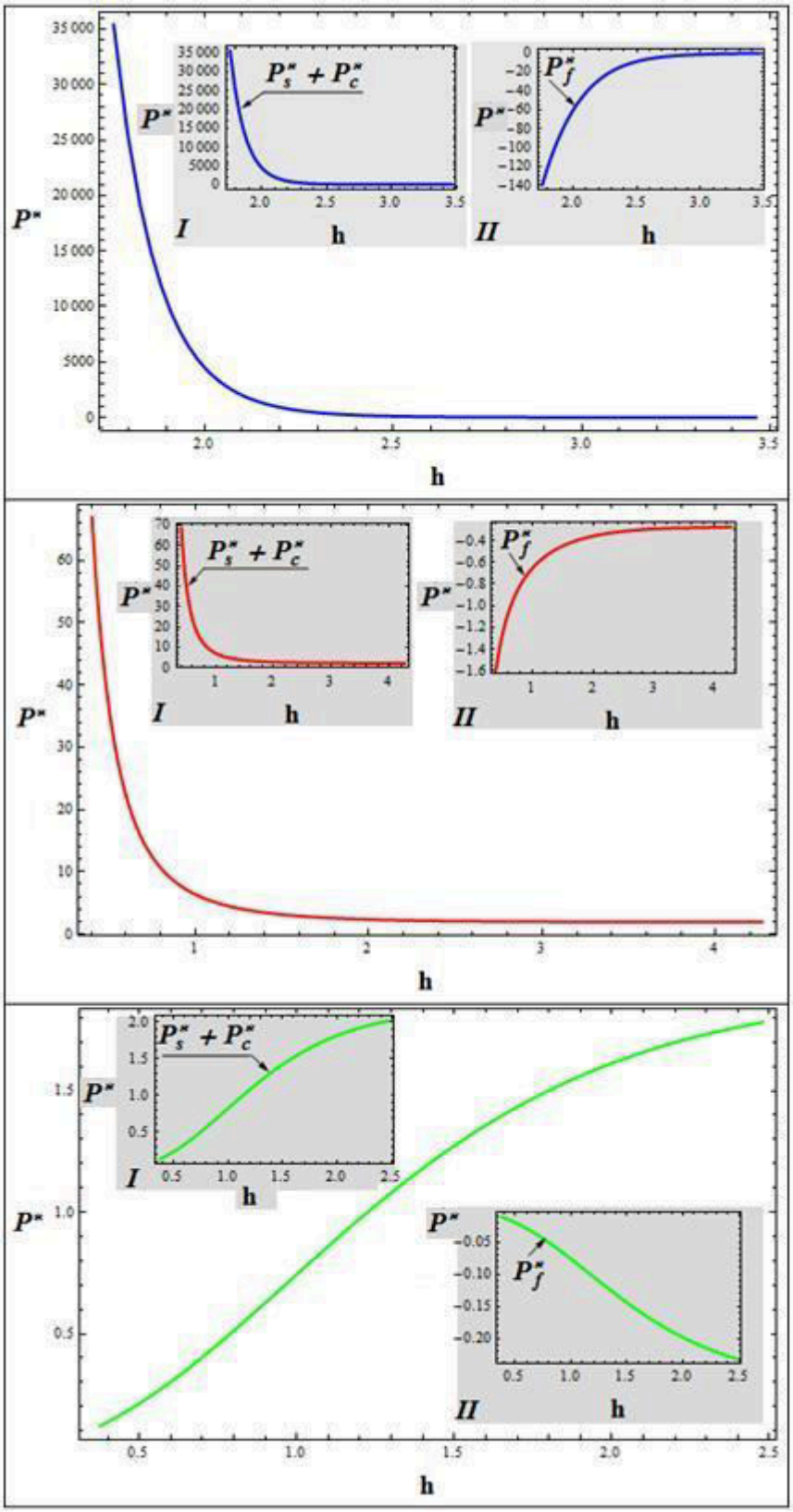

Figure 50: Total power flow transported by the nonlinear TM_0- mode (cf. Figure 48) (presented by blue, red and green colour corresponding to the dispersion curves DC_1, DC_2, and DC_3, respectively) (evaluated according to (3.2.3)). Gray section I: power flow in the substrate and cladding. Gray section II: power flow in the film

4.2 Uniaxial medium in the film bounded by linear substrate and cladding

TM- electromagnetic waves guided by a dielectric film filled with a nonlinear uniaxial medium[29] characterized by a dielectric tensor

$$\varepsilon_f = \begin{pmatrix} \varepsilon_{1f} + a_f\,|E_x|^2 & 0 & 0 \\ 0 & 0 & 0 \\ 0 & 0 & \varepsilon_{2f} \end{pmatrix} \tag{4.2.1}$$

are considered in the present subsection. Using (3.1.15) an analytical closed form dispersion relation can be presented in this case[30].

Instead of equations (3.1.4), (3.1.5) now the first integral for $\nu = f$ is given by

$$G_f(Z_f, X_f) :=$$

$$:= \frac{a_f^2 X_f^6}{2} + a_f\left(\varepsilon_{1f} - \frac{3\gamma^2}{4}\right)X_f^4 + \frac{\varepsilon_{1f}\left(\varepsilon_{1f} - \gamma^2\right)}{2}X_f^2 + \frac{\varepsilon_{2f}\gamma^2 Z_f^2}{2} + C_f = 0 \tag{4.2.2}$$

with the integration constant

$$C_f = \frac{1}{4}\left(2\varepsilon_{1f}\left(\gamma^2 - \varepsilon_{1f}\right)X_{0f}^2 + a\left(3\gamma^2 - 4\varepsilon_{1f}\right)X_{0f}^4 - 2a^2 X_{0f}^6 - 2\varepsilon_{2f}\gamma^2 Z_{0f}^2\right). \tag{4.2.3}$$

According to (4.2.1) the diagonal elements (2.6) are written as

$$\begin{aligned} \varepsilon_{xf} &= \varepsilon_{1f} + a_f\, X_f^2(x), \\ \varepsilon_{zf} &= \varepsilon_{2f}. \end{aligned} \tag{4.2.4}$$

Equation (3.1.10) with $\nu = f$ reads

$$F_{X_f}^{\pm}(X_f, \gamma) = \frac{\varepsilon_{1f} + 3a_f X_f^2}{\pm\sqrt{Z_f^2(X_f, \gamma)}\cdot\varepsilon_{2f}\,\gamma}. \tag{4.2.5}$$

Following the steps I- IV, V*- VII* of Section 3 (assuming $\varepsilon_{1c} = \varepsilon_{2c} = \varepsilon_c$, $\varepsilon_{1s} = \varepsilon_{2s} = \varepsilon_s$ and omitting the subscript $\nu = f$ (apart from $\varepsilon_{xf}, \varepsilon_{zf}, \varepsilon_{1f}, \varepsilon_{2f}, C_f$)) one obtains:

I. According to (4.1.2) solution $X_s(0+0)$ is given by

$$X_s(0-0) = \frac{\gamma\, Z(0)}{\sqrt{\gamma^2 - \varepsilon_s}}. \tag{4.2.6}$$

II. The boundary condition for the interface $x = 0$ for the present case is represented by a cubic equation (cf. (3.1.11))

$$\left[\varepsilon_{1f} + a\, X^2(0+0)\right] X(0+0) = \frac{\gamma\, \varepsilon_s\, Z(0)}{\sqrt{\gamma^2 - \varepsilon_s}} \tag{4.2.7}$$

with roots

$$\begin{cases} X_1(0+0) = \dfrac{\vartheta^{1/3}}{2^{1/3}3^{2/3}a} - \dfrac{2^{1/3}\varepsilon_{1f}}{3^{1/3}\vartheta^{1/3}}, \\ X_2(0+0) = -\dfrac{(1-i\sqrt{3})\vartheta^{1/3}}{2 2^{1/3}3^{2/3}a} + \dfrac{(1+i\sqrt{3})\varepsilon_{1f}}{2^{2/3}3^{1/3}\vartheta^{1/3}}, \\ X_3(0+0) = -\dfrac{(1+i\sqrt{3})\vartheta^{1/3}}{2 2^{1/3}3^{2/3}a} + \dfrac{(1-i\sqrt{3})\varepsilon_{1f}}{2^{2/3}3^{1/3}\vartheta^{1/3}}, \end{cases} \tag{4.2.8}$$

where

$$\vartheta = -\frac{9\, a^2 \varepsilon_s\, \gamma\, Z(0)}{\sqrt{\gamma^2 - \varepsilon_s}} + \sqrt{3}\sqrt{a^3\left(4\varepsilon_{1f}^3 + \frac{27a\, \varepsilon_s^2 \gamma^2 Z^2(0)}{\gamma^2 - \varepsilon_s}\right)}. \tag{4.2.9}$$

III. Choosing a real root $X_i(0+0)$ ($i = 1, 2$ or 3) according to (4.2.8) and inserting into (4.2.3) the constant of integration C_f is defined (in the numerical example below only one real root (4.2.8) exists).

IV. From the second equation (4.1.2) follows

$$X_c(h+0) = -\frac{\gamma\, Z(h)}{\sqrt{\gamma^2 - \varepsilon_c}}, \tag{4.2.10}$$

where $Z(h)$ will be defined on the step V*.

V*. Solving (4.2.2) with respect to Z^2 one obtains

$$Z^2 = \frac{-4C_f + X^2\left((2\varepsilon_{1f} + 3aX^2)\gamma^2 - 2(\varepsilon_{1f} + aX^2)^2\right)}{2\gamma^2\varepsilon_{2f}}, \qquad (4.2.11)$$

hence, assuming hereafter $Z^2 > 0$ two real solutions $Z(h)$ exist

$$Z_{1,2}(h) =$$

$$= \pm\sqrt{\frac{-4C_f + X^2(h-0)\left(\left(2\varepsilon_{1f} + 3a\,X^2(h-0)\right)\gamma^2 - 2\left(\varepsilon_{1f} + a\,X^2(h-0)\right)^2\right)}{2\gamma^2\varepsilon_{2f}}} \qquad (4.2.12)$$

If $Z^2 < 0$ no analytical solution in this case is possible. Thus, $Z^2 > 0$ is a restriction for the experimental parameters.

VI*. The boundary condition for the interface $x = h$ is represented by a cubic equation (with respect to $X(h-0)$) (cf. (3.1.12))

$$\left[\varepsilon_{1f} + a\,X^2(h-0)\right]X(h-0) = -\frac{\gamma\,\varepsilon_c\,Z(h)}{\sqrt{\gamma^2 - \varepsilon_c}}. \qquad (4.2.13)$$

Taking the square of (4.2.13) (with $Z(h)$ from (4.2.12)) and solving the resulting equation for $X^2(h-0)$ three solutions are possible

$$\begin{cases} X_1^2(h-0) = p_1 - \dfrac{\sqrt[3]{2}\;p_2}{p_0\,\sqrt[3]{p_4}} + \dfrac{\sqrt[3]{p_4}}{\sqrt[3]{2}\;p_0}, \\ X_2^2(h-0) = p_1 + \dfrac{(1+i\sqrt{3})\,p_2}{\sqrt[3]{4}\,p_0\,\sqrt[3]{p_4}} - \dfrac{\left(1-i\sqrt{3}\right)\sqrt[3]{p_4}}{\sqrt[3]{16}\;p_0}, \\ X_3^2(h-0) = p_1 + \dfrac{(1-i\sqrt{3})\,p_2}{\sqrt[3]{4}\,p_0\,\sqrt[3]{p_4}} - \dfrac{\left(1+i\sqrt{3}\right)\sqrt[3]{p_4}}{\sqrt[3]{16}\;p_0}, \end{cases} \qquad (4.2.14)$$

where

$$p_0 = 3a^2\left(1 + \frac{\varepsilon_c^2}{\varepsilon_{2f}(\gamma^2 - \varepsilon_c)}\right),$$

$$p_1 = 3\frac{4\varepsilon_{1f}\varepsilon_c(\varepsilon_c - \varepsilon_{2f}) + (4\varepsilon_{1f}\varepsilon_{2f} - 3\varepsilon_c^2)\gamma^2}{6a(\varepsilon_{2f} - \varepsilon_c)\varepsilon_c - 6a\varepsilon_{2f}\gamma^2},$$

$$p_2 = -\frac{(2a\varepsilon_{1f}(\varepsilon_{2f}-\varepsilon_c)\varepsilon_c + a(3\varepsilon_c^2 - 2\varepsilon_{1f}\varepsilon_{2f})\gamma^2)^2}{4\varepsilon_{2f}^2(\varepsilon_c-\gamma^2)^2},$$

$$p_3 = -\frac{a^3}{4\varepsilon_{2f}^3(\varepsilon_c-\gamma^2)^3}\Big(8\big(\varepsilon_{1f}\big(\varepsilon_{2f}-\varepsilon_c\big)\varepsilon_c - \varepsilon_{1f}\varepsilon_{2f}\gamma^2\big)^3 +$$

$$+54\varepsilon_{1f}\varepsilon_c^4\gamma^4\big(\varepsilon_c^2+\varepsilon_{2f}(\gamma^2-\varepsilon_c)\big) - 18{\varepsilon_{1f}^2}^2\varepsilon_c^2\gamma^2\big(\varepsilon_c^2+\varepsilon_{2f}(\gamma^2-\varepsilon_c)\big)^2 +$$

$$+27\varepsilon_c^2\Big(-{\varepsilon_c}^4\gamma^6 + 8aC_f\big(\varepsilon_c^2+\varepsilon_{2f}\gamma^2-\varepsilon_{2f}\varepsilon_c\big)^2\Big)\Big),$$

$$p_4 = \sqrt{p_3^2 - 4p_2^3} - p_3.$$

VII*. Setting $X = \xi$ in (4.2.11) the solution $Z^2(\xi,\gamma)$ reads

$$Z^2(\xi,\gamma) = \frac{-4C_f + \xi^2\Big(\big(2\varepsilon_{1f}+3a\xi^2\big)\gamma^2 - 2\big(\varepsilon_{1f}+a\xi^2\big)^2\Big)}{2\gamma^2\varepsilon_{2f}}. \quad (4.2.15)$$

Using (4.2.5) with $X = \xi$ and (4.2.15) equation (3.1.15) can be written as

$$\int_{X(0+0,\gamma,Z(0))}^{X(h-0,\gamma,Z(0))} \frac{\big(\varepsilon_{2f}\,\gamma\big)^{-1}\big(\varepsilon_{1f}+3a\xi^2\big)d\xi}{Z^{\pm}(\xi,\gamma)} = h > 0, \quad (4.2.16)$$

where

$$Z^{\pm}(\xi,\gamma) := \pm\sqrt{Z^2(\xi,\gamma) =}$$

$$= \pm\sqrt{\frac{-4C_f + \xi^2\Big(\big(2\varepsilon_{1f}+3a\xi^2\big)\gamma^2 - 2\big(\varepsilon_{1f}+a\xi^2\big)^2\Big)}{2\gamma^2\varepsilon_{2f}}}. \quad (4.2.17)$$

and the sign " + " or " − " has to be chosen subject to

$$sgn[Z(\xi = X(0+0),\gamma)] \equiv sgn[Z(0)],$$
$$sgn[Z(\xi = X(h-0),\gamma)] \equiv sgn[Z(h)]. \quad (4.2.18)$$

With $\sigma = \xi^2$ in the integral (4.2.16) the dispersion relation reads

$$DR_X\left(\gamma, Z(0), \varepsilon_c, \varepsilon_s, \varepsilon_{1f}, \varepsilon_{2f}, a\right) = \\ = \int\limits_{X^2(0+0,\gamma,Z(0))}^{X^2(h-0,\gamma,Z(0))} \frac{\pm\left(\varepsilon_{1f} + 3a\,\sigma\right)\cdot\sqrt{\gamma^2\varepsilon_{2f}}}{\left(\pm\sqrt{A\sigma^4 + B\sigma^3 + C\sigma^2 + D\sigma}\right)\cdot\sqrt{2}\,\gamma\,\varepsilon_{2f}}\,d\sigma = h, \tag{4.2.19}$$

where

$$\begin{aligned} A &= -2a^2, \\ B &= 3a\gamma^2 - 4a\varepsilon_{1f}, \\ C &= 2\varepsilon_{1f}\left(\gamma^2 - \varepsilon_{1f}\right), \\ D &= -4C_f. \end{aligned} \tag{4.2.20}$$

and the sign in the numerator is " + " (" − ") if $\xi > 0$ ($\xi < 0$) on the path $\xi \in [X(0+0), X(h-0)]$.

The integrand in (4.2.19) (without sign $\pm$) has a primitive function expressed in terms of elliptic integrals as follows

$$\mathcal{F}(x) = \tilde{\alpha}(x)\cdot\frac{\left(\varepsilon_{1f}\cdot R_3\,F\left[\varphi\left(\tilde{s}(x)\right)\middle|\tilde{m}\right] + 3\,a\,\cdot\Pi\left(\tilde{n};\varphi\left(\tilde{s}(x)\right)\middle|\tilde{m}\right)\right)}{R_3\cdot\sqrt{Ax^4 + Bx^3 + Cx^2 + Dx}}, \tag{4.2.21}$$

where

$F[\varphi(s(z))|m]$ and $\Pi(n;\varphi(s(z))|m)$ denote the elliptic integrals of the first and third kinds, respectively[26], and

$$\tilde{\alpha}(x) = \ (R_3 - R_2)\frac{\sqrt{2\,\gamma^2\varepsilon_{2f}}}{\gamma\,\varepsilon_{2f}}\,x^2\sqrt{\frac{R_1x - 1}{(R_1 - R_3)x}}\sqrt{\frac{-(R_2x - 1)(R_3x - 1)}{(R_2 - R_3)^2\,x^2}},$$

$$\varphi\left(\tilde{s}(x)\right) = Arcsin\sqrt{\tilde{s}(x)},$$

$$\tilde{s}(x) = \sqrt{\frac{1 - R_3x}{(R_2 - R_3)x}},$$

$$\widetilde{m} = \frac{R_2 - R_3}{R_1 - R_3},$$

$$\tilde{n} = 1 - \frac{R_2}{R_3},$$

$$R_1 = \tilde{k}_1 - \frac{2^{1/3}\,\tilde{p}}{\tilde{k}_2\,(\sqrt{4\,\tilde{p}^3 + \tilde{q}^2} + \tilde{q}\,)^{1/3}} + \frac{(\sqrt{4\,\tilde{p}^3 + \tilde{q}^2} + \tilde{q}\,)^{1/3}}{2^{1/3}\,\tilde{k}_2},$$

$$R_2 = \tilde{k}_1 + \frac{\left(1 + i\sqrt{3}\right)\tilde{p}}{2^{2/3}\tilde{k}_2\,(\sqrt{4\,\tilde{p}^3 + \tilde{q}^2} + \tilde{q}\,)^{1/3}} - \frac{(1 - i\sqrt{3})\,(\sqrt{4\,\tilde{p}^3 + \tilde{q}^2} + \tilde{q})^{1/3}}{2^{4/3}\,\tilde{k}_2},$$

$$R_3 = \tilde{k}_1 + \frac{(1 - i\sqrt{3})\,\tilde{p}}{2^{2/3}\,\tilde{k}_2\,(\sqrt{4\,\tilde{p}^3 + \tilde{q}^2} + \tilde{q})^{1/3}} - \frac{(1 + i\sqrt{3})\,(\sqrt{4\,\tilde{p}^3 + \tilde{q}^2} + \tilde{q})^{1/3}}{2^{4/3}\,\tilde{k}_2}$$

with

$$\tilde{k}_1 = -\frac{C}{3D}, \quad \tilde{k}_2 = 3D, \quad \tilde{p} = 3BD - C^2, \quad \tilde{q} = -27AD^2 + 9BCD - 2C^3.$$

Hence, the dispersion relation (4.2.9) can be presented in the closed analytical form:

$$sgn\,(\mathcal{F}[X^2(h)] - \mathcal{F}[X^2(0)]\,) = h > 0, \tag{4.2.22}$$

where

$$X^2(h) = X^2\big(h - 0, \gamma, Z(0)\big) \tag{4.2.23}$$

and $X^2\big(h - 0, \gamma, Z(0)\big)$ is a real and positive root chosen according to (4.2.14), and

$$X^2(0) = X^2\big(0 + 0, \gamma, Z(0)\big) \tag{4.2.24}$$

is a real root chosen according to (4.2.8), and

$$sgn = \begin{cases} +, & \begin{cases} X(0) > 0, X(h) > 0 \text{ and } Z^+(\xi,\gamma) \text{satisfies (4.2.18)} \\ \text{or} \\ X(0) < 0, X(h) < 0 \text{ and } Z^-(\xi,\gamma) \text{satisfies (4.2.18)}, \end{cases} \\ -, & \begin{cases} X(0) > 0, X(h) > 0 \text{ and } Z^-(\xi,\gamma) \text{satisfies (4.2.18)} \\ \text{or} \\ X(0) < 0, X(h) < 0 \text{ and } Z^+(\xi,\gamma) \text{satisfies (4.2.18)}. \end{cases} \end{cases} \tag{4.2.25}$$

In general, the functions X and $Z(X,\gamma)$ (cf. (4.2.15)) can also change sign within the integration interval $\big(X\big(0+0,\gamma,Z(0)\big),X(h-0,\gamma,Z(0))\big)$. This has to be taken into account evaluating (4.2.16), and hence in applying (4.2.22).

If higher modes are possible (see numerical example below) the period T_X of the dispersion relation (4.2.16) with (4.2.5) reads[28]

$$T_X = \left|\oint_{G(Z,X)=0} F_X^{\pm}(\xi,\gamma)d\xi\right|. \tag{4.2.26}$$

To obtain the higher modes solutions $N\cdot T_X$ $(N=1,2,3,\dots)$ has to be added on the left- hand side of (4.2.16):

$$h_N = (h+\mathrm{k}\cdot T_X)+N\cdot T_X\,, \tag{4.2.27}$$

where

$$\mathrm{k}=\begin{cases}0, & \text{if } h>0,\\ 1, & \text{if } h<0.\end{cases}$$

The total power flow can be evaluated according to (3.2.7) and (C.1.10)

$$P_X^{*}=\frac{\varepsilon_s\,\gamma\,Z^2(0)}{2\sqrt{(\gamma^2-\varepsilon_s)^3}}+P_{film,X}^{\pm}+\frac{\varepsilon_c\,\gamma\,Z^2(h)}{2\sqrt{(\gamma^2-\varepsilon_c)^3}}, \tag{4.2.28}$$

where

$$P_{film,X}^{\pm}=\pm\int_{X(0+0,\gamma,Z(0))}^{X(h-0,\gamma,Z(0))}\frac{(\varepsilon_{1f}+a\,\xi^2)(\varepsilon_{1f}+3a\,\xi^2)\,\xi^2\,d\xi}{\varepsilon_{2f}\,\gamma^2\sqrt{\frac{\Big(\big(2\varepsilon_{1f}+3a\,\xi^2\big)\gamma^2-2\big(\varepsilon_{1f}+a\,\xi^2\big)\Big)\xi^2-4C_f}{2\,\varepsilon_{2f}\,\gamma^2}}} \tag{4.2.29}$$

is the power flow in the film.

The primitive function in (4.2.29) (omitting sign " $\pm$ ") reads

$$\begin{aligned}\tilde{\mathcal{P}}(x)=\tilde{\beta}_0(x)+\tilde{\beta}_1(x)E\big[\varphi\left(\tilde{s}(x)\right)/\tilde{m}\big]+\\ +\tilde{\beta}_2(x)F[\varphi\left(\tilde{s}(x)\right)/\tilde{m}]+\tilde{\beta}_3(x)\,\Pi\big(\tilde{n};\varphi\big(\tilde{s}(x)\big)/\tilde{m}\big),\end{aligned} \tag{4.2.30}$$

where

$E\left[\varphi\left(m\cdot s(x)\right)\middle|m\right]$ denotes the elliptic integrals of the second kind[26], and

$$\tilde{\beta}_0(x) = -\frac{\sqrt{f(x)}\,(-4\,\varepsilon_{1f} + 12a\,x^2 + 27\gamma^2)}{16\sqrt{2}\,a\,x^2},$$

$$\tilde{\beta}_1(x) = \\ = \frac{C_f(R_2-R_3)x^2(R_1x^2-1)\sqrt{-\frac{(R_2x^2-1)(R_3x^2-1)}{(R_2-R_3)^2\;x^4}(4\varepsilon_{1f}-27\gamma^2)}}{4\sqrt{2}a\;\varepsilon_{2f}\sqrt{f(x)}\sqrt{\frac{R_1x^2-1}{(R_1-R_3)x^2}\gamma^2}},$$

$$\tilde{\beta}_2(x) = \frac{C_f(R_2-R_3)x^2}{4a\;\varepsilon_{2f}\sqrt{f(x)}\,\gamma^2}\times \\ \times\sqrt{\frac{R_1x^2-1}{2(R_1-R_3)x^2}}\sqrt{-\frac{(R_2x^2-1)(R_3x^2-1)}{(R_2-R_3)^2\;x^4}}\left(12a+4\,\varepsilon_{1f}R_1-27R_1\gamma^2\right),$$

$$\tilde{\beta}_3(x) = \frac{9(R_3-R_2)\left(9\gamma^2-8\varepsilon_{1f}\right)x^2}{16\;\varepsilon_{2f}R_3\sqrt{f(x)}}\times \\ \times\sqrt{\frac{R_1x^2-1}{2(R_1-R_3)x^2}}\sqrt{-\frac{(R_2x^2-1)(R_3x^2-1)}{(R_2-R_3)^2\;x^4}}.$$

For periodic Z, X the total power flow for higher modes can be written as (cf. (3.2.10) and (3.2.11))

$$P_N^* = (P_X^* + \mathrm{k}\cdot T^*) + N\cdot T^* \tag{4.2.31}$$

with[28]

$$T^* = \left|\oint_{G(Z,X,\gamma)=0} P_{film,X}^{\pm}(\xi,\gamma)d\xi\right|. \tag{4.2.32}$$

Thus, using (4.2.21) and (4.2.30) the dispersion relation and the total power flow can be evaluated straightforwardly (as exemplified in Appendix J).

For numerical evaluation the material parameters are chosen as follows

$$\varepsilon_{1s} = \varepsilon_{2s} = \varepsilon_s = 1, \qquad \varepsilon_{1c} = \varepsilon_{2c} = \varepsilon_c = 4, \qquad \varepsilon_{1f} = 9,\ \varepsilon_{2f} = 6,$$
$$a_s = b_s = a_c = b_c = b_f = 0, \qquad Z(0) = 1\,.$$

The first integral $G(Z,X) = 0$ evaluated for fixed γ (cf. equation (4.2.2)) is presented by closed curves as shown in Figure 51, thus the functions $Z(x), X(x)$ and $H(x)$ are periodic (for a certain range of γ).

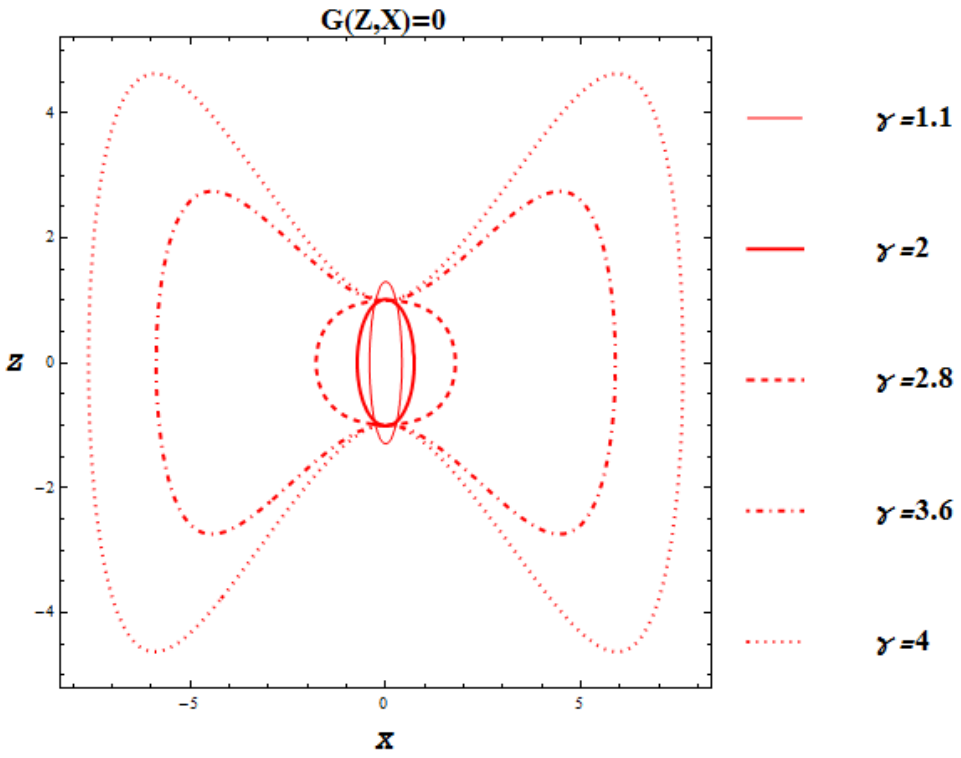

a)

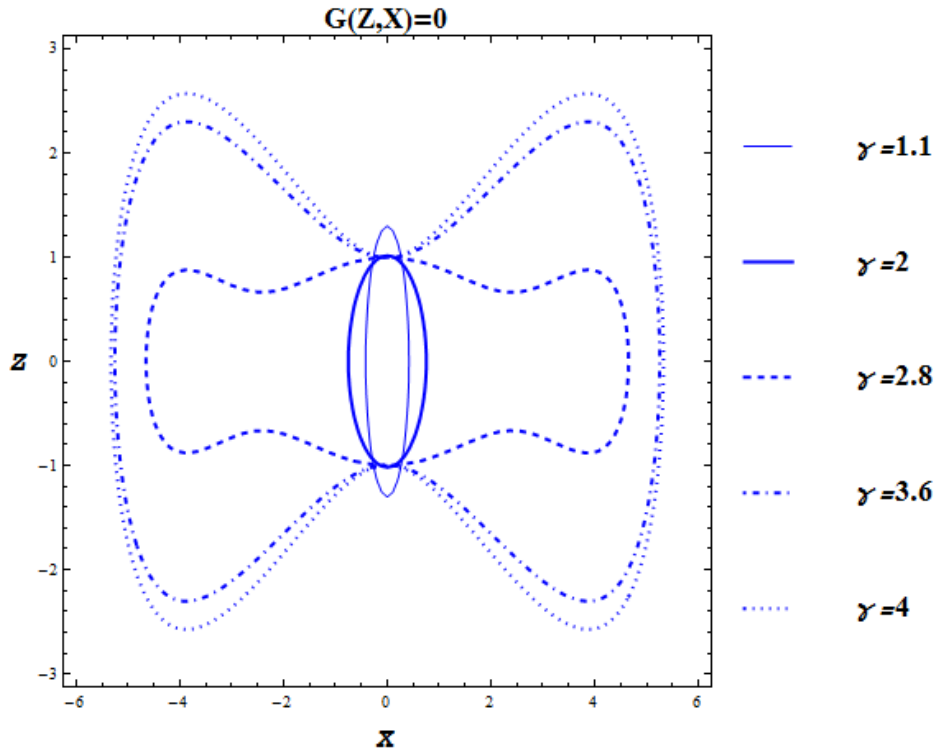

b)

Figure 51: The first integral $G(Z,X,\gamma)=0$ (cf. (3.1.4)) **a)** for $a=0.2$ **b)** for $a=-0.2$

Taking into account the periodicity of the field components $Z(x), X(x)$ and $H(x)$ the dispersion relation including higher modes is evaluated (cf. equation (4.2.2), (4.2.3) and (4.2.4)). Results are depicted in Figure 52.

It can be seen that the solutions for a special modes have a cut- off with respect to h in the focusing case ($a=0.2$). In the defocusing one ($a=-0.2$) there is a cut- off with respect to h as well as to γ (γ, h are real only on the branches AA*, BB*, CC*).

Figure 53 shows solutions of the dispersion relation for the TM_0- mode in comparison with the linear case ($a=0$, cf. equation (C.1.8)). Points A, B and C on the dispersion curves are chosen to present the field patterns of the nonlinear TM_0- wave propagating in the film with the thickness $h=3$ in the focusing, defocusing and linear cases with the propagation constant $\gamma=2.89$, $\gamma=2.70$ and $\gamma=2.78$, respectively. Results are given in Figure 54.

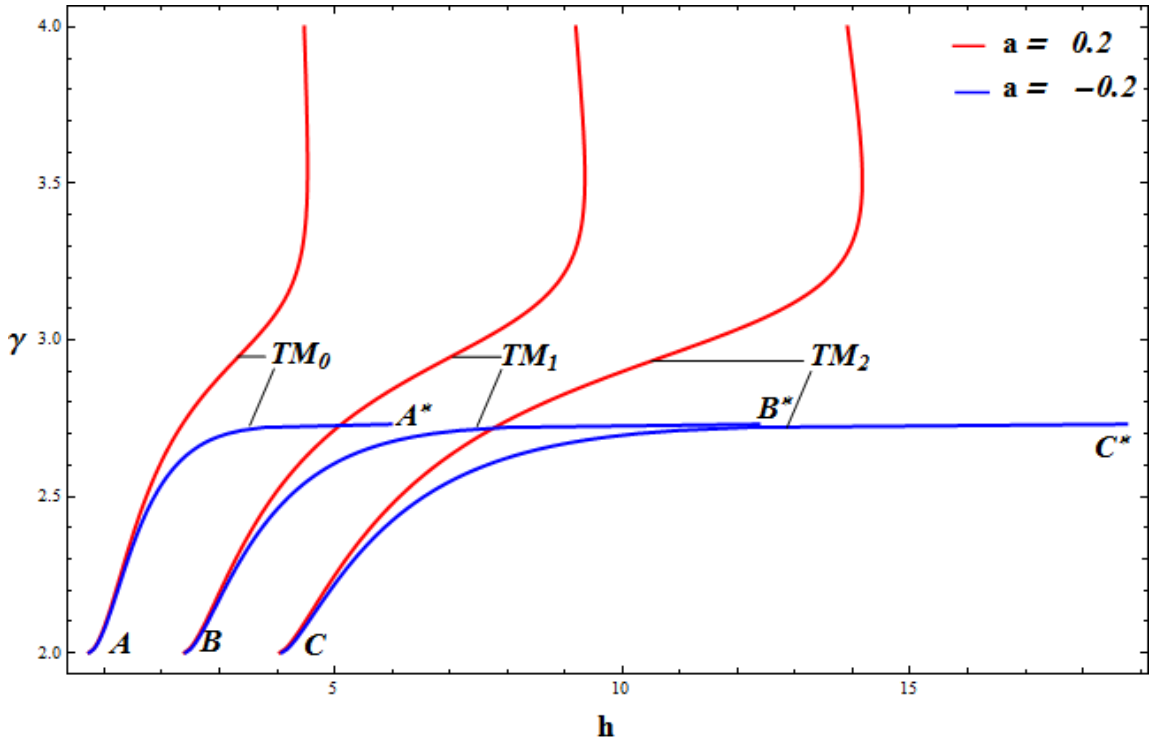

Figure 52: The fundamental mode TM_0 and the first two higher modes TM_1, TM_2 as solutions of the dispersion relation (4.2.2) (by using (4.2.3) and (4.2.4))

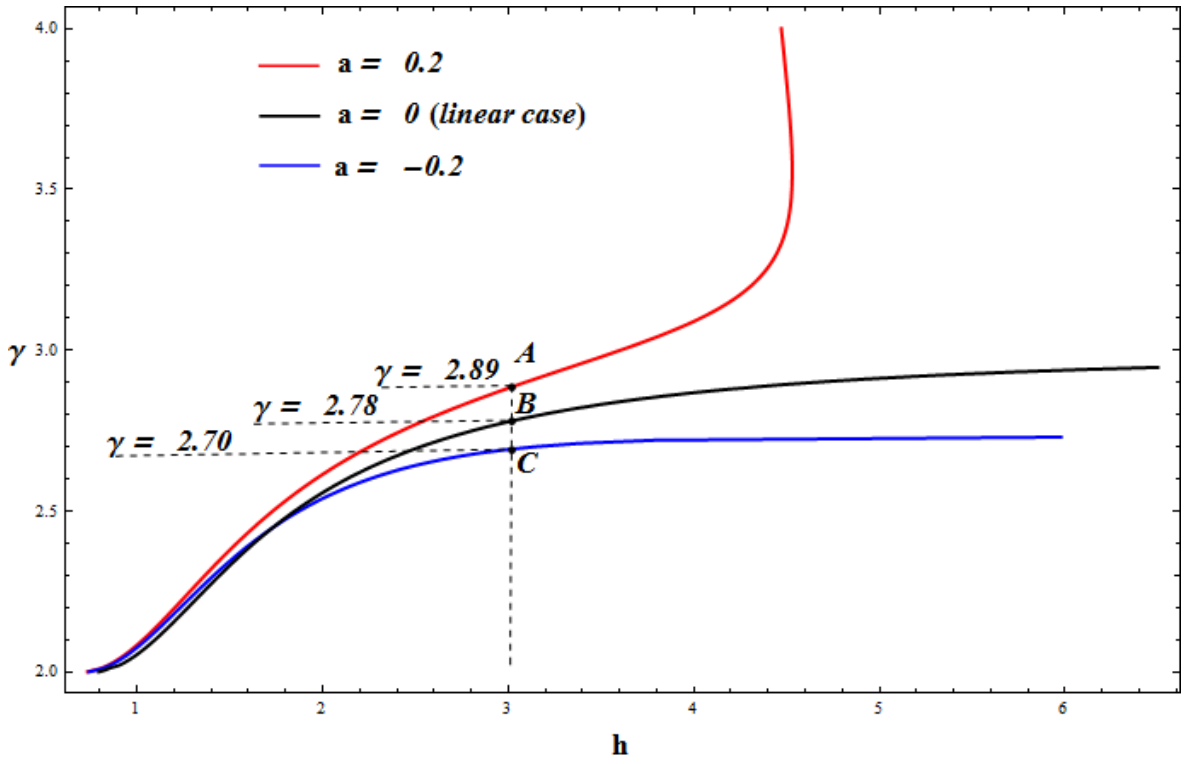

Figure 53: Comparison of the dispersion relation solutions in the focusing ($a = 0.2$), linear ($a = 0$) and defocusing ($a = -0.2$) cases (cf. (4.2.2), (4.2.3), (4.2.4) and (C.1.8))

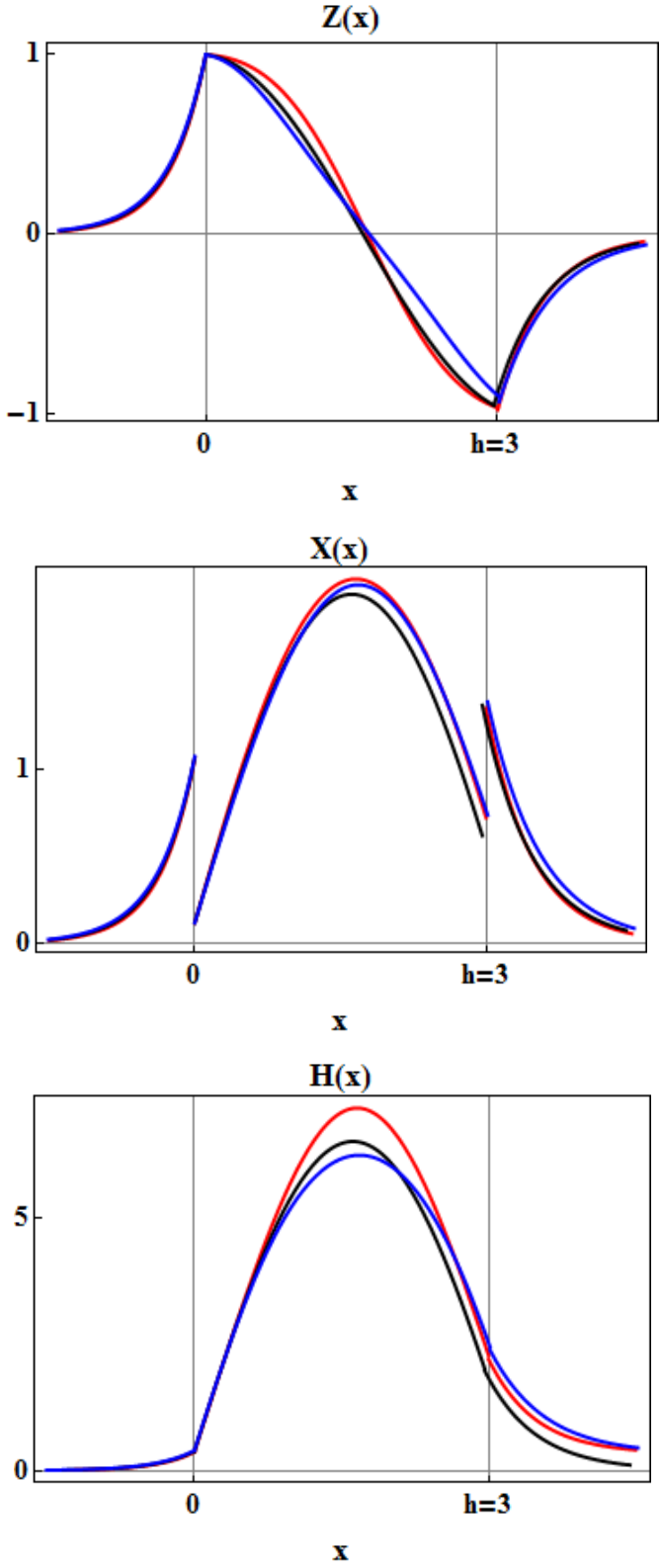

Figure 54: Comparison of the field patterns $Z(x)$, $X(x)$ and $H(x)$ of the nonlinear TM_0- mode in the focusing ($a = 0.2$, red curve), linear ($a = 0$, black curve) and defocusing ($a = -0.2$, blue curve) cases (cf. Figure 53) (evaluated according to (4.1.1), (4.1.2) and (4.1.3)[20])

Figure 55 illustrates the TM_0- mode solutions obtained for small nonlinearity coefficients a in comparison with the solution of the linear problem ($a = 0$).

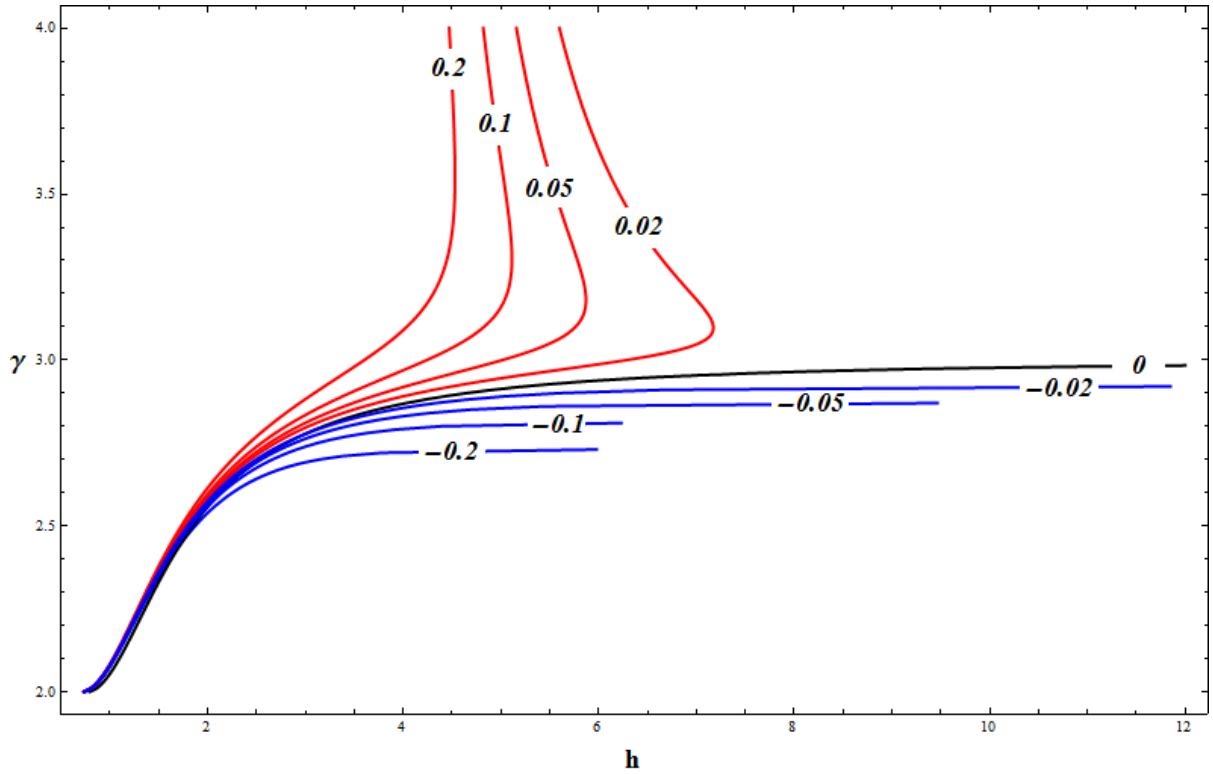

Figure 55: γ versus h for TM_0- mode evaluated for different values of the nonlinearity coefficient a. Dispersion curves are labelled by a (cf. (4.2.2) (4.2.3), (4.2.4) and (C.1.8)).

Varying the field component $Z(0)$ in the dispersion relation (4.2.4) solutions shown in Figure 56 in comparison with the linear solution (does not depend on $Z(0)$) are obtained.

The total power flow carried by the nonlinear TM_0- wave in the focusing, defocusing and linear cases ($a = 0.2$, $a = -0.2$ and $a = 0$, respectively) is depicted in Figure 57. It can be noted here, that the shape of the power flow curves is similar to the shape in the TM, TE cases considered in [29].

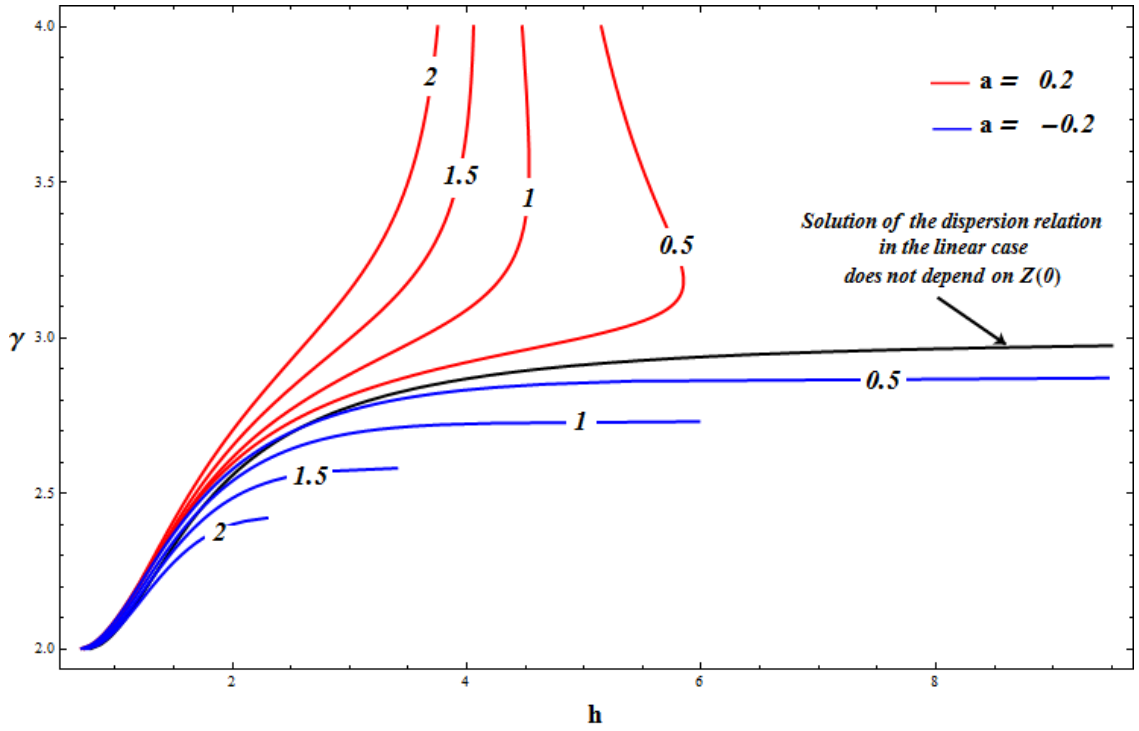

Figure 56: Dependence of the propagation constant γ on the film thickness h for TM_0- mode evaluated for different values of the field component $Z(0)$. Dispersion curves are labelled by $Z(0)$ (cf. (4.2.2), (4.23), (4.2.4) and (C.1.8)). Red curves represent solutions in the focusing case ($a = 0.2$), blue – in the defocusing one ($a = -0.2$).

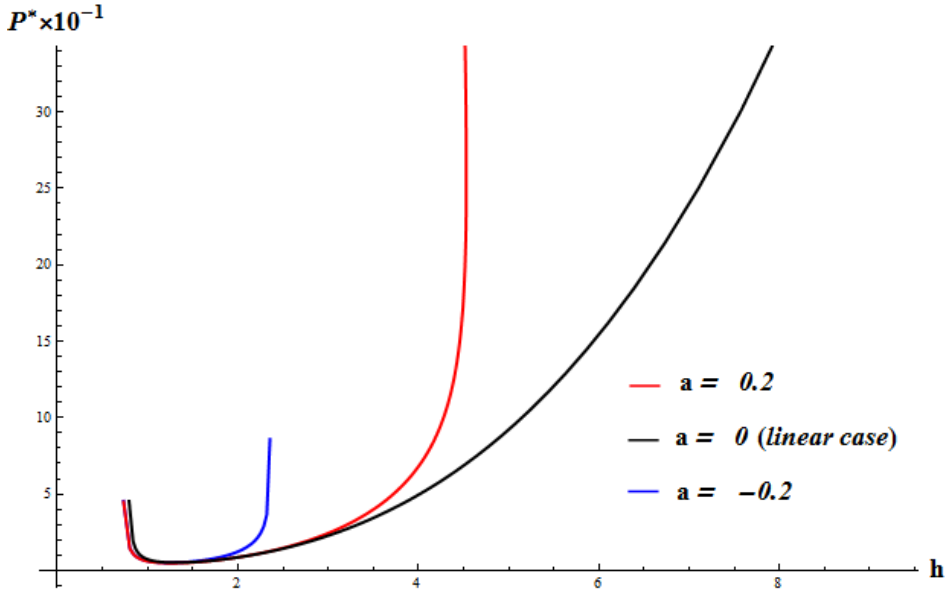

Figure 57: Total power flow of the TM_0- nonlinear wave as function of h corresponding to the dispersion curves represented in the Figure 53 (cf. (4.2.5), (4.2.6) and (3.2.3))

4.3 Saturating medium in the film bounded by linear substrate and cladding

In the previous subsections a Kerr- type nonlinearity (and its variations) in the film has been considered. But the method to obtain the dispersion relation outlined in Section 3 can be also used for more general permittivities as given by (2.5). Necessary for using the method is the integrability condition (3.1.3).

TM- wave- propagation in a dielectric film with a saturable permittivity is described by a tensor

$$\varepsilon_f = \begin{pmatrix} \varepsilon_{1f} + \dfrac{a_f\,|E_x|^2}{1+\lambda\,|E_x|^2} + b_f\,|E_z|^2 & 0 \\ 0 & 0 \\ 0 & \varepsilon_{2f} + \dfrac{a_f\,|E_z|^2}{1+\lambda\,|E_z|^2} + b_f\,|E_x|^2 \end{pmatrix},$$

$$|\lambda| \ll 1. \tag{4.3.1}$$

Obviously, the integrability condition (3.1.3) is satisfied.

Omitting the subscript $\nu = f$ (apart from $\varepsilon_{1f}, \varepsilon_{2f}, C_f$) and using the expression for the first integral given in [28, Table 3] with respect to (4.3.1) one obtains

$$G(Z,X,\gamma) := \frac{M_3(Z)\,(X^2)^3 + M_2(Z)\,(X^2)^2 + M_1(Z)\,X^2 + M_0(Z)}{\lambda^2\,(1+\lambda\,X^2)} = 0, \tag{4.3.2}$$

where

$$M_3(Z) = \lambda^2\left(\left(a+\lambda(\varepsilon_{1f}+b\,Z^2)\right)^2 - \lambda(2a+\lambda(\varepsilon_{1f}+b\,Z^2))\gamma^2\right), \tag{4.3.3}$$

$$\begin{aligned} M_2(Z) = \lambda^2\big(&2a\left(\varepsilon_{1f}+b\,Z^2\right) + a(\lambda\,Z^2-2)\gamma^2 + \\ &+\lambda\left(C_f\lambda + 2\left(\varepsilon_{1f}+b\,Z^2\right)^2 + \left(\left(\lambda\varepsilon_{2f}-2b\right)Z^2 - 2\varepsilon_{1f}\right)\gamma^2\right) - \\ &-a\,\gamma^2\,ln(1+\lambda\,Z^2)\big), \end{aligned} \tag{4.3.4}$$

$$M_1(Z) = \lambda\Big(\lambda\,(2C_f\lambda + \big(\varepsilon_{1f} + b\,Z^2\big)^2 - (\varepsilon_{1f} + \big(b - 2a - 2\varepsilon_{2f}\lambda\big)Z^2)\gamma^2) -,$$
$$-2a\gamma^2 ln(1 + \lambda\,Z^2)\Big), \tag{4.3.5}$$

$$M_0(Z) = \lambda\big(C_f\lambda + \gamma^2\big(a + \varepsilon_{2f}\lambda\big)Z^2\big) - a\,\gamma^2\,ln(1 + \lambda\,Z^2), \tag{4.3.6}$$

$$C_f = -X_0^2\left(\varepsilon_{1f} - \gamma^2 + \frac{a\,X_0^2}{1 + \lambda\,X_0^2} + b\,Z_0^2\right)^2 - \gamma^2\left(\big(\varepsilon_{1f} - \gamma^2\big)X_0^2 + \varepsilon_{2f}Z_0^2\right) -$$
$$-\gamma^2\left(Z_0^2(\lambda + b\,X_0^2) - \frac{a\,ln[1 + \lambda\,Z_0^2]}{\lambda^2}\right). \tag{4.3.7}$$

Formula (4.3.2) is a particular case of formula (9) in [28, Table 3].

The same arguments as in Section 3 and steps the I-VII applied to the dispersion relation (3.1.14) lead to

$$DR_Z\big(\gamma, Z(0), \varepsilon_{1f}, \varepsilon_{2f}, a\big) = \int_{Z(0)}^{Z(h,\gamma,Z(0))} F_Z^{\pm}(\zeta,\gamma)d\zeta = h, \tag{4.3.8}$$

where

$$F_Z^{\pm}(Z,\gamma) = \frac{\gamma}{\pm\sqrt{X^2(Z,\gamma)}\left(\gamma^2 - \varepsilon_{1f} - \dfrac{a\,X^2(Z,\gamma)}{1 + \lambda\,X^2(Z,\gamma)} - b\,Z^2\right)} \tag{4.3.9}$$

with the real and positive root $X^2(Z,\gamma)$ of equation (4.3.2).

If the first integral (4.3.2) is represented by closed curves in the plane (Z,X) (for each fixed γ), the dispersion relation including higher modes is written as (according to (3.1.20), (3.1.18) and (4.3.9))

$$h_N = (h + \mathrm{k}\cdot T_Z) + N\cdot T_Z\,, \tag{4.3.10}$$

where

$$\mathrm{k} = \begin{cases} 0, & \text{if } h > 0, \\ 1, & \text{if } h < 0, \end{cases}$$

and

$$T_Z = \left| \oint\limits_{G(Z,X,\gamma)=0} F_Z^{\pm}(\zeta,\gamma)d\zeta \right|. \tag{4.3.11}$$

Taking into account (3.2.3) and (C.1.10) the total power flow for the present case reads

$$P_Z^* = \frac{\varepsilon_{1s}\,\gamma\,Z^2(0)}{2\sqrt{(\gamma^2-\varepsilon_{1s})^3}} + P_f^{\pm} + \frac{\varepsilon_{1c}\,\gamma\,Z^2(h)}{2\sqrt{(\gamma^2-\varepsilon_{1c})^3}}, \tag{4.3.12}$$

where

$$P_f^* = \pm \int\limits_{Z(0)}^{Z(h,\gamma,Z(0))} \frac{\left(\varepsilon_{1f} + \dfrac{a\,X^2(\zeta,\gamma)}{1+\lambda\,X^2(\zeta,\gamma)} + b\,\zeta^2\right)}{\left(\gamma^2 - \varepsilon_{1f} - \dfrac{a\,X^2(\zeta,\gamma)}{1+\lambda\,X^2(\zeta,\gamma)} - b\,\zeta^2\right)} \cdot \sqrt{X^2(\zeta,\gamma)}d\zeta. \tag{4.3.13}$$

Thus, the method proposed in Section 3 can be applied to rather general permittivities as (2.5) or as shown in [28, Table 3].

To the best of my knowledge, the exact dispersion relation for the case of the saturating film is obtained for the first time in the present work (compare, for example, [14, Table 3]).

For numerical evaluation the following material parameters are chosen:

$$\varepsilon_{1s} = \varepsilon_{2s} = \varepsilon_s = 1,\ \ \varepsilon_{1c} = \varepsilon_{2c} = \varepsilon_c = 1,\ \ \varepsilon_{1f} = 4,\ \ \ \varepsilon_{2f} = 2,$$

$$a = 0.03,\ \ b = 0.01,\ \ Z(0) = 1,\ \ \lambda = 0.02$$

(the discriminant D of the equation (4.1.7) is negative, so that equation (4.1.6) has a unique real root $X(0+0)$).

Figure 58, representing the first integral (4.3.2), shows that periodic functions Z, X exist only fo $\gamma < \sqrt{\varepsilon_f}$ (here $\sqrt{\varepsilon_f} = 2$). Furthermore, numerical evaluation of the dispersion relation including higher modes (cf. (4.3.10)) implies that the solutions have a cut- off with respect to $\gamma = \sqrt{\varepsilon_f}$. Results are depicted in Figure 59.

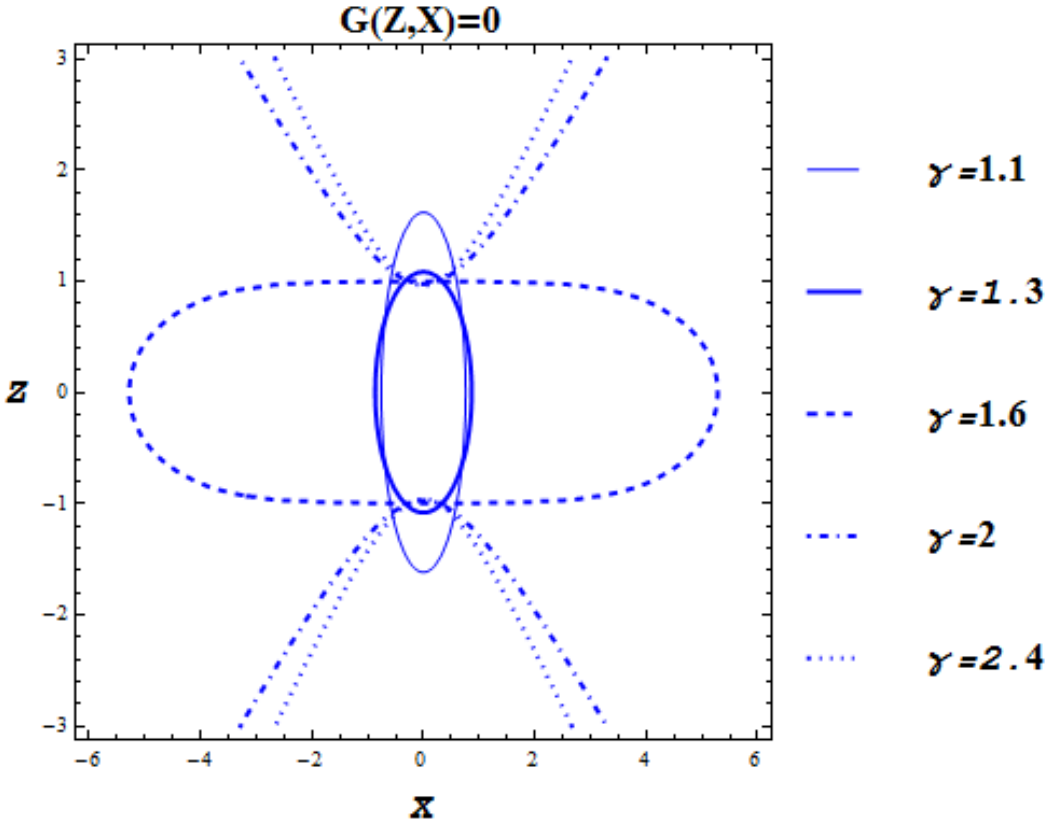

Figure 58: The first integral $G(Z, X, \gamma) = 0$ (cf. (4.3.2))

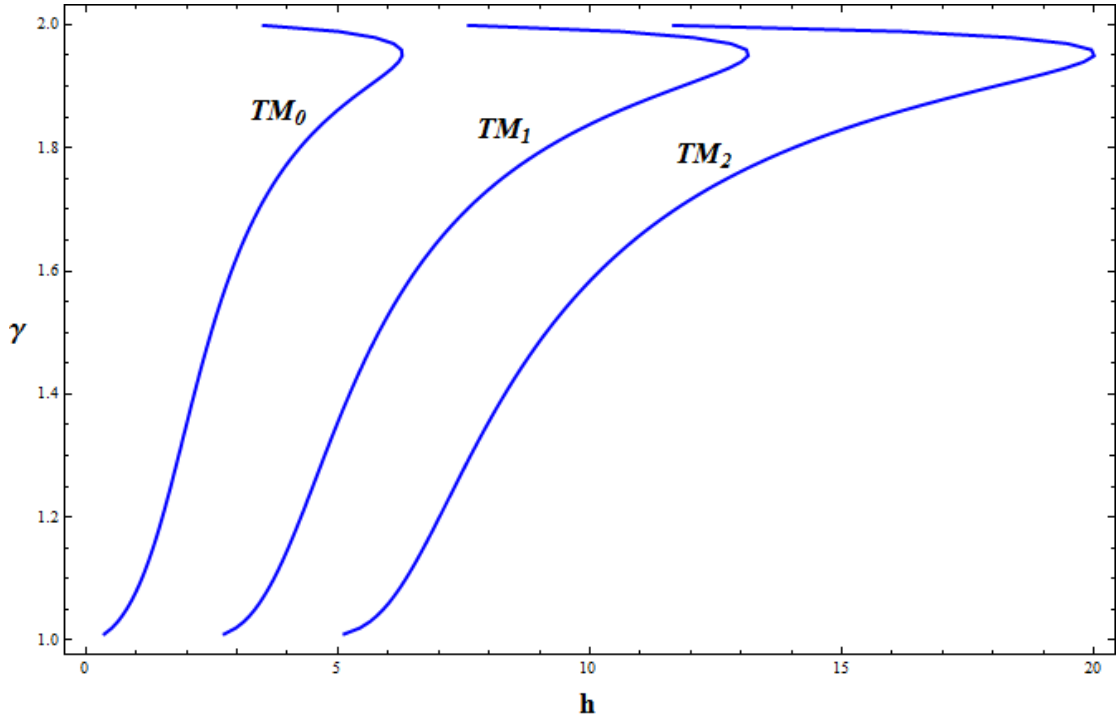

Figure 59: Fundamental mode TM_0 and the higher modes TM_1, TM_2 solutions of the dispersion relation (4.3.10)

Figure 60 illustrates the dispersion relation for the TM_0- mode compared with the case $\lambda = 0$ (Kerr nonlinearity in the film).

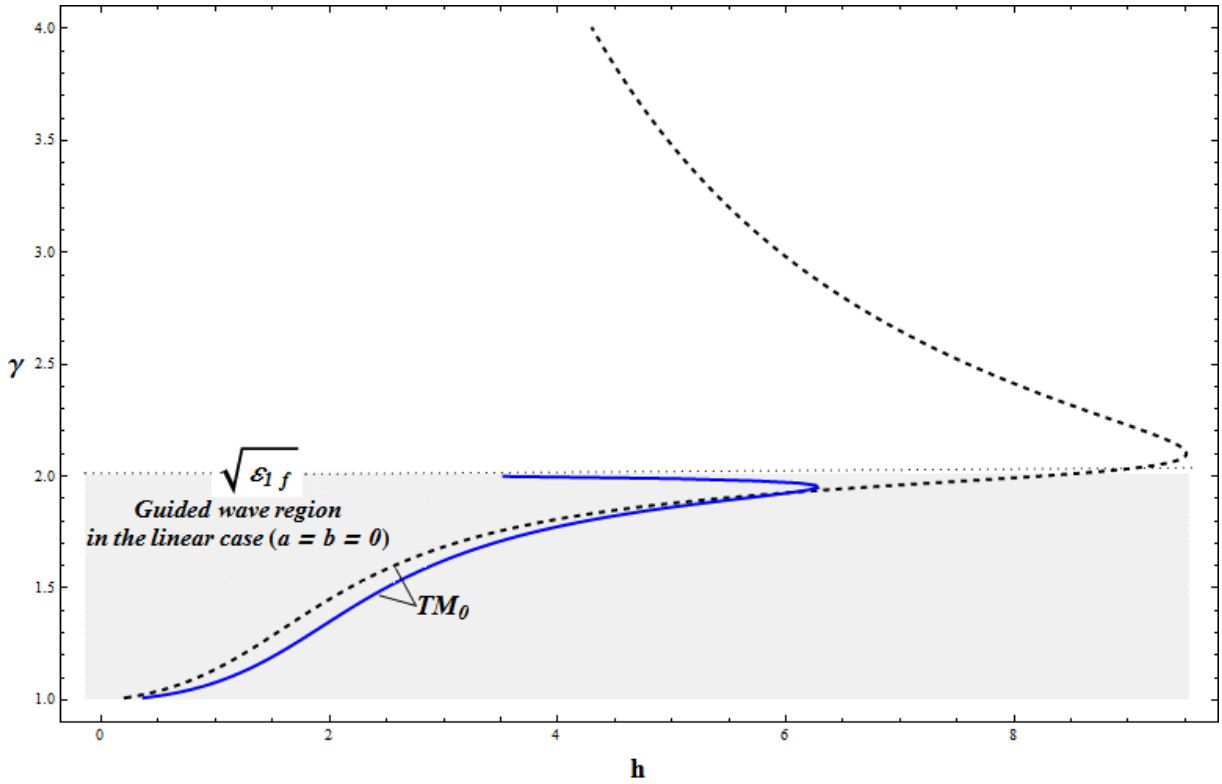

Figure 60: γ versus h (for TM_0 mode). Blue curve – dispersion relation (4.3.8), black dashed one – dispersion relation if $\lambda = 0$ (cf. Figure 5, p. 38)

Field components of the TM_0- mode propagating in the film with thickness $h = 4$ and the propagation constant $\gamma = 1.7814$ are shown in Figure 61. The total power flow transported by the TM_0- wave through the waveguide described by Figure 60 (blue curve) is depicted in Figure 62.

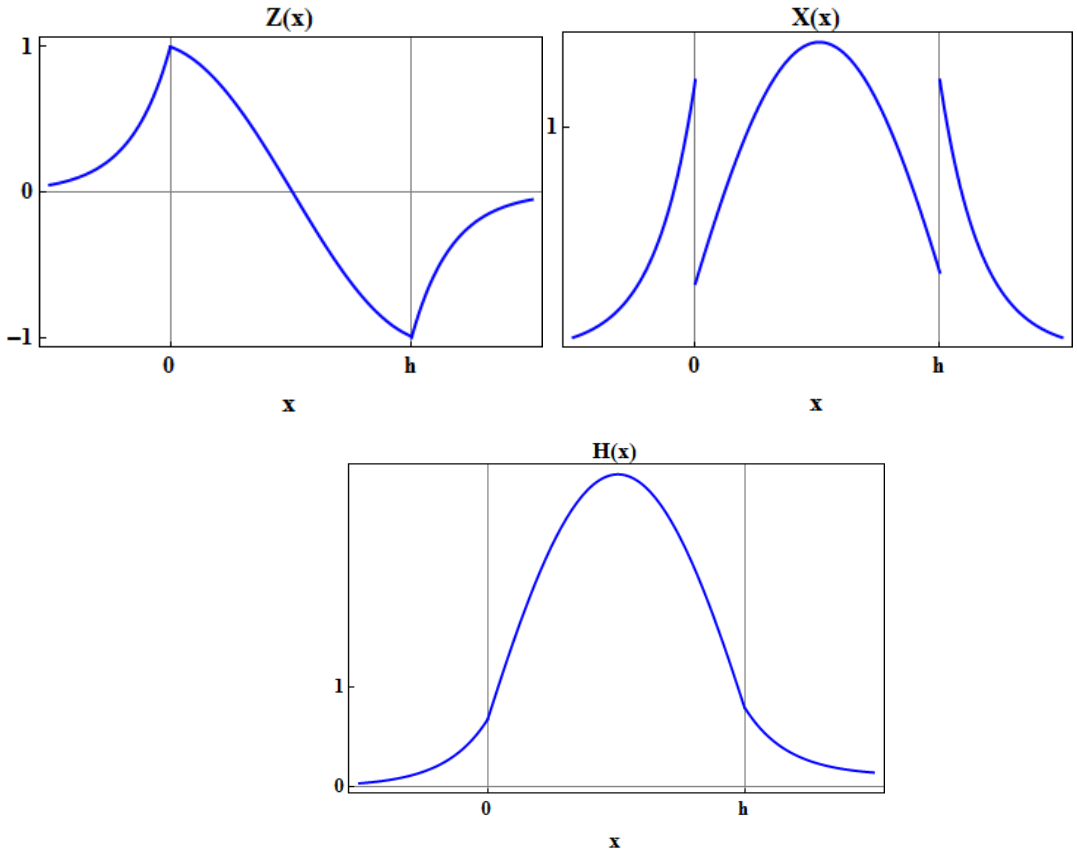

Figure 61: Field patterns $Z(x), X(x)$, and $H(x)$ for the TM_0- mode (corresponding to the blue dispersion curve in Figure 58) (evaluated according to (4.1.1), (4.1.2) and (4.1.3)[20])

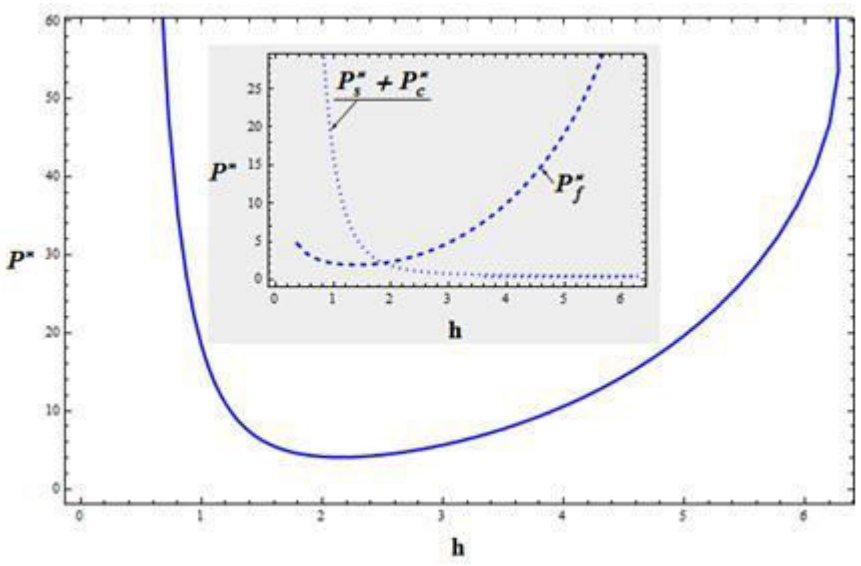

Figure 62: Total power flow transported by the TM_0- wave (corresponding to the blue dispersion curve in Figure 58) (cf. (4.3.12- 13) Gray region: separation of the total power flow into the flow carried by the substrate and cladding and power flow in the film

4.4 Kerr- nonlinear substrate, film and cladding

Propagation of the TM-electromagnetic waves through a Kerr- nonlinear waveguide with the dielectric permittivity (2.5) is considered in the present subsection.

Numerical evaluation proceeds according to steps the I- VII of Section 3 (for details see Appendix K) with the following material parameters:

$$\varepsilon_{1s} = 4, \quad \varepsilon_{2s} = 1, \quad \varepsilon_{1f} = 9, \quad \varepsilon_{2f} = 6, \quad \varepsilon_{1c} = 1, \quad \varepsilon_{2c} = 0.5,$$
$$a_s = 0.1, \quad b_s = 0.05, \quad a_f = 0.2, \quad b_f = 0.1, \quad a_c = 0.15, \quad b_c = 0.08,$$
$$Z(0) = 1.$$

As shown in Appendix K there are four real solutions $X_f(0+0) = \{X_{f1}^{p1}, X_{f1}^{m1}, X_{f1}^{p3}, X_{f1}^{m3}\}$ of the equation (3.1.11) depicted in Figure 63, each of those leads to the two different and periodic solutions of the dispersion relation (3.1.14) as shown in Figures 64, 65.

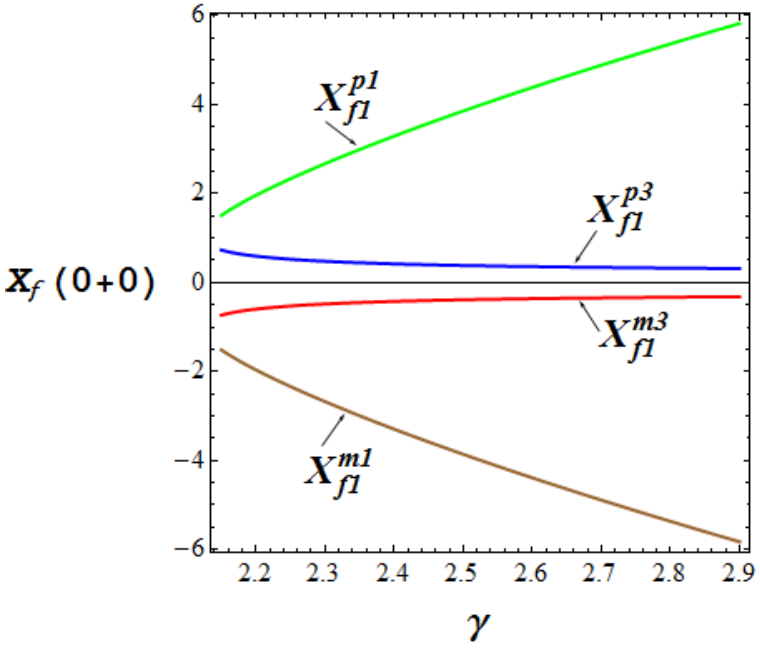

Figure 63: Real solutions $X_f(0+0)$ (cf. (3.1.11))

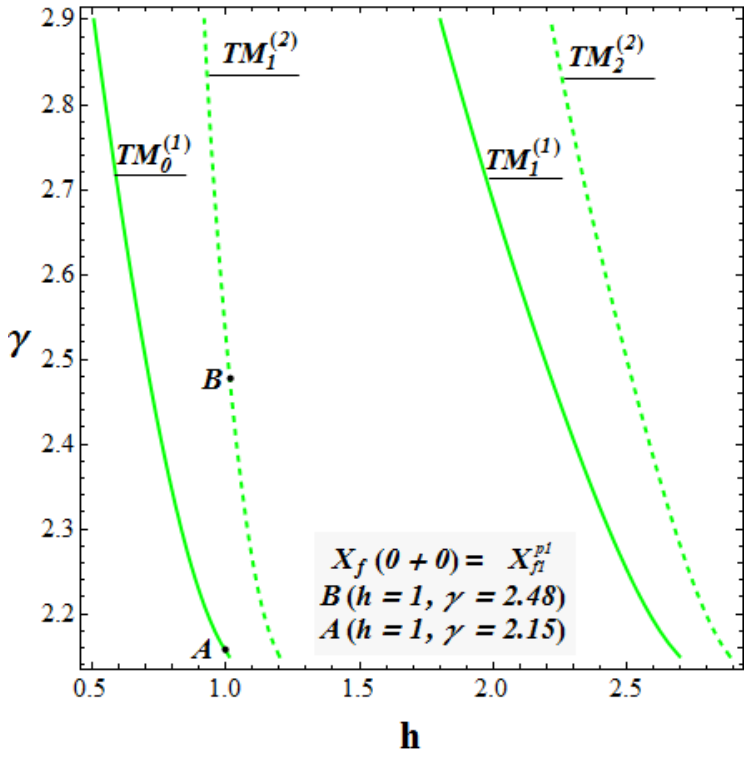

a)

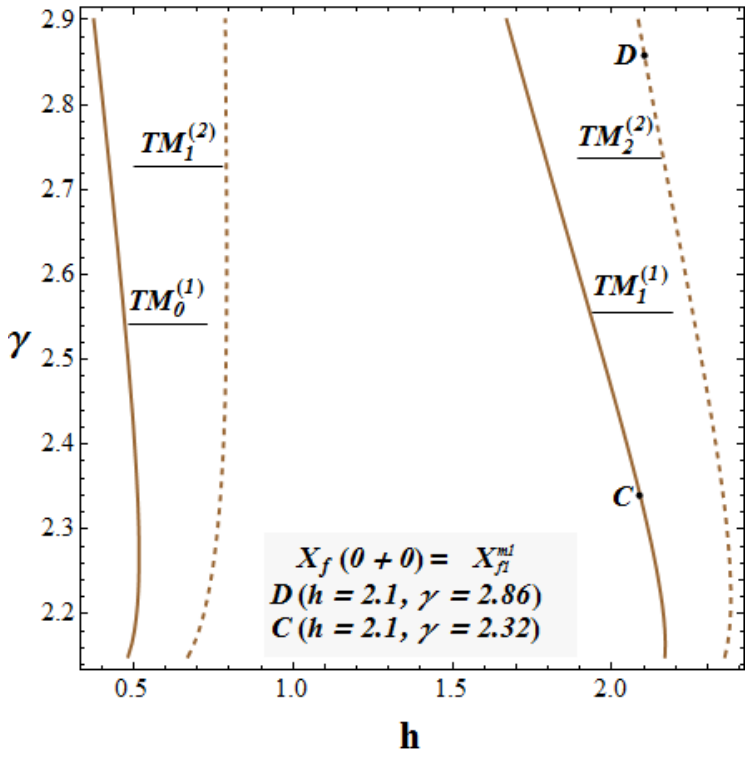

b)

Figure 64: Solutions of the dispersion relation (3.1.14) in the case **a)** $X_f(0+0) = X_{f1}^{p1}$(green curves) **b)** $X_f(0+0) = X_{f1}^{m1}$ (brown curves). Labelling $TM_i^{(j)}$ denotes i –th mode for the j -th solution ($i = 0,1,2,\ldots;\ j = 1,2$).

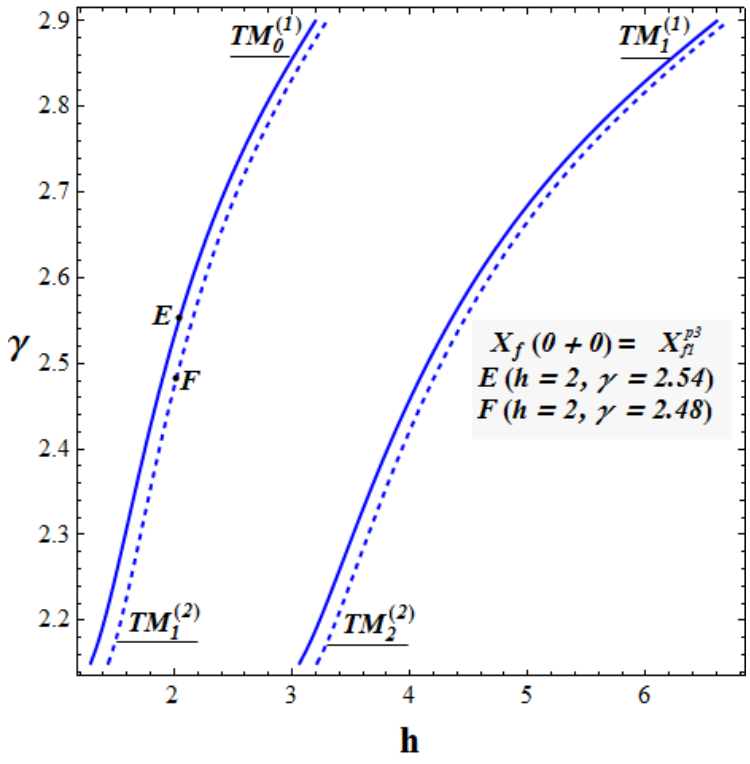

a)

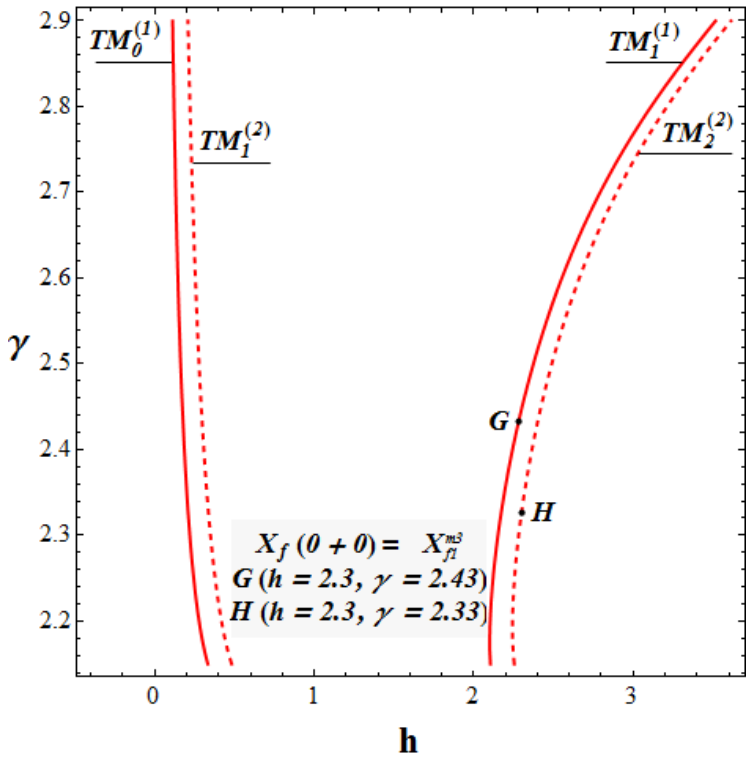

b)

Figure 65: Solutions of the dispersion relation (3.1.14) in the case **a)** $X_f(0+0) = X_{f1}^{p3}$(green curves) **b)** $X_f(0+0) = X_{f1}^{m3}$ (brown curves). Labelling $TM_i^{(j)}$ denotes i –th mode for the j -th solution ($i = 0,1,2,\ldots;\ j = 1,2$).

Figure 66 illustrates the field patterns of the nonlinear TM- wave propagating in the waveguide with the film thickness h and propagation constant γ with values given in Figures 64, 65 by points A,B,C,D,E,F,G,H.

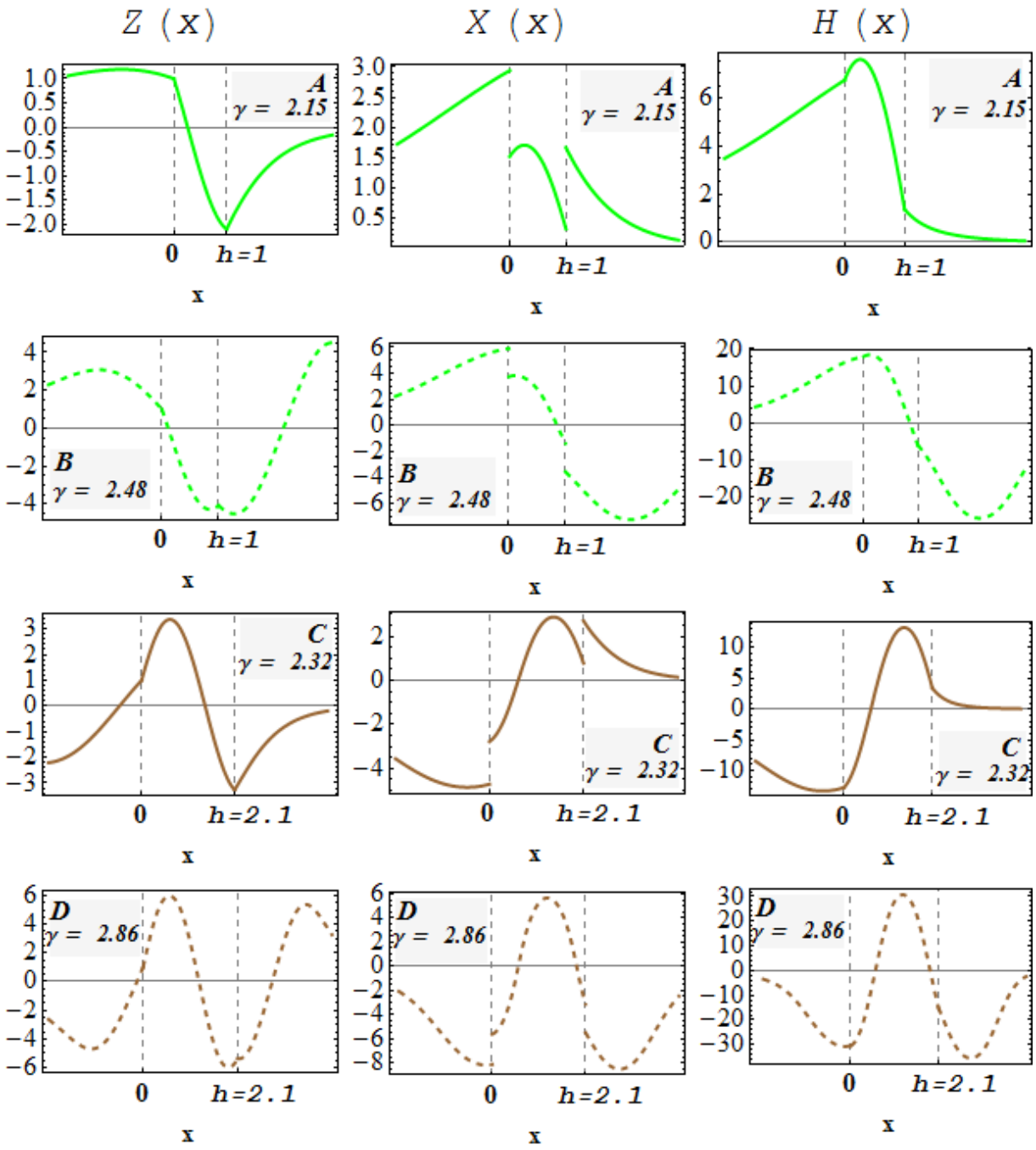

a)

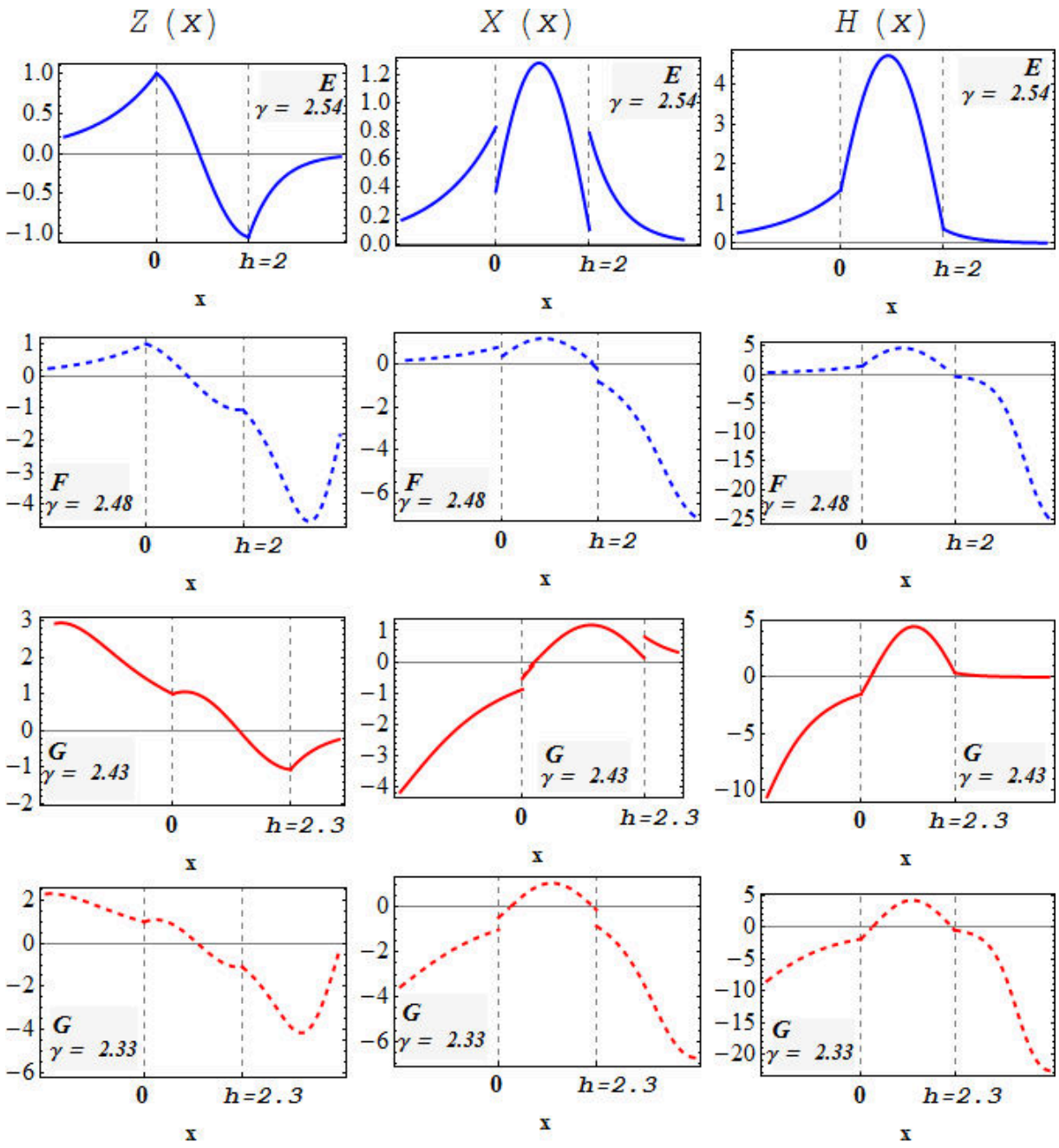

b)

Figure 66: Field patterns of the nonlinear TM- wave[20] for different values h and γ **a)** cf. Figures 63 **b)** cf. Figure 64

The total power flow (and components in the substrate, cladding, and in the film) transported by the nonlinear TM wave through a waveguide described by Figures 64, 65 is presented in Figure 67.

As can be seen in Figures 67 b), d), the transport of the energy exhibits opposite signs in the layers $\left(P_f^* > 0,\ P_s^* < 0,\ P_c^* < 0\right)$ (for comparison, see Figure 19, p. 50). To the best of my knowledge, these results in the present case are not reported in the pertinent literature (see for example, Table 3).

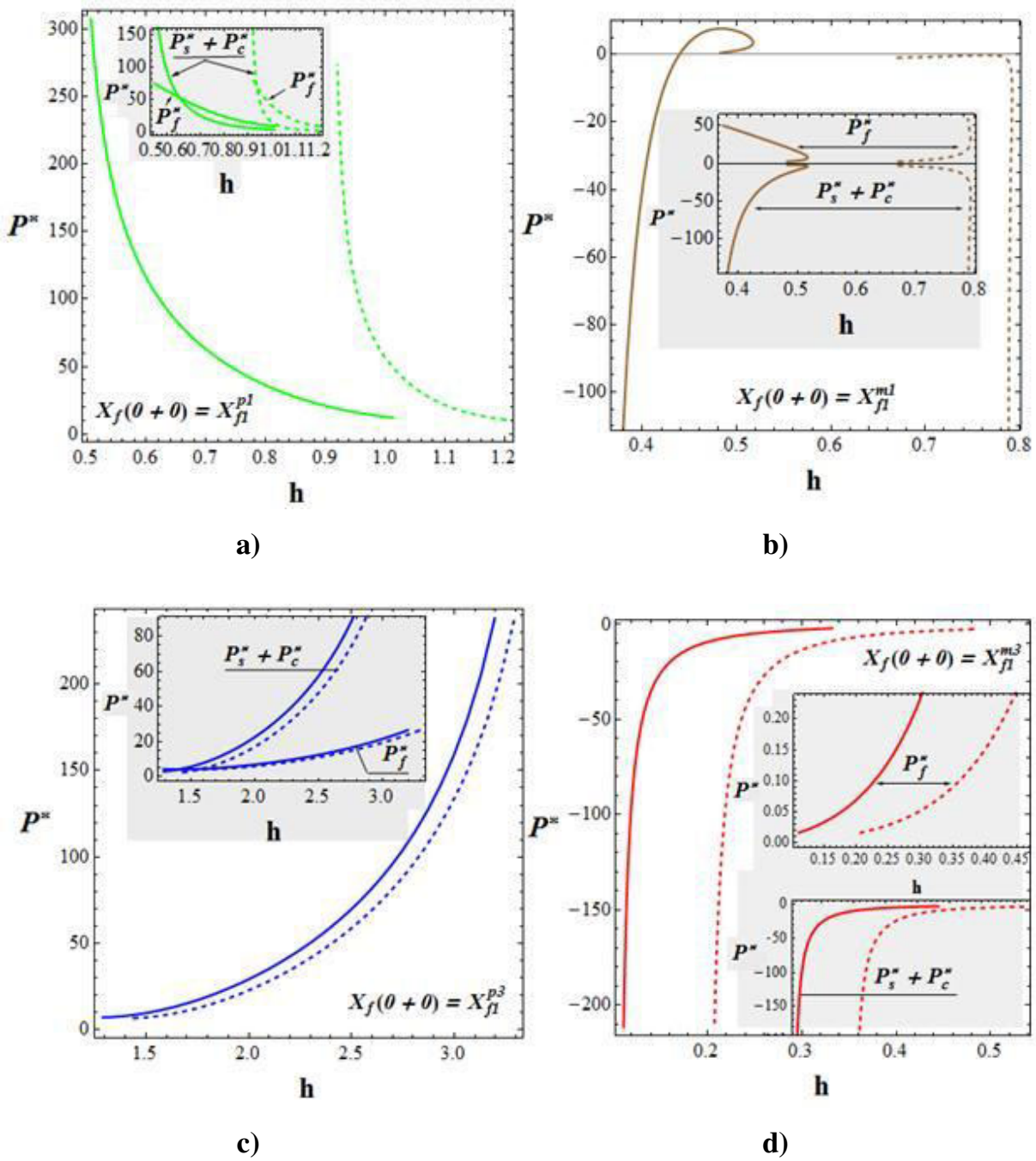

Figure 67: The total power flow (cf. (3.2.3)) of the $TM_0^{(1)}$ and $TM_1^{(2)}$- modes corresponding to **a)** Figure 64a) **b)** Figure 64b) **c)** Figure 65a) **d)** Figure 65b). Gray region: components of the total power flow in the substrate, cladding, and in the film

5 Integral equations approach to TM- electromagnetic waves guided by a (nonlinear) dielectric film with a spatially varying permittivity

TM- electromagnetic waves guided by a (nonlinear) dielectric film with the permittivity (2.7) situated between two linear and isotropic media ($\varepsilon_{1s} = \varepsilon_{2s} = \varepsilon_s,\ \varepsilon_{1c} = \varepsilon_{2c} = \varepsilon_c,\ a_s = b_s = a_c = b_c = 0$) are considered in the present section [24, Table 3].

As follows from (2.10), (2.12- 13) the diagonal elements of the tensor in (2.7) (omitting the subscript $\nu = f$ for the functions $X(x), Z(x)$) are

$$\begin{aligned} \varepsilon_{xf} &= \varepsilon_{1f} + f(x) + a_f\, X^2(x) + b_f\, Z^2(x), \\ \varepsilon_{zf} &= \varepsilon_{2f} + f(x) + b_f\, X^2(x) + a_f\, Z^2(x). \end{aligned} \tag{5.1}$$

Subject to these assumptions the system (2.11) (with $\nu = f$) cannot be reduced to an exact differential equation as in Section 3. And thus, an integral equation approach[31] (see also [24, Table 3]) as a solution of the problem is proposed in the following.

5.1 Reduction of the problem to the integral equations

Separating the linear part ε_{2f} in (5.1) the system (2.11) with $\nu = f$ can be rewritten as (the subscript f hereafter is omitted)

$$\begin{cases} \dfrac{d^2Z(x)}{dx^2} + \varepsilon_2 Z(x) = \gamma \dfrac{dX(x)}{dx} - \tilde{\varepsilon}_z Z(x), \\ -\gamma \dfrac{dZ(x)}{dx} + \gamma^2 X(x) = \tilde{\varepsilon}_x X(x), \end{cases} \tag{5.1.1}$$

where

$$\begin{aligned} \tilde{\varepsilon}_x &= f(x) + a X^2(x) + b Z^2(x), \\ \tilde{\varepsilon}_z &= f(x) + b X^2(x) + a Z^2(x). \end{aligned} \tag{5.1.2}$$

From the first equation (5.1.1) follows

$$\frac{dX(x)}{dx} = \frac{\varepsilon_2 Z(x)}{\gamma} + \frac{\tilde{\varepsilon}_z Z(x)}{\gamma} + \frac{1}{\gamma}\frac{d^2Z(x)}{dx^2}. \tag{5.1.3}$$

Inserting (5.1.3) into the second equation (5.1.1) leads to

$$\frac{d^2Z(x)}{dx^2} + \frac{\varepsilon_2(\varepsilon_1 - \gamma^2)}{\varepsilon_1} Z(x) = \frac{\gamma^2 - \varepsilon_1}{\varepsilon_1} \tilde{\varepsilon}_z Z(x) - \frac{\gamma}{\varepsilon_1}\frac{d}{dx}\left(\tilde{\varepsilon}_x X(x)\right). \tag{5.1.4}$$

Assuming $\gamma^2 < \varepsilon_1$ and applying the second Green's formula[32] equation (5.1.4) can be transformed to the integral equation (for details see Appendix L.2)

$$\begin{aligned} Z(x) = Z_0(x) - \\ -\frac{(\varepsilon_1 - \gamma^2)}{\varepsilon_1} \int_0^h G(x,y)\, \tilde{\varepsilon}_z(y) Z(y) dy - \frac{\gamma}{\varepsilon_1} \int_0^h G(x,y) \left(\tilde{\varepsilon}_x(y) X(y)\right)' dy, \end{aligned} \tag{5.1.5}$$

where $Z_0(x)$ is given by

$$Z_0(x) = Z(0)\cos \hbar x + \frac{Z(h) - Z(0)\cos \hbar h}{\sin \hbar h} \sin \hbar x, \tag{5.1.6}$$

with

$$\hbar = \sqrt{\frac{\varepsilon_2\,(\varepsilon_1 - \gamma^2)}{\varepsilon_1}}. \tag{5.1.7}$$

The value $Z(0)$ is prescribed and $Z(h)$ will be determined in the following subsection.

The Green's function $G(x,y)$, corresponding to (5.1.4) is defined by[32] (for details see Appendix L.1)

$$G(x,y) = \begin{cases} \dfrac{\sin \hbar x \;\; \sin \hbar(y-h)}{\hbar \sin \hbar h}, & x \le y \\ \dfrac{\sin \hbar y \;\; \sin \hbar(x-h)}{\hbar \sin \hbar h}, & y \le x \end{cases} \tag{5.1.8}$$

where $\hbar\, h \neq \pi\, l, l = 1,2, \ldots$.

Integration by parts in (5.1.5) yields

$$Z(x) = Z_0(x) - \\ -\frac{\varepsilon_1 - \gamma^2}{\varepsilon_1}\int_0^h G(x,y)\tilde{\varepsilon}_z(y)Z(y)dy + \frac{\gamma}{\varepsilon_1}\int_0^h \frac{\partial G(x,y)}{\partial y}\tilde{\varepsilon}_x(y)X(y)dy. \tag{5.1.9}$$

Using the second equation (5.1.1) and using (5.1.9) leads to the integral equation for the x - component of the electric field

$$X(x) = \frac{\gamma\varepsilon_1}{\varepsilon_x(\gamma^2 - \varepsilon_1)}\frac{dZ_0(x)}{dx} + \\ +\frac{\gamma}{\varepsilon_x}\int_0^h \frac{\partial G(x,y)}{\partial x}\tilde{\varepsilon}_z(y)Z(y)dy + \frac{\gamma^2}{\varepsilon_x(\gamma^2 - \varepsilon_1)}\int_0^h \frac{\partial^2 G(x,y)}{\partial y \partial x}\tilde{\varepsilon}_x(y)X(y)dy. \tag{5.1.10}$$

Thus, the problem is reduced to the system (5.1.9), (5.1.10) that has to be solved subject to the boundary conditions.

5.2 Boundary conditions and dispersion relation

Continuity of the function $Z(x)$ given by (5.1.9) at the interfaces $x = 0$ and $x = h$ implies

$$\begin{cases} Z_0(0) = Z(0), \\ Z_0(h) = Z(h), \end{cases} \tag{5.2.1}$$

where $Z(0)$ is assumed to be prescribed and $Z(h)$ has to be determined.

Taking into account the well- known solutions $Z(x)$, $X(x)$ for the substrate and cladding (cf. (C.1.4), (C.1.6)) the boundary conditions (3.1.11), (3.1.12) read

$$\varepsilon_x\big(X(0+0,\gamma,Z(0)),Z(0)\big)\,X(0+0,\gamma,Z(0)) = \frac{\gamma\,\varepsilon_s\,Z(0)}{\sqrt{\gamma^2-\varepsilon_s}}, \tag{5.2.2}$$

$$\varepsilon_x\big(X(h-0,\gamma,Z(0)),Z(h)\big)X(h-0,\gamma,Z(0)) = -\frac{\gamma\,\varepsilon_c\,Z(h)}{\sqrt{\gamma^2-\varepsilon_c}}. \tag{5.2.3}$$

As outlined in Appendix M $Z(h)$ can be written as

$$Z(h) = Z_{lin}(h) + \\ + \frac{\varepsilon_1-\gamma^2}{\varepsilon_1\,\hbar}\int_0^h sin\,\hbar(y-h)\,\tilde{\varepsilon}_z(y)Z(y)dy - \frac{\gamma}{\varepsilon_1}\int_0^h cos\,\hbar(y-h)\,\tilde{\varepsilon}_x(y)X(y)dy, \tag{5.2.4}$$

where

$$Z_{lin}(h) = Z(0)(\cos\hbar h + \beta\sin\hbar h) \tag{5.2.5}$$

is a solution of the problem in the linear case ($f(x) = 0, a = b = 0$) (for details see Appendix C.1) with $x = h$ and

$$\beta = -\varepsilon_s\sqrt{\frac{\varepsilon_1-\gamma^2}{\varepsilon_1\,\varepsilon_2\,(\gamma^2-\varepsilon_s)}}. \tag{5.2.6}$$

Equations (5.1.9), (5.1.10), (5.2.2) and (5.2.3) are a representation of dispersion relation for the present case. It relates $h, \gamma, Z(0)$ to the parameters $a, b, \varepsilon_s, \varepsilon_1, \varepsilon_2, \varepsilon_c$ and function $f(x)$.

5.3 Iteration procedure

The system (5.1.9) and (5.1.10) can be written in matrix form as follows

$$\vec{v}(x) = \vec{v}_0(x) + \int_0^h M(\vec{v})\,(y)\vec{v}(y)dy + L(\vec{v})(x) \tag{5.3.1}$$

where

$$\vec{v}_0(x) = \begin{pmatrix} Z_0(x) \\ 0 \end{pmatrix}, \quad \vec{v}(x) = \begin{pmatrix} Z(x) \\ X(x) \end{pmatrix}, \quad L(\vec{v})(x) = \begin{pmatrix} 0 \\ \dfrac{\gamma\varepsilon_1}{\varepsilon_x(\gamma^2 - \varepsilon_1)} \dfrac{dZ_0(x)}{dx} \end{pmatrix}, \tag{5.3.2}$$

and M is given by

$$M = \begin{pmatrix} m_{11} & m_{12} \\ m_{21} & m_{22} \end{pmatrix} = \\ = \begin{pmatrix} -\dfrac{\varepsilon_1 - \gamma^2}{\varepsilon_1}\, G(x,y)\tilde{\varepsilon}_z(y) & \dfrac{\gamma}{\varepsilon_1}\dfrac{\partial G(x,y)}{\partial y}\tilde{\varepsilon}_x(y) \\ \dfrac{\gamma}{\varepsilon_x(x)}\dfrac{\partial G(x,y)}{\partial x}\tilde{\varepsilon}_z(y) & \dfrac{\gamma^2}{\varepsilon_x(x)\,(\gamma^2 - \varepsilon_1)}\dfrac{\partial^2 G(x,y)}{\partial y \partial x}\tilde{\varepsilon}_x(y) \end{pmatrix}. \tag{5.3.3}$$

Considering equation (5.3.1) in the Banach vector space $C[0,h]$ of continuous complex-valued functions on the segment $[0,h]$ and solving it by iterations using the Banach fixed-point theorem[33] (for details see Appendix N.1) the exact solution $\vec{v}(x)$ can be represented as the limit of a uniformly convergent sequence[33]

$$\vec{v}_j(x) = \vec{v}_0(x) + \textstyle\int_0^h M\left(\vec{v}_{j-1}\right)(y)\vec{v}_{j-1}(y)dy + L\left(\vec{v}_{j-1}\right)(x). \quad {\scriptstyle j=1,2,\ldots} \tag{5.3.4}$$

Contraction conditions of the Banach fixed-point theorem are given as follows (cf. Appendix N.2)

$$\begin{cases} I_0^2 \le \dfrac{4\,(1-f_0\,b_0)^3}{27\,a_0\,b_0}\,, \\ 1-f_0\,b_0>0, \\ \quad 0<q<1, \end{cases} \tag{5.3.5}$$

where

$$q = \frac{2a_0R\,\varepsilon_1|\gamma|}{(\varepsilon_1-\gamma^2)\,(\varepsilon_1-f_0)^2}\left\|\frac{dZ_0(x)}{dx}\right\| + b_0(f_0+a_0R^2) + \frac{\not{k}hR^2}{|\sin\not{k}h|}\times$$
$$\times\left[\frac{\varepsilon_1-\gamma^2}{\varepsilon_1}\cdot\frac{h^2}{4} + h|\gamma|\cdot\frac{a_0(\varepsilon_1+2f_0)+R^2|a^2-b^2|}{(\varepsilon_1-f_0)^2} + \right.$$
$$\left. + \frac{a_0|\gamma|h}{\varepsilon_1} + \frac{2a_0\varepsilon_1\gamma^2}{(\varepsilon_1-\gamma^2)(\varepsilon_1-f_0)^2}\right], \tag{5.3.6}$$

and

$$0 < R_{min} \le R \le R_{max}\ , \tag{5.3.7}$$

where R_{min}, R_{max} are two positive roots of the polynomial

$$a_0\,b_0\,R^3 - (1-f_0\,b_0)R + I_0 = 0, \tag{5.3.8}$$

$$f_0 = max|f(x)|\,, \tag{5.3.9}$$

$$a_0 = max(a\,,b)\,, \tag{5.3.10}$$

$$b_0 = \frac{\not{k}\,h}{2|\sin\not{k}h|}\cdot\ max\left\{\frac{h^2\,|\varepsilon_1-\gamma^2|}{4\,\varepsilon_1} + \frac{h\,|\gamma|}{\varepsilon_1-f_0}\ ;\ \frac{h\,|\gamma|}{\varepsilon_1} + \frac{2\,\gamma^2}{|\varepsilon_1-\gamma^2|\,(\varepsilon_1-f_0)}\right\}, \tag{5.3.11}$$

and

$$I_0 = \|Z_0(x)\| + \frac{|\gamma|\,\varepsilon_1}{|\varepsilon_1-\gamma^2|\,(\varepsilon_1-f_0)}\left\|\frac{dZ_0(x)}{dx}\right\|. \tag{5.3.12}$$

The a priory error estimate[33] for $\vec{v}$ reads

$$\left\|\vec{v}-\vec{v}_j\right\| \le \frac{q^j}{1-q}\|\vec{v}_1-\vec{v}_0\|. \tag{5.3.13}$$

5.4 Numerical results

To illustrate the analysis of the present section the material parameters and function $f(x)$ are chosen as follows

$$\varepsilon_s = 1, \quad \varepsilon_c = 12.25, \quad \varepsilon_1 = 16, \quad \varepsilon_2 = 4, \quad a = 0.03,$$
$$Z(0) = 0.1, \quad f(x) = m\,Cos^2 nx, \quad m = 0.3, \quad n = 0.2, \quad b = 0.01. \tag{5.4.1}$$

Figure 68 shows solution of the dispersion relation (5.3.4), (5.2.2) and (5.2.3) in the first iteration ($j = 1$) obtained for the pure Kerr-case ($f(x) = 0$) compared with the exact solution according to (3.1.14) ($m = n = 0$). Blue region depicts the domain where the contraction conditions (5.3.5) are satisfied.

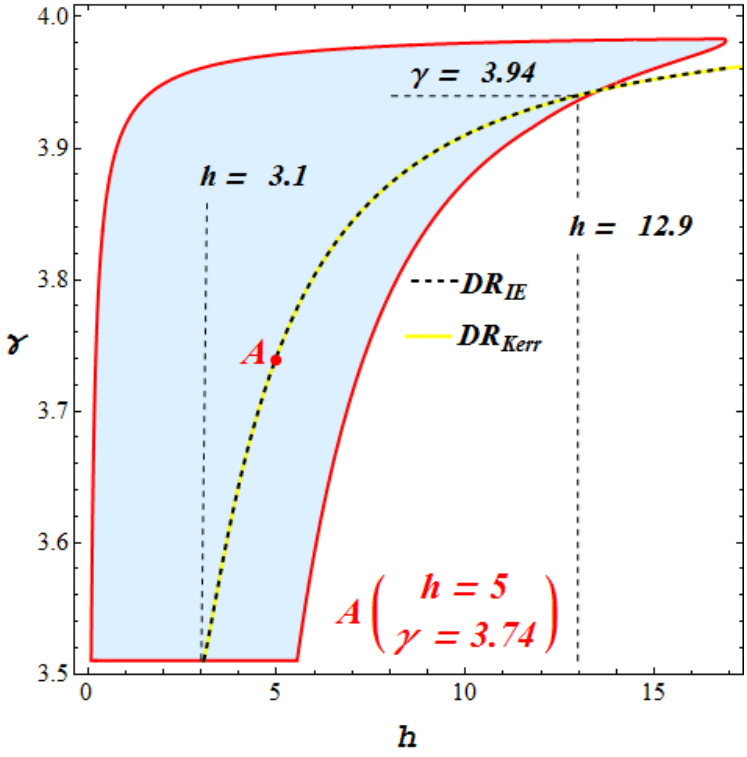

Figure 68: First iteration of the dispersion relation for the pure Kerr-case (black dashed curve DR_{IE}) compared with the exact solution according to (3.1.14) (yellow curve DR_{Kerr}); $m = n = 0$. Blue region: contraction conditions (5.3.5) are satisfied for $3.1 \leq h \leq 12.9$.

As follows from Figure 68, there is a good agreement between the solutions obtained by the two different methods: according to steps the I- VII of Section 3 on the one hand, and according to the integral approach of the present Section on the other one. This is also valid for the solution $Z(h)$ as shown in Figure 69.

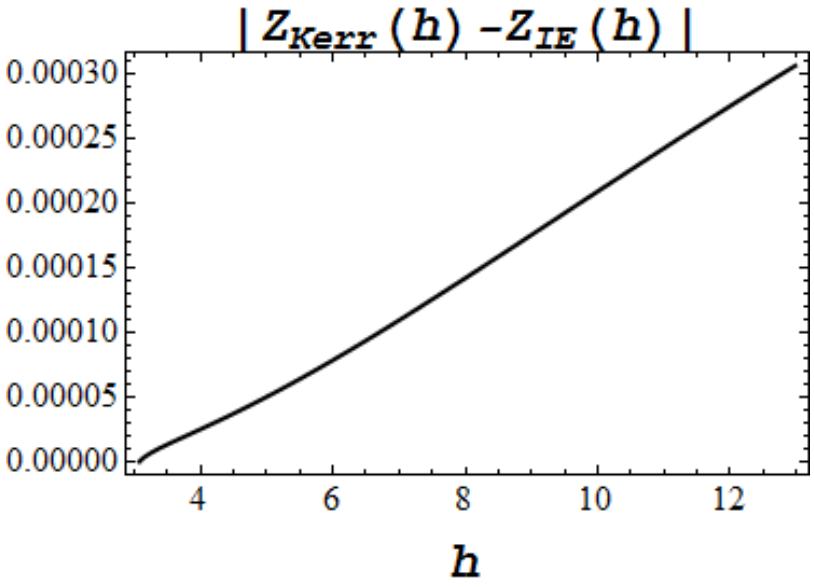

Figure 69: The difference between solutions $Z(h)$ obtained according to (5.2.4) (in Figure denoted as $Z_{IE}(h)$) and Step VI. of Section 3 (in Figure denoted as $Z_{Kerr}(h)$)

Solution of the dispersion relation (5.3.4), (5.2.2), (5.2.3) in the first iteration ($j = 1$) for the case of the spatially varying permittivity ($f(x) \neq 0, a = b = 0$) in the film in comparison with the solution of the linear problem (cf. (C.1.8), $f(x) = 0, a = b = 0$) is presented in Figure 70. As above the blue region shows the domain where the contraction conditions (5.3.5) are satisfied.

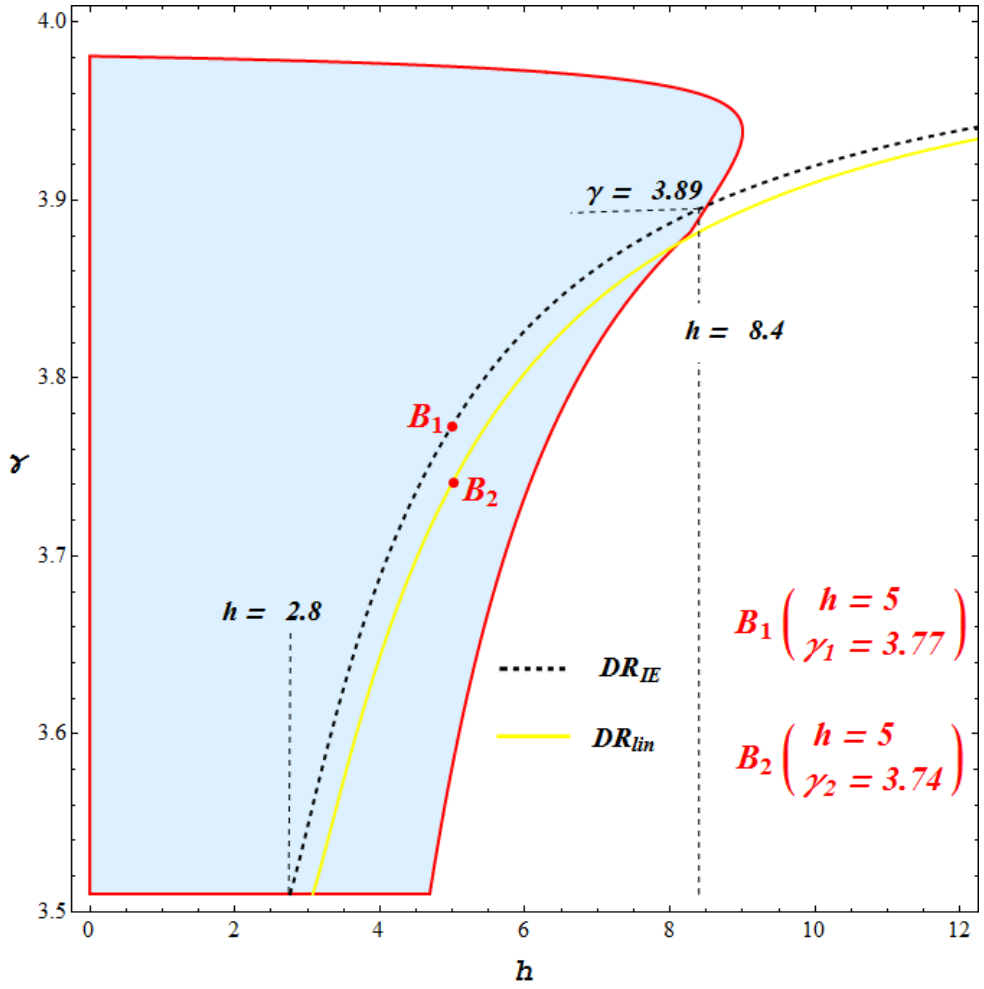

Figure 70: Dispersion relation for $a = b = 0$ (black dashed curve DR_{IE}) compared with the solution in the linear case (cf. (C.1.8)) (yellow curve DR_{lin}). Blue region: contraction conditions (5.3.5) are satisfied for $2.8 \leq h \leq 8.4$.

Figure 71 illustrates the solution of the problem if the dielectric function in the film (cf. (5.1)) depends on the transverse coordinate x as well as on the field intensity $|\boldsymbol{E}|^2$ $(f(x) \neq 0, a \neq 0, b \neq 0)$. The total power flow transported by the TM- wave in this case is depicted in Figure 72.

Choosing the propagation constant γ and the film thickness h as shown by the points A, B_1 and B_2, C in Figures 68, 70, 71, respectively, the corresponding field patterns $Z(x), X(x), H(x)$ of the nonlinear TM- wave are represented in Figures 73, 74.

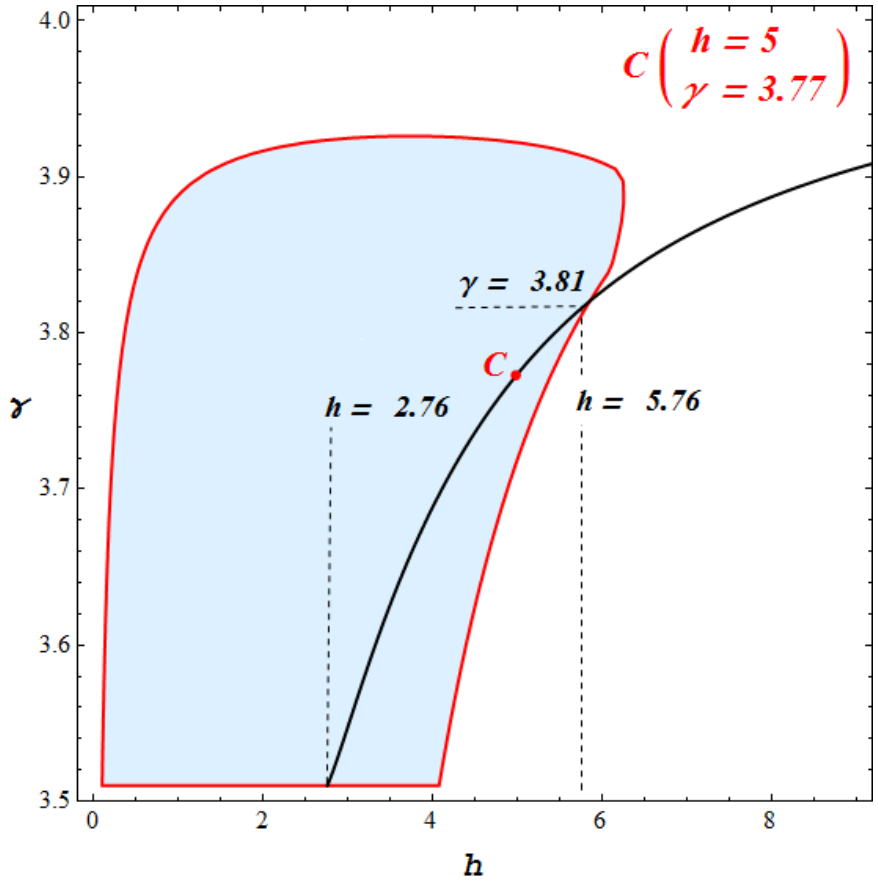

Figure 71: Dispersion relation for the general case with parameters cf. (5.4.1). Blue region: contraction conditions (5.3.5) are satisfied for $2.76 \leq h \leq 5.76$.

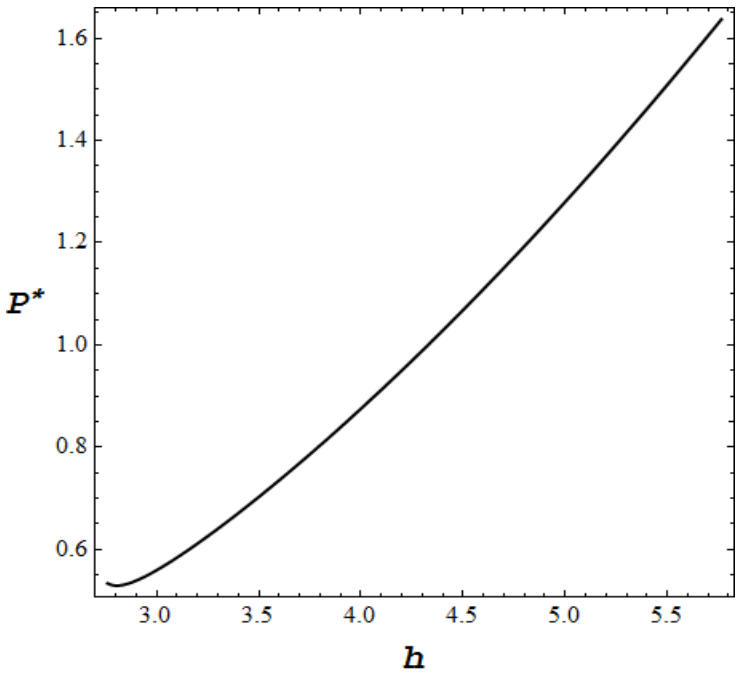

Figure 72: The total power flow corresponding to the dispersion relation in Figure 71

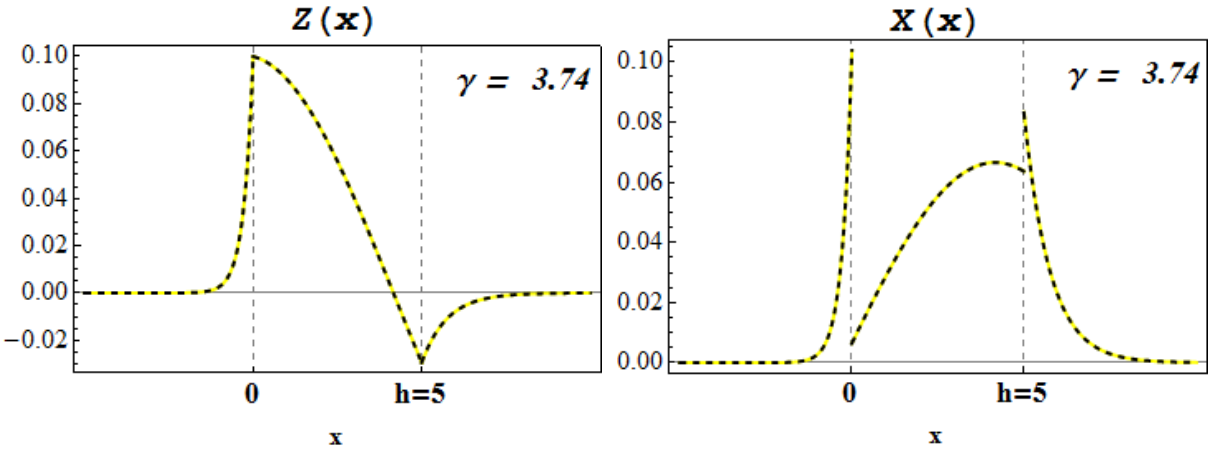

a)

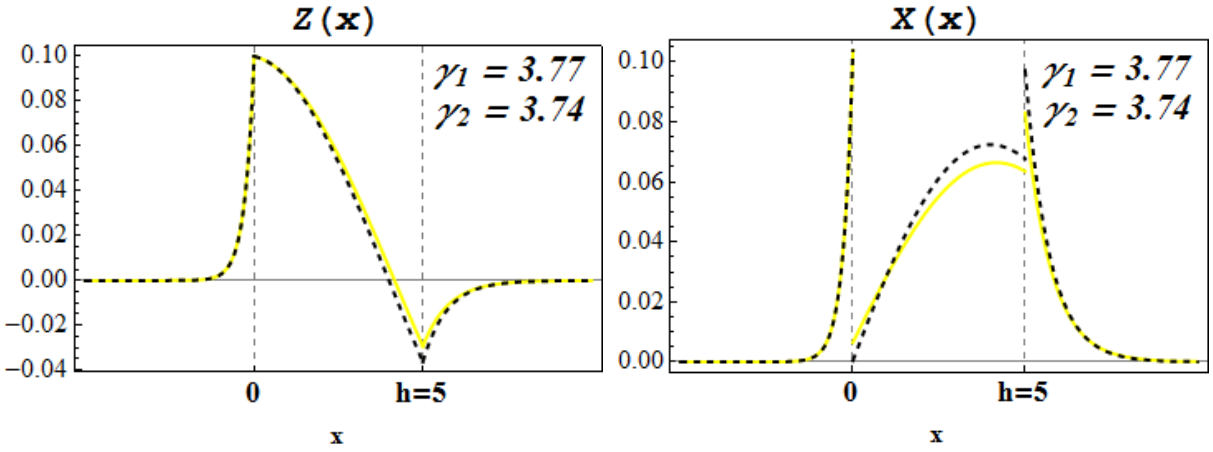

b)

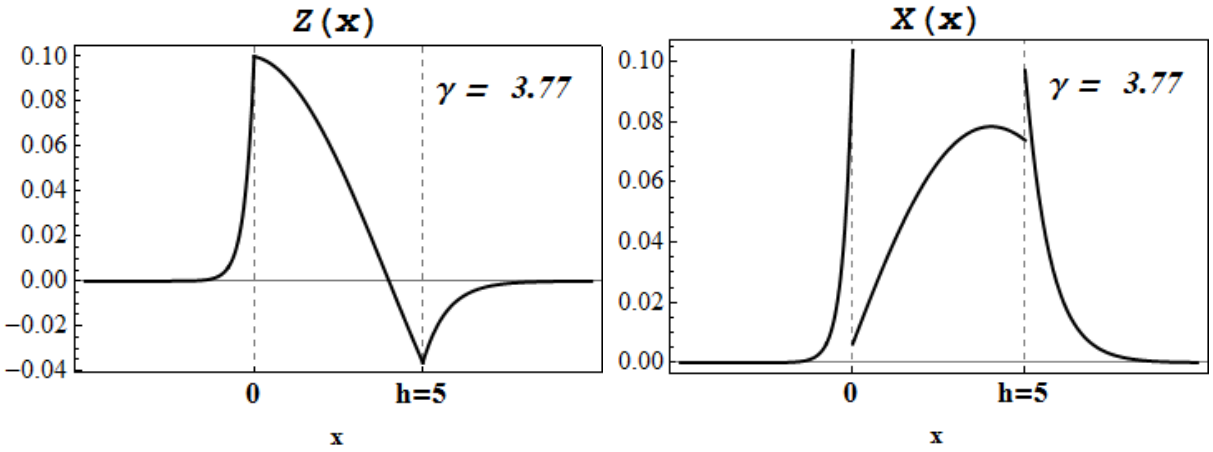

c)

Figure 73: Electric field patterns of the TM_0 wave propagating in the waveguide prescribed in **a)** Figure 68 (values h, γ are given by point A), **b)** Figure 70 (values h, γ are given by points B_1, B_2), **c)** Figure 71 (values h, γ are given by point C)

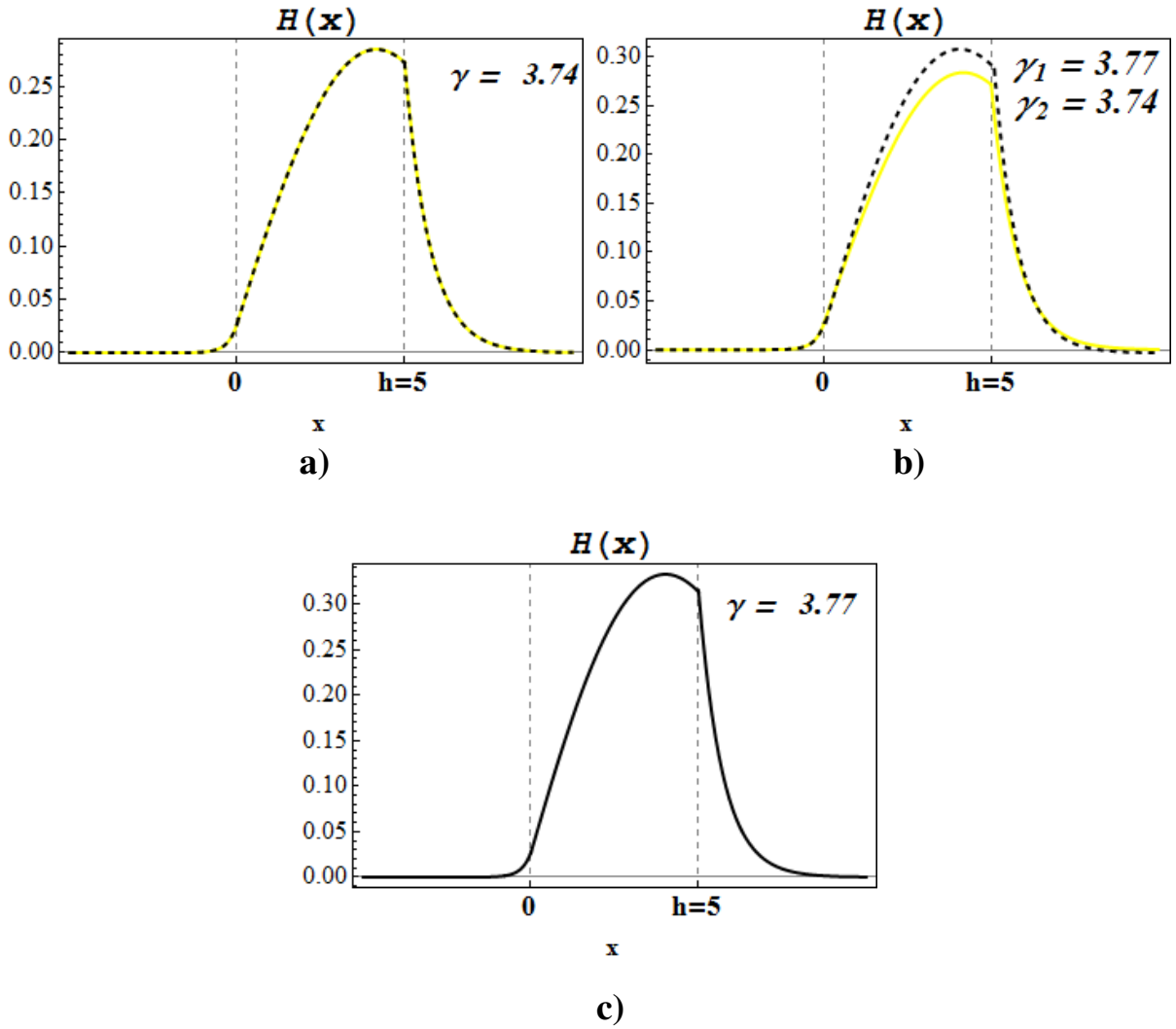

Figure 74: Magnetic field patterns of the TM_0 wave propagating in the waveguide prescribed in **a)** Figure 68 (values $h,\ \gamma$ are given by point A) **b)** Figure 70 (values $h,\ \gamma$ are given by points B_1, B_2) **c)** Figure 71 (values $h,\ \gamma$ are given by point C)

As follows from Figures 73 a), 74 a) the agreement between the wave solutions obtained according to the methods of Section 3 and the integral approach procedure of the present Section is satisfactory. – This consistency proofs (to a certain extent) the validity of results presented in this dissertation.

6 Summary, Open Problems, and Outlook

In the present dissertation travelling TM- $\left(A(x,z)e^{-i(\omega t-\gamma z)}\right)$ waves with phase velocity $\frac{\omega}{\gamma}$ in a three- layer waveguide with homogeneous, lossless and nonmagnetic media has been studied for two types of permittivities:

III.

$$\varepsilon_\nu = \begin{pmatrix} \varepsilon_{x\nu} & 0 & 0 \\ 0 & \varepsilon_{y\nu} & 0 \\ 0 & 0 & \varepsilon_{z\nu} \end{pmatrix}, \tag{6.1}$$

where

$$\begin{aligned} \varepsilon_{x\nu} &= \varepsilon_{1\nu} + a_\nu |E_x|^2 + b_\nu |E_z|^2, \\ \varepsilon_{z\nu} &= \varepsilon_{2\nu} + b_\nu |E_x|^2 + a_\nu |E_z|^2, \end{aligned} \tag{6.2}$$

$\varepsilon_{1\nu}$, $\varepsilon_{2\nu}$, a_ν, b_ν real constants, and $\nu = s, f, c$ for the substrate, film, and cladding, respectively[9];

IV.

$$\varepsilon_\nu = \begin{cases} \varepsilon_s = const, & \nu = s, \\ \begin{pmatrix} \varepsilon_{xf} & 0 & 0 \\ 0 & \varepsilon_{yf} & 0 \\ 0 & 0 & \varepsilon_{zf} \end{pmatrix}, & \nu = f, \\ \varepsilon_c = const, & \nu = c, \end{cases} \tag{6.3}$$

where[9]

$$\begin{aligned} \varepsilon_{xf} &= \varepsilon_{1f} + \tilde{\varepsilon}_x, \\ \varepsilon_{zf} &= \varepsilon_{2f} + \tilde{\varepsilon}_z, \end{aligned} \tag{6.4}$$

$$\begin{aligned} \tilde{\varepsilon}_x &= f(x) + a_f |E_x|^2 + b_f |E_z|^2, \\ \tilde{\varepsilon}_z &= f(x) + b_f |E_x|^2 + a_f |E_z|^2, \end{aligned} \tag{6.5}$$

ε_{1f}, ε_{2f}, a_f, b_f are real constants, and $f(x)$ a continuously differentiable real- valued function of the transverse coordinate x.

Permittivities of type I satisfy an integrability condition that leads to an exact differential equation with a first integral (expressed by a polynomial equation in Z^2, X^2) of Maxwell's equations. Using the first integral, combination of Maxwell's equations with the boundary conditions leads to exact analytical dispersion relations expressed in terms of integrals.
In general, these integrals do not possess a primitive function (only for special cases, e.g., uniaxial media, a primitive function exists). Thickness h and propagation constant γ satisfying the dispersion relation, are associated to the possible modes propagating in the waveguide. The corresponding power flow is calculated straightforwardly. Comparison with publications of Tables 2, 3 shows that results obtained are new to a certain extent.

If permittivities do not satisfy an integrability condition (e.g. like type II) Maxwell's equations are solved by means of an integral equation approach applying an iterative procedure based on the Banach fixed- point theorem. As for type I permittivities, dispersion relation, field components, and power flow have been evaluated and compared (for $f(x) \equiv 0$) with results for type I nonlinearity. The consistency is remarkably good.
With regards to novelty it seems that the integral equation approach has been applied for the first time to the present problem[34] (cf. [24, Table 3]). It presents a general analytical approximate solution of the problem.

Further investigations are motivated by the following open problems:

- The left- hand side of the equations (3.1.14), (3.1.15) must be real and positive, it seems interesting and nontrivial to analyze these conditions analytically, in order to obtain constrains for the parameters $\varepsilon_{1\nu}$, $\varepsilon_{2\nu}$, a_ν, b_ν ($\nu = s, f, c$), and the value $Z(0)$.

- Numerical results given in subsections 4.1.2.1- 2 (self-defocusing film bounded by the linear media), 4.1.4 (metamaterial nonlinear film) and 4.4 (nonlinear substrate, film and cladding) have shown
  - that more than one real root $X_f(0+0,\gamma,Z(0))$ or $Z(h)$ of the equations (3.1.11) and (3.1.12), respectively, can exist, leading to the different dispersion relations. The question which of these solutions will be dominate can be approached by a stability analysis,
  - that the transport of the energy inside and outside the film exhibits opposite signs – it seems interesting to analyze these remarkable results.
- It seems, the method outlined in Sections 3, 4 can be generalized to more general nonlinearities of the dielectric function (if the integrability condition is satisfied, for example,
  $\varepsilon_v \sim |\boldsymbol{E}|^{2n},\ n = 2, 3, \ldots$).

With respect to the integral equation approach

- it is interesting to obtain the parameters ε_s, ε_c, ε_1, ε_2, a, b, $Z(0)$ such that contraction conditions are valid also for higher modes solutions,
- permittivities more general that given by (5.1) (for example, absorbing or saturating film, nonlinearity of higher order) could be investigated.

Appendixes

A On the transformation of the system (2.4)

With the ansatz (2.10) the system (2.4) reads

$$\begin{cases} i\gamma \hat{E}_x - \dfrac{d\hat{E}_z}{dx} = i\omega\mu \hat{H}_y, \\ \dfrac{d\hat{H}_y}{dx} = -i\omega\varepsilon \hat{E}_z, \\ i\gamma \hat{H}_y = i\omega\varepsilon \hat{E}_x. \end{cases} \tag{A.0.1}$$

Differentiating the first equation of (A.0.1) and using the second one leads to

$$-\frac{d^2\hat{E}_z(x)}{dx^2} + \gamma i \frac{d\hat{E}_x(x)}{dx} = \omega^2\mu\varepsilon \hat{E}_z(x). \tag{A.0.2}$$

Combining the first and third equations of (A.0.1) gives

$$-\frac{d\hat{E}_z(x)}{dx} + \gamma i \hat{E}_x(x) = \frac{\omega^2\mu\varepsilon i \hat{E}_x(x)}{\gamma}. \tag{A.0.3}$$

Division on both sides of (A.0.2) and (A.0.3) by $k^2 = \omega^2\mu\varepsilon_0$ implies

$$\begin{cases} -\dfrac{1}{k^2}\dfrac{d^2\hat{E}_z(x)}{dx^2} + \dfrac{\gamma}{k^2} i \dfrac{d\hat{E}_x(x)}{dx} = \dfrac{\varepsilon}{\varepsilon_0}\hat{E}_z(x), \\ -\dfrac{1}{k^2}\dfrac{d\hat{E}_z(x)}{dx} + \dfrac{\gamma}{k^2} i \hat{E}_x(x) = \dfrac{\varepsilon}{\varepsilon_0}\dfrac{i\hat{E}_x(x)}{\gamma}. \end{cases} \tag{A.0.4}$$

Applying to the system (A.0.4) the normalization procedure according to (2.12) (A.0.4) reads (in dimensionless quantities)

$$\begin{cases} -\dfrac{d^2\hat{E}_z(\tilde{x})}{d\tilde{x}^2} + \tilde{\gamma}\ \dfrac{di\hat{E}_x(\tilde{x})}{d\tilde{x}} = \tilde{\varepsilon}\ \hat{E}_z(\tilde{x}), \\ -\dfrac{d\hat{E}_z(\tilde{x})}{d\tilde{x}} + \tilde{\gamma}\ i\hat{E}_x(\tilde{x}) = \dfrac{\tilde{\varepsilon}}{\tilde{\gamma}}\ i\hat{E}_x(\tilde{x}). \end{cases} \tag{A.0.5}$$

Using notation (2.13) and omitting the tilde sign in (A.0.5) the system (2.11) is obtained.

B Expression for the magnetic field *H*

Rewriting the first equation of the system (A.0.1) gives

$$\widehat{H}_y = \frac{1}{i\omega\mu}\left(i\gamma\hat{E}_x - \frac{d\hat{E}_z}{dx}\right). \tag{B.0.1}$$

According to the normalization (2.12) and the notation (2.13) expression (B.0.1) can be rewritten as (noting here that $\mu = \mu_0$)

$$\widehat{H}_y(\tilde{x}) = \frac{-i\sqrt{\varepsilon_0\,\mu_0}}{k\,\mu_0}\left(k\tilde{\gamma}\cdot i\hat{E}_x(\tilde{x}) - k\frac{d\hat{E}_z(\tilde{x})}{d\tilde{x}}\right),$$

$$\widehat{H}_y(\tilde{x}) = -i\sqrt{\frac{\varepsilon_0}{\mu_0}}\left(\tilde{\gamma}\cdot i\hat{E}_x(\tilde{x}) - \frac{d\hat{E}_z(\tilde{x})}{d\tilde{x}}\right),$$

$$\widehat{H}_y(\tilde{x}) = -i\sqrt{\frac{\varepsilon_0}{\mu_0}}\left(-\frac{dZ(\tilde{x})}{d\tilde{x}} + \tilde{\gamma}X(\tilde{x})\right),$$

$$H_v(x) =: i\sqrt{\frac{\mu_0}{\varepsilon_0}}\widehat{H}_y = \left(\gamma X_v(x) - \frac{dZ_v(x)}{dx}\right), \tag{B.0.2}$$

where the tilde sign has been omitted.

C. On the solutions of the linear problem

C.1 Dispersion relation, field solutions and the total power flow

If $a_\nu = b_\nu = 0$ (linear case) the system (2.11) reads

$$\begin{cases} -\dfrac{d^2 Z_\nu(x)}{dx^2} + \gamma \dfrac{dX_\nu(x)}{dx} = \varepsilon_{2\nu}\, Z_\nu(x), \\ -\gamma \dfrac{dZ_\nu(x)}{dx} + \gamma^2 X_\nu(x) = \varepsilon_{1\nu}\, X_\nu(x) \end{cases} \tag{C.1.1}$$

and hence

$$\frac{d^2 Z_\nu(x)}{dx^2} + \hbar_\nu^2 Z_\nu(x) = 0, \tag{C.1.2}$$

where

$$\hbar_\nu^2 = \frac{\varepsilon_{2\nu}(\varepsilon_{1\nu} - \gamma^2)}{\varepsilon_{1\nu}}. \tag{C.1.3}$$

Due to the well- known theory of linear differential equations the solution of (C.1.2) can be found directly[35]. Taking into account the boundary conditions at the interfaces and the infinity the solutions $Z_\nu(x)$ are given by

$$\begin{aligned} Z_s(x) &= Z(0) e^{\sqrt{-\hbar_s^2}\, x}, && x < 0 \\ Z_f(x) &= Z(0)\left(\cos \hbar_f x + p_{sf} \sin \hbar_f x\right), && 0 < x < h \\ Z_c(x) &= Z(h)\, e^{-\sqrt{-\hbar_c^2}(x-h)}, && x > h \end{aligned} \tag{C.1.4}$$

where

$$p_{sf} = -\sqrt{\frac{\varepsilon_{1s}\,\varepsilon_{2s}\,(\varepsilon_{1f}-\gamma^2)}{\varepsilon_{1f}\,\varepsilon_{2f}\,(\gamma^2-\varepsilon_{1s})}}, \tag{C.1.5}$$

($\gamma^2 < \varepsilon_{1f}$ but $\gamma^2 > \varepsilon_{1\nu}$ for $\nu = s, c$.)

Using the second equation of the system (C.1.1) the solutions $X_\nu(x)$ are

$$\begin{aligned} X_s(x) &= \frac{\gamma\, Z(0)}{(\gamma^2-\varepsilon_{1s})}\sqrt{-\hbar_s^2}\;\, e^{\sqrt{-\hbar_s^2}\,x}, && x<0\\ X_f(x) &= \frac{\gamma\;\, Z(0)\,\hbar_f}{(\gamma^2-\varepsilon_{1f})}\left(p_{sf}\,cos\,\hbar_f x - sin\hbar_f x\right), && 0<x<h\\ X_c(x) &= -\frac{\gamma\, Z(h)}{(\gamma^2-\varepsilon_{1c})}\sqrt{-\hbar_c^2}\;\, e^{-\sqrt{-\hbar_c^2}(x-h)}. && x>h \end{aligned} \tag{C.1.6}$$

Using (A.0.1) the magnetic field components are given by

$$\begin{aligned} H_s(x) &= \frac{\varepsilon_{1s}\, Z(0)}{(\gamma^2-\varepsilon_{1s})}e^{\sqrt{-\hbar_s^2}\,x}, && x<0\\ H_f(x) &= \frac{\varepsilon_{1f}\,\hbar_f\, Z(0)}{(\gamma^2-\varepsilon_{1f})}\left(p_{sf}\,cos\hbar_f x - sin\hbar_f x\right), && 0<x<h\\ H_c(x) &= -\frac{\varepsilon_{1c}\, Z(h)}{(\gamma^2-\varepsilon_{1c})}e^{-\sqrt{-\hbar_c^2}(x-h)}. && x>h \end{aligned} \tag{C.1.7}$$

Taking into account the boundary conditions at the interfaces and the solutions (C.1.4), (C.1.7) the dispersion relation reads

$$tan\,\hbar_f h = \frac{\hbar_f\,(\sqrt{-k_s^2}+\sqrt{-k_c^2})}{k_f^2-\sqrt{-k_s^2}\cdot\sqrt{-k_c^2}} \tag{C.1.8}$$

consistent with the well- known result of linear wave- guide theory[12, 13].

The total power flow in a waveguide with the film thickness h is given in Section 3.2

$$P^* = \frac{P}{P_0} = P_s^* + P_f^* + P_c^*, \tag{C.1.9}$$

where

$$P_s^* = \frac{\varepsilon_{1s}\,\gamma\,Z^2(0)}{2\sqrt{(\gamma^2-\varepsilon_{1s})^3}},$$
$$P_f^* = \frac{\gamma\varepsilon_{1s}\hbar_f Z^2(0)}{4\,(\varepsilon_{1f}-\gamma^2)^2}\times$$
$$\times\left(2\left(p_{sf}cos\,2\hbar_f h + 2\hbar_f h\left(p_{sf}^2+1\right)-p_{sf}\right)+(p_{sf}^2-1)sin\,2\hbar_f h\right)$$
$$P_c^* = \frac{\varepsilon_{1c}\,\gamma\,Z^2(h)}{2\sqrt{(\gamma^2-\varepsilon_{1c})^3}} \qquad \text{(C.1.10)}$$

are the parts of the total power flow in the substrate, film and cladding, respectively.

C.2 On the inversion of equations (3.1.7) and (3.1.8) in the linear case

The linear solutions $Z_\nu(x)$ can also be obtained by integration and inversion of the integral (3.1.7) (with $a_\nu = b_\nu = 0$) as follows.

Setting $Z_s(x_0) = Z(0)$, $\nu = s$, and choosing plus sign of the square root in (3.1.9) gives

$$\int_{Z(0)}^{Z_s(x)} \frac{\gamma\,d\zeta}{+\sqrt{\frac{\varepsilon_{2s}\,\gamma^2\,\zeta^2}{\varepsilon_{1s}\,(\gamma^2-\varepsilon_{1s})}}\,(\gamma^2-\varepsilon_{1s})} = x,$$
$$\frac{1}{\sqrt{-\hbar_s^2}}\,log\,Z\Big|_{Z=Z(0)}^{Z=Z_s(x)} = x,$$
$$log\,Z_s(x) = \sqrt{-\hbar_s^2}\,x + log\,Z(0). \qquad \text{(C.2.1)}$$

Solving (C.2.1) with respect to $Z_s(x)$ the solution in the substrate is obtained.

Setting $Z_f(x_0) = Z(0)$, $\nu = f$, and choosing plus sign of the square root in (3.1.9) gives

$$\int_{Z(0)}^{Z_f(x)} \frac{\gamma\, d\zeta}{\sqrt{-\dfrac{2\,C_f + \varepsilon_{2f}\,\gamma^2\,\zeta^2}{\varepsilon_{1f}\,(\gamma^2-\varepsilon_{1f})}\,(\gamma^2-\varepsilon_{1f})}} = x,$$

$$\frac{1}{\hbar_f} arctan\,\gamma Z \sqrt{-\frac{\varepsilon_{1f}}{2\,C_f + \varepsilon_{2f}\,\gamma^2\,Z^2}}\Bigg|_{Z=Z(0)}^{Z=Z_f(x)} = x,$$

$$arctan\,\gamma Z_f(x) \sqrt{-\frac{\varepsilon_{1f}}{2\,C_f + \varepsilon_{2f}\gamma^2 Z_f^2(x)}} =$$

$$= \hbar_f x + arctan\,\gamma Z(0) \sqrt{-\frac{\varepsilon_{1f}}{2\,C_f + \varepsilon_{2f}\gamma^2 Z^2(0)}}, \qquad \text{(C.2.2)}$$

where

$$C_f = \frac{1}{2}\,\gamma^2\,Z^2(0)\left(\frac{\varepsilon_{1s}\,\varepsilon_{2s}\,(\varepsilon_{1f}-\gamma^2)}{\varepsilon_{1f}(\varepsilon_{1s}-\gamma^2)} - \varepsilon_{2f}\right). \qquad \text{(C.2.3)}$$

Taking the tangent of (C.2.2) and solving the resulting equation with respect to $Z_f(x)$ the solution in the film is found (see (C.1.4)).

Setting $Z_c(x_0) = Z(h)$, $\nu = c$, and choosing minus sign of the square root in (3.1.9) gives

$$\int_{Z(h)}^{Z_c(x)} \frac{\gamma\, d\zeta}{-\sqrt{\dfrac{\varepsilon_{2c}\,\gamma^2\,\zeta^2}{\varepsilon_{1c}\,(\gamma^2-\varepsilon_{1c})}\,(\gamma^2-\varepsilon_{1c})}} = x - h,$$

$$\frac{-1}{\sqrt{-\hbar_c^2}} \log Z\Big|_{Z=Z(h)}^{Z=Z_c(x)} = x - h,$$

$$\log Z_c(x) = -\sqrt{-\hbar_c^2}\,(x-h) + \log Z(h). \qquad \text{(C.2.4)}$$

Solving (C.2.4) with respect to $Z_c(x)$ the solution in the cladding is obtained.

Integrating and inverting the integral (3.1.8) (with $a_\nu = b_\nu = 0$) leads to the linear solutions $X_\nu(x)$ as follows.

Setting $X_s(x_0) = X(0-0)$, $\nu = s$, (value $X(0-0)$ is defined below) and choosing plus sign of the square root in (3.1.9) gives

$$\int_{X(0-0)}^{X_s(x)} \frac{\varepsilon_{1s}\, d\xi}{+\sqrt{\frac{\varepsilon_{1s}\,(\gamma^2-\varepsilon_{1s})\xi^2}{\varepsilon_{2s}\gamma^2}\cdot\varepsilon_{2s}\gamma}} = x,$$

$$\frac{1}{\sqrt{-\hbar_s^2}}\log X\Big|_{X=X(0-0)}^{X=X_s(x)} = x,$$

$$\log X_s(x) = \sqrt{-\hbar_s^2}\,x + \log X(0-0). \qquad \text{(C.2.5)}$$

Solving (C.2.5) with respect to $X_s(x)$ the solution in the substrate is obtained.

Setting $X_f(x_0) = X(0+0)$, $\nu = f$, and choosing plus sign of the square root in (3.1.9) gives

$$\int_{X(0+0)}^{X_f(x)} \frac{\varepsilon_{1f}\ d\xi}{\sqrt{-\frac{2\,C_f + \varepsilon_{1f}\left(\varepsilon_{1f}-\gamma^2\right)\xi^2}{\varepsilon_{2f}\,\gamma^2}\cdot\varepsilon_{2f}\gamma}} = x,$$

$$\frac{1}{\hbar_f}\arctan X\sqrt{-\frac{\varepsilon_{2f}\gamma^2}{2\,C_f + \varepsilon_{1f}\left(\varepsilon_{1f}-\gamma^2\right)X^2}}\Bigg|_{X=X(0+0)}^{X=X_f(x)} = x,$$

$$\arctan X_f(x)\sqrt{-\frac{\varepsilon_{2f}\gamma^2}{2\,C_f + \varepsilon_{1f}\left(\varepsilon_{1f}-\gamma^2\right)X_f^2(x)}} =$$

$$= \hbar_f x + \arctan X(0+0)\sqrt{-\frac{\varepsilon_{2f}\gamma^2}{2\,C_f + \varepsilon_{1f}\left(\varepsilon_{1f}-\gamma^2\right)X^2(0+0)}}. \qquad \text{(C.2.6)}$$

From the boundary conditions at the interface $x = 0$ it follows

$$X(0+0) = \frac{\gamma\varepsilon_{1s}Z(0)}{\varepsilon_{1f}(\gamma^2-\varepsilon_{1s})}, \qquad \text{(C.2.7)}$$

$$X(0-0) = \frac{\varepsilon_{1f}X(0+0)}{\varepsilon_{1s}}. \qquad \text{(C.2.8)}$$

Taking the tangent of (C.2.6) and solving the resulting equation with respect to $X_f(x)$ the solution in the film is found.

Setting $X_c(x_0) = X(h+0)$, $\nu = c$, and choosing minus sign of the square root in (3.1.9) gives

$$\int_{X(h+0)}^{X_c(x)} \frac{\varepsilon_{1c}\, d\xi}{-\sqrt{\frac{\varepsilon_{1c}\,(\gamma^2-\varepsilon_{1c})\xi^2}{\varepsilon_{2c}\gamma^2}\cdot\varepsilon_{2c}\gamma}} = x-h,$$

$$\frac{-1}{\sqrt{-\varkappa_c^2}}\log X\Big|_{X=X(h+0)}^{X=X_c(x)} = x-h,$$

$$\log X_c(x) = -\sqrt{-\varkappa_c^2}\,(x-h) + \log X(h+0). \tag{C.2.9}$$

Using the boundary conditions at the interface $x = h$ implies

$$X(h-0) = -\frac{\gamma\varepsilon_{1c}Z(h)}{\varepsilon_{1f}(\gamma^2-\varepsilon_{1c})}, \tag{C.2.10}$$

$$X(h+0) = \frac{\varepsilon_{1f}X(h-0)}{\varepsilon_{1c}}. \tag{C.2.11}$$

Solving (C.2.9) with respect to $X_c(x)$ the solution in the cladding is obtained.

D On the evaluation of the power flow

D.1 On the expression for the power flow (3.2.2)

Inserting ansatz (2.1) into (3.2.1) gives

$$\bar{S}_z = \frac{1}{2}\, Re\big[\vec{\mathcal{E}} \times \vec{\mathcal{H}}^*\big]_z = \frac{1}{2}\, Re[\boldsymbol{E} \times \boldsymbol{H}^*]_z = \frac{1}{2}\, Re\big[E_x H_y^*\big] = \frac{1}{2}\, Re\big[\hat{E}_x(x)\, \hat{H}_y^*(x)\big]. \tag{D.1.1}$$

Using the third equation of the system (A.0.1) the expression (D.1.1) can be rewritten as

$$\bar{S}_z = \frac{1}{2}\, \frac{\omega\, \varepsilon}{\gamma}\, \hat{E}_x(x)\, \hat{E}_x^*(x) = \frac{1}{2}\, \frac{\omega\, \varepsilon}{\gamma}\, \big|\hat{E}_x(x)\big|^2. \tag{D.1.2}$$

Rewriting (D.1.2) using (2.12) and normalizing by $P_0 = \frac{\omega\, \varepsilon_0}{2}$ implies

$$\frac{\bar{S}_z}{P_0} = \frac{\tilde{\varepsilon}\, \big|\hat{E}_x(\tilde{x})\big|^2}{\tilde{\gamma}}. \tag{D.1.3}$$

Omitting the tilde sign in (D.1.3) and using (2.19), (2.6) the power flow transported by the nonlinear wave (per unit width in the y- direction) is given by

$$P^* = \int_{-\infty}^{\infty} \frac{\bar{S}_z(x)}{P_0}\, dx = \int_{-\infty}^{\infty} \frac{\varepsilon_{xv} X_v(x)}{\gamma}\, dx =$$

$$= \int_{-\infty}^{0} \frac{\varepsilon_{xs}\, X_s^2(x)}{\gamma}\, dx + \int_{0}^{h} \frac{\varepsilon_{xf}\, X_f^2(x)}{\gamma}\, dx + \int_{h}^{\infty} \frac{\varepsilon_{xc}\, X_c^2(x)}{\gamma}\, dx. \tag{D.1.4}$$

D.2 On the evaluation of the power flow according to (3.2.3)

To evaluate the power flow given by (3.2.2) it is useful to rewrite the second equation of the system (2.11) according to $(\gamma^2 - \varepsilon_{xv})X_v dx = \gamma\, dZ_v(x)$.

Hence

$$\frac{\varepsilon_{xv} X_v^2(x)}{\gamma}\, dx = \frac{\varepsilon_{xv}\, X_v(Z_v, \gamma)}{\gamma^2 - \varepsilon_{xv}}\, dZ_v,$$

and

$$\frac{\omega\, \varepsilon_0}{2} \int_{-\infty}^{\infty} \frac{\varepsilon_{xv} X_v^2(x)}{\gamma}\, dx = \frac{\omega\, \varepsilon_0}{2} \int_{-\infty}^{\infty} \frac{\varepsilon_{xv} X_v(\zeta, \gamma)}{\gamma^2 - \varepsilon_{xv}}\, d\zeta. \tag{D.2.1}$$

Taking into account (D.1.4) and the boundary conditions at the interfaces and at infinity the power flow can be evaluated as

$$P^* = \frac{P}{P_0} = \left[\int_0^{Z(0)} \frac{\varepsilon_{xs}\, X_s(\zeta, \gamma)}{\gamma^2 - \varepsilon_{1s}} d\zeta + \int_{Z(0)}^{Z(h)} \frac{\varepsilon_{xf}\, X_f(\zeta, \gamma)}{\gamma^2 - \varepsilon_{1f}} d\zeta + \int_{Z(h)}^{0} \frac{\varepsilon_{xc}\, X_c(\zeta, \gamma)}{\gamma^2 - \varepsilon_{1c}} d\zeta \right]. \tag{D.2.2}$$

where

$$P_0 = \frac{2}{\omega\, \varepsilon_0}. \tag{D.2.3}$$

D.3 On the evaluation of the power flow according to (3.2.7)

The power flow given by (3.2.2) can be evaluated alternatively by inserting the second equation of (2.11) into the first one leading to

$$dx\left[2a_\nu b_\nu X_\nu^4(x) + b_\nu(2\varepsilon_{1\nu} + 2b_\nu Z_\nu^2(x) - \gamma^2)X_\nu^2(x) + \left(\varepsilon_{2\nu} + a_\nu Z_\nu^2(x)\right)\gamma^2\right] \times$$
$$\times Z_\nu(x) = \left(\varepsilon_{1\nu} + 3a_\nu\, X_\nu^2(x) + b_\nu\, Z_\nu^2(x)\right)\gamma dX_\nu(x)$$

Thus

$$\frac{\varepsilon_{x\nu}X_\nu^2(x)}{\gamma}dx = \frac{\varepsilon_{x\nu}X_\nu^2}{\gamma}\cdot\frac{f_X(X,\gamma)\,dX_\nu}{Z_\nu(X_\nu,\gamma)},$$

and

$$\frac{\omega\,\varepsilon_0}{2}\int_{-\infty}^{\infty}\frac{\varepsilon_{x\nu}X_\nu^2(x)}{\gamma}dx = \frac{\omega\,\varepsilon_0}{2}\int_{-\infty}^{\infty}\frac{\varepsilon_{x\nu}\,\xi^2}{\gamma}\cdot\frac{f_X(\xi,\gamma)}{Z_\nu(\xi,\gamma)}\,d\xi. \qquad \text{(D.3.1)}$$

Using (D.1.4) and the boundary conditions at the interfaces and at infinity the power flow reads

$$P^* = \frac{P}{P_0} = \left[\int_0^{X_s(0-0,\gamma,Z(0))}\frac{\varepsilon_{xs}\,\xi^2}{\gamma}\cdot\frac{f_{Xs}(\xi,\gamma)\,d\xi}{Z_s(\xi,\gamma)} + \right.$$
$$+\int_{X_f(0+0,\gamma,Z(0))}^{X_f(h-0,\gamma,Z(0))}\frac{\varepsilon_{xf}\,\xi^2}{\gamma}\cdot\frac{f_{Xf}(\xi,\gamma)\,d\xi}{Z_f(\xi,\gamma)} +$$
$$\left.+\int_{X_c(h+0,\gamma,Z(0))}^{0}\frac{\varepsilon_{xc}\,\xi^2}{\gamma}\cdot\frac{f_{Xc}(\xi,\gamma)\,d\xi}{Z_c(\xi,\gamma)}\right], \qquad \text{(D.3.2)}$$

where

$$P_0 = \frac{2}{\omega\,\varepsilon_0}.$$

E On the evaluation of the dispersion relation in the self-focusing case

Evaluation of the dispersion relation presented in Figure 5 proceeds according to steps the I- IV, V*- VII* outlined in Section 3 (with omitting subscript $\nu = f$ (apart from $\varepsilon_{1f}, \varepsilon_{2f}$ and C_f)).

Following notation is used below:

$$\begin{cases} X_1(Z,\gamma) = \pm\sqrt{[X^2(Z,\gamma)]_1}\,, \\ X_2(Z,\gamma) = \pm\sqrt{[X^2(Z,\gamma)]_2}\,, \\ X_3(Z,\gamma) = \pm\sqrt{[X^2(Z,\gamma)]_3}\,, \end{cases} \tag{E.0.1}$$

$$\begin{cases} X_1^+(Z,\gamma) = +\sqrt{[X^2(Z,\gamma)]_1}\,, & X_1^-(Z,\gamma) = -\sqrt{[X^2(Z,\gamma)]_1}\,, \\ X_2^+(Z,\gamma) = +\sqrt{[X^2(Z,\gamma)]_2} & X_2^-(Z,\gamma) = -\sqrt{[X^2(Z,\gamma)]_2}\,, \\ X_3^+(Z,\gamma) = +\sqrt{[X^2(Z,\gamma)]_3} & X_3^-(Z,\gamma) = -\sqrt{[X^2(Z,\gamma)]_3}\,, \end{cases} \tag{E.0.2}$$

$$\begin{cases} Z_1(X,\gamma) = \pm\sqrt{[Z^2(X,\gamma)]_1}\,, \\ Z_2(X,\gamma) = \pm\sqrt{[Z^2(X,\gamma)]_2}\,, \end{cases} \tag{E.0.3}$$

$$\begin{cases} Z_1^+(X,\gamma) = +\sqrt{[Z^2(X,\gamma)]_1}\,, & Z_1^-(X,\gamma) = -\sqrt{[Z^2(X,\gamma)]_1}\,, \\ Z_2^+(X,\gamma) = +\sqrt{[Z^2(X,\gamma)]_2} & Z_2^-(X,\gamma) = -\sqrt{[Z^2(X,\gamma)]_2}\,, \end{cases} \tag{E.0.4}$$

where

- $[X^2(Z,\gamma)]_i$ is the first, second and third root of (with respect to X^2, cubic) equation $G(Z,X,\gamma) = 0$ for $i = 1,2,3$, respectively (cf. (3.1.4) for $\nu = f$),

- $[Z^2(X,\gamma)]_j$ is the first and second square root of (with respect to Z^2, quadratic) equation $G(Z,X,\gamma)=0$ for $j=1,2$, respectively (cf. (3.1.4) for $\nu=f$).

Using (E.0.2- 4) notation (3.1.9- 10) can be rewritten as

$$F^{\pm}_{Z_i}(Z,\gamma)=\frac{\gamma}{X_i^{\pm}(Z,\gamma)\left(\gamma^2-\varepsilon_{1f}-a\,X_i^2(Z,\gamma)-b\,Z^2\right)}, \tag{E.0.5}$$

$$F^{\pm}_{X_j}(X,\gamma)=\frac{1}{Z_j^{\pm}(X,\gamma)}\times$$

$$\times\frac{\left(\varepsilon_{1f}+3aX^2+b\,Z_j^2(X,\gamma)\right)\gamma}{\left(2abX^4+b\left(2\varepsilon_{1f}+2b\,Z_j^2(X,\gamma)-\gamma^2\right)X^2+\left(\varepsilon_{2f}+a\,Z_j^2(X,\gamma)\right)\gamma^2\right)}. \tag{E.0.6}$$

I. Using the first equation (4.1.2) solution $X_s(0-0)$ reads

$$X_s(0-0)=\frac{\gamma\,Z(0)}{\sqrt{\gamma^2-\varepsilon_s}}. \tag{E.0.7}$$

II. Equation (3.1.11) rewritten as equation (4.1.6) has a unique real and positive root $X(0+0)$ presented in Figure E.1.

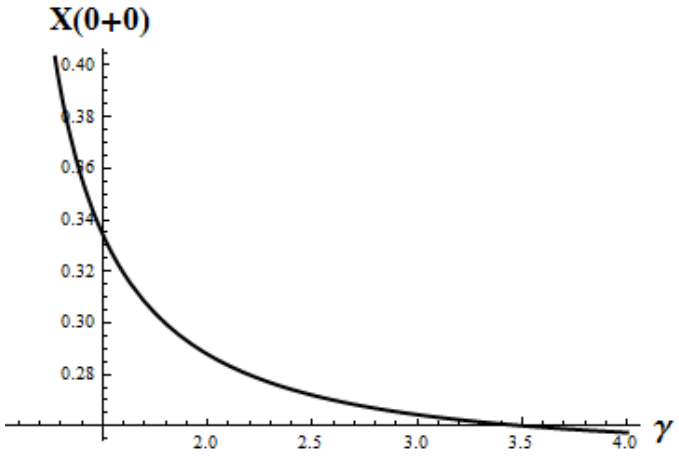

Figure E.1: Solution $X(0+0)$ of equation (4.1.6)

III. The constant of the integration C_f is depicted in Figure E.2.

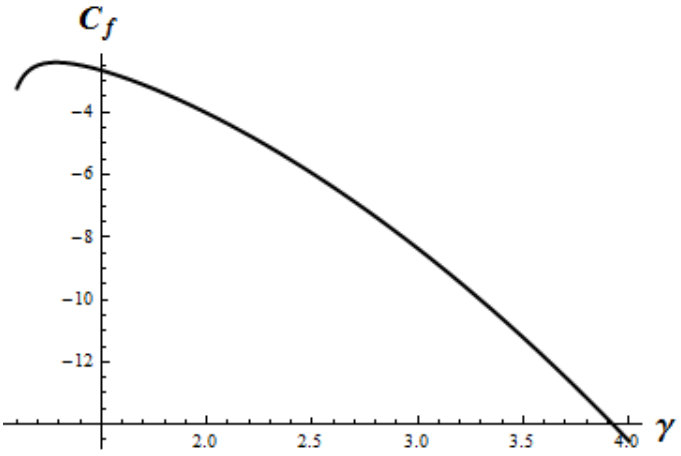

Figure E.2: Constant of the integration C_f (cf. (3.1.5))

IV. Solution $X_c(h+0)$ is obtained from the second equation (4.1.2)

$$X_c(h+0) = -\frac{\gamma\, Z(h)}{\sqrt{\gamma^2 - \varepsilon_c}}\,, \tag{E.0.8}$$

where $Z(h)$ is not determined till now.

V*. Solving equation (3.1.4) with respect to $Z^2(X,\gamma)$ yields

$$[Z^2(X,\gamma)]_{1,2} = \frac{1}{2r_1}\left(-r_2 \pm \sqrt{r_2^2 - 4r_1 r_3}\right), \tag{E.0.9}$$

where

$r_1 = 2b^2X^2 + a\gamma^2,$

$r_2 = 4b\varepsilon_{1f}X^2 + 4abX^4 + 2\varepsilon_{2f}\gamma^2 - 2bX^2\gamma^2,$

$r_3 = 4C_f + 2a^2X^6 + aX^4\left(4\varepsilon_{1f} - 3\gamma^2\right) + 2\varepsilon_{1f}X^2\left(\varepsilon_{1f} - \gamma^2\right).$

Plotting the roots $Z_j^+(X,\gamma), Z_j^-(X,\gamma)$ $(j = 1,2)$ (cf. (E.0.4) and (E.0.9)) together with the equations (3.1.4), (3.1.11) and (3.1.12) for each fixed value $\gamma \in (1,4]$ has shown that the function $Z_2^+(X,\gamma)$ satisfies equations (3.1.11), the function $Z_2^-(X,\gamma)-$ equation (3.1.12) as shown in Figure E.3. Points $X_0 = X\big(0+0,\gamma,Z(0)\big)$, X_{h1} and X_{h2} denote the solutions of equations (3.1.11), (3.1.12), respectively. The function $Z_2(X,\gamma)$ changes sign in the points $X_*^{\pm}$ [36].

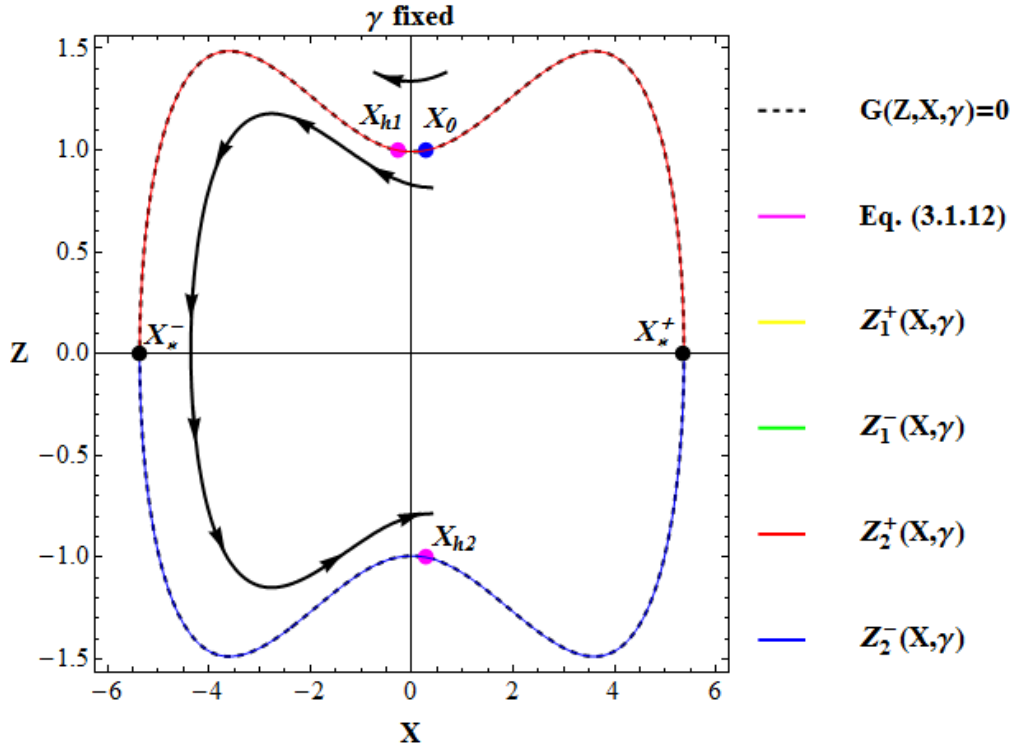

Figure E.3: The first integral $G(Z,X,\gamma)=0$ with the roots $Z_j^{\pm}(X,\gamma)(j=1,2)$ and solutions of equations (3.1.11), (3.1.12) plotted for any fixed γ.

Hence, there are two solutions $Z(h)$ defined as

$$Z_1(h)=Z_2^-\big(X\big(h-0,\gamma,Z(0)\big),\gamma\big), \tag{E.0.10}$$

$$Z_2(h)=Z_2^+(X\big(h-0,\gamma,Z(0)\big),\gamma), \tag{E.0.11}$$

so that the function $X_c(h+0)$ on step IV. is determined.

VI* Solution $X(h-0)=X\big(h-0,\gamma,Z(0)\big)$ is presented in Figure E.4.

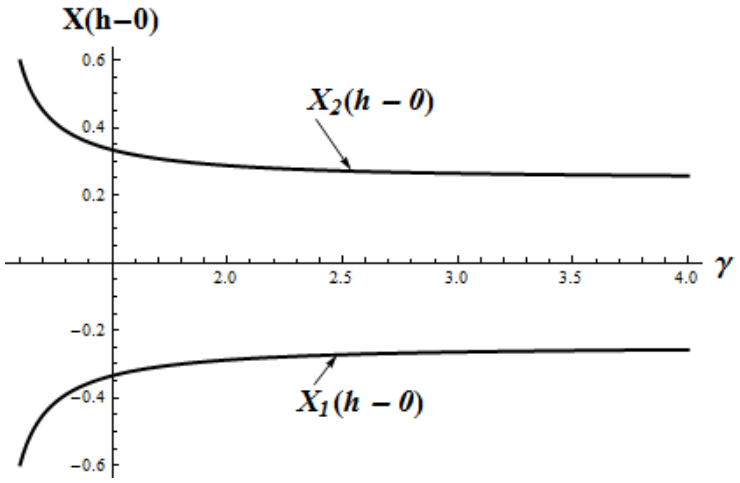

Figure E.4: Two solutions of the function $X(h-0)=X\big(h-0,\gamma,Z(0)\big)$

VII* Considering the integration contour (X_0, X_{h1}) one obtains

$$h_I = \int_{X_0}^{X_{h1}} F_{X_2}^{+}(\xi,\gamma)d\xi. \qquad \text{(E.0.12)}$$

For the integration contour (X_0, X_{h2}) comes

$$h_{II} = \int_{X_0}^{X_*^-} F_{X_2}^{+}(\xi,\gamma)d\xi + \int_{X_*^+}^{X_{h2}} F_{X_2}^{-}(\xi,\gamma)d\xi. \qquad \text{(E.0.13)}$$

Numerical evaluation of (E.0.12) and (E.0.13) implies the positive values h_I, h_{II} leading the fundamental (first even TM_0) and the first odd (TM_1) mode, respectively, presented in Figures 5, 7 (pp. 38, 40, respectively). Setting $N = 1, 2, 3, \ldots$ in (3.1.20) the higher modes presented in Figure 7 are obtained.

According to (3.2.7) and the analysis above the total power flow transported by the nonlinear TM_0- wave through a waveguide with the thickness h can be written as

$$P^* = P_s^* + P_f^* + P_c^* =$$

$$= \frac{\varepsilon_s \gamma\, Z(0)}{2\,(\gamma^2 - \varepsilon_s)^{3/2}} + \int_{X_0}^{X_{h1}} \frac{\varepsilon_{xf}\,\xi^2}{\gamma} \cdot \frac{f_{X_2}(\xi,\gamma)\,d\xi}{Z_2^{+}(\xi,\gamma)} + \frac{\varepsilon_c\,\gamma\,Z^2(h)}{2\,(\gamma^2 - \varepsilon_c)^{3/2}} \qquad \text{(E.0.14)}$$

where

$$\varepsilon_{xf} = \varepsilon_{1f} + a\,\xi^2 + [Z_2^{+}(\xi,\gamma)]^2,$$

$$Z(h) = Z_2(h),\ X(h-0) = X_{h1} \text{ (see (E.0.11))}$$

and P_s^*, P_f^*, P_c^* denote the parts of the total power flow in the substrate, film and cladding, respectively.

Numerical evaluation of (E.0.14) gives result presented in Figure 11 (p. 43).

F On the evaluation of the dispersion relation in the defocusing case I

The dispersion relation in the defocusing case I (subsection 4.1.2.1) is evaluated according to steps the I-VII of Section 3 (using notation (E.0.1- 6)) as follows:

I. Equation (4.1.2) leads to

$$X_s(0-0) = \frac{\gamma\, Z(0)}{\sqrt{\gamma^2 - \varepsilon_s}}. \tag{F.0.1}$$

II. Taking parameters b) of subsection 4.1 (cf. Figure 3) and choosing

$$1 < \gamma \leq 5$$

the first root of (4.1.6) presented in Figure F.1 is considered in the present case.

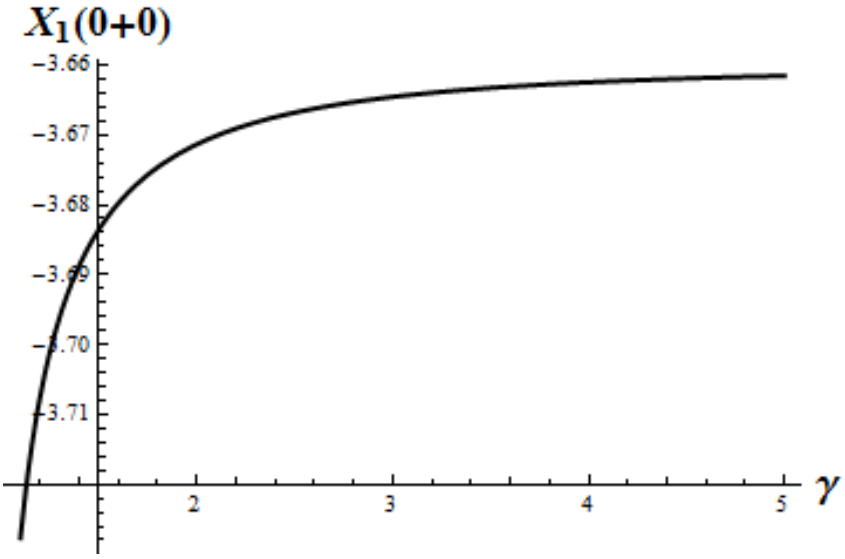

Figure F.1: The first root $X_1(0+0)$ of (4.1.6)

III. Figure F.2 shows the constant of the integration C_f in dependence on γ.

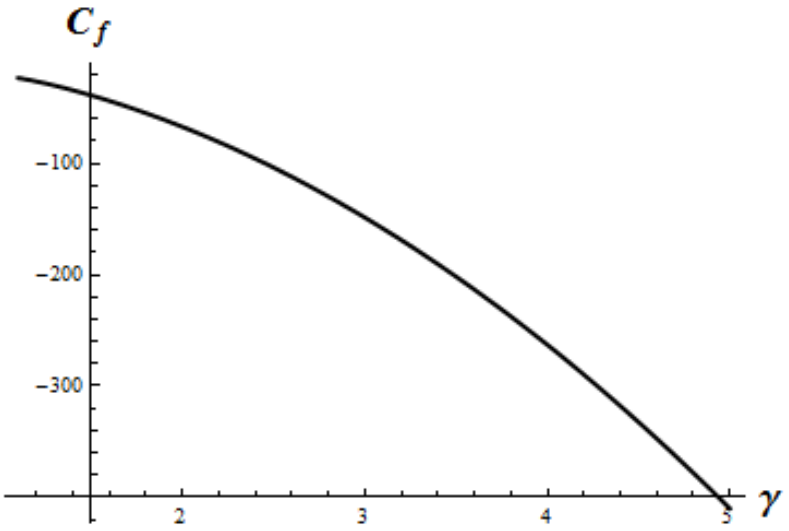

Figure F.2: The integration constant C_f (cf. (3.1.5))

IV. According to the second equation (4.1.2) solution $X_c(h+0)$ is written as

$$X_c(h+0) = -\frac{\gamma\, Z(h)}{\sqrt{\gamma^2 - \varepsilon_c}}\,, \tag{F.0.2}$$

where $Z(h)$ will be defined in step VI.

V. As follows from Figure 13 the functions Z and X are not periodic and the function $X_1(0+0)$ is negative (see also Figure F.1), hence, only the roots $X_i^-(Z,\gamma)$ $(i = 1,2,3)$ (cf. notation (E.0.2)) have to be considered. Plotting all three roots $X_i^-(Z,\gamma)$ $(i = 1,2,3)$ of equation $G(Z,X,\gamma) = 0$ (for simplicity not given here) has shown that only the first root $X_1^-(Z,\gamma)$ is real and satisfies equations (3.1.11) and (3.1.12) as depicted in Figure F.3, so that there are two solutions $X(h-0)$ defined as

$$X_{h1} = X_1^-\big(h-0,\gamma,Z(0);Z_1(h)\big), \tag{F.0.3}$$

$$X_{h2} = X_1^-\big(h-0,\gamma,Z(0);Z_2(h)\big). \tag{F.0.4}$$

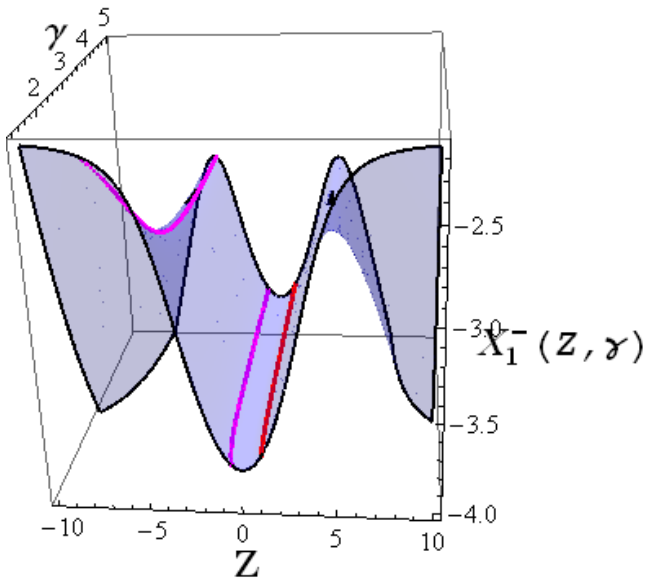

Figure F.3: The root $X_1^-(Z,\gamma)$ of equation $G(Z,X,\gamma)=0$ (cf. (3.1.4) and notation (E.0.2)). Red curve on the surface depicts the solution $X_1(0+0)$ (cf. (4.1.6) and Figure F.1), magenta curves – numerical solutions of equation (3.1.12).

VI.-VII.

Figure F.4 shows two solutions $Z_i(h)=Z_i\big(h,\gamma,Z(0)\big)(i=1,2)$ (according to step V) labelled by Z_{h1} and Z_{h2} for $i=1$ and $i=2$, respectively, together with the corresponding integrand of (3.1.14) $F_{Z_1}^-(\zeta,\gamma)$.

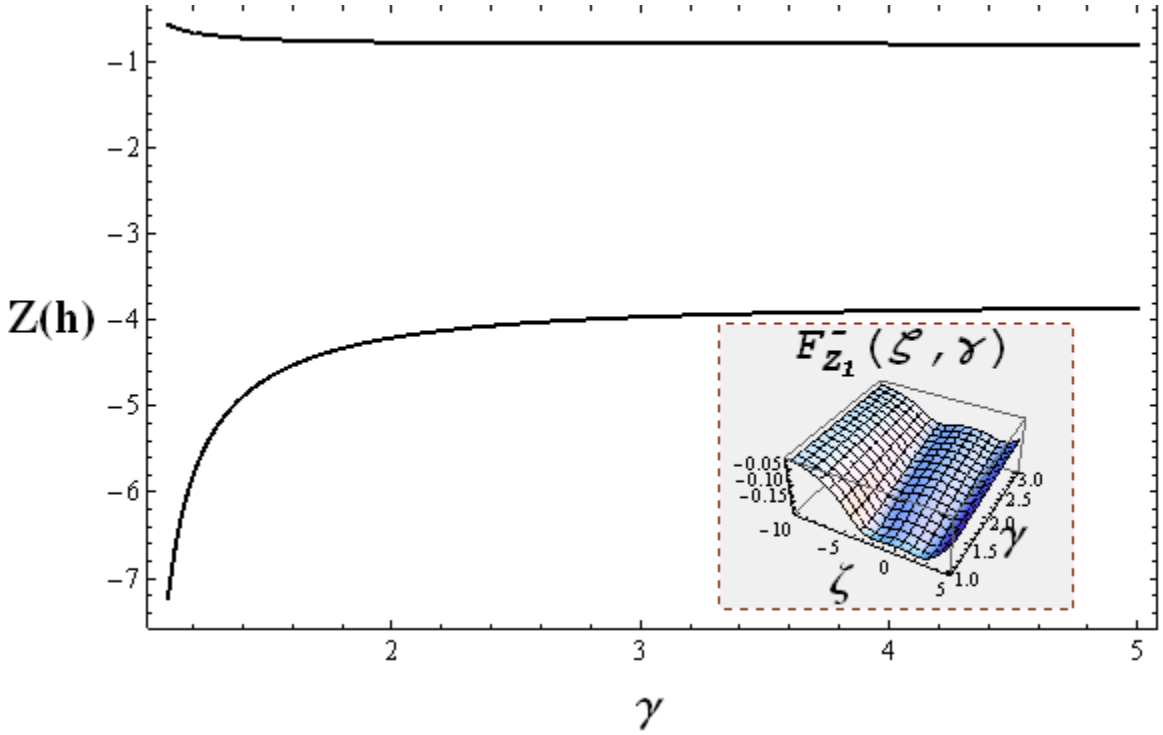

Figure F.4: Solutions $Z(h)$ of equation (3.1.12) and the integrand $F_{Z_1}^-(\zeta,\gamma)$

Hence, inserting $Z_i(h)(i = 1,2)$ into (F.0.2) two solutions for $X_c(h + 0)$ are defined.

As follows from Figure F.4, the integrand $F_{Z_1}^{-}(\zeta, \gamma)$ is a negative function, hence the both negative solutions $Z_1(h)$ and $Z_2(h)$ have to be taken in evaluation of (3.1.14) leading to positive h (cf. parameters in this case $Z(0) > 0$). Denoting solution of the dispersion relation (3.1.14) evaluated with $Z_i(h)$ as DC_i for $i = 1,2$, respectively, one obtains

$$DC_1 := \int_{Z(0)}^{Z_1(h)} F_{Z_1}^{-}(\zeta, \gamma) d\zeta, \tag{F.0.5}$$

$$DC_2 := \int_{Z(0)}^{Z_2(h)} F_{Z_1}^{-}(\zeta, \gamma) d\zeta. \tag{F.0.6}$$

Numerical evaluation of (F.0.5) and (F.0.6) gives results presented in Figure F.5.

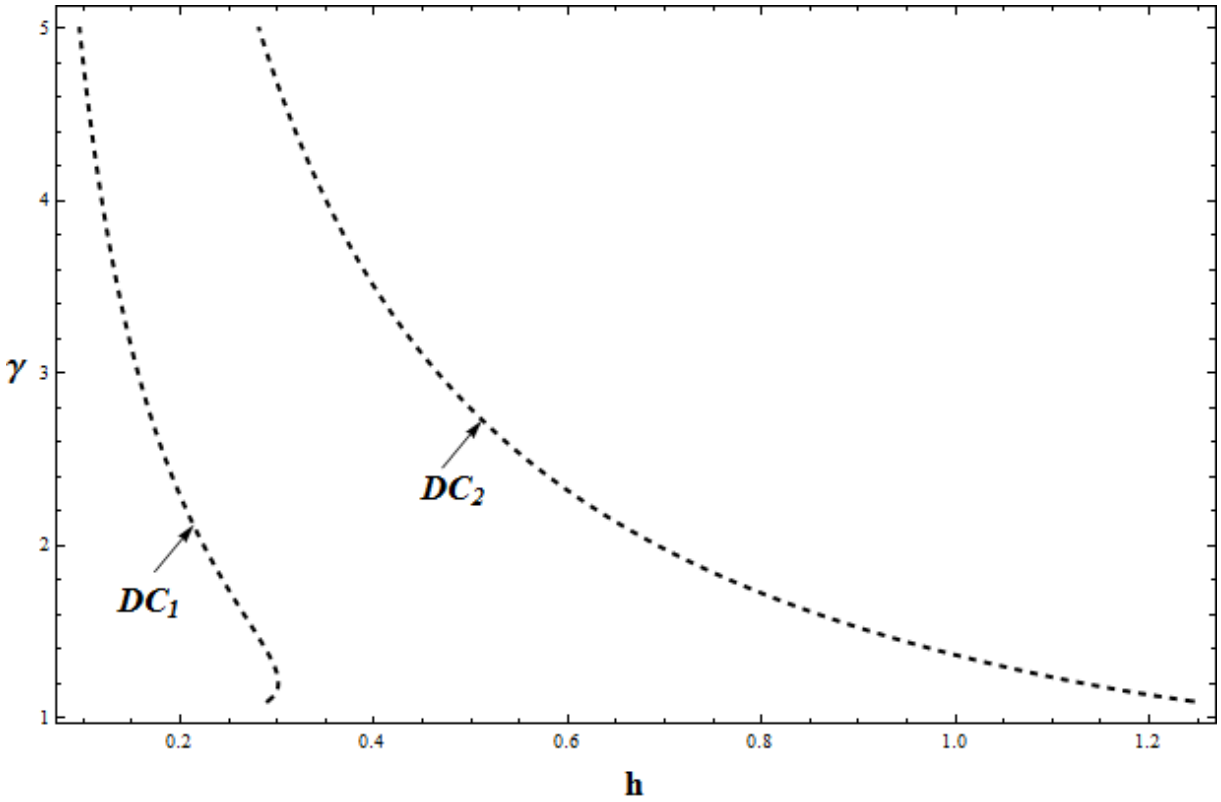

Figure F.5: Dispersion relation (cf. (3.1.14))

According to equation (3.2.3) and analysis above the total power flow transported by the TM- wave through the nonlinear film bounded by linear media and characterized by the dispersion relation DC_i $(i = 1,2)$ can be written as follows

$$P^* = P_s^* + P_f^* + P_c^* =$$
$$= \frac{\varepsilon_s \gamma\, Z(0)}{2\,(\gamma^2 - \varepsilon_s)^{3/2}} +$$
$$+ \int_{Z(0)}^{Z_i(h)} \frac{\varepsilon_{1f} + b\,\zeta^2 + a\,[X_1^-(\zeta,\gamma)]^2}{\gamma^2 - \varepsilon_{1f} - b\,\zeta^2 - a\,[X_1^-(\zeta,\gamma)]^2} \cdot X_1^-(\zeta,\gamma)\, d\zeta$$
$$+ \frac{\varepsilon_c \gamma\, Z_i^2(h)}{2\,(\gamma^2 - \varepsilon_c)^{3/2}},$$

(F.0.7)

where P_s^*, P_f^*, P_c^* denote the parts of the total power flow in the substrate, film and cladding, respectively.

Numerical evaluation of (F.0.7) with $i = 1$ yields result depicted in Figure 19, taking $i = 2$ in (F.0.7) implies result depicted in Figure 20.

The dispersion relation presented in Figure F.5 can be also obtained by using equation (3.1.15) following steps the V*- VII*:

V*. Plotting of the roots $Z_i^{\pm}(X,\gamma), (i = 1,2)$ (cf. notation (E.0.4)) (for simplicity not given here) has shown that only the roots $Z_2^-(X,\gamma)$, $Z_2^+(X,\gamma)$ are real. As shown in Figure F.6 the root $Z_2^+(X,\gamma)$ satisfies equation (3.1.11) (red curve), equation (3.1.12) has two solutions satisfied by the root $Z_2^-(X,\gamma)$ (magenta curves), hence, there are two solutions $Z(h)$ defined as

$$Z_{h1} = Z_2^-\big(h,\gamma,Z(0);X_1\big(h-0,\gamma,Z(0)\big),\gamma\big), \qquad \text{(F.0.8)}$$
$$Z_{h2} = Z_2^-\big(h,\gamma,Z(0);X_2\big(h-0,\gamma,Z(0)\big),\gamma\big), \qquad \text{(F.0.9)}$$

so that two solutions solutions for $X_c(h+0)$ (see step IV.) are defined.

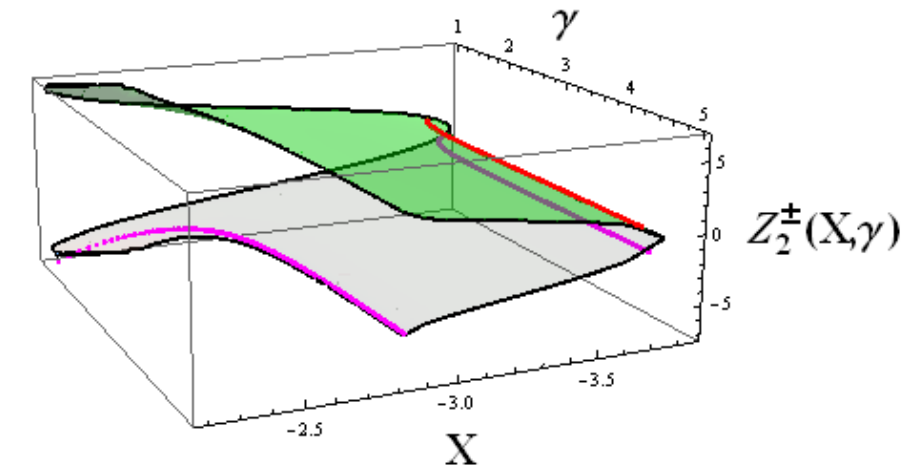

Figure F.6: Green and gray colours present the roots $Z_2^+(X,\gamma)$ and $Z_2^-(X,\gamma)$, respectively (cf. notation (E.0.4)). Red curve depicts the solution $X_1(0+0)$ (cf. (4.1.6) and Figure F.1), magenta curves – numerical solutions of equation (3.1.12).

VI*. According to step V* there are two solutions $X_i\big(h-0,\gamma,Z(0)\big)$ $(i=1,2)$ presented in Figure F.7 and labelled by X_{h1} and X_{h2}.

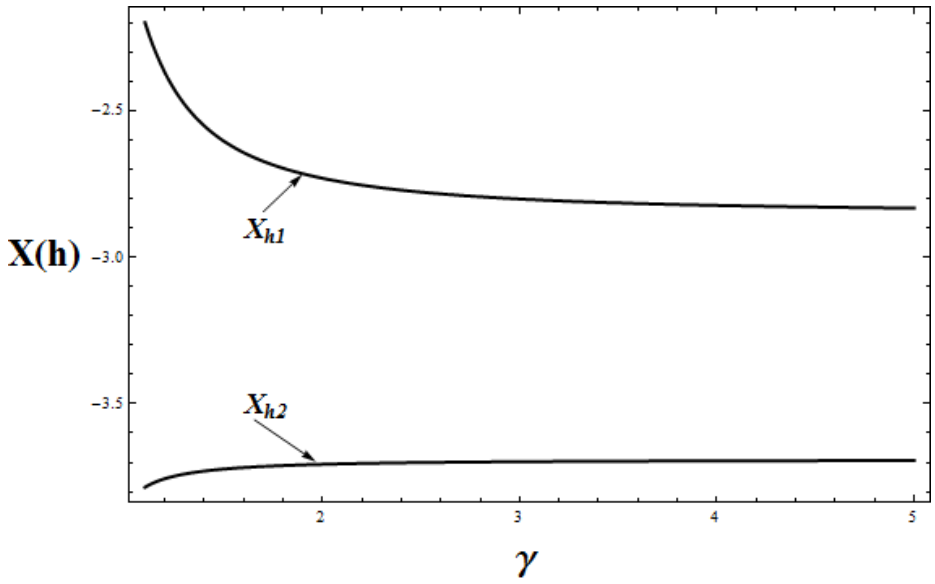

Figure F.7: Solutions $X(h-0)$ of equation (3.1.12)

VII*. Taking into account results of steps I and V*, and denoting solutions of the dispersion relation (3.1.15) evaluated with $X_i\big(h-0,\gamma,Z(0)\big)$ as DC_i^* for $i=1,2$, respectively, one obtains

$$DC_1^* := \int_{X_1(0+0)}^{X_*^-(\gamma)} F_{X_2}^+(\xi,\gamma)d\xi + \int_{X_*^-(\gamma)}^{X_1(h-0,\gamma,Z(0))} F_{X_2}^-(\xi,\gamma)d\xi, \qquad \text{(F.0.10)}$$

$$DC_2^* := \int_{X_1(0+0)}^{X_*^-(\gamma)} F_{X_2}^+(\xi,\gamma)d\xi + \int_{X_*^-(\gamma)}^{X_2(h-0,\gamma,Z(0))} F_{X_2}^-(\xi,\gamma)d\xi, \qquad \text{(F.0.11)}$$

where $X_*^-(\gamma)$ is real and negative root (due to $X_1(0+0)<0$, $X_i\big(h-0,\gamma,Z(0)\big)<0$ $(i=1,2)$ and function X is not periodic) of equation $G(Z=0,X,\gamma)=0$ (see (3.1.4)).

Numerical evaluation of (F.0.10) and (F.0.11) yields results presented in Figure F.8 by yellow curves in comparison with Figure F.5. As can be seen, there is agreement of the solutions obtained by using equations (3.1.15) and (3.1.14), showing consistency of the two approaches in Section 3.

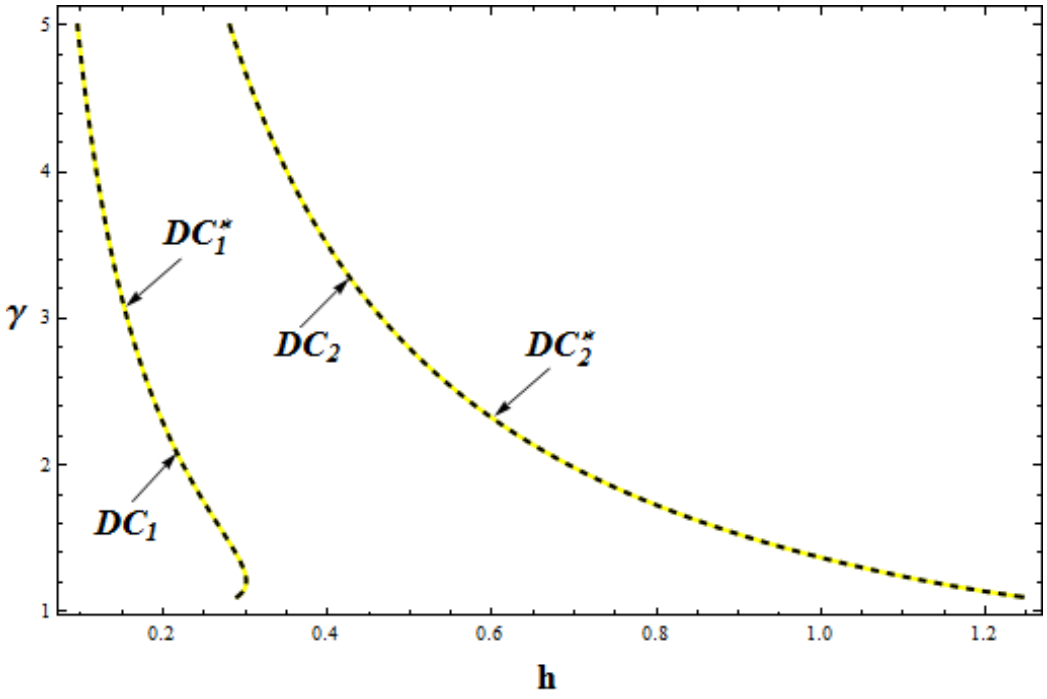

Figure F.8: Agreement of the dispersion relations obtained cf. (3.1.14) (black) and (3.1.15) (yellow)

G On the evaluation of the dispersion relation in the defocusing case II

Following steps the I-VII of Section 3 and using notation (E.0.1- 6) the dispersion relation in the defocusing case II (subsection 4.1.2.2) is evaluated as shown below:

VI. Equation (4.1.2) implies

$$X_s(0-0) = \frac{\gamma\, Z(0)}{\sqrt{\gamma^2 - \varepsilon_s}}. \qquad \text{(G.0.1)}$$

VII. Figure G.1 shows the second root of (4.1.6) (cf. parameters b)) of subsection 4.1 (see Figure 3). A range of the propagation constant γ is chosen as

$$1 < \gamma \leq 3.$$

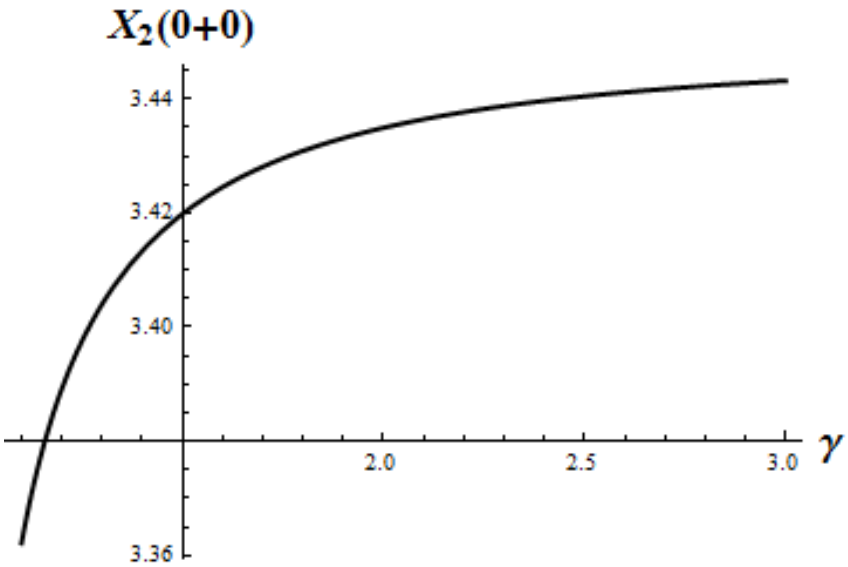

Figure G.1: The second root of (4.1.4)

VIII. Figure G.2 shows the constant of the integration C_f.

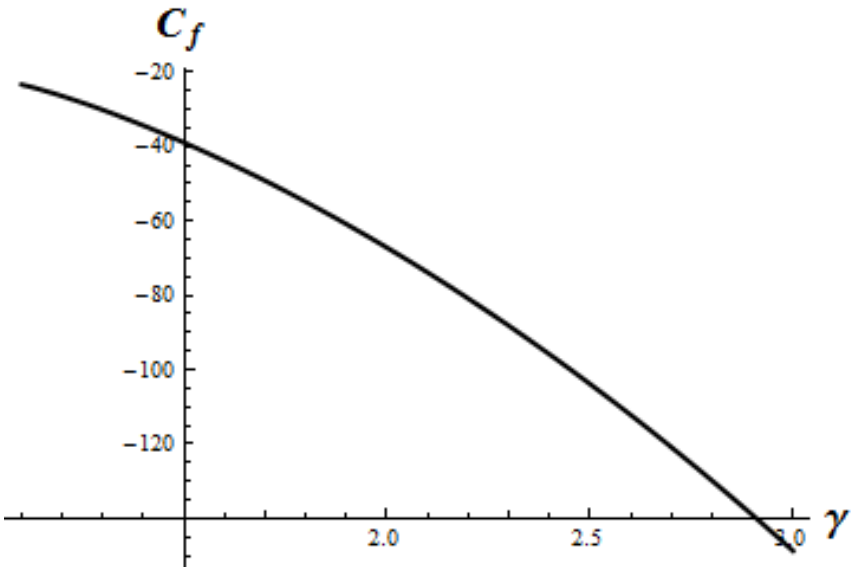

Figure G.2: The integration constant C_f (cf. (3.1.5))

IX. According to the second equation (4.1.2) solution $X_c(h+0)$ is written as

$$X_c(h+0) = -\frac{\gamma\, Z(h)}{\sqrt{\gamma^2 - \varepsilon_c}}\,, \tag{G.0.2}$$

where $Z(h)$ will be defined in step VI.

X. As follows from Figure 21 the functions Z and X are not periodic and the function $X_2(0+0)$ is positive (see also Figure G.1), hence, only the roots $X_i^+(Z,\gamma)$ $(i = 1,2,3)$ (cf. notation (E.0.2)) have to be considered. Plotting all three roots $X_i^+(Z,\gamma)$ $(i = 1,2,3)$ of equation $G(Z,X,\gamma) = 0$ (for simplicity not given here) has shown that only the first root $X_1^+(Z,\gamma)$ is real and satisfies equations (3.1.11) and (3.1.12) as depicted in Figure G.3, so that there are two solutions $X(h-0)$ defined as

$$X_{h1} = X_1^+\big(h-0,\gamma,Z(0);Z_1(h)\big), \tag{G.0.3}$$

$$X_{h2} = X_1^+\big(h-0,\gamma,Z(0);Z_2(h)\big). \tag{G.0.4}$$

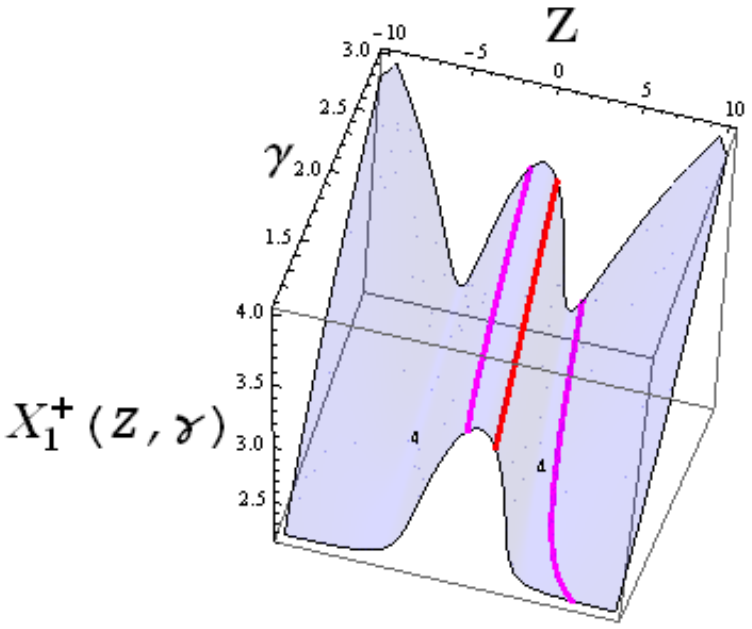

Figure G.3: The root $X_1^+(Z,\gamma)$ of equation $G(Z,X,\gamma)=0$ (cf. (3.1.4) and notation (E.0.2)). Red curve on the surface depicts the solution $X_2(0+0)$ (cf. (4.1.6) and Figure G.1), magenta curves – numerical solutions of equation (3.1.12).

VI.-VII.

Figure G.4 shows two solutions $Z_i(h)=Z_i\big(h,\gamma,Z(0)\big)(i=1,2)$ (according to step V) labelled by Z_{h1} and Z_{h2} for $i=1$ and $i=2$, respectively, together with the corresponding integrand of (3.1.14) $F_{Z_1}^+(\zeta,\gamma)$.

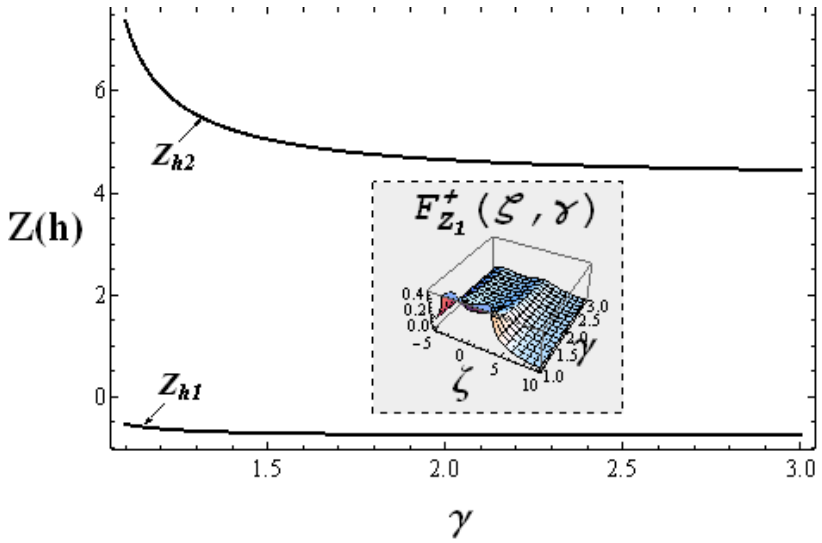

Figure G.4: Solutions $Z(h)$ of equation (3.1.12) and the integrand $F_{Z_1}^+(\zeta,\gamma)$

As follows from Figure G.4, the integrand $F_{Z_1}^{+}(\zeta,\gamma)$ and the integral upper limit $Z_2(h)$ in (3.1.14) are positive functions, the solution $Z_1(h)$ is negative, hence, only one solution $Z_2(h)$ is to be taken by evaluation of (3.1.14) leading to positive h (cf. parameters in this case $Z(0) > 0$):

$$\begin{matrix} Z(0) > 0 \\ Z_1(h) < 0 \\ F_{Z1}^{p}(\zeta,\gamma) > 0 \end{matrix} \Rightarrow \int_{Z(0)}^{Z_1(h)} F_{Z1}^{p}(\zeta,\gamma) < 0, \qquad \text{(G.0.5)}$$

$$\begin{matrix} Z(0) > 0 \\ Z_2(h) > 0 \\ F_{Z1}^{p}(\zeta,\gamma) > 0 \end{matrix} \Rightarrow \int_{Z(0)}^{Z_2(h)} F_{Z1}^{p}(\zeta,\gamma) > 0. \qquad \text{(G.0.6)}$$

Numerical evaluation of the integral in (G.0.6) gives results presented in Figure 22 a).

Inserting $Z_2(h)$ into (G.0.2) solution $X_c(h+0)$ is defined.

According to equation (3.2.3) and analysis above the total power flow transported by the TM- wave through the nonlinear film bounded by linear media in the present case can be written as follows

$$\begin{aligned} P^* &= P_s^* + P_f^* + P_c^* = \\ &= \frac{\varepsilon_s \gamma\, Z(0)}{2\,(\gamma^2-\varepsilon_s)^{3/2}} + \\ &+ \int_{Z(0)}^{Z_2(h)} \frac{\varepsilon_{1f} + b\,\zeta^2 + a\,[X_1^{+}(\zeta,\gamma)]^2}{\gamma^2 - \varepsilon_{1f} - b\,\zeta^2 - a\,[X_1^{+}(\zeta,\gamma)]^2} \cdot X_1^{+}(\zeta,\gamma)\, d\zeta \\ &+ \frac{\varepsilon_c \gamma\, Z_2^2(h)}{2\,(\gamma^2-\varepsilon_c)^{3/2}}, \end{aligned} \qquad \text{(G.0.7)}$$

where P_s^*, P_f^*, P_c^* denote the parts of the total power flow in the substrate, film and cladding, respectively.

Numerical evaluation of (G.0.7) leads to results presented in Figure 25.

H On the evaluation of the dispersion relation in the defocusing case III

Evaluation of the dispersion relation in the defocusing case III (subsection 4.1.2.3) proceeds according to steps the I-IV, V*-VII* outlined in Section 3 by using notation (E.0.1- 6) for $1 < \gamma < 3.2$.

V. From the first equation (4.1.2) it follows

$$X_s(0-0) = \frac{\gamma\, Z(0)}{\sqrt{\gamma^2 - \varepsilon_s}}. \qquad \text{(H.0.1)}$$

VI. The third root of (4.1.6) presented in Figure H.1 is considered below.

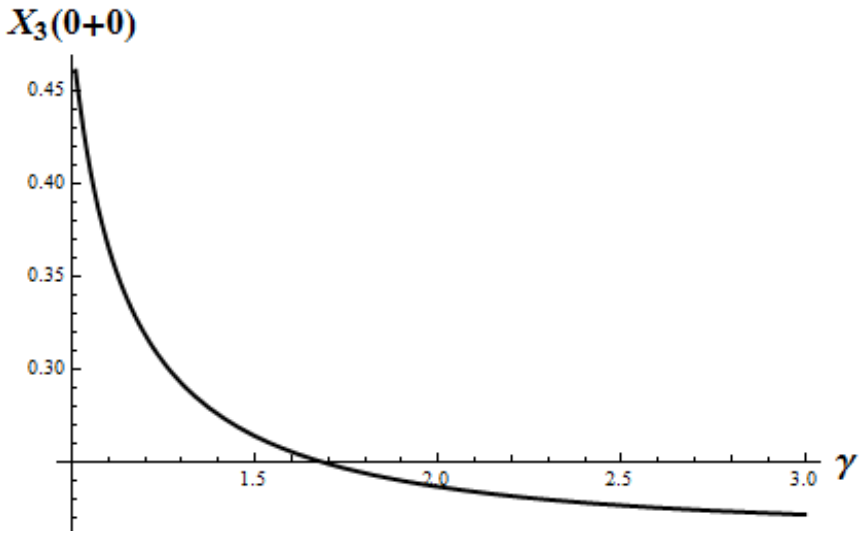

Figure H.1: The third root $X(0+0)$ of equation (4.1.6)

VII. The constant of the integration C_f as a negative function is depicted in Figure H.2.

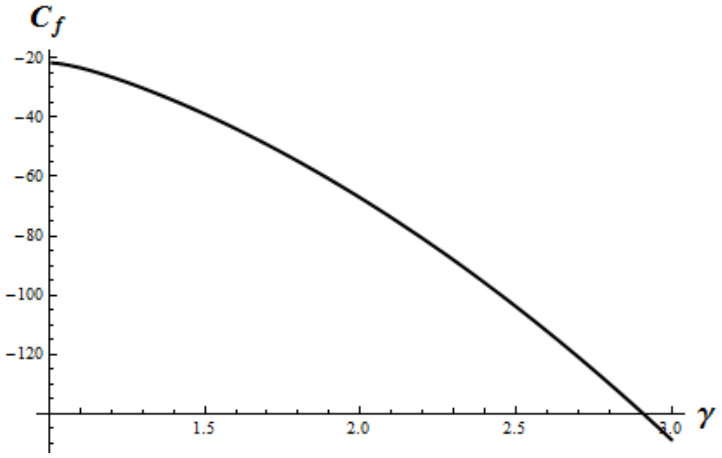

Figure H.2: The constant of integration C_f (cf. (3.1.5))

Using the second equation (4.1.2) solution $X_c(h+0)$ is obtained as

$$X_c(h+0) = -\frac{\gamma\, Z(h)}{\sqrt{\gamma^2 - \varepsilon_c}}\,, \tag{H.0.2}$$

where $Z(h)$ will be defined below.

V*. Figure H.3 shows the real roots $Z_j^+(X,\gamma), Z_j^-(X,\gamma)$ $(j = 1,2)$ of equation $G(Z,X,\gamma) = 0$ and the first integral (3.1.4) together with solutions of equations (3.1.11), (3.1.12). As can be seen only the roots $Z_2^+(X,\gamma)$, $Z_2^-(X,\gamma)$ satisfy equations (3.1.11) and (3.1.12), so that there are two solutions $Z(h)$ defined as

$$Z_{h1} = Z_2^+\big(h,\gamma,Z(0);X_1\big(h-0,\gamma,Z(0)\big),\gamma\big), \tag{H.0.3}$$

$$Z_{h2} = Z_2^-\big(h,\gamma,Z(0);X_2\big(h-0,\gamma,Z(0)\big),\gamma\big). \tag{H.0.4}$$

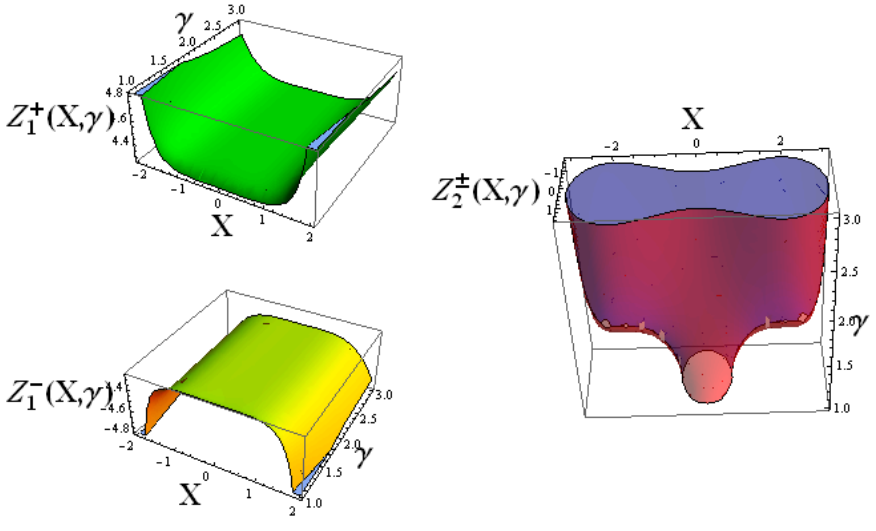

a) **b)**

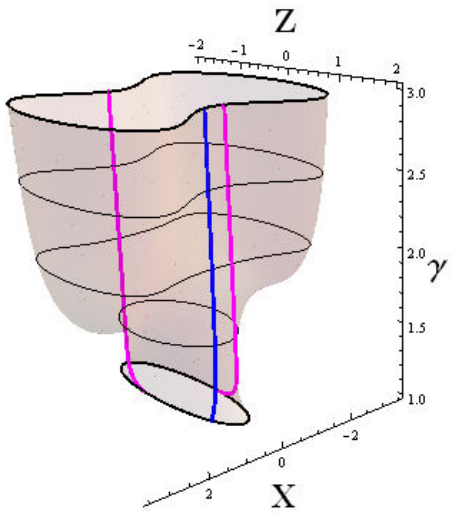

c)

Figure H.3: **a)** Green colour: $Z_1^+(X,\gamma)$, yellow colour: $Z_1^-(X,\gamma)$ **b)** Red colour: $Z_2^+(X,\gamma)$, blue colour: $Z_2^-(X,\gamma)$ **c)** the first integral $G(Z,X,\gamma)=0$ (cf. eq. (3.1.4)); blue curve on the first integral surface depicts the solution $X_3(0+0)$ (cf. Figure H.1), the magenta curves – numerical solutions of equation (3.1.12).

VI*. According to step V* there are two solutions $X_i\big(h-0,\gamma,Z(0)\big)$ $(i=1,2)$ presented in Figure H.4 and labelled by X_{h1} and X_{h2}.

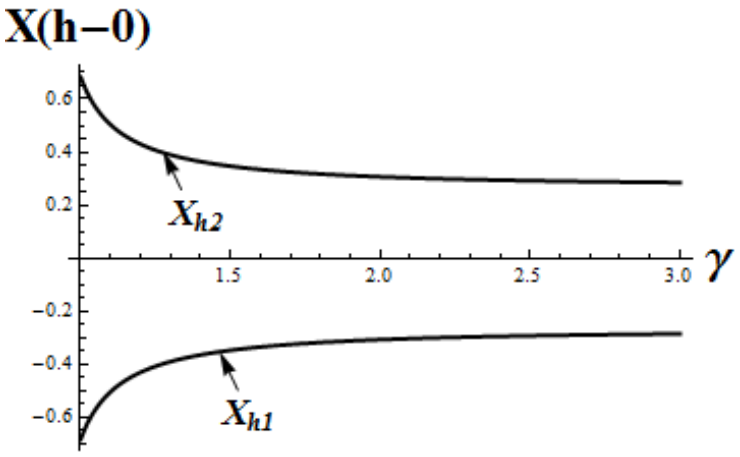

Figure H.4: Two solutions $X\big(h-0,\gamma,Z(0)\big)$ (cf. (3.1.12))

VII*. Figure H.5 presents the first integral $G(Z,X)=0$ together with equation (3.1.12) (magenta curve) and the roots $Z_2^+(X,\gamma), Z_2^-(X,\gamma)$ for fixed $\gamma\in(1,3.2)$. Blue point $X_0=X(0+0,\gamma;Z(0))$ depicts lower limit of the integral (3.1.15). The function $Z_2(X,\gamma)$ changes sign in the points $X_*^{\pm}$ (see [36]).

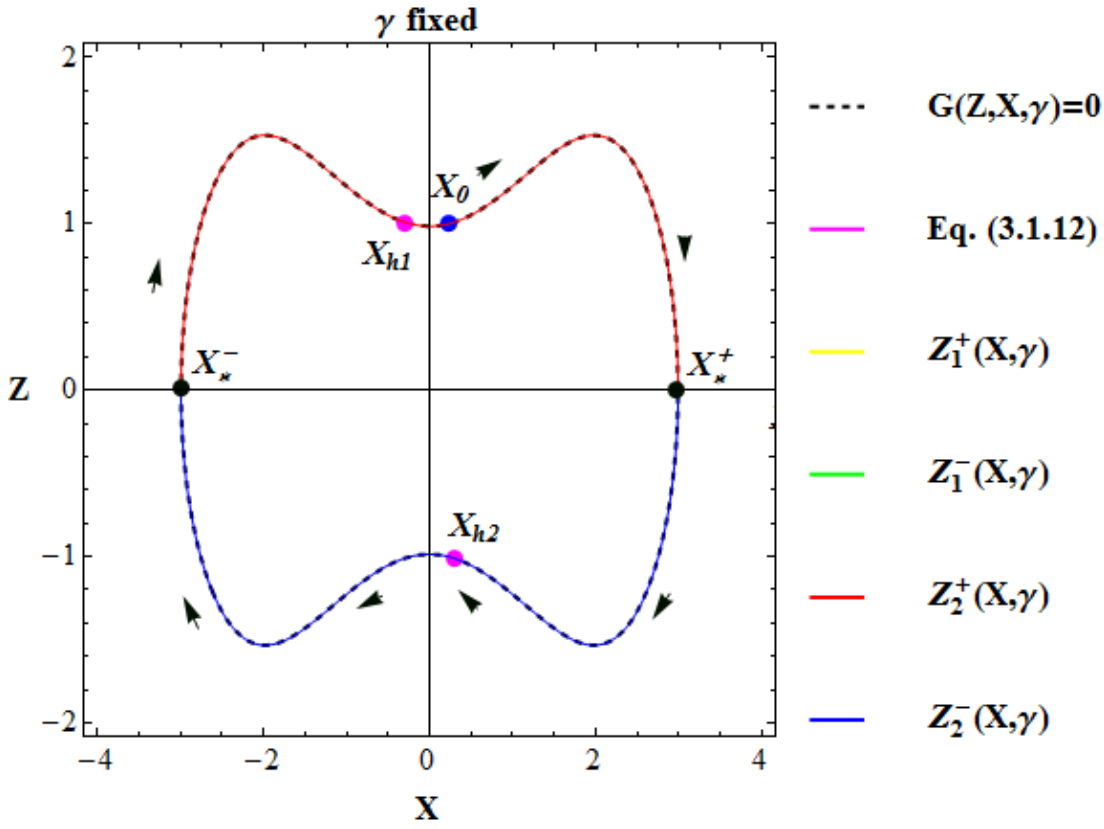

Figure H.5: The first integral $G(Z,X,\gamma)=0$ with the roots $Z_j^{\pm}(X,\gamma)(j=1,2)$ and solutions of equations (3.1.11), (3.1.12) plotted for any fixed $\gamma \in (1,3.2)$

Using the integration contour (X_0, X_{h1}) leads to

$$h_I = \int_{X_0}^{X_*^+} F_{X_2}^+(\xi,\gamma)d\xi + \int_{X_*^+}^{X_*^-} F_{X_2}^-(\xi,\gamma)d\xi + \int_{X_*^-}^{X_{h1}} F_{X_2}^-(\xi,\gamma)d\xi. \quad \text{(H.0.5)}$$

Considering an integration contour (X_0, X_{h2}) one obtains:

$$h_{II} = \int_{X_0}^{X_*^-} F_{X_2}^+(\xi,\gamma)d\xi + \int_{X_*^+}^{X_{h2}} F_{X_2}^-(\xi,\gamma)d\xi. \quad \text{(H.0.6)}$$

Evaluation of (H.0.5) yields Figure H.6.

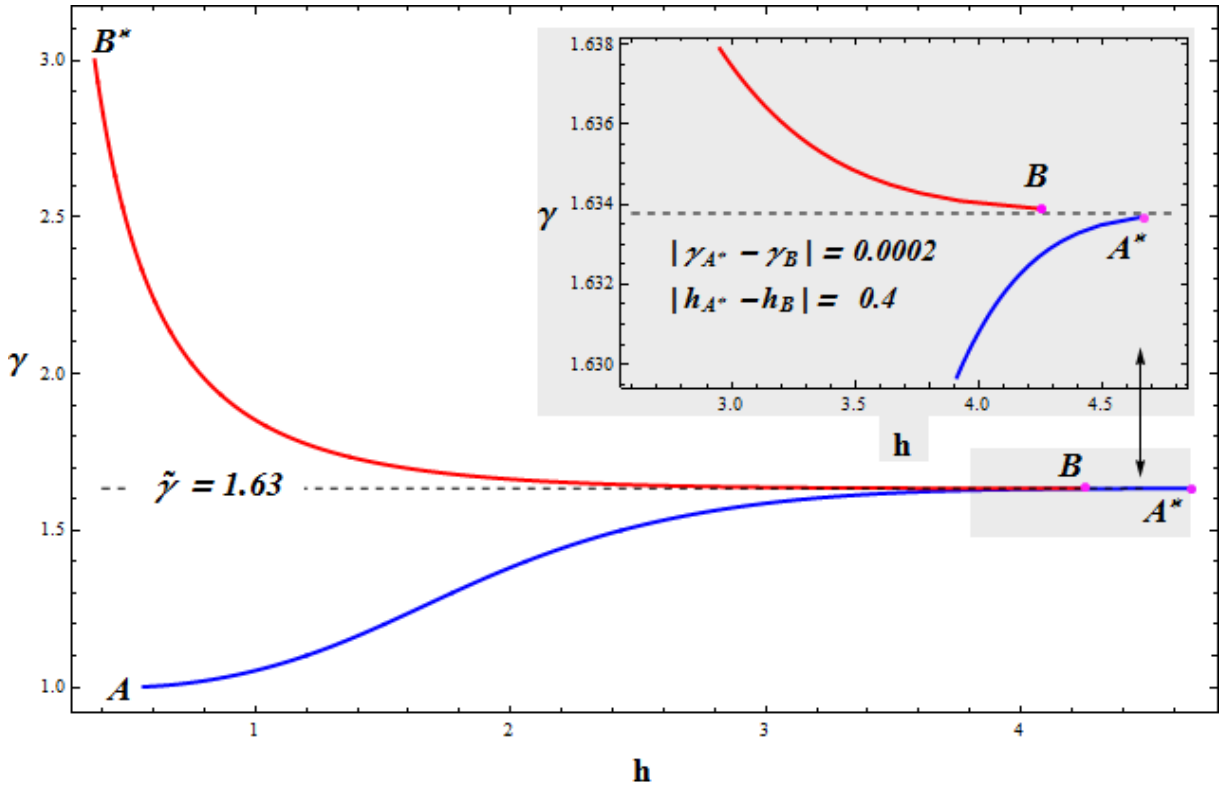

Figure H.6: Dispersion relation (TM_0- mode) (cf. (3.1.15))

As can be seen in Figure H.6 the solution of the dispersion relation represented by two curves AA^* and BB^* is a discontinuous function for $\gamma = 1.63$. A jump discontinuity is shown in a gray region. I suppose that this discontinuity of the dispersion curve follows from the discontinuity of the integral limits $X_*^{\pm}$ in (H.0.5) as shown in Figure H.7.

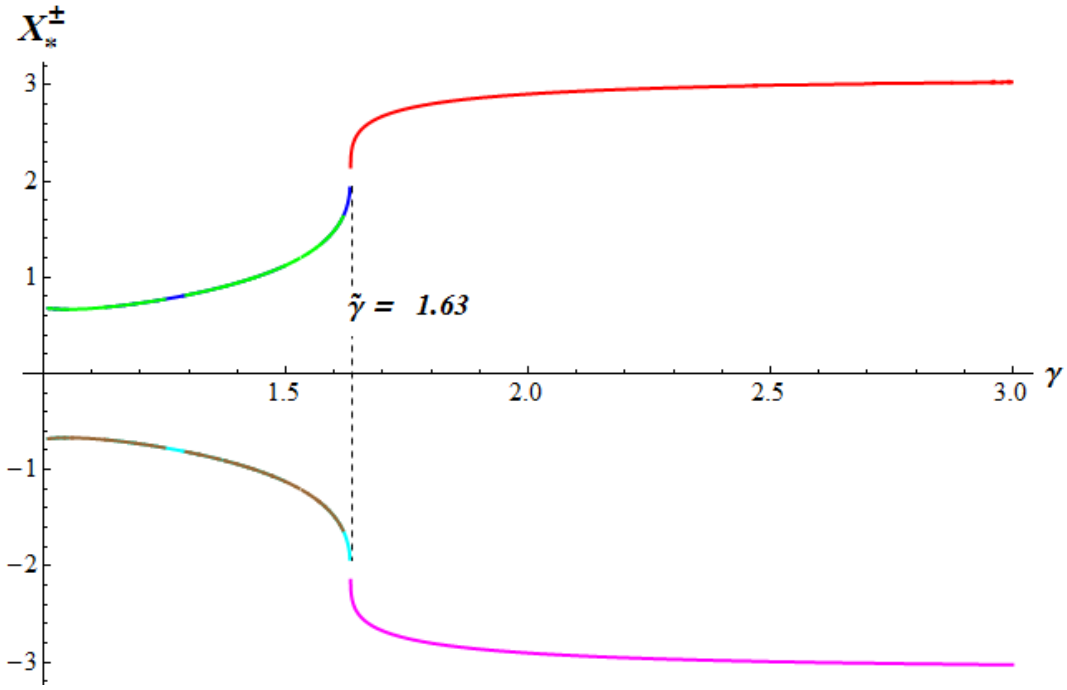

Figure H.7: Solutions $X_*^{\pm}(\gamma)$ of $G(Z=0,X,\gamma)=0$. Red, blue and green curves denote the first, second and third positive roots of equation $G(Z=0,X,\gamma)=0$, respectively. Magenta, cyan and brown− the first, second and third negative roots of equation $G(Z=0,X,\gamma)=0$

Furthermore, only $(\gamma,h)\in AA^*$ lead to the real and continuous (on the interval $x\in[0,h]$) functions $Z(x),X(x)$ and $H(x)$. Figure H.8 shows field patterns for fixed $\gamma=1.7\in BB^*$ and the corresponding film thickness $h=1.576$ (obtained according to (H.0.5)). The continuity condition for the functions $Z(x),X(x)$ and $H(x)$ are violated in point $\tilde{x}\in[0,h]$. This holds for all values $(\gamma,h)\in BB^*$, so that only solutions of the dispersion relation (evaluated according to (H.0.5), (H.0.6)) for $\gamma\in(1,\tilde{\gamma}=1.63)$ are presented in subsection 4.1.2.3. Further (analytical) investigation seems suitable for this exceptional case.

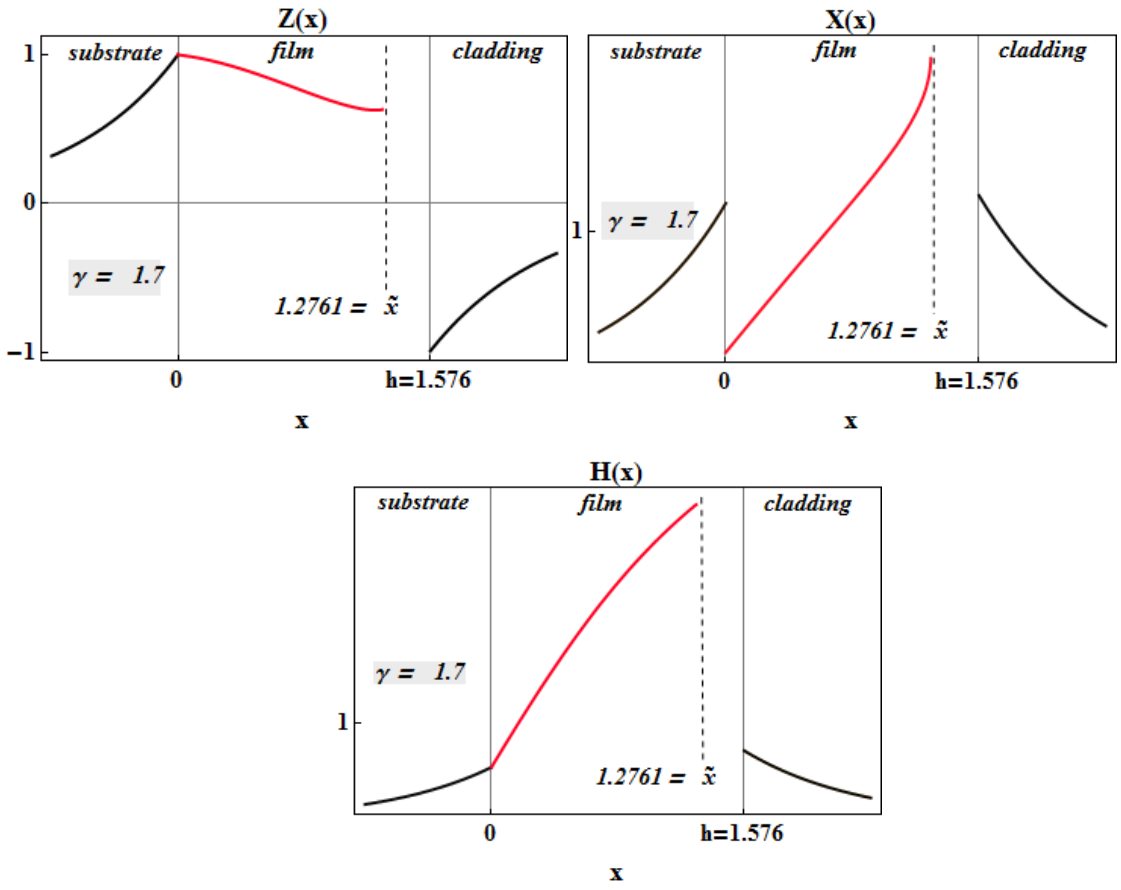

Figure H.8: Solutions $Z(x), X(x)$ and $H(x)$ for $h = 1.576$ and $\gamma = 1.7$

According to (3.2.7) and the analysis above the total power flow transported by the nonlinear TM_0- wave (see Figure 32, p. 61) through a waveguide with the thickness h can be evaluated as follows

$$P^* = P_s^* + P_c^* + P_f^* = \frac{\varepsilon_s \gamma\, Z(0)}{2\,(\gamma^2 - \varepsilon_s)^{3/2}} + \frac{\varepsilon_c \gamma\, Z^2(h)}{2\,(\gamma^2 - \varepsilon_c)^{3/2}} +$$

$$+ \int_{X_0}^{X_*^+} \frac{\varepsilon_{xf}\,\xi^2}{\gamma} \cdot F_{X_2}^+(\xi,\gamma)\,d\xi + \int_{X_*^-}^{X_{h2}} \frac{\varepsilon_{xf}\,\xi^2}{\gamma} \cdot F_{X_2}^-(\xi,\gamma)\,d\xi, \qquad 1 < \gamma < \tilde{\gamma} = 1.63$$

(H.0.8)

where

$$\varepsilon_{xf} = \varepsilon_{1f} + a\,\xi^2 + [Z_2^+(\xi,\gamma)]^2,$$

$$Z^2(h) = Z_2^+(X(h-0),\gamma) \text{ with } X(h-0) = X_{h2},$$

and P_s^*, P_f^*, P_c^* denote the parts of the total power flow in the substrate, film and cladding, respectively.

I On the evaluation of the dispersion relation for the case $a_f = 0$ (special Kerr- nonlinearity of the film)

An analytical closed form dispersion relation in the case of special Kerr-nonlinearity of the film ($a_f = 0$) is obtained following steps the I- VII as shown below (material parameters for corresponding numerical evaluation are given in subsection 4.1.3, nonlinearity coefficient b is chosen as $b = 0.35$).

I. Solution $X_s(0-0)$ is defined as (cf. (4.1.2))

$$X_s(0-0) = \frac{\gamma\, Z(0)}{\sqrt{\gamma^2 - \varepsilon_s}}. \tag{I.0.1}$$

II. Equation (3.1.11), rewritten for the present case as,

$$\varepsilon_s\, X_s(0-0) = \left[\varepsilon_{1f} + b\, Z^2(0)\right] X(0+0), \tag{I.0.2}$$

has a unique solution

$$X(0+0) = \frac{\gamma\, \varepsilon_s\, Z(0)}{\left(\varepsilon_{1f} + b\, Z^2(0)\right)\sqrt{\gamma^2 - \varepsilon_s}} \tag{I.0.3}$$

presented in Figure I.1.

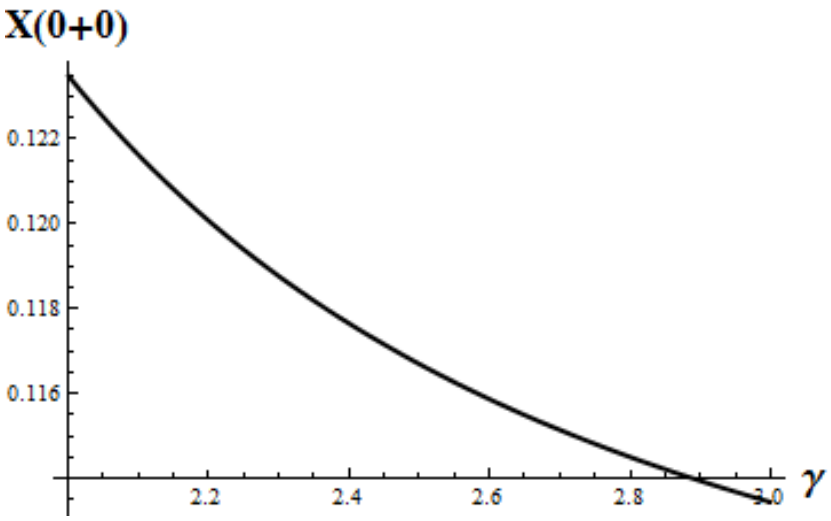

Figure I.1: Solution $X(0+0)$ (cf. (I.0.3)) (parameters cf. subsection 4.1.3, $b = 0.35$)

III. Inserting (I.0.3) into (4.1.3.3) the constant of integration is determined as

$$C_f = \frac{\gamma^2 Z^2(0)}{2}\left(\frac{\varepsilon_s^2\left(\varepsilon_{1f} + b\,Z^2(0) - \gamma^2\right)}{\left(\varepsilon_{1f} + b\,Z^2(0)\right)(\varepsilon_s - \gamma^2)} - \varepsilon_{2f}\right). \qquad \text{(I.0.4)}$$

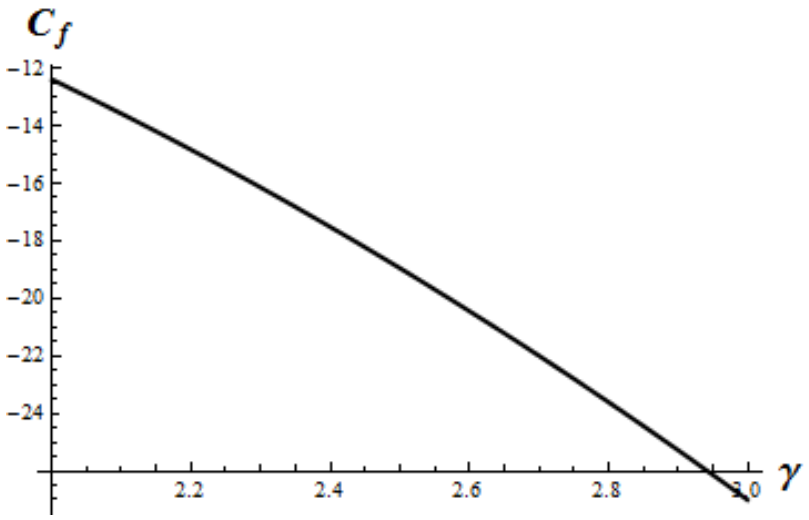

Figure I.2: Constant of integration C_f (cf. (I.0.4)) (parameters cf. Section 4.1.3, $b = 0.35$)

IV. The second equation (4.1.2) implies

$$X_c(h+0) = -\frac{\gamma\, Z(h)}{\sqrt{\gamma^2 - \varepsilon_c}}, \qquad \text{(I.0.5)}$$

where $Z(h)$ will be defined below.

V. Equation $G(Z, X, \gamma) = 0$ (cf. (4.1.3.2)) has only a one solution

$$X^2(Z,\gamma) = -\frac{2\,C_f + \gamma^2 \varepsilon_{2f}\, Z^2}{\left(\varepsilon_{1f} + b\, Z^2\right)\left(\varepsilon_{1f} + b\, Z^2 - \gamma^2\right)}, \tag{I.0.6}$$

hence, by setting $Z = Z(h)$ in the right-hand side of (I.0.6), solutions $X(h-0)$ are

$$X_{1,2}(h-0) = \pm\sqrt{-\frac{2\,C_f + \gamma^2 \varepsilon_{2f}\, Z^2(h)}{\left(\varepsilon_{1f} + b\, Z^2(h)\right)\left(\varepsilon_{1f} + b\, Z^2(h) - \gamma^2\right)}}. \tag{I.0.7}$$

VI. With (I.0.5) and (I.0.7) equation (3.1.12) reads

$$\left(\varepsilon_{1f} + b\, Z^2(h)\right)\left(\pm\sqrt{-\frac{2\,C_f + \gamma^2 \varepsilon_{2f}\, Z^2(h)}{\left(\varepsilon_{1f} + b\, Z^2(h)\right)\left(\varepsilon_{1f} + b\, Z^2(h) - \gamma^2\right)}}\right) = \\ = \frac{\gamma\, Z(h)\,(\varepsilon_c + b\, Z^2(h))}{\sqrt{\gamma^2 - \varepsilon_c}}, \tag{I.0.8}$$

so that two solutions $Z^2(h)$ exist

$$Z^2_{1,2}(h) = \frac{1}{q_0}\left(q_1 \pm \sqrt{{q_1}^2 + q_0\, q_2}\right), \tag{I.0.9}$$

where

$$q_0 = 2b\,\gamma^2\left(\varepsilon_c^2 + \varepsilon_{2f}(\gamma^2 - \varepsilon_c)\right),$$
$$q_1 = \gamma^4\left(\varepsilon_c^2 - \varepsilon_{2f}\varepsilon_{2f}\right) + \gamma^2\left(\varepsilon_{2f} - \varepsilon_c\right)\varepsilon_c\varepsilon_{2f} + 2b(\varepsilon_c - \gamma^2)C_f,$$
$$q_2 = 4\varepsilon_{2f}(\varepsilon_c - \gamma^2)C_f.$$

For material parameters given in subsection 4.1.3 (with $b = 0.35$) both solutions $Z^2_{1,2}(h)$ are real but only solution $Z_2^2(h)$ is positive as shown in Figure I.3.

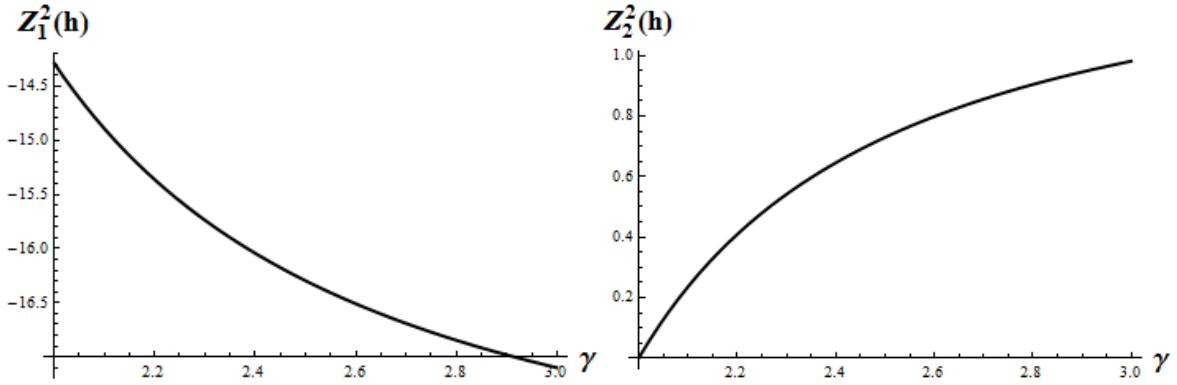

Figure I.3: Roots $Z_{1,2}^2(h)$ (cf. (I.0.9)) (parameters cf. subsection 4.1.3, $b = 0.35$)

VII. Setting $Z \equiv \zeta$ in (I.0.7) solution $X^2(\zeta, \gamma)$ is given by

$$X^2(\zeta,\gamma) = -\frac{2\,C_f + \gamma^2 \varepsilon_{2f}\,\zeta^2}{\left(\varepsilon_{1f} + b\,\zeta^2\right)\left(\varepsilon_{1f} + b\,\zeta^2 - \gamma^2\right)}. \tag{I.0.10}$$

With (I.0.10) and (4.1.3.4) equation (3.1.14) reads

$$\int_{Z(0)}^{Z(h)} \frac{\gamma\, d\zeta}{\pm\sqrt{-\dfrac{2\,C_f + \gamma^2 \varepsilon_{2f}\,\zeta^2}{\left(\varepsilon_{1f} + b\,\zeta^2\right)\left(\varepsilon_{1f} + b\,\zeta^2 - \gamma^2\right)}} \times \left(\gamma^2 - \varepsilon_{1f} - b\,\zeta^2\right)} = h > 0, \tag{I.0.11}$$

where the sign " + " or " − " has to be chosen in dependence on the function (cf. (I.0.10))

$$X^{\pm}(\zeta,\gamma) = \pm\sqrt{-\frac{2\,C_f + \gamma^2 \varepsilon_{2f}\,\zeta^2}{\left(\varepsilon_{1f} + b\,\zeta^2\right)\left(\varepsilon_{1f} + b\,\zeta^2 - \gamma^2\right)}} \tag{I.0.12}$$

subject to

$$\begin{aligned} sgn[X(\zeta = Z(0),\gamma)] &\equiv sgn[X(0+0)], \\ sgn[X(\zeta = Z(h),\gamma)] &\equiv sgn[X(h-0)]. \end{aligned} \tag{I.0.13}$$

Substitution of $\xi = \zeta^2$ in the integral (I.0.11) leads to

$$\int_{Z^2(0)}^{Z^2(h)} \frac{\pm\gamma\, d\xi}{2\left(\pm\sqrt{-\dfrac{\left(2\,C_f + \gamma^2 \varepsilon_{2f}\,\xi\right)\xi}{\left(\varepsilon_{1f} + b\,\xi\right)\left(\varepsilon_{1f} + b\,\xi - \gamma^2\right)}}\right) \times \left(\gamma^2 - \varepsilon_{1f} - b\,\xi\right)} = h, \tag{I.0.14}$$

where the sign in the numerator is " + " (" − ") if $\zeta > 0$ ($\zeta < 0$) on the path $\zeta \in [Z(0), Z(h)]$.

The integrand in (I.0.14) (omitting the signs " $\pm$ ") has a primitive function expressed in terms of elliptic integrals:

$$\Phi[z] = \alpha_1(z)\, F[\varphi(s(z)), m] + \alpha_2(z)\, \Pi(n; \varphi(s(z)), m), \tag{I.0.15}$$

where

$$\alpha_1(z) = \frac{\gamma\, \varepsilon_{1f}^2 (\varepsilon_{1f} - \gamma^2 + b\, z)}{b\, (\varepsilon_{1f} - \gamma^2)(\varepsilon_{1f} + b\, z)} \times$$

$$\times \sqrt{\frac{b^2 (\varepsilon_{1f} - \gamma^2)^2\, (\varepsilon_{1f} + b\, z)^2}{\varepsilon_{1f}^3\, (\varepsilon_{1f} + b\, z - \gamma^2)^2\, (\varepsilon_{2f}\, \gamma^2\, (\varepsilon_{1f} - \gamma^2) - 2\, b\, C_f)}},$$

$$a_2(z) = -\frac{\gamma\, z}{\varepsilon_{1f} + b\, z} \sqrt{\frac{(\varepsilon_{1f} - \gamma^2)^2\, (\varepsilon_{1f} + b\, z)^2}{\varepsilon_{1f}\, z\, (\varepsilon_{2f}\, \gamma^2\, (\varepsilon_{1f} - \gamma^2) - 2\, b\, C_f)}},$$

$$\varphi(s(z)) = Arcsin\sqrt{s(z)}\,,$$

$$s(z) = \frac{\varepsilon_{1f} (\varepsilon_{1f} - \gamma^2 + b\, z)}{b\, \gamma^2 z},$$

$$n = \frac{\gamma^2}{\varepsilon_{1f}},$$

$$m = \frac{2\, b\, \gamma^2\, C_f}{\varepsilon_{1f}\, (2\, b\, C_f - \varepsilon_{2f}\, \gamma^2\, (\varepsilon_{1f} - \gamma^2))}.$$

Thus, the dispersion relation in the present case can be presented in the closed analytical form:

$$sgn\, (\Phi[Z^2(h)] - \Phi[Z^2(0)]\,) = h > 0, \tag{I.0.16}$$

where

$$sgn = \begin{cases} +, & \begin{cases} Z(0) > 0, Z(h) > 0 \text{ and } X^+(\zeta,\gamma) \text{ satisfies (I.0.14)} \\ \text{or} \\ Z(0) < 0, Z(h) < 0 \text{ and } X^-(\zeta,\gamma) \text{ satisfies (I.0.14)} \end{cases} \\ -, & \begin{cases} Z(0) > 0, Z(h) > 0 \text{ and } X^-(\zeta,\gamma) \text{ satisfies (I.0.14)} \\ \text{or} \\ Z(0) < 0, Z(h) < 0 \text{ and } X^+(\zeta,\gamma) \text{ satisfies (I.0.14)} . \end{cases} \end{cases} \tag{I.0.17}$$

In general, the functions Z and $X(Z,\gamma)$ (cf. (I.0.6)) can also change sign within the integration interval $(Z(0), Z(h))$. This has to be taken into account in evaluation of (I.0.11), and hence in applying (I.0.16).

This can be illustrated by numerical evaluation of the dispersion relation (I.0.16) for $\gamma \in (1,3)$ with material parameters of subsection 4.1.3 (with $b = 0.35$). Figure I.4 presents the functions $X^{\pm}(Z,\gamma)$ (blue and red curves), solutions $Z_0 = Z(0)$, $Z_{h1} = -\sqrt{Z_2(h)}$, $Z_{h2} = +\sqrt{Z_2(h)}$ (cf. (I.0.9)), $X_{h1} = X_2(h-0)$, $X_{h2} = X_1(h-0)$ (cf. (I.0.7)), $Z_*^{\pm}$ (black points)[37] and the first integral $G(Z,X,\gamma) = 0$ (cf. (4.1.3.2)) (black dashed curve) for fixed $\gamma = 2.5$.

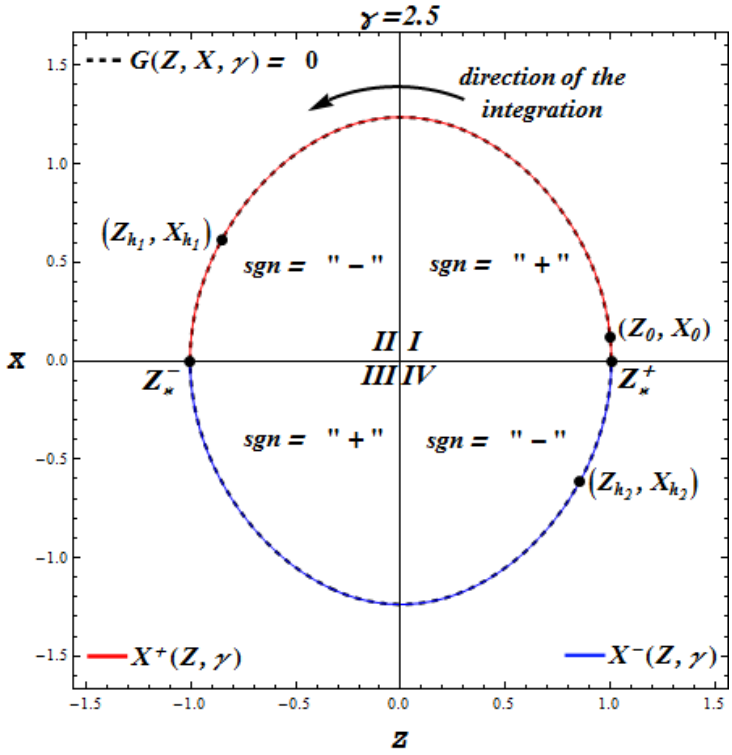

Figure I.4: The first integral $G(Z,X,\gamma = 2.5) = 0$ (cf. (4.1.3.2)) (parameters cf. subsection 4.1.3, $b = 0.35$)

According to Figure I.4 the dispersion relation (I.0.11) corresponding to the solutions Z_{h1}, Z_{h2} reads (using (I.0.14) and (I.0.16))

$$\int_{Z_0}^{Z_{h1}} F_Z^{\pm}(\zeta,\gamma)d\zeta = \int_{Z_0}^{0} F_Z^{+}(\zeta,\gamma)d\zeta + \int_{0}^{Z_{h1}} F_Z^{+}(\zeta,\gamma)d\zeta =$$

$$= + \left(\lim_{\varepsilon\to 0}\Phi[\varepsilon] - \Phi[Z_0^2]\right) + \left(-\left(\Phi[Z_{h1}^2] - \lim_{\varepsilon\to 0}\Phi[\varepsilon]\right)\right) =$$

$$= 2\lim_{\varepsilon\to 0}\Phi[\varepsilon] - \Phi[Z_0^2] - \Phi[Z_{h1}^2] = 1.8 > 0$$

$$\int_{Z_0}^{Z_{h2}} F_Z^{\pm}(\zeta,\gamma)d\zeta =$$

$$= \int_{Z_0}^{0} F_Z^{+}(\zeta,\gamma)d\zeta + \int_{0}^{Z_*^-} F_Z^{+}(\zeta,\gamma)d\zeta + \int_{Z_*^-}^{0} F_Z^{-}(\zeta,\gamma)d\zeta + \int_{0}^{Z_{h2}} F_Z^{-}(\zeta,\gamma)d\zeta =$$

$$= \left(+\left(\lim_{\varepsilon\to 0}\Phi[\varepsilon] - \Phi[Z_0^2]\right)\right) + \left(-\left(\Phi[(Z_*^-)^2] - \lim_{\varepsilon\to 0}\Phi[\varepsilon]\right)\right) +$$

$$+ \left(+\left(\lim_{\varepsilon\to 0}\Phi[\varepsilon] - \Phi[(Z_*^-)^2]\right)\right) + \left(-\left(\Phi[Z_{h2}^2] - \lim_{\varepsilon\to 0}\Phi[\varepsilon]\right)\right) =$$

$$= 4\lim_{\varepsilon\to 0}\Phi[\varepsilon] - 2\Phi[(Z_*^-)^2] - \Phi[Z_0^2] - \Phi[Z_{h2}^2] = 4.1.$$

Evaluation for $\gamma \in (1,3)$ shows that the structure of Figure I.4 is independent on γ, Z_0, X_0 in this domain ($(Z_0, X_0) \in X^+(Z,\gamma)$ is located in the quadrant I, $(Z_{h1}, X_{h1}) \in X^+(Z,\gamma)$ and $(Z_{h2}, X_{h2}) \in X^-(Z,\gamma)$ are located in the quadrant II and IV, respectively), hence, the dispersion relations for the present case can be rewritten as

$$2\lim_{\varepsilon\to 0}\Phi[\varepsilon] - \Phi[Z_0^2] - \Phi[Z_{h1}^2(\gamma)] = h = h1, \qquad \text{(I.0.18)}$$

$$4\lim_{\varepsilon\to 0}\Phi[\varepsilon] - 2\Phi[Z_*^2(\gamma)] - \Phi[Z_0^2] - \Phi[Z_{h2}^2(\gamma)] = h = h2. \qquad \text{(I.0.19)}$$

Figure I.4 gives also information about the mode number. The integrand in (I.0.11) does not change sign on the integration path (Z_0, Z_{h1}) $(X(Z,\gamma) = X^+(Z,\gamma) \in (Z_0, Z_*^-))$ but changes the sign once on the integration path (Z_0, Z_{h2}) $\left(X(Z,\gamma) = X^+(Z,\gamma) \in (Z_0, Z_*^-),\ X(Z,\gamma) = X^-(Z,\gamma) \in (Z_*^-, Z_{h2})\right)$.
Therefore, equations (I.0.18) and (I.0.19) present the solutions for the first even (fundamental TM_0) and the first odd (TM_1) modes, respectively. Results of numerical evaluation of (I.0.18), (I.0.19) are presented in Figure 42.
As has been shown in Figure 40 the functions Z and X are periodic. Using Figure I.4 and (I.0.16) the period (4.1.3.7) for higher mode solutions can be evaluated according to[28]

$$T_Z = 4\left|\lim_{\varepsilon\to 0}\Phi\,[\varepsilon] - \Phi[Z_*^2]\right|, \tag{I.0.20}$$

where $Z_*^2 = (Z_*^{\pm})^2$.
Adding T_Z (cf. (4.1.3.8) with $N = 1, \mathrm{k} = 0$) to the right- hand side of equations (I.0.18) and (I.0.19) the solutions for the second (even) and third (odd) modes given in Figure 42, are obtained.

Following the same arguments as in step the VII above the integral (4.1.3.10) (setting $\xi = \zeta^2$) reads

$$P_{film}^{\pm} = \int_{Z^2(0)}^{Z^2(h)} \frac{\pm(\varepsilon_{1f} + b\,\xi)}{2\,(\gamma^2 - \varepsilon_{1f} - b\,\xi)}\left(\pm\sqrt{-\frac{\left(2\,C_f + \gamma^2\varepsilon_{2f}\,\xi\right)}{\left(\varepsilon_{1f} + b\,\xi\right)\left(\varepsilon_{1f} + b\,\xi - \gamma^2\right)\xi}}\right)d\xi, \tag{I.0.21}$$

where selection of the signs " $\pm$ " is defined above (see formulas (I.0.11)-(I.0.14)).
The primitive function of (I.0.21) (omitting the signs " $\pm$ ") is a function expressed in terms of elliptic integrals:

$$\mathcal{P}[z] = \beta_1(z)\,E\left[m\cdot\varphi\left(s(z)\right), m\right] + \beta_2(z)\,F\left[\varphi\left(s(z)\right), m\right] + \\ + \beta_3\,(z)\,\Pi\left(n; \varphi\left(s(z)\right), m\right) + \beta_4(z), \tag{I.0.22}$$

where

$$\beta_1(z) = \frac{(\varepsilon_{1f} + b\,z)\sqrt{-2\,\gamma^2 b\,C_f}}{b\sqrt{(\varepsilon_{1f} + b\,z)^2\,(\varepsilon_{1f} - \gamma^2)^2}},$$

$$\beta_2(z) = -z\sqrt{\frac{2\,C_f}{b\,\gamma^2 z^2}},$$

$$\beta_3(z) = -\frac{\varepsilon_{2f}\,\gamma^4 z^2}{\varepsilon_{1f}\,(2\,C_f + \varepsilon_{2f}\,\gamma^2 z)}\sqrt{-\frac{\varepsilon_{1f}(\varepsilon_{1f} - \gamma^2)^2\,(2\,C_f + \varepsilon_{2f}\,\gamma^2 z)^2}{b^2\gamma^4 z^4\,(2\,b\,C_f - \varepsilon_{2f}\,\gamma^2\,(\varepsilon_{1f} - \gamma^2))}},$$

$$\beta_4(z) = \frac{(\varepsilon_{1f} + b\,z)}{b}\sqrt{-\frac{2\,C_f + \varepsilon_{2f}\,\gamma^2 z}{z\,(\varepsilon_{1f} + b\,z)((\varepsilon_{1f} + b\,z - \gamma^2)}}.$$

In a similar way to (I.0.16) the power flow in the film can be presented as

$$P^{\pm}_{film} = sgn\left(\mathcal{P}\left[Z^2(h) - \mathcal{P}[Z^2(0)]\right]\right), \tag{I.0.23}$$

where sgn is defined by (I.0.17).

If the functions Z and $X(Z,\gamma)$ (cf. (I.0.6)) change sign in the interval $(Z(0), Z(h))$, change of sgn within this interval has to be considered in (I.0.23) in more details, but evaluation is straightforward.

Taking into account (4.1.3.9), (I.0.22), (I.0.18), (I.0.19) and (I.0.20) the total power flow for the TM_0 and TM_1 modes and its periodicity can be evaluated as (material parameters cf. subsection 4.1.3, $b = 0.35$)

$$P^{\pm}_{film,h1} = 2\lim_{\varepsilon\to 0}\mathcal{P}\,[\varepsilon] - \mathcal{P}[Z_0^2] - \mathcal{P}[Z_{h1}^2(\gamma)], \tag{I.0.24}$$

$$P^{\pm}_{film,h2} = 4\lim_{\varepsilon\to 0}\mathcal{P}[\varepsilon] - 2\,\mathcal{P}[Z_*^2(\gamma)] - \mathcal{P}[Z_0^2] - \mathcal{P}[Z_{h2}^2(\gamma)], \tag{I.0.25}$$

$$T^* = 4\left|\lim_{\varepsilon\to 0}\mathcal{P}\,[\varepsilon] - \mathcal{P}[Z_*^2(\gamma)]\right|, \tag{I.0.26}$$

respectively. Hence, the total power flow corresponding to the dispersion relation including higher modes reads (according to (4.1.3.12))

$$P^*_{TM_j} = \frac{\varepsilon_{1s}\,\gamma\,Z^2(0)}{2\sqrt{(\gamma^2-\varepsilon_{1s})^3}} + P^{\pm}_{film,l} + \frac{\varepsilon_{1c}\,\gamma\,Z^2(h)}{2\sqrt{(\gamma^2-\varepsilon_{1c})^3}} + N\cdot T^*, \tag{I.0.27}$$

where (cf. (I.0.18), (I.0.19))

$$\begin{cases} \text{if} & j=0, \text{ then } l=h1 \text{ and } N=0, \\ & j=1, \text{ then } l=h2 \text{ and } N=0, \\ & j=2, \text{ then } l=h1 \text{ and } N=1, \\ & j=3, \text{ then } l=h2 \text{ and } N=1. \end{cases} \tag{I.0.28}$$

Results of the numerical evaluation of (I.0.27) is presented in Figure 46.

J On the evaluation of the dispersion relation in the case of a uniaxial medium in the film

Numerical results presented in subsection 4.2 have been evaluated for

$$1 < \gamma \leq 4. \tag{J.01}$$

Case $a = 0.2$ is considered below.

As follows from Figure J.1 only the first solution of equation (4.2.7) from three possible solutions is real. This has been taken for further evaluation.

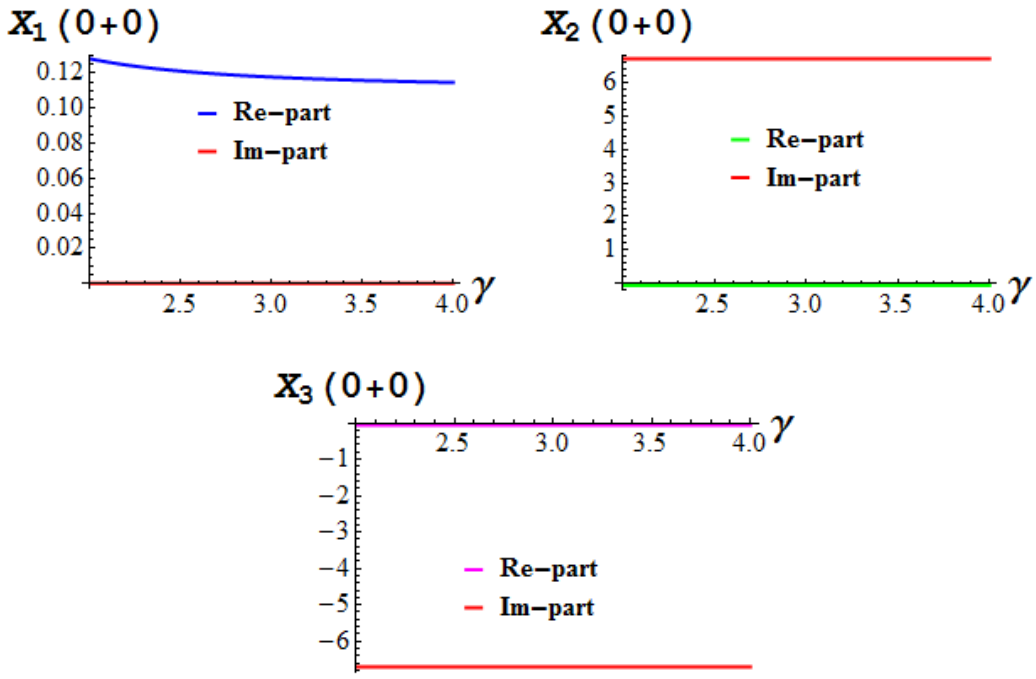

Figure J.1: Three roots of eq. (4.2.7) (cf. (4.2.8))

Assuming $X_{0f} = X_1(0+0)$ in (4.2.3) the constant of integration is evaluated. Result is depicted in Figure J.2.

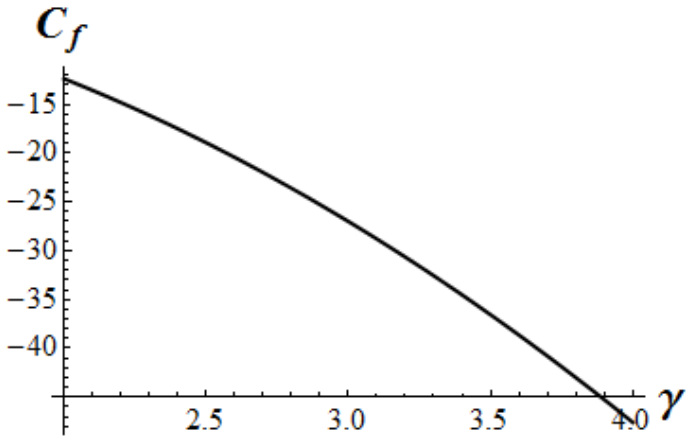

Figure J.2: The constant of integration C_f evaluated with $X_{0f} = X_1(0+0)$ (cf. equations (4.2.3) and (4.2.8))

Figure J.3 presents three solutions $X^2(h-0)$ of equation (4.2.13). As can been seen in Figure J.3 only the first solution $X^2(h-0) = X_1^2(h-0)$ is real and positive. This has been taken for the evaluation of the dispersion relation and the power flow.

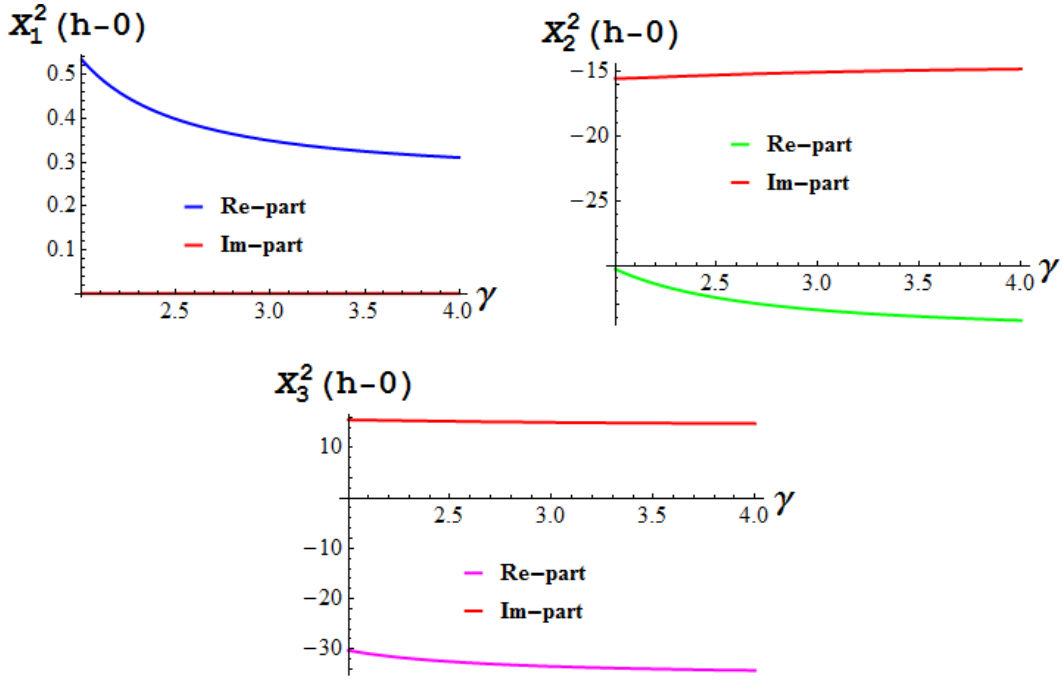

Figure J.3: Three roots of eq. (4.2.13) (cf. (4.2.14))

Figure J.4 represents the first integral $G(Z, X, \gamma) = 0$ (cf. (4.2.2)) plotted with the functions $Z^{\pm}(\xi = X, \gamma)$ (cf. (4.2.17)) and the solutions $X_0 = X_1(0 + 0)$ (cf. (4.2.8)), $X_{h1,h2} = \pm\sqrt{X_1^2(h - 0)}$ (cf. (4.2.14)) of equations (4.2.7) and (4.2.13), respectively, for a fixed $\gamma \in (1, 4]$.

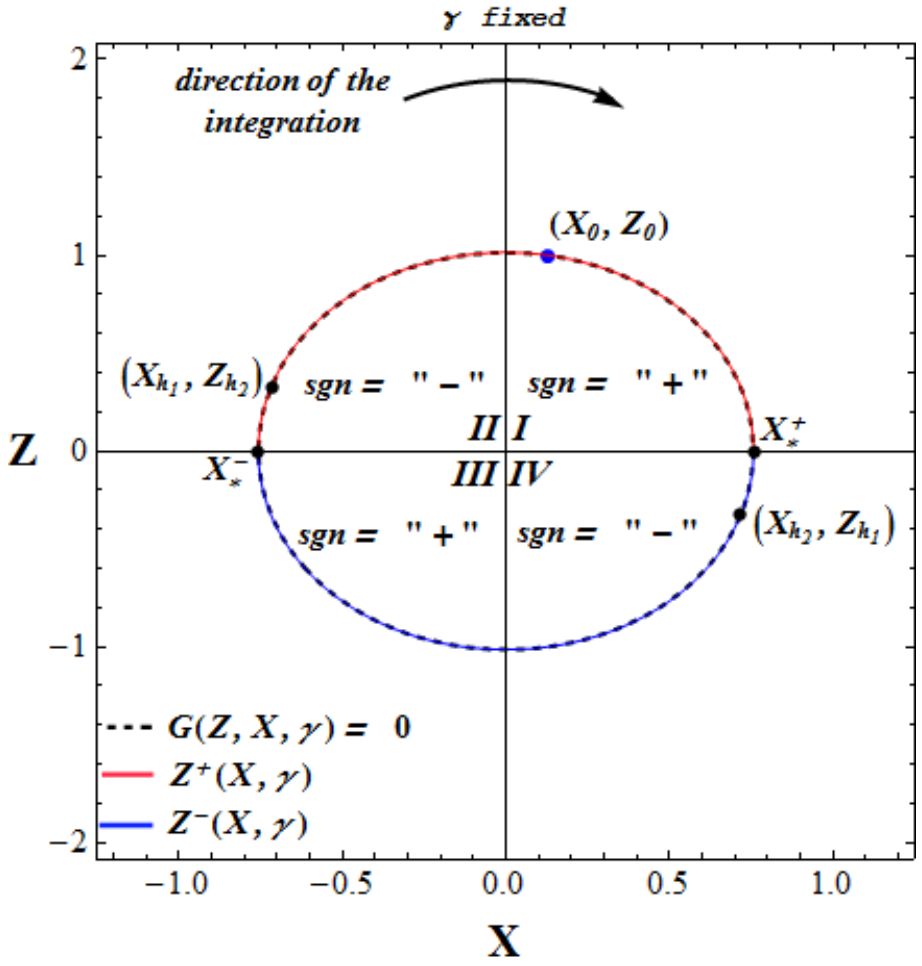

Figure J.4: The first integral $G(Z, X, \gamma) = 0$ with the solutions $Z_j^{\pm}(X, \gamma)(j = 1,2)$ and solutions of equations (4.2.7), (4.2.13) plotted for a fixed γ. Here $Z_0 = Z(0)$, $Z_{h1,h2} = Z_{1,2}(h)$ (cf. (4.2.12))

Structure presented in Figure J.4 (point $(X_0, Z_0) \in Z^+(X, \gamma)$ is located in the quadrant I, points $(X_{h1}, Z_{h2}) \in Z^+(X, \gamma)$ and $(X_{h2}, Z_{h1}) \in Z^-(X, \gamma)$ are located in the quadrant II and IV, respectively) is the same for all $\gamma \in (1,4]$. Hence, the dispersion relation (4.2.22) for the two solutions X_{h1}, X_{h2} in the present case reads

$$\int_{X_0}^{X_{h1}} F_X^{\pm}(\xi,\gamma)d\xi =$$

$$= \int_{X_0}^{X_*^+} F_X^+(\xi,\gamma)d\xi + \int_{X_*^+}^{0} F_X^-(\xi,\gamma)d\xi + \int_{0}^{X_*^-} F_X^-(\xi,\gamma)d\xi + \int_{X_*^-}^{X_{h1}} F_X^+(\xi,\gamma)d\xi =$$

$$= \left(+\left(\mathcal{F}[(X_*^+)^2] - \mathcal{F}[X_0^2]\right)\right) + \left(-\left(\lim_{\varepsilon\to 0}\mathcal{F}[\varepsilon] - \mathcal{F}[(X_*^+)^2]\right)\right)$$

$$+ \left(+\left(\mathcal{F}[(X_*^-)^2] - \lim_{\varepsilon\to 0}\mathcal{F}[\varepsilon]\right)\right) + \left(-(\mathcal{F}[X_{h1}^2] - \mathcal{F}[(X_*^-)^2])\right)$$

$$= 2\left(\mathcal{F}[(X_*^+)^2] + \mathcal{F}[(X_*^-)^2] - \lim_{\varepsilon\to 0}\mathcal{F}[\varepsilon]\right) - \mathcal{F}[X_0^2] - \mathcal{F}[X_{h1}^2(\gamma)] = h1 > 0, \quad \text{(J.0.2)}$$

$$\int_{X_0}^{X_{h2}} F_X^{\pm}(\xi,\gamma)d\xi = \int_{X_0}^{X_*^+} F_X^+(\xi,\gamma)d\xi + \int_{X_*^+}^{X_{h2}} F_X^-(\xi,\gamma)d\xi =$$

$$= \left(+\left(\mathcal{F}\left[(X_*^p)^2\right] - \mathcal{F}[X_0^2]\right)\right) + \left(-\left(\mathcal{F}[X_{h2}^2] - \mathcal{F}\left[(X_*^p)^2\right]\right)\right) =$$

$$= 2\mathcal{F}[(X_*^+)^2] - \mathcal{F}[X_0^2] - \mathcal{F}[X_{h1}^2] = h2 > 0, \quad \text{(J.0.3)}$$

where X_*^+, X_*^- are solutions of $G(Z \equiv 0, X, \gamma) = 0$.

Numerical evaluation of (J.0.2) and (J.0.3) leads to the results presented in Figure 52 (TM_0 and TM_1 modes, blue curves).

Using (4.2.30) and the analysis given for the dispersion relation above the power flow in the film for the solution X_{h1} can be written as follows

$$P_{film,X}^{\pm}(X_{h1}) = 2\left(\tilde{\mathcal{P}}[(X_*^+)^2] + \tilde{\mathcal{P}}[(X_*^-)^2] - \lim_{\varepsilon\to 0}\tilde{\mathcal{P}}[\varepsilon]\right) - \tilde{\mathcal{P}}[X_0^2] - \tilde{\mathcal{P}}[X_{h1}^2(\gamma)], \quad \text{(J.0.4)}$$

Numerical evaluation of (4.2.28) with $P_{film,X}^{\pm}$ according to (J.0.4) leads to the result presented in Figure 57 (the total power flow of the TM_0 mode, blue curve). Evaluation of the dispersion relation and the total power flow for the other values a (or $Z(0)$) proceeds analogously.

K On the evaluation of the dispersion relation in the case of nonlinear substrate, film, and cladding

Choosing a domain of the propagation constant γ as in the linear case

$$Max\left[\sqrt{\varepsilon_{1s}}, \sqrt{\varepsilon_{2s}}, \sqrt{\varepsilon_{1c}}, \sqrt{\varepsilon_{1c}}\right] < \gamma \leq \sqrt{\varepsilon_{1f}} \qquad \text{(K.0.1)}$$

solutions of the dispersion relation in the present case are obtained by using (3.1.14) according to steps the I- VII of Section 3 as shown in the following:

I. Figure K.1 presents the three solutions of equation (3.1.4) (with $\nu = s$) solved with respect to $X_s^2(0-0) = X_s^2(0-0;\gamma, Z(0))$. The first (green curve) and third (blue curve) roots are real and positive, these will be taken for further consideration.

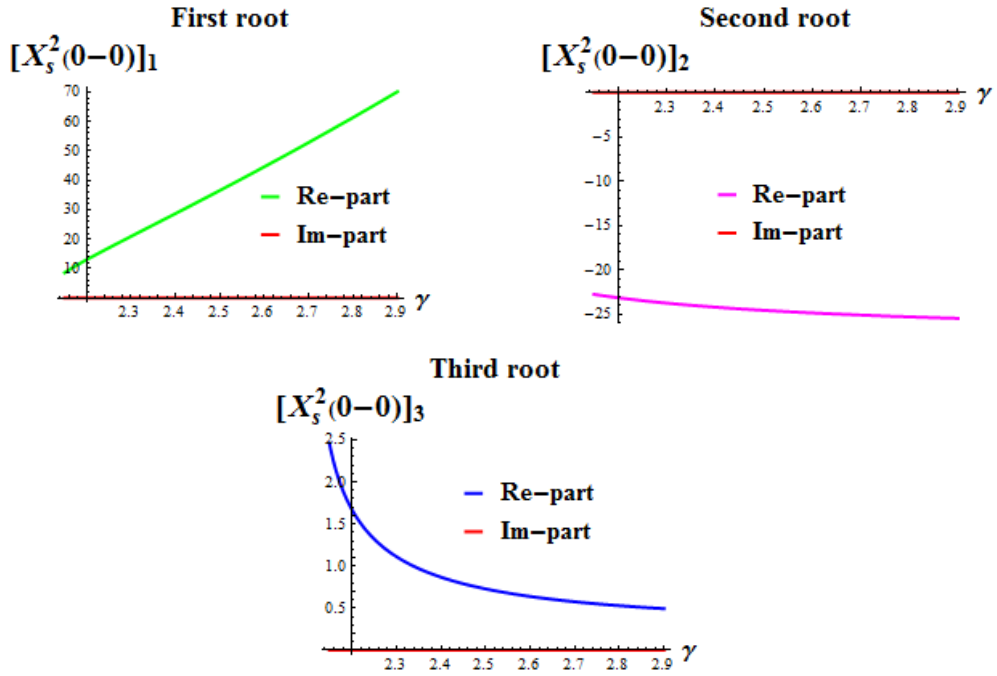

Figure K.1: Three solutions $X_s^2(0-0)$ of equation $G_s(Z_s, X_s, \gamma) = 0$ (cf. (3.1.4))

II. Inserting the solutions $\pm\sqrt{[X_s^2(0-0)]_i}$, $(i = 1,3)$ into equation (3.1.11) solutions $X_f(0+0)$, presented in Figure K.2, are obtained. Following notation is used

$$X_{si}^{p} = +\sqrt{[X_s^2(0-0)]_i}\,,$$
$$X_{si}^{m} = -\sqrt{[X_s^2(0-0)]_i}\,,$$

X_{fj}^{pi}: the $j-$th root $X_f(0+0)$ of equation (3.1.11) evaluated with X_{si}^{p},

X_{fj}^{mi}: the $j-$th root $X_f(0+0)$ of equation (3.1.11) evaluated with X_{si}^{m},

$$(i = 1,3;\ \ j = 1,2,3)$$

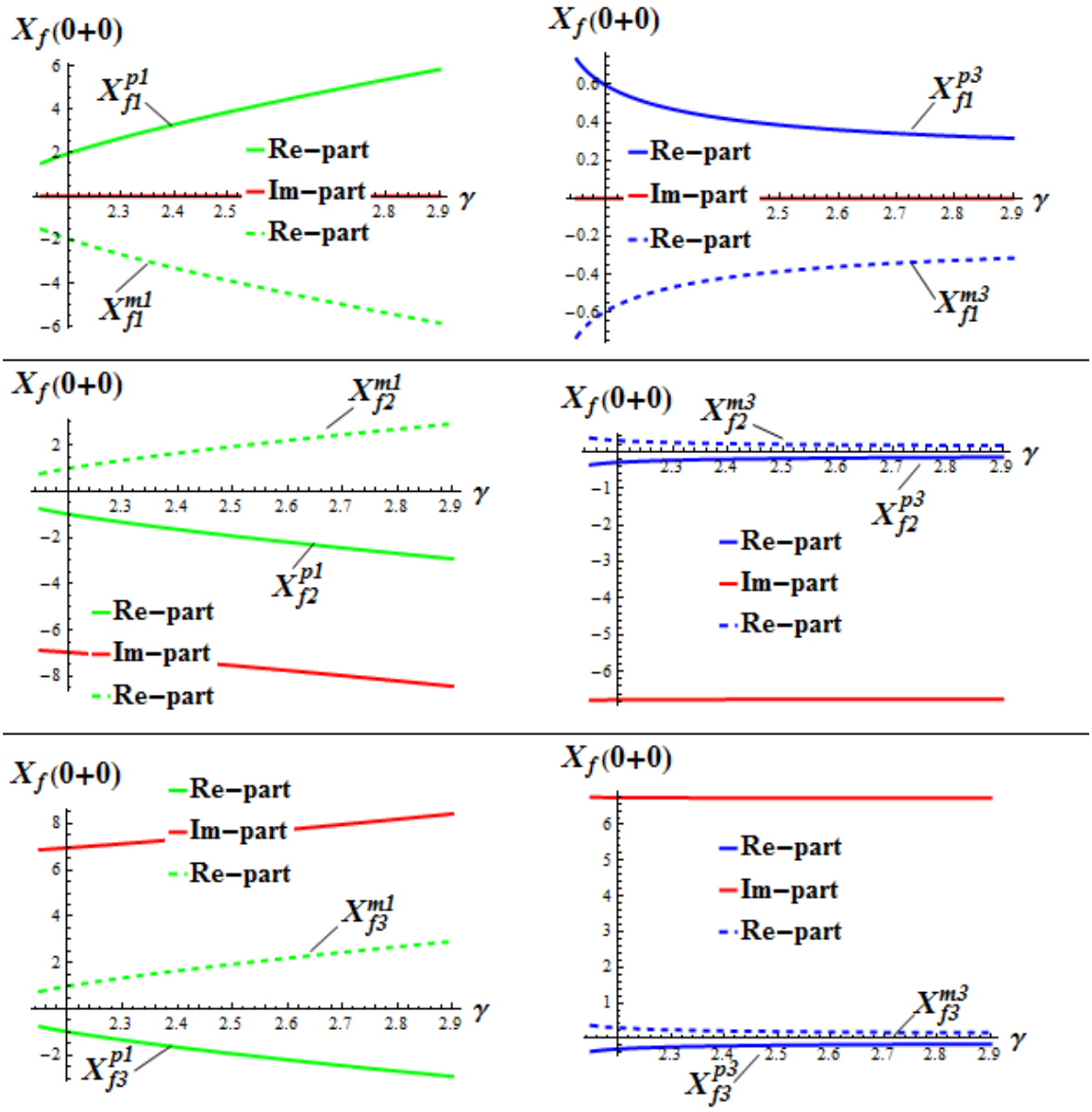

Figure K.2: Solutions $X_f(0+0)$ of equation (3.1.11)

As can be seen from Figure K.2 only the roots X_{f1}^{pi} and X_{f1}^{mi} $(i = 1,3)$ are real. Hereafter all results on steps the III- VI evaluated with X_{f1}^{pi} and X_{f1}^{mi} will be represented graphically by green (for $i = 1$) and blue (for $i = 3$) colour $\left(\text{solid curve for } X_{f1}^{pi}\ (i = 1,3) \text{ and dashed curve for } X_{f1}^{mi}\ (i = 1,3)\right)$.

III. The constants of the integration C_f are shown in Figure K.3. Taking into account that (see also Figure K.2)

$$\left|X_{f1}^{pi}\right| = \left|X_{f1}^{mi}\right| \ (i = 1,3),$$

and that C_f is quadratic with respect to $X_f(0+0)$ (cf. (3.1.5)) the following equalities hold

$$C_{f1} = C_f\left(Z^2(0),\ X_{0f}^2 = \left(X_{f1}^{p1}\right)^2\right) = C_f\left(Z^2(0),\ X_{0f}^2 = \left(X_{f1}^{m1}\right)^2\right),$$
$$C_{f3} = C_f\left(Z^2(0),\ X_{0f}^2 = \left(X_{f1}^{p3}\right)^2\right) = C_f\left(Z^2(0),\ X_{0f}^2 = \left(X_{f1}^{m3}\right)^2\right). \tag{K.0.2}$$

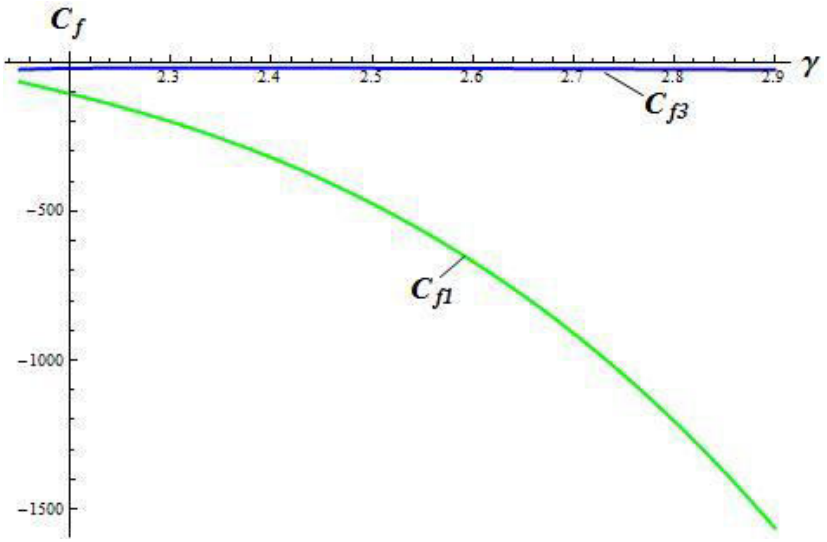

Figure K.3: The integration constants C_f (cf. (3.1.5))

IV. Figure K.4 depicts the three solutions of equation (3.1.4) (with $\nu = c$) solved with respect to $X_c^2(h+0) = X_c^2(h+0, \gamma, Z(0); Z(h))$ (on the figure labelled by $X_{c1}^2(h+0)$, $X_{c2}^2(h+0)$, $X_{c3}^2(h+0)$ for the first, second and third root, respectively). Roots $X_{c1}^2(h+0)$ and $X_{c3}^2(h+0)$

as real and positive have to be taken for evaluation of the equation (3.1.12) (in step the V below).

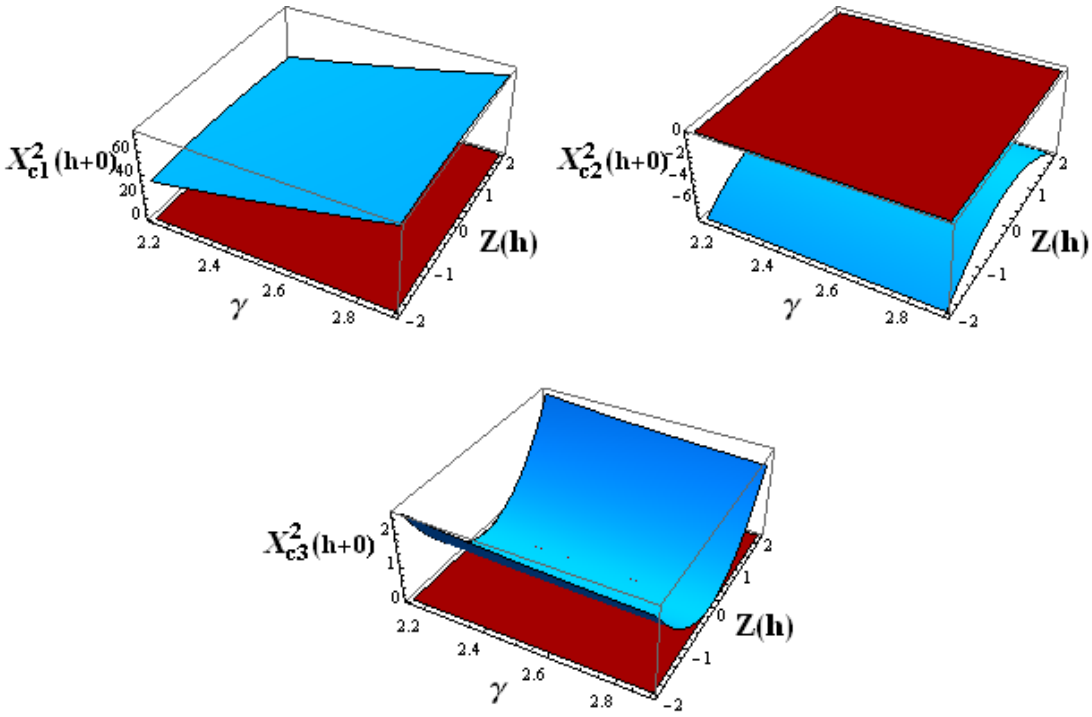

Figure K.4: Cyan colour surface shows real part of the root $X^2_{cj}(h+0)$, red one – imaginary part of the root $X^2_{cj}(h+0)(j=1,2,3)$.

V.-VI.

Figure K.5 shows the first integral (3.1.4) evaluated with $C_f = C_{f1}$ (cf. (3.1.5) and Step IV.) and $C_f = C_{f3}$ (cf. (3.1.5) and Step IV.). As can be seen the first integrals $G_f(Z_f, X_f, \gamma; C_{fi}) = 0$ $(i = 1,3)$ are presented by closed curves (for fixed γ) so that the functions Z_f, X_f, H_f are periodic.

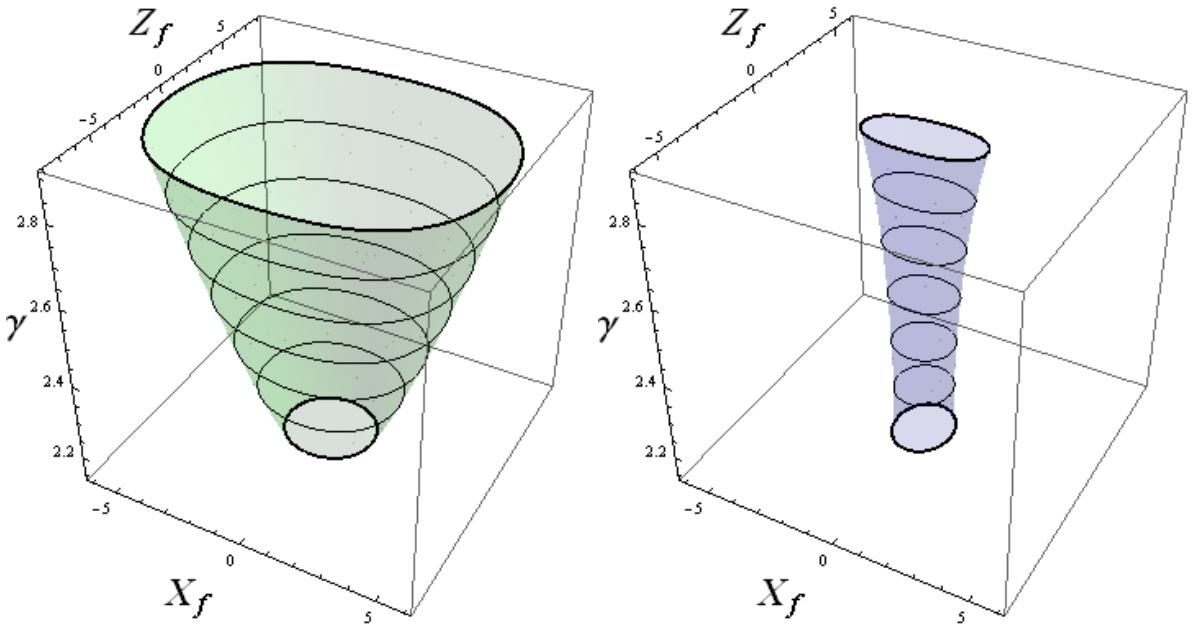

Figure K.5: **a)** The first integral $\boldsymbol{G_f(Z_f, X_f, \gamma) = 0}$ evaluated with $\boldsymbol{C_{f1}}$ (cf. (3.1.4), (3.1.5) and result on Step III) **b)** The first integral $\boldsymbol{G_f(Z_f, X_f, \gamma) = 0}$ evaluated with $\boldsymbol{C_{f3}}$ (cf. (3.1.4), (3.1.5) and result on Step III)

Solving equation $G_f(Z_f, X_f, \gamma; C_f = C_{fi}) = 0$ with respect to $X_f^2(Z_f, \gamma)$ and plotting all solutions $X_{fj}^2(Z_f, \gamma; C_{fi})(i = 1,3;\ j = 1,2,3)$ (for simplicity not given here) yields that only roots $X_{f1}^2(Z_f, \gamma; C_{f1})$ and $X_{f1}^2(Z_f, \gamma; C_{f3})$ are real and positive, hence these solutions have to be considered for evaluation of equation (3.1.12) (with $Z_f = Z(h)$). Rewriting (3.1.12) for each combination $\pm\sqrt{X_{f1}^2(Z(h), \gamma; C_{fi})}$ and $\pm\sqrt{X_{ci}^2(h+0)}$ $(i = 1,3)$ as follows

$$BC_{\pm,ci}^{\pm,C_{fi}} := \varepsilon_{xf}^{\left(\pm\sqrt{X_{f1}^2(Z(h),\gamma;C_{fi})}\right)^2} \cdot \left(\pm\sqrt{X_{f1}^2(Z(h), \gamma; C_{fi})}\right) - \\ -\varepsilon_{cf}^{\left(\pm\sqrt{X_{ci}^2(h+0)}\right)^2} \cdot \left(\pm\sqrt{X_{ci}^2(h+0)}\right) = 0, \qquad (i = 1,3) \tag{K.0.3}$$

where

$$\varepsilon_{xf}^{\left(\pm\sqrt{X_{f1}^2(Z(h),\gamma;C_{fi})}\right)^2} = \varepsilon_{1f} + a_f\left(\pm\sqrt{X_{f1}^2\big(Z(h),\gamma;C_{fi}\big)}\right)^2 + b_f Z^2(h),$$

$$\varepsilon_{cf}^{\left(\pm\sqrt{X_{ci}^2(h+0)}\right)^2} = \varepsilon_{1c} + a_c\left(\pm\sqrt{X_{ci}^2(h+0)}\right)^2 + b_c Z^2(h),$$

contour plots of (K.0.3) (see Figure K.6) show that only equations $BC_{+,c3}^{+,C_{f1}}$, $BC_{-,c3}^{-,C_{f1}}$, $BC_{+,c3}^{+,C_{f3}}$, and $BC_{-,c3}^{-,C_{f3}}$ are satisfied.

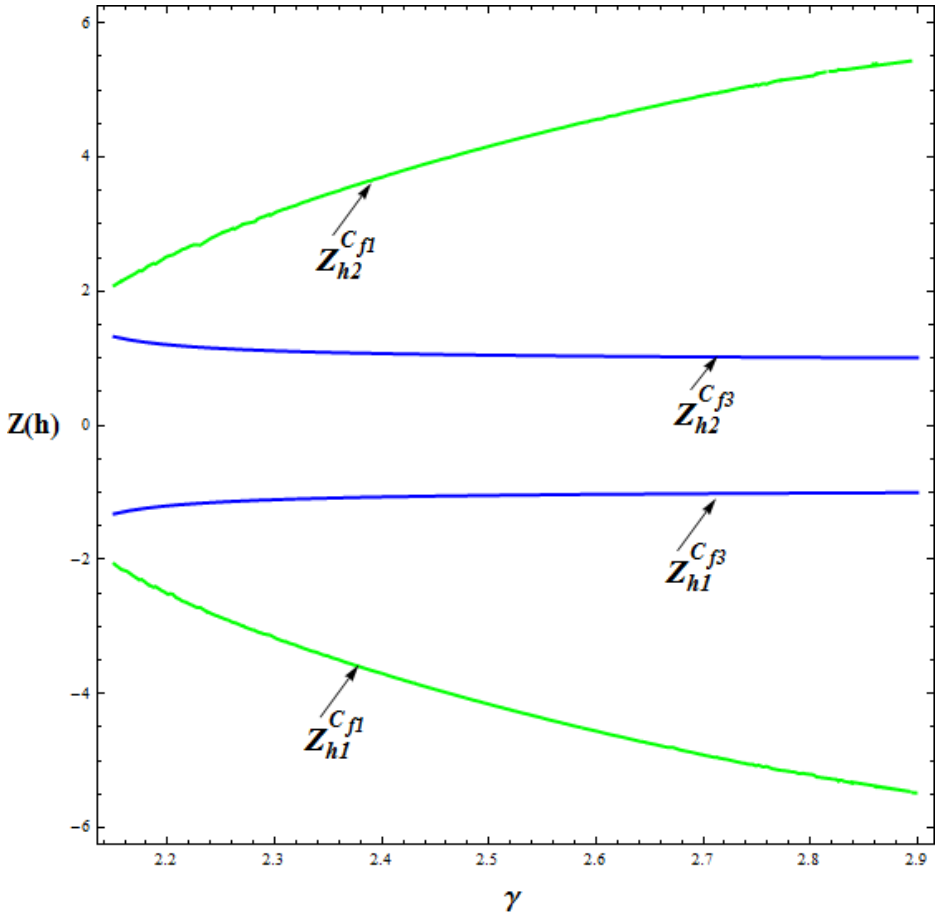

Figure K.6: Solutions $\boldsymbol{Z(h)}$ of equations (K.0.2)

Furthermore, equations $BC_{+,c3}^{+,C_{f1}}$, $BC_{-,c3}^{-,C_{f1}}$ have the same solutions $Z(h) = Z_{h1}^{C_{f1}}$, $Z(h) = Z_{h2}^{C_{f1}}$, analogously, equations $BC_{+,c3}^{+,C_{f3}}$, $BC_{-,c3}^{-,C_{f3}}$

have the same solutions $Z(h) = Z_{h1}^{C_{f3}}$, $Z(h) = Z_{h2}^{C_{f3}}$. Hence, taking into account (K.0.2) one obtains:

Solutions $X_f(0+0) = X_{f1}^{p1}$ and $X_f(0+0) = X_{f1}^{m1}$ lead to the same solutions $Z(h)$

- $Z(h) = Z_{h1}^{p,C_{f1}}$, where $Z_{h1}^{p,C_{f1}}$ is a solution of equation $BC_{+,c3}^{+,C_{f1}}$,
- $Z(h) = Z_{h1}^{m,C_{f1}}$, where $Z_{h1}^{m,C_{f1}}$ is a solution of equation $BC_{-,c3}^{-,C_{f1}}$,
- $Z(h) = Z_{h2}^{m,C_{f1}}$, where $Z_{h2}^{m,C_{f1}}$ is a solution of equation $BC_{-,c3}^{-,C_{f1}}$,
- $Z(h) = Z_{h2}^{p,C_{f1}}$, where $Z_{h2}^{p,C_{f1}}$ is a solution of equation $BC_{+,c3}^{+,C_{f1}}$.

Solutions $X_f(0+0) = X_{f1}^{p3}$ and $X_f(0+0) = X_{f1}^{m3}$ imply the same solutions $Z(h)$

- $Z(h) = Z_{h1}^{p,C_{f3}}$, where $Z_{h1}^{p,C_{f3}}$ is a solution of equation $BC_{+,c3}^{+,C_{f3}}$,
- $Z(h) = Z_{h1}^{m,C_{f3}}$, where $Z_{h1}^{m,C_{f3}}$ is a solution of equation $BC_{-,c3}^{-,C_{f3}}$,
- $Z(h) = Z_{h2}^{m,C_{f3}}$, where $Z_{h2}^{m,C_{f3}}$ is a solution of equation $BC_{-,c3}^{-,C_{f3}}$,
- $Z(h) = Z_{h2}^{p,C_{f3}}$, where $Z_{h2}^{p,C_{f3}}$ is a solution of equation $BC_{+,c3}^{+,C_{f3}}$.

The positions of the points $\left(Z_0 = Z(0), X_{f1}^{pi}\right)$, $\left(Z_0 = Z(0), X_{f1}^{mi}\right)$, $Z_{hk}^{sign,C_{fi}}$ $(sign = p, m; k = 1,2)$, $Z_*^{p,C_{fi}} = \sqrt{Z_{f*}^2}$, $Z_*^{m,C_{fi}} = -\sqrt{Z_{f*}^2}$ (here Z_{f*}^2 is real and positive solution of equation $G_f\left(Z_f, X_f = 0, \gamma\right) = 0$) and the roots $\pm\sqrt{X_{f1}^2\left(Z_f\right)} = \pm\sqrt{X_{f1}^2\left(Z_f, \gamma; C_{fi}\right)}$ on the curve $G_f\left(Z_f, X_f, \gamma; C_{fi}\right) = 0$ for fixed γ are shown in Figures K.7 and K.8 for $i = 1,3$, respectively.

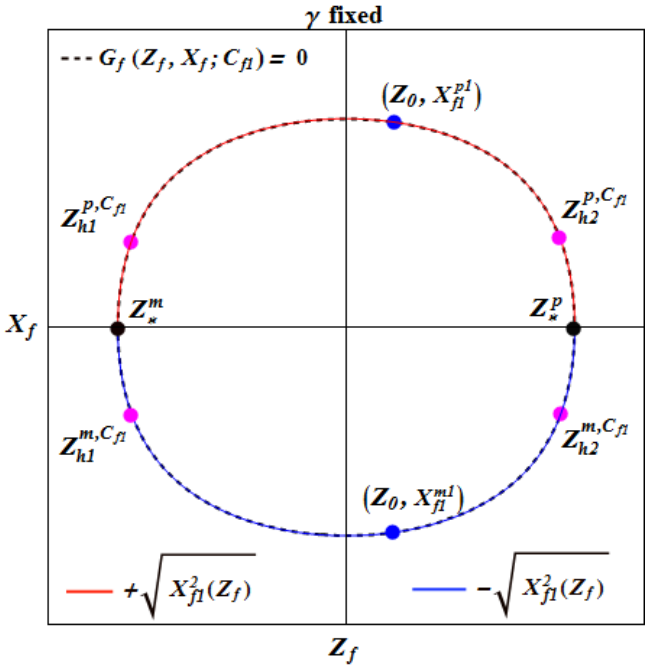

Figure K.7: The first integral $G_f(Z_f, X_f, \gamma = const; C_{f1}) = 0$ (black dashed curve) with the roots $\pm\sqrt{X_{f1}^2(Z_f)}$ (blue and red curves, respectively) and the solutions of equations (3.1.11) (blue points) and (3.1.12) (magenta points)

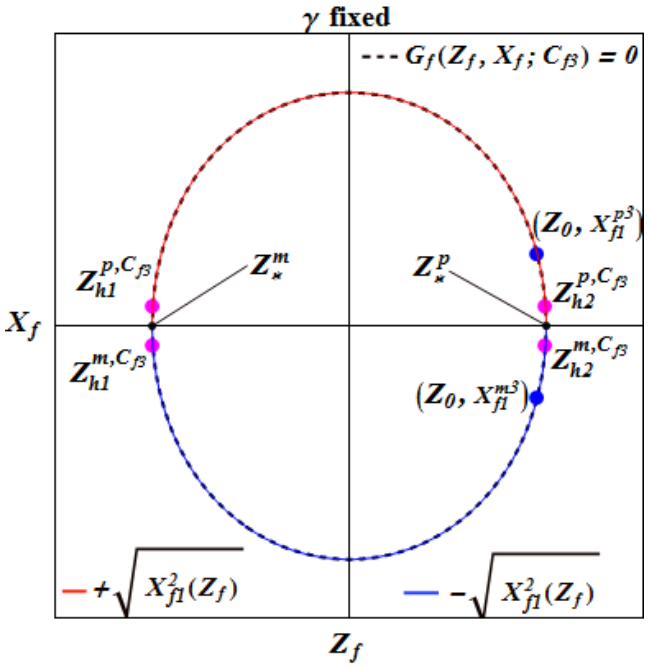

Figure K.8: The first integral $G_f(Z_f, X_f, \gamma = const; C_{f3}) = 0$ (black dashed curve) with the roots $\pm\sqrt{X_{f1}^2(Z_f)}$ (blue and red curves, respectively) and the solutions of equations (3.1.11) (blue points) and (3.1.12) (magenta points)

VII. Summing results of the foregoing steps there are four possibilities to evaluate the dispersion relation using the solutions $X_f(0+0)=\{X_{f1}^{p1}, X_{f1}^{m1}, X_{f1}^{p3}, X_{f1}^{m3}\}$. Each solution $X_f(0+0)$ leads to the two different sets of solutions for the dispersion relation as shown below for the case $X_f(0+0) = X_{f1}^{p1}$. Evaluation of the dispersion relation for the other solutions $X_f(0+0)$ proceeds analogously (results are shown in Figure 64 b), 65 a), 65 b) for X_{f1}^{m1}, X_{f1}^{p3}, and X_{f1}^{m3}, respectively).

Assuming $X_f(0+0) = X_{f1}^{p1}$, setting $X_f^2(Z_f,\gamma) = X_{f1}^2(Z_f,\gamma;C_{f1})$ in (3.1.9) (with $\nu = f$), taking into account (3.1.14), and choosing the integration path $\left(Z_0, Z_{hk}^{sign,C_{f1}}\right)$ $(sign = p,m; k = 1,2)$ (counterclockwise sense, cf. Figure K.7) for each fixed γ in the interval (K.0.1) one obtains

$$h_I = \int_{Z(0)}^{Z_{h1}^{p,C_{f1}}} F_{Z_f}^{+}(\zeta,\gamma)d\zeta, \qquad \text{(K.0.4)}$$

where the integrand function $F_{Z_f}^{+}(\zeta,\gamma)$ does not change its sign in $\left(Z_0, Z_{h1}^{p,C_{f1}}\right)$,

$$h_{II} = \int_{Z(0)}^{Z_*^m} F_{Z_f}^{+}(\zeta,\gamma)d\zeta + \int_{Z_*^m}^{Z_{h2}^{m,C_{f1}}} F_{Z_f}^{-}(\zeta,\gamma)d\zeta\,, \qquad \text{(K.0.5)}$$

where the integrand function $F_{Z_f}^{\pm}(\zeta,\gamma)$ changes sign in the interval $\left(Z_0, Z_{h2}^{m,C_{f1}}\right)$.

Numerical evaluation of (K.0.4)- (K.0.5) gives results shown in Figure 64 a) by the solid curves denoted as $TM_0^{(1)}$(the first even (fundamental) mode), $TM_1^{(1)}$ (the first odd mode), respectively. Thus, a combination of

X_{f1}^{p1}, $Z_{h1}^{p,C_{f1}}$ and $Z_{h2}^{m,C_{f1}}$ in (3.1.14), (3.1.20) yields the one set of periodic solutions of the dispersion relation (for given parameters).

$$h_{III} = \int_{Z(0)}^{Z_*^m} F_{Z_f}^{+}(\zeta,\gamma)d\zeta + \int_{Z_*^m}^{Z_{h1}^{m,C_{f1}}} F_{Z_f}^{-}(\zeta,\gamma)d\zeta\,, \qquad \text{(K.0.6)}$$

where the integrand function $F_{Z_f}^{\pm}(\zeta,\gamma)$ changes sign in the interval $\left(Z_0, Z_{h1}^{m,C_{f1}}\right)$,

$$h_{IV} = \int_{Z(0)}^{Z_*^m} F_{Z_f}^{+}(\zeta,\gamma)d\zeta + \int_{Z_*^m}^{Z_*^p} F_{Z_f}^{-}(\zeta,\gamma)d\zeta \int_{Z_*^p}^{Z_{h2}^{p,C_{f1}}} F_{Z_f}^{+}(\zeta,\gamma)d\zeta\,, \quad \text{(K.0.7)}$$

where the integrand function $F_{Z_f}^{\pm}(\zeta,\gamma)$ changes sign in $\left(Z_0, Z_{h2}^{p,C_{f1}}\right)$ twice.

Results of the numerical evaluation of (K.0.6)- (K.0.7) are shown in Figure 64 a) by the dashed curves denoted as $TM_1^{(2)}$(the first odd mode), $TM_2^{(2)}$ (the second even mode), respectively. Hence, a combination of X_{f1}^{p1}, $Z_{h1}^{m,C_{f1}}$ and $Z_{h2}^{p,C_{f1}}$ in (3.1.14), (3.1.20) yields the second set of periodic solutions of the dispersion relation (for given parameters).

According to equation (3.2.3) and to the evaluation of the dispersion relation according to (K.0.4) and (K.0.6) above the total power flow transported by the $TM_0^{(1)}$- and $TM_1^{(2)}$ wave through the nonlinear film bounded by nonlinear media can be written as follows

$$P_I^*\left(Z_{h1}^{p,C_{f1}}\right) = P_s^* + P_f^* + P_c^* =$$

$$= \int_0^{Z_0} P_{s1}^+(\zeta,\gamma)d\zeta + \int_{Z_0}^{Z_{h1}^{p,C_{f1}}} P_{f1}^+(\zeta,\gamma)d\zeta + \int_{Z_{h1}^{p,C_{f1}}}^{0} P_{c3}^+(\zeta,\gamma)\,d\zeta,$$

(K.0.8)

$$P_{III}^*\left(Z_{h1}^{m,C_{f1}}\right) = P_s^* + P_f^* + P_c^*$$

$$= \int_0^{Z_0} P_{s1}^+(\zeta,\gamma)d\zeta + \int_{Z_0}^{Z_*^m} P_{f1}^+(\zeta,\gamma)d\zeta + \int_{Z_*^m}^{Z_{h1}^{m,C_{f1}}} P_{f1}^-(\zeta,\gamma)d\zeta + \int_{Z_{h1}^{m,C_{f1}}}^{0} P_{c3}^-(\zeta,\gamma)\,d\zeta$$

(K.0.9)

where P_s^*, P_f^*, P_c^* denote the parts of the total power flow in the substrate, film and cladding, respectively, and

$$P_{s1}^+(Z_s,\gamma) = \frac{\varepsilon_{1s} + b_s\,Z_s^2 + a_s\,X_{s1}^2(Z_s,\gamma)}{\gamma^2 - \varepsilon_{1s} - b_s\,Z_s^2 - a_s\,X_{s1}^2(Z_s,\gamma)} \cdot \left(+\sqrt{X_{s1}^2(Z_s,\gamma)}\right),$$

(K.0.10)

$$P_{f1}^{\pm}(Z_f,\gamma) = \frac{\varepsilon_{1f} + b_f\,Z_f^2 + a_f\,X_{f1}^2(Z_f,\gamma)}{\gamma^2 - \varepsilon_{1f} - b_f\,Z_f^2 - a_f\,X_{f1}^2(Z_f,\gamma)} \cdot \left(\pm\sqrt{X_{f1}^2(Z_f,\gamma)}\right),$$

(K.0.11)

$$P_{c3}^{\pm}(Z_c,\gamma) = \frac{\varepsilon_{1c} + b_c\,Z_c^2 + a_c\,X_{c3}^2(Z_c,\gamma)}{\gamma^2 - \varepsilon_{1c} - b_c\,Z_c^2 - a_c\,X_{c3}^2(Z_c,\gamma)} \cdot \left(\pm\sqrt{X_{c3}^2(Z_c,\gamma)}\right).$$

(K.0.12)

Numerical evaluation of (K.0.8) and (K.0.9) leads to results presented in Figure 67 a) by the solid and dashed curves, respectively.

L. Integral equation for the function $Z(x)$

L.1 On the construction of the Green's function $G(x,y)$

Equation (5.1.4) can be rewritten as

$$LZ(x) = \tilde{f}(x), \quad (0 < x < h) \tag{L.1.1}$$

where

$$L \coloneqq \alpha_2 \frac{d^2}{dx^2} + \alpha_1 \tag{L.1.2}$$

with

$$\alpha_2 = 1 \tag{L.1.3}$$

and

$$\alpha_1 \coloneqq \hbar^2 = \frac{\varepsilon_2\,(\varepsilon_1 - \gamma^2)}{\varepsilon_1}, \tag{L.1.4}$$

$$\tilde{f}(x) = \frac{\gamma^2 - \varepsilon_1}{\varepsilon_1}\,\tilde{\varepsilon}_z\,Z(x) - \frac{\gamma}{\varepsilon_1}\,\frac{d}{dx}\big(\tilde{\varepsilon}_x\;X(x)\big). \tag{L.1.5}$$

Continuity of the function $Z(x)$ at the interfaces $x = 0$ and $x = h$ leads to

$$\begin{cases} Z(x)|_{x=0-0} = Z(x)|_{x=0+0} = Z(0), \\ Z(x)|_{x=h-0} = Z(x)|_{x=h+0} = Z(h). \end{cases} \tag{L.1.6}$$

According to [32] the Green's function $G(x,y)$ to the problem (L.1.1), (L.1.6) can be found as a solution of

$$LG(x,y) = 0, \quad \begin{pmatrix} 0 < x < y \\ y < x < h \end{pmatrix} \tag{L.1.7}$$

$$G(0,y) = G(h,y) = 0, \tag{L.1.8}$$

$G(x,y)$ continuous at $x = y$,

$$\left.\frac{dG(x,y)}{dx}\right|_{x=y+} - \left.\frac{dG(x,y)}{dx}\right|_{x=y-} = \alpha_2. \tag{L.1.9}$$

Using the well- known results[35] with assumptions $\gamma^2 < \varepsilon_1$ and $\hbar > 0$ the linear differential equation (L.1.7) has a solution

$$G(x,y) = \begin{cases} A\sin \hbar x + C\cos \hbar x\,, & 0 < x < y, \\ B\sin \hbar x + D\cos \hbar x\,, & y < x < h. \end{cases} \tag{L.1.10}$$

Applying the boundary conditions (L.1.8) to (L.1.10) implies

$$\begin{cases} A\sin 0 + C\cos 0 = 0, \\ B\sin \hbar h + D\cos \hbar h = 0, \end{cases}$$

hence

$$C = 0, \tag{L.1.11}$$

$$D = -\frac{B\sin \hbar h}{\cos \hbar h}. \tag{L.1.12}$$

Therefore, the Green's function has a form

$$G(x,y) = \begin{cases} A\,u_1(x), & 0 < x < y, \\ Bu_2(x), & y < x < h, \end{cases} \tag{L.1.13}$$

where

$$\begin{cases} u_1(x) = \sin \hbar x\,, \\ u_2(x) = \sin \hbar x - \dfrac{\sin \hbar h}{\cos \hbar h}\cos \hbar x. \end{cases} \tag{L.1.14}$$

Using continuity of the function $G(x,y)$ at $x = y$ in (L.1.3) yields

$$Au_1(y) - Bu_2(y) = 0, \tag{L.1.15}$$

Applying (L.1.9) to the function $G(x,y)$ (cf. (L.1.13)) implies

$$-A\,u_1'(y) + Bu_2'(y) = 1. \tag{L.1.16}$$

Solutions $u_1(x)$ and $u_2(x)$ of system (L.1 15- 16) are independent because the Wronskian of $u_1(y)$ and $u_2(y)$ does not vanish if $\hbar h \neq \pi\, l,\ l = 1,2,\ldots$[38]:

$$W\big(u_1(y), u_2(y)\big) = u_1(y)u_2'(y) - u_2(y)u_1'(y), \tag{L.1.17}$$

$$W\big(u_1(y), u_2(y)\big) = \hbar \sin \hbar y \left(\cos \hbar y + \frac{\sin \hbar h}{\cos \hbar h} \sin \hbar y\right) -$$

$$-\hbar \left(\sin \hbar y - \frac{\sin \hbar h}{\cos \hbar h} \cos \hbar y\right) \cos \hbar y = \frac{\hbar \sin \hbar h}{\cos \hbar h}.$$

Hence, the coefficients A and B can be obtained as

$$A = \frac{u_2(y)}{W\big(u_1(y), u_2(y)\big)} = \left(\sin \hbar y - \frac{\sin \hbar h}{\cos \hbar h} \cos \hbar y\right) \frac{\cos \hbar h}{\hbar \sin \hbar h} =$$

$$= \frac{\sin \hbar(y-h)}{\hbar \sin \hbar h},$$

$$B = \frac{u_1(y)}{W\big(u_1(y), u_2(y)\big)} = \frac{\sin \hbar y \cos \hbar h}{\hbar \sin \hbar h},$$

and hence, the Green's function corresponding to (5.1.4) has a following form

$$G(x,y) = \begin{cases} \dfrac{\sin \hbar(y-h) \sin \hbar x}{\hbar \sin \hbar h}, & 0 < x < y, \\ \dfrac{\sin \hbar(x-h) \sin \hbar y}{\hbar \sin \hbar h}, & y < x < h. \end{cases} \tag{L.1.18}$$

L.2 On the integral equation for the function $Z(x)$

As prescribed in Appendix L.1 equation (5.1.4) can be presented as

$$LZ(x) = \tilde{f}(x), \quad (0 < x < h) \tag{L.2.1}$$

where the solution $Z(x)$ satisfies the boundary conditions

$$\begin{cases} Z(x)|_{x=0-0} = Z(x)|_{x=0+0} = Z(0), \\ Z(x)|_{x=h-0} = Z(x)|_{x=h+0} = Z(h). \end{cases} \tag{L.2.2}$$

The boundary value problem (L.1.7) – (L.1.9) associated to the system (L.2.1), (L.2.2) can be rewritten as[32]

$$LG(x,y) = \delta(x-y), \quad \begin{pmatrix} 0 < x < y \\ y < x < h \end{pmatrix} \tag{L.2.3}$$

$$G(0,y) = G(h,y) = 0. \tag{L.2.4}$$

Multiplying (L.2.1) by $G(x,y)$ and (L.2.3) by $(-Z(x))$one obtains

$$G(x,y)LZ(x) = G(x,y)\tilde{f}(x), \tag{L.2.5}$$

$$-Z(x)LG(x,y) = -Z(x)\delta(x-y). \tag{L.2.6}$$

Adding equations (L.2.5), (L.2.6) and integrating leads to

$$\int_0^h dy\big(G(x,y)LZ(y) - Z(y)LG(x,y)\big) = \int_0^h dy\left(G(x,y)\tilde{f}(y) - Z(y)\delta(x-y)\right). \tag{L.2.7}$$

On the other hand, applying to the left-hand side of (L.2.7) the second Green's formula[32] gives

$$\int_0^h dy\big(G(x,y)LZ(y) - Z(y)LG(x,y)\big) = \left(G(x,y)\frac{dZ(y)}{dy} - Z(y)\frac{\partial G(x,y)}{\partial y}\right)\Big|_{y=0}^{h}. \tag{L.2.8}$$

Combining equations (L.2.7) and (L.2.8) implies

$$\int_0^h dy\left(G(x,y)\tilde{f}(y) - Z(y)\delta(x-y)\right) = \left(G(x,y)\frac{dZ(y)}{dy} - Z(y)\frac{\partial G(x,y)}{\partial y}\right)\Big|_{y=0}^{y=h}. \tag{L.2.9}$$

According to (L.1.17) the derivative of the Green's function with respect to y is given as

$$\frac{\partial G(x,y)}{\partial y} = \begin{cases} \dfrac{\cos \hbar(y-h)\sin \hbar x}{\sin \hbar h}, & 0 < x < y, \\ \dfrac{\sin \hbar(x-h)\cos \hbar y}{\sin \hbar h}, & y < x < h, \end{cases} \tag{L.2.10}$$

hence,

$$\begin{cases} \left.\dfrac{\partial G(x,y)}{\partial y}\right|_{y=h} = \dfrac{\sin \kappa x}{\sin \kappa h}, \\ \left.\dfrac{\partial G(x,y)}{\partial y}\right|_{y=0} = \dfrac{\sin \kappa (x-h)}{\sin \kappa h}. \end{cases} \tag{L.2.11}$$

Using the well- known properties of the delta function and the condition

$$G(x,0) = G(x,h) = 0 \tag{L.2.12}$$

(L.2.9) reads

$$\begin{aligned} \int_0^h G(x,y)\tilde{f}(y)dy - Z(x) &= Z(0)\left.\frac{\partial G(x,y)}{\partial y}\right|_{y=0} - Z(h)\left.\frac{\partial G(x,y)}{\partial y}\right|_{y=h} = \\ &= Z(0)\frac{\sin \kappa (x-h)}{\sin \kappa h} - Z(h)\frac{\sin \kappa x}{\sin \kappa h} = \\ &= \frac{Z(0)\cos \kappa h - Z(h)}{\sin \kappa h}\sin \kappa x - Z(0)\cos \kappa x. \end{aligned} \tag{L.2.13}$$

Therefore, the solution of (5.1.4) can be presented as follows

$$\begin{aligned} Z(x) = Z_0(x) + \int_0^h G(x,y)\tilde{f}(y)dy = Z_0(x) - \\ -\frac{(\varepsilon_1 - \gamma^2)}{\varepsilon_1}\int_0^h G(x,y)\,\tilde{\varepsilon}_z(y)Z(y)dy - \frac{\gamma}{\varepsilon_1}\int_0^h G(x,y)\left(\tilde{\varepsilon}_x(y)X(y)\right)'dy, \end{aligned} \tag{L.2.14}$$

where

$$Z_0(x) = Z(0)\cos \kappa x + \frac{Z(h) - Z(0)\cos \kappa h}{\sin \kappa h}. \tag{L.2.15}$$

M On the evaluation of the solution $Z(h)$

Equation (5.1.10) can be rewritten as follows

$$\frac{\varepsilon_x\, X(x)}{\gamma} = \frac{\varepsilon_1}{(\gamma^2-\varepsilon_1)}\,\frac{dZ_0(x)}{dx} + \\ + \int_0^h \frac{\partial G(x,y)}{\partial x}\,\tilde{\varepsilon}_z(y)Z(y)dy + \frac{\gamma}{(\gamma^2-\varepsilon_1)}\int_0^h \frac{\partial^2 G(x,y)}{\partial y \partial x}\,\tilde{\varepsilon}_x(y)X(y)dy. \tag{M.0.1}$$

Setting in (M.0.1) $x = 0+0$ and comparing the result equation with the boundary condition (5.2.2) yields

$$\frac{\varepsilon_s\, Z(0)}{\sqrt{\gamma^2-\varepsilon_s}} = \frac{\varepsilon_1}{(\gamma^2-\varepsilon_1)}\left(\frac{dZ_0(x)}{dx}\right)\Big|_{x=0} + \\ + \int_0^h \frac{\sin \kappa(y-h)}{\sin \kappa h}\,\tilde{\varepsilon}_z(y)Z(y)dy + \frac{\gamma}{(\gamma^2-\varepsilon_1)}\int_0^h \frac{\kappa \cos \kappa(y-h)}{\sin \kappa h}\,\tilde{\varepsilon}_x(y)X(y)dy. \tag{M.0.2}$$

Using (5.1.6) in (M.0.2) leads to

$$\frac{\varepsilon_s\, Z(0)}{\sqrt{\gamma^2-\varepsilon_s}} = \frac{\varepsilon_1 \kappa}{(\gamma^2-\varepsilon_1)\ \sin \kappa h}\ Z(h) - \frac{\varepsilon_1\, \kappa \cos \kappa h}{(\gamma^2-\varepsilon_1)\ \sin \kappa h}\ Z(0) + \\ + \int_0^h \frac{\sin \kappa(y-h)}{\sin \kappa h}\,\tilde{\varepsilon}_z(y)Z(y)dy + \frac{\gamma}{(\gamma^2-\varepsilon_1)}\int_0^h \frac{\kappa \cos \kappa(y-h)}{\sin \kappa h}\,\tilde{\varepsilon}_x(y)X(y)dy. \tag{M.0.3}$$

Solving (M.0.3) with respect to $Z(h)$ one obtains

$$Z(h) = \ Z(0)\ \left(\cos \kappa h - \frac{\varepsilon_1-\gamma^2}{\varepsilon_1}\ \frac{\varepsilon_s}{\sqrt{\gamma^2-\varepsilon_s}}\ \frac{\sin \kappa h}{\kappa}\right) + \\ + \frac{\varepsilon_1-\gamma^2}{\varepsilon_1\ \kappa}\ \int_0^h \sin \kappa(y-h)\ \tilde{\varepsilon}_z(y)Z(y)dy - \frac{\gamma}{\varepsilon_1}\ \int_0^h \cos \kappa(y-h)\ \tilde{\varepsilon}_x(y)X(y)dy.$$

The coefficient of $Z(0)$ can be simplified by using (5.1.7)

$$cos\,\hbar h - \frac{\varepsilon_1 - \gamma^2}{\varepsilon_1}\,\frac{\varepsilon_s}{\sqrt{\gamma^2 - \varepsilon_s}}\,\frac{sin\,\hbar h}{\hbar} =$$

$$= cos\,\hbar h - \frac{\varepsilon_1 - \gamma^2}{\varepsilon_1}\,\frac{\varepsilon_s}{\sqrt{\gamma^2 - \varepsilon_s}}\sqrt{\frac{\varepsilon_2(\varepsilon_1 - \gamma^2)}{\varepsilon_1}}\,sin\,\hbar h =$$

$$= cos\,\hbar h \;-\; \varepsilon_s\sqrt{\frac{(\varepsilon_1 - \gamma^2)}{\varepsilon_1\varepsilon_2\,(\gamma^2 - \varepsilon_s)}}\;sin\,\hbar h = \cos\hbar h + \beta\,sin\,\hbar h,$$

where

$$\beta = -\varepsilon_s\sqrt{\frac{\varepsilon_1 - \gamma^2}{\varepsilon_1\,\varepsilon_2\,(\gamma^2 - \varepsilon_s)}}$$

is given by (C.1.5) if $\varepsilon_{1s} = \varepsilon_{2s} = \varepsilon_s, \varepsilon_{1f} = \varepsilon_1, \varepsilon_{2f} = \varepsilon_2$.

Hence, the equation for the $Z(h)$ can be written as

$$Z(h) = Z_{lin}(h) + \frac{\varepsilon_1 - \gamma^2}{\varepsilon_1\hbar}\int_0^h sin\,\hbar(y-h)\,\tilde{\varepsilon}_z(y)Z(y)dy -$$

$$-\frac{\gamma}{\varepsilon_1}\int_0^h cos\,\hbar(y-h)\,\tilde{\varepsilon}_x(y)X(y)dy, \tag{M.0.4}$$

where

$$Z_{lin}(h) = Z(0)(\cos\hbar h + \beta\,sin\,\hbar h) \tag{M.0.6}$$

is a solution of the linear problem ($a = b = 0, \varepsilon_{1s} = \varepsilon_{2s} = \varepsilon_s, \varepsilon_{1f} = \varepsilon_1$, $\varepsilon_{2f} = \varepsilon_2, f(x) = 0$) in $x = h$ (cf. (C.1.4)).

N On the application of the Banach theorem

N.1 The Banach fixed- point theorem[33]

The Banach fixed- point theorem represents a fundamental convergence theorem for a broad class of iteration methods.

The problem is to solve the operator equation

$$u = Au, \quad u \in M, \tag{N.1.1}$$

by means of the iteration method:

$$u_{n+1} = Au_n, \quad n = 0,1, \dots, \tag{N.1.2}$$

where $u_n \in M$. Each solution of ((N.1.1) is called a fixed point of the operator A.

Theorem (The fixed- point theorem of Banach)

Assuming that:

(a)M is a closed nonempty set in the Banach space X over $\mathbb{K}$, and

(b) the operator $A: M \to M$ is k- contractive, i.e., by definition,

$$\|Au - Av\| \leq k\|u - v\| \quad \text{for all } u, v \in M, \tag{N.1.3}$$

and fixed $k, 0 \leq k < 1$.

Then, the following is valid

(i) **Existence and uniqueness.** The original equation (N.1.1) has exactly one solution u, i.e., the operator A has exactly one fixed point u on the set M.

(ii) **Convergence of the iteration method.** For each given $u_0 \in M$, the sequence (u_n) constructed by (N.1.2) converges to the unique solution u of equation (N.1.1).

(iii) **Error estimates.** For all $n = 0,1,...$ one obtains the so- called a priori error estimate

$$\|u_n - u\| \leq k^n(1-k)^{-1}\|u_1 - u_0\|, \qquad \text{(N.1.4)}$$

and the so- called a posterior error estimate

$$\|u_{n+1} - u\| \leq k(1-k)^{-1}\|u_{n+1} - u_n\|. \qquad \text{(N.1.5)}$$

(iv) **Rate of convergence.** For all $n = 0,1,...$

$$\|u_{n+1} - u\| \leq k\|u_n - u\| \qquad \text{(N.1.6)}$$

holds.

This theorem was proved by Banach in 1920. It is called the Banach fixed- point theorem or the contraction principle.

N.2 Application of the Banach fixed-point theorem [31, 39]

The Banach vector space $(C[0,h])^2$ of continuous complex- valued functions $\vec{v}(x)$ on the segment $[0,h]$ with the norm

$$\|\vec{v}\| := \|v_1\| + \|v_2\|, \quad \vec{v} = col(v_1, v_2), \quad \|v_j\| = \max_{x\in[0,h]}|v_j(x)|, \quad j = 1,2 \qquad \text{(N.2.1)}$$

is considered in the following.

Equation (5.3.1) reads

$$\vec{v}(x) = \vec{v}_0(x) + \int_0^h M(\vec{v})\,(y)\vec{v}(y)dy + L(\vec{v})(x). \qquad \text{(N.2.2)}$$

The estimate of (N.2.2) implies

$$\|\vec{v}\| \leq I_0 + \max(|m_{11}| + |m_{21}|; |m_{12}| + |m_{22}|)\,\|\vec{v}\|, \qquad \text{(N.2.3)}$$

where

$$I_0 = \|Z_0(x)\| + \frac{|\gamma|\,\varepsilon_1}{(\varepsilon_1 - \gamma^2)\,(\varepsilon_1 - f_0)}\left\|\frac{dZ_0(x)}{dx}\right\| \qquad \text{(N.2.4)}$$

and the values m_{ij} $(i,j = 1,2)$ can be estimated as (cf. (5.3.3))

$$|\, m_{11}| \leq \frac{\varepsilon_1 - \gamma^2}{\varepsilon_1}\ (f_0 + a\ \|Z\|^2 + b\ \|X\|^2)\ \max_{x\in[0,h]} \int_0^h |G(x,y)|dy$$

$$\leq \frac{\varepsilon_1 - \gamma^2}{8\ \varepsilon_1}\ \frac{\hbar h^3}{|sin\hbar h|}\ (f_0 + a_0\|\vec{v}\|^2), \tag{N.2.5}$$

$$|\, m_{21}| \leq \frac{|\gamma|}{\varepsilon_1}\ (f_0 + a\ \|Z\|^2 + b\ \|X\|^2)\ \max_{x\in[0,h]} \int_0^h \left|\frac{\partial G(x,y)}{\partial x}\right| dy$$

$$\leq \frac{|\gamma|}{2\ (\varepsilon_1 - f_0)}\ \frac{\hbar h^2}{|sin\hbar h|}\ (f_0 + a_0\|\vec{v}\|^2), \tag{N.2.6}$$

$$|m_{12}| \leq \frac{|\gamma|}{\varepsilon_1}\ (f_0 + a\ \|Z\|^2 + b\ \|X\|^2)\ \max_{x\in[0,h]} \int_0^h \left|\frac{\partial G(x,y)}{\partial y}\right| dy$$

$$\leq \frac{|\gamma|}{2\ \varepsilon_1}\ \frac{\hbar h^2}{|sin\hbar h|}\ (f_0 + a_0\|\vec{v}\|^2), \tag{N.2.7}$$

$$|m_{22}| \leq \frac{\gamma^2}{|\varepsilon_1 - \gamma^2|(\varepsilon_1 - f_0)}\ (f_0 + a\ \|Z\|^2 + b\ \|X\|^2)\ \max_{x\in[0,h]} \int_0^h \left|\frac{\partial^2 G(x,y)}{\partial y \partial x}\right| dy$$

$$\leq \frac{\gamma^2}{(\varepsilon_1 - \gamma^2)(\varepsilon_1 - f_0)}\ \frac{\hbar h}{|sin\hbar h|}\ (f_0 + a_0\|\vec{v}\|^2), \tag{N.2.8}$$

where

$$f_0 = max|f(x)| \tag{N.2.9}$$

and

$$a_0 = max(a\ , b). \tag{N.2.10}$$

Combining (N.2.3), (N.2.4)- (N.2.8) one obtains

$$\|\vec{v}\| \leq I_0 + b_0(f_0 + a_0\|\vec{v}\|^2)\|\vec{v}\|, \tag{N.2.11}$$

where

$$b_0 = \frac{\hbar\ h}{2\ |\sin \hbar h|}\ max\left\{\frac{h^2\ (\varepsilon_1 - \gamma^2)}{4\ \varepsilon_1} + \frac{h\ |\gamma|}{\varepsilon_1 - f_0}\ ;\ \frac{h\ |\gamma|}{\varepsilon_1} + \frac{2\ \gamma^2}{(\varepsilon_1 - \gamma^2)\ (\varepsilon_1 - f_0)}\right\}. \tag{N.2.12}$$

Denoting

$$F(\vec{v}) \coloneqq \vec{v}_0(x) + \int_0^h M(\vec{v})\,(y)\vec{v}(y)dy + L(\vec{v})(x) \qquad \text{(N.2.13)}$$

equation (N.2.2) can be rewritten in operator form as

$$\vec{v}(y) = F(\vec{v})(y). \qquad \text{(N.2.14)}$$

To solve the operator equation (N.2.14) with the help of the Banach- fixed point theorem it must be proofed at first that operator F maps the ball

$$B_R(0) = \{\vec{v}(x) \in (C[0,h])^2,\ \ \|\vec{v}\| \le R\} \qquad \text{(N.2.15)}$$

to itself.

Since (N.2.11) is satisfied, the condition $\vec{v} \in B_R(0)$ implies the inequality

$$g(R) \le 0, \qquad \text{(N.2.16)}$$

where

$$g(R) = a_0 b_0 R^3 - (1 - b_0 f_0)R + I_0. \qquad \text{(N.2.17)}$$

The polynomial $g(R)$ has three real roots if its discriminant is positive or equal to zero

$$D_{g(R)} \coloneqq a_0 b_0(-4(1 - b_0 f_0)^3 - 27 a_0 b_0 I_0^2) \ge 0. \qquad \text{(N.2.18)}$$

From (N.2.18) it follows

$$I_0^2 \le \frac{4(1 - b_0 f_0)^3}{27 a_0 b_0}, \qquad \text{(N.2.19)}$$

and hence,

$$1 - b_0 f_0 > 0. \qquad \text{(N.2.20)}$$

If (N.2.20) is satisfied, equation (N.2.18) has two positive ($R_{min} \le R_{max}$) roots and one negative root[40], i.e., the radius R of the ball $B_R(0)$ must satisfy the condition

$$0 < R_{min} \le R \le R_{max}. \qquad \text{(N.2.21)}$$

Choosing radius R according to (N.2.21) (i.e., equation (N.2.14) has at least one solution inside $B_R(0)$) the contraction operator F is estimated as follows.

Considering

$$F(\vec{v}_1) - F(\vec{v}_2) = \int_0^h \big(M(\vec{v}_1)\vec{v}_1(y) - M(\vec{v}_2)\vec{v}_2(y)\big)dy + L(\vec{v}_1) - L(\vec{v}_2) =$$

$$= \int_0^h M(\vec{v}_1)\big(\vec{v}_1(y) - \vec{v}_2(y)\big)dy +$$

$$+ \int_0^h \big(M(\vec{v}_1) - M(\vec{v}_2)\big)\vec{v}_2(y)dy + L(\vec{v}_1) - L(\vec{v}_2) \tag{N.2.22}$$

one obtains

$$\|F(\vec{v}_1) - F(\vec{v}_2)\| \le \|I_1\| + \|I_2\| + \|I_3\|, \tag{N.2.23}$$

where I_1, I_2 correspond to the integral part of operator F, and I_3 corresponds to the nonlinear part L of operator F. The following estimations hold:

$$\|I_1\| \le max\{|m_{11}(\vec{v}_1)| + |m_{21}(\vec{v}_1)|; |\, m_{12}(\vec{v}_1)| + |m_{22}(\vec{v}_1)|\}\,\|\vec{v}_1 - \vec{v}_2\|$$

$$\le b_0(f_0 + a_0R^2)\|\vec{v}_1 - \vec{v}_2\|, \tag{N.2.24}$$

$$\|I_2\| \le \frac{\varepsilon_1 - \gamma^2}{\varepsilon_1} \cdot \frac{\not{k}h^3}{8|\sin \not{k}\mathrm{h}|} \cdot\ 2a_0R \cdot \|\vec{v}_1 - \vec{v}_2\| \cdot \|Z_2\| +$$

$$+ \frac{|\gamma|\not{k}h^2}{2|\sin \not{k}h|} \cdot \left[\frac{2a_0R(\varepsilon_1 + 2f_0)}{(\varepsilon_1 - f_0)^2} + \frac{2R^3|a^2 - b^2|}{(\varepsilon_1 - f_0)^2}\right] \cdot \|\vec{v}_1 - \vec{v}_2\| \cdot \|Z_2\| +$$

$$+ \frac{|\gamma|}{\varepsilon_1} \cdot \frac{\not{k}h^2}{2|\sin \not{k}h|} \cdot 2a_0R \cdot \|\vec{v}_1 - \vec{v}_2\| \cdot \|X_2\| +$$

$$+ \frac{\gamma^2\varepsilon_1}{\varepsilon_1 - \gamma^2} \cdot \frac{\not{k}h}{|\sin \not{k}h|} \cdot \frac{2a_0R}{(\varepsilon_1 - f_0)^2} \cdot \|\vec{v}_1 - \vec{v}_2\| \cdot \|X_2\|$$

$$\le \left[\frac{\varepsilon_1 - \gamma^2}{\varepsilon_1} \cdot \frac{\not{k}h^3R^2}{4|\sin \not{k}\mathrm{h}|} + \frac{|\gamma|\not{k}h^2}{|\sin \not{k}h|} \cdot \left(\frac{a_0R^2(\varepsilon_1 + 2f_0) + R^4|a^2 - b^2|}{(\varepsilon_1 - f_0)^2}\right) +\right.$$

$$\left. + \frac{|\gamma|}{\varepsilon_1} \cdot \frac{\not{k}h^2}{|\sin \not{k}h|} \cdot a_0R^2 + \frac{\gamma^2\varepsilon_1}{\varepsilon_1 - \gamma^2} \cdot \frac{\not{k}h}{|\sin \not{k}h|} \cdot \frac{2a_0R^2}{(\varepsilon_1 - f_0)^2}\right] \cdot \|\vec{v}_1 - \vec{v}_2\|$$

$$\le \left[\frac{(\varepsilon_1 - \gamma^2)h^2}{4\varepsilon_1} + \frac{a_0h|\gamma|(\varepsilon_1 + 2f_0)}{(\varepsilon_1 - f_0)^2} + \frac{h|\gamma|R^2|a^2 - b^2|}{(\varepsilon_1 - f_0)^2} + \frac{a_0h|\gamma|}{\varepsilon_1} +\right.$$

$$\left. + \frac{2a_0\varepsilon_1\gamma^2}{(\varepsilon_1 - \gamma^2)(\varepsilon_1 - f_0)^2}\right] \cdot \frac{\not{k}hR^2}{|\sin \not{k}h|} \cdot \|\vec{v}_1 - \vec{v}_2\|, \tag{N.2.25}$$

and

$$\| I_3\| \leq \frac{\varepsilon_1|\gamma|}{\varepsilon_1-\gamma^2}\left\|\frac{dZ_0(x)}{dx}\right\|\cdot\left\|\frac{1}{\varepsilon_x(X_1,Z_1)}-\frac{1}{\varepsilon_x(X_2,Z_2)}\right\| =$$

$$= \frac{\varepsilon_1|\gamma|}{\varepsilon_1-\gamma^2}\left\|\frac{dZ_0(x)}{dx}\right\|\cdot\left\|\frac{\varepsilon_x(X_2,Z_2)-\varepsilon_x(X_1,Z_1)}{\varepsilon_x(X_1,Z_1)\cdot\varepsilon_x(X_2,Z_2)}\right\|$$

$$\leq \frac{\varepsilon_1|\gamma|}{\varepsilon_1-\gamma^2}\left\|\frac{dZ_0(x)}{dx}\right\|\cdot\frac{\|a(X_1^2-X_2^2)+b(Z_1^2-Z_2^2)\|}{(\varepsilon_1-f_0)^2}$$

$$\leq \frac{\varepsilon_1|\gamma|}{\varepsilon_1-\gamma^2}\left\|\frac{dZ_0(x)}{dx}\right\|\cdot\frac{a\|X_1-X_2\|\|X_1+X_2\|+b\|Z_1-Z_2\|\|Z_1+Z_2\|}{(\varepsilon_1-f_0)^2}$$

$$\leq \frac{\varepsilon_1|\gamma|}{\varepsilon_1-\gamma^2}\left\|\frac{dZ_0(x)}{dx}\right\|\cdot\frac{2aR\,\|X_1-X_2\|+2bR\|Z_1-Z_2\|}{(\varepsilon_1-f_0)^2}$$

$$\leq \frac{\varepsilon_1|\gamma|}{\varepsilon_1-\gamma^2}\cdot\frac{2a_0R\,\|\vec{v}_1-\vec{v}_2\|}{(\varepsilon_1-f_0)^2}\cdot\left\|\frac{dZ_0(x)}{dx}\right\|. \qquad \text{(N.2.26)}$$

Combining (N.2.24)- (N.2.26) and using (N.2.12) leads to

$$\|F(\vec{v}_1)-F(\vec{v}_2)\| \leq q\|\vec{v}_1-\vec{v}_2\|, \qquad \text{(N.2.27)}$$

where

$$q = \frac{2a_0R\,\varepsilon_1|\gamma|}{(\varepsilon_1-\gamma^2)\,(\varepsilon_1-f_0)^2}\left\|\frac{dZ_0(x)}{dx}\right\| + b_0(f_0+a_0R^2) + \frac{\hbar hR^2}{|\sin\hbar h|}\times$$

$$\times\left[\frac{\varepsilon_1-\gamma^2}{\varepsilon_1}\cdot\frac{h^2}{4}+h|\gamma|\cdot\frac{a_0(\varepsilon_1+2f_0)+R^2|a^2-b^2|}{(\varepsilon_1-f_0)^2}+\right.$$

$$\left.+\frac{a_0|\gamma|h}{\varepsilon_1}+\frac{2a_0\varepsilon_1\gamma^2}{(\varepsilon_1-\gamma^2)(\varepsilon_1-f_0)^2}\right]. \qquad \text{(N.2.28)}$$

If the condition

$$q<1 \qquad \text{(N.2.29)}$$

holds, the operator F is contractive, and hence, the iteration sequence (5.3.4), rewritten here as

$$\vec{v}_j(x)=\vec{v}_0(x)+\int_0^h M\left(\vec{v}_{j-1}\right)(y)\vec{v}_{j-1}(y)dy+L\left(\vec{v}_{j-1}\right)(x), \qquad j=1,2,\ldots \qquad \text{(N.2.30)}$$

converges to the unique solution $\vec{v}(x)$ of equation (N.2.14).

References

Section 1:

[1] Michael Bass et. al., "Handbook of Optics", Vol. II, New York (2010), pp. 6.2- 6

[2] Bahaa E. A. Saleh, Malvin Carl Teich, "Grundlagen der Photonik", Wiley- VCH Verlag GmbH & Co. KGaA (2008), p. 346

[3] Guenther Robert D., "Encyclopedia of modern optics", Amsterdam (2005), Vol. 1, p. 470

[4] Publications by Smirnov, Valovik [21, 25, 27- 8, Table 3] and Rukhlenko et. a1. [29- 30, Table 3] are similar to the present dissertation thematically and partly methodically. Nevertheless, there are important differences.
Procedure of a reduction of Maxwell's equations to a system of two nonlinear differential equations together with normalization and introducing of new variables is the same in the papers of Smirnov, Valovik as well as in the present work. But the analysis leading to an exact dispersion relation has been provided in different ways (next introducing of new variables have been proposed in [21, 25, 27- 8]). Furthermore, more details have been taken into account in the present work:

- Geometry of the problem in the present work (Kerr- nonlinear tensorial dielectric permittivity in all three media) is more general than that considered by Smirnov, Valovik (Kerr- nonlinear isotropic film bounded by the linear media) and Rukhlenko et. a1. (Kerr- nonlinear isotropic film bounded by the metalic media).
- There are no restrictions to the nonlinearity coefficients a, b in the present dissertation − the particular case $a = b$ such that $a > 0$ has been discussed in [21, 25, 27].

- The total power flow carried by the nonlinear TM- wave is derived in this work but hasn't been examined in [21, 25, 27-30].

Section 2:

[5] The ansatz (2.1) with $\omega = \omega_0$ follows from the assumption that the time-dependence of the optical response of the nonlinear medium is described by one frequency ω_0. For example, in absence of phase matching the small amplitudes of higher harmonics can be neglected[6].

[6] Serov V. S., Schürmann H. W., „Reflection and transmission of a plane TE-wave at a lossy, saturating nonlinear dielectric film", in "Nonlinear optics" edited by Kamanina N. V., InTexOpen (2012), ISBN: 979-953-307-375-9

[7] This is an approximate representation of the dielectric function. Considering the dipole moment per unit volume it is difficult to control the permittivity by the electric (macroscopic) field at the point y, because the medium reacts with delay. Moreover, the response of the medium is not local in space. These facts are not taken into account by modeling of the permittivity (2.5). However, experimental measurements show that the representation of the dielectric function as (2.5) has physical significance[6].

[8] Boardman A. D., Maradudin A. A., Stegeman G. I., Twardowski T. and Wright E. M., "Exact theory of nonlinear p- polarized optical waves", Physical Review A (1987), Vol. 35, No. 3, pp. 1159- 1164

[9] The diagonal element of the dielectric tensor ε_{yv} $(v = s, f, c)$ has not to be taken into account due to the geometry of the problem.

Section 3:

[10] Hubbard J. H., West B. H., "Differential equations, a dynamical systems approach, Part *I*", New York (1991), pp. 85-87

[11] Joseph R. I. and D. N. Christodoulides, "Exact field decomposition for TM-waves in nonlinear media", Optics Letters (1987), Vol. 12, No.10, pp. 826- 828

[12] Markuse D., "Theory of dielectric optical waveguides", San Diego (1991), pp. 14- 17

[13] Yeh Pochi, "Optical Waves in Layered Media", Wiley, New York (1988), pp. 313- 314

[14] It seems remarkable that $Z(0)$ appears as the third argument in the functions $X_\nu(x,\gamma,\dots)$ $(\nu = s,f,c)$ in equations (3.1.11), (3.1.12). If $x_0 = 0$ or $x_0 = h$ the functions $X_\nu(x_0)$ depend on $Z(0)$. Thus the dependence on $Z(0)$ has been indicated as the third argument of the functions $X_\nu(x,\gamma,\dots)$ in (3.1.11) and (3.1.12).

[15] Choosing $Z(0) = 0$ and $C_f = 0$ leads to the particular solutions of (2.11) that are not considered within this dissertation.

[16] For a given $Z(0)$ equation (3.1.12) has four, two or zero real roots $Z(h)$. Hereafter it is formulated for one real $Z(h)$.

[17] There are six, four, two or zero real roots $X_f\big(h-0,\gamma,Z(0)\big)$ of equation (3.1.12) for a given $Z(0)$. Hereafter it is formulated for one real $X_f\big(h-0,\gamma,Z(0)\big)$.

Section 4:

[18] Case $D = 0$ is not considered in the present work, because it yields nothing new.

[19] In general, there is more than one real root $X_f\big(0+0,\gamma,Z(0)\big)$ of the equation (3.1.11) for a given $Z(0)$. The question which solution $X_f\big(0+0,\gamma,Z(0)\big)$

will be prevalent can be answered by performing a stability analysis that is not considered in the present work.

[20] Field patterns in the film are obtained by means of the routine "NDSolve" (Mathematica 7.0).

[21] Schürmann H. W., "On the theory of TE-polarized waves guided by a nonlinear three-*layer structure"*, Zeitschrift für Physik B 97 (1995), pp. 515-522

[22] Boardman A. D., Egan P., Lederer F., Langbein U. and Michalache D., "Third-*order nonlinear electromagnetic TE and TM guided waves",* Nonlinear surface electromagnetic phenomena edited by H. –E. Ponath and G. I. Stegeman, Chapter 2, North- Holland, Amsterdam (1991)

[23] Mitsuhiro Yokota., "Guided transverse- magnetic waves supported by a weakly nonlinear slab waveguide*"*, Optical Society of America (1993) pp. 1096-1101

[24] Jasinski J., "*Balanced modes approximation for TM fields in Kerr thin films"*, JOSA B (1995), Vol. 12, Issue 12, pp. 2412-2419

[25] An analytical closed form dispersion relation in this case $(a = 0, b \neq 0)$ can be obtained only using (3.1.14). Using equation (3.1.15) only a numerical solution of the problem is possible. The dispersion relation for the special case $a \neq 0, b = 0$ can be solved only numerically (using (3.1.14) or (3.1.15)) – this is not considered in the present work.

[26] Abramowitz M., Stegun. I. A. " Handbook of mathematical functions with formulas, graphs, and mathematical tables*"*, Dover Publications, INC., New York (1971), pp. 589-590

[27] If $G(Z, X, \gamma) = 0$ is a closed curve in the plane (Z, X) for each fixed γ (for example, see Figure 40)).

[28] It is difficult to give a general formula for the period in terms of the primitive function without knowledge of the geometry of $G(Z, X, \gamma) = 0$ but it is simple to do it if the material parameters are given. For details, see Appendix I (Appendix J).

[29] Boardman A. D., Maradudin A. A., Stegeman G. I., Twardowski T., Wright E. M. "Exact theory of nonlinear p- polarized optical waves", Physical Review A (1987), Vol. 56, No. 3, pp. 1159- 1164

[30] An analytical closed form dispersion relation in this case is possible provided that using (3.1.15). Equation (3.1.14) enables to solve this problem only numerically.

Section 5:

[31] Serov V. S., Schürmann H. W., Svetogorova E., " Integral equation approach to reflection and transmission of a plane TE-wave at a (linear/nonlinear) dielectric film with spatially varying permittivity", Journal of Physics A: Mathematical and General (2004), Vol. 37, No. 10, pp. 3489-3500

[32] Stakgold I., "*Green's functions and boundary value* problems, Second Edition", New York (1998), Springer- Verlag, pp.191-197

[33] Zeidler E., "Applied functional analysis [Part1]: Applications to mathematical physics", New York (1995), Springer-Verlag, pp. 18-26

Section 6:

[34] For a cylindrical waveguide − an approach using an integral equation has been proposed by Schürmann H. W., Serov V., Shestopalov Y., Smirnov Y. in Report of the "Research in Pairs"- project "*Green's function approach to* the solution of nonlinear differential equations with constant and variable coefficients", Mathematisches Forschungsinstitut Oberwolfach (Oktober 29- November 11, 2006). See further Smirnov Yu. G., Valovik D. V.,

"Electromagnetic wave propagation in nonlinear layered waveguide structures", PSU Press, Penza (2011)

Appendix C:

[35] Polyanin Andrei D., Zaitsev Valentin F., "Hanbook of Exact Solutions for Ordinary Differential Equations", CRC Press, Boca Raton (1995), p. 130

Appendix E:

[36] Points $X_*^{\pm}$ are obtained as real solutions of equation $G(Z \equiv 0, X, \gamma) = 0$.

Appendix I:

[37] Points $Z_*^{\pm} = \pm\sqrt{\frac{-2\,C_f}{\varepsilon_{2f}\,\gamma^2}}$ are obtained as solutions of Eq. $G(Z, X \equiv 0, \gamma) = 0$.

Appendix L:

[38] The case $\hbar h = \pi\, l, l = 1,2,\ldots$ must be solved by using different Green's function.

Appendix N:

[39] Contents of N.2 are mainly based on hints by and discussion with Prof. V. S. Serov, Department of Mathematical Sciences, University of Oulu, Finland

[40] cf. Descartes' rule of signs, see, for example, Korn G., Korn T., "Mathematical handbook for scientists and engineers : definitions, theorems, and formulas for reference and review", New York (1968), McGraw-Hill

Acknowledgement

I would like to gratefully and sincerely thank Prof. Dr. Hans Werner Schürmann, my first scientific advisor, for the help, guidance, understanding he has given me during my PhD studies at the Department of Physics, University Osnabrück.

I owe my gratitude to my second and third advisors, Prof. Dr. Heinz- Jürgen Schmidt and Prof. Dr. Valery Sergeevich Serov, for their care, suggestions and valuable comments.

I would like also to acknowledge Prof. Dr. Klaus Betzler, the chair of the Graduate College 695, for the help with any problems and the support of my PhD project.

A special thank goes to Prof. Dr. Yuri Gennad'evich Smirnov for his support of my first steps into scientific world and recommendations.

I am indebted to the members of the working group "Didaktik der Physik", Prof. Dr. Roland Berger, Daniel Schwarz, Stefan Korte, Michael Kant, Marion von Landsberg and other for their help and warm atmosphere at the department.

Thanks to all my friends and my family for being there for me.

Financial support by the Deutsche Forschungsgemeinschaft (Graduate College 695: Nonlinearities of optical materials) is gratefully acknowledged.

Eidesstattliche Erklärung

Hiermit erkläre ich an Eides Statt, die vorliegende Abhandlung selbstständig und ohne unerlaubte Hilfe verfasst, die benutzten Hilfsmittel vollständig angegeben und noch keinen Promotionsversuch unternommen zu haben.

Osnabrück, 13.08.2012

Kadriya Yuskaeva